European Commission

JRC SCIENCE AND POLICY REPORTS

Feasibility study on the extension of the Real Driving Emissions (RDE) procedure to Particle Number (PN)

Chassis dynamometer evaluation of portable emission measurement systems (PEMS) to measure particle number (PN) concentration: Phase II

Barouch Giechaskiel
Francesco Riccobono
Pierre Bonnel

2015

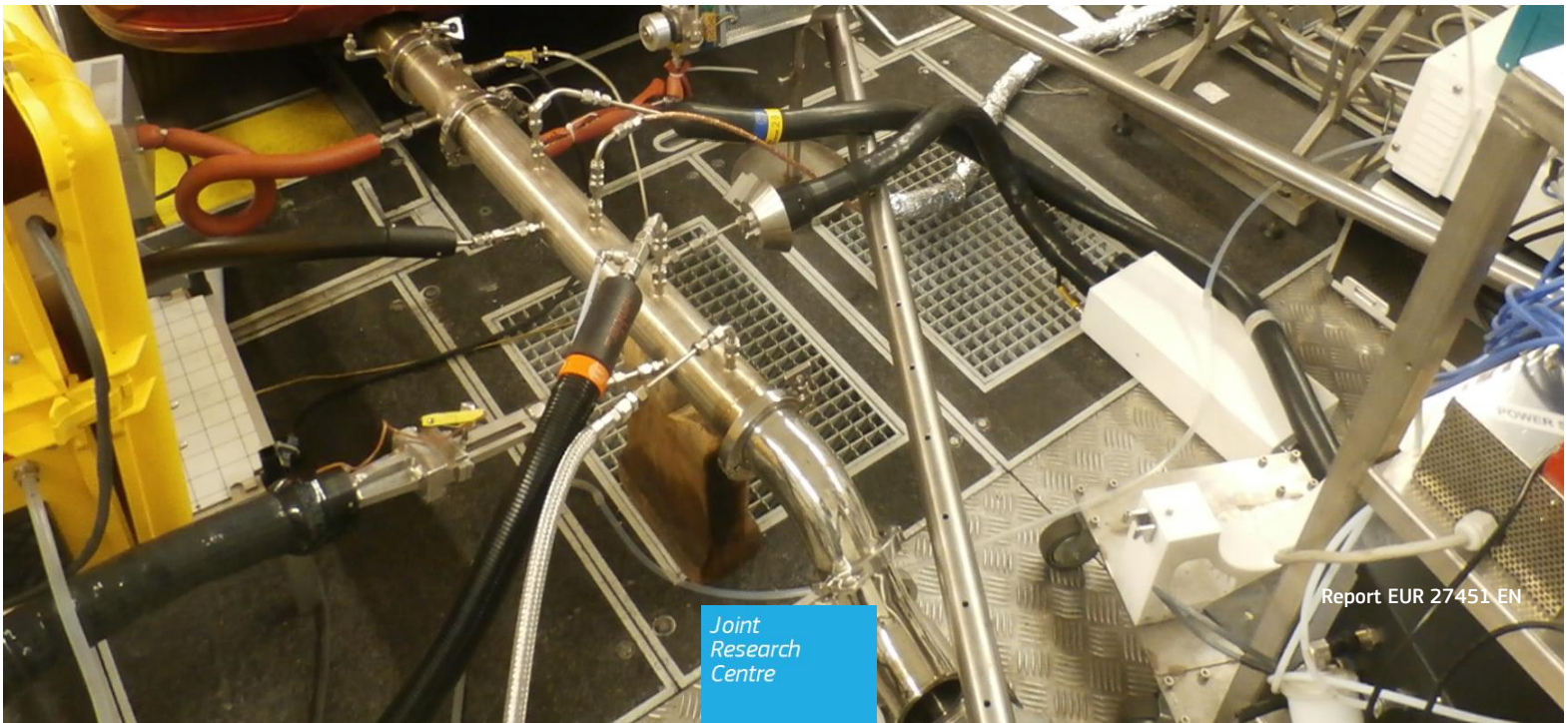

Report EUR 27451 EN

European Commission
Joint Research Centre
Institute for Energy and Transport

Contact information
Barouch Giechaskiel
Address: Joint Research Centre, Via Enrico Fermi 2749, TP 230, 21027 Ispra (VA), Italy
E-mail: Barouch.Giechaskiel@jrc.ec.europa.eu
Tel.: +39 0332 78 5312

https://ec.europa.eu/jrc

JRC97357

EUR 27451 EN

ISBN 978-92-79-51003-8 (PDF)

ISSN 1831-9424 (online)

doi:10.2790/74218

Luxembourg: Publications Office of the European Union, 2015

Abstract

This report presents the results of Phase II evaluation of Particle Number (PN) Portable Measurement Systems (PEMS). 8 PN-PEMS were compared with legislation compliant PN systems connected to the tailpipe and the dilution tunnel (CVS). In total 7 Gasoline Direct Injection (GDI), 3 Port Fuel Injection (PFI), 2 Diesel Particulate Filter (DPF) equipped vehicle, 1moped and 3 motorcycles were tested with >130 test cycles. The results confirmed the findings of Phase I: Diffusion Charging (DC) based systems are a feasible option to measure PN and thermal pre-treatment is necessary to avoid volatile artefacts. At least two of the DC based PN-PEMS showed good agreement with the reference PMP system (#1, #3). A third one (#4) also had very good behaviour, but higher scatter. The best performing PN-PEMS had differences from the reference instrument at the tailpipe within -25% and +30% with a scatter of 20%.. The differences from the reference system at the dilution tunnel were within -35% and +50% (scatter 25%) (including all technologies tested); slightly higher due to the particle transformation processes that take place between the tailpipe and the dilution tunnel, exhaust flow accuracy and time alignment. It was also shown that a well calibrated PN-PEMS can cover a wide range of engine technologies with similar differences to the reference system. Based on the experimental data new PN-PEMS efficiencies were recommended for the technical requirements. The CPC based PN-PEMS had issues (prototypes). However, one CPC based PN-PEMS, which arrived late in the program, had behaviour equivalent to the reference systems and better real time comparability with the reference systems compared to the DC based systems. Further evaluation of the system after the campaign with another 10 vehicles confirmed these findings.

Table of Contents

1 Introduction 9
1.1 Main findings 10
1.1.1 Lab calibration 10
1.1.2 Chassis tests 11
2 Experimental 13
2.1 Instrumentation 13
2.2 Setup 13
2.3 Vehicles 13
2.4 Protocol 14
2.5 Calculations 14
3 PMP systems 16
3.1 Calibration of PMP systems 16
3.2 Real time (CVS) 16
3.3 Real time (TP) 17
3.4 Emission levels 19
3.5 Size dependency 20
3.6 Summary PMP 21
4 EEPS 23
4.1 Monodisperse calibration 23
4.2 Polydisperse comparisons 25
4.3 Vehicle results 28
5 PN-PEMS #1' 30
5.1 Description 30
5.2 Calibration 30
5.3 Real time 32
5.4 Comparison to PMP-CVS 33
5.5 Comparison to PMP-TP 34
5.6 Particle size effect 34
5.7 Ambient temperature 36
5.8 Challenge aerosol (motorcycles) 36
5.9 Volatile removal efficiency 38
5.10 DPF Regeneration 38
5.11 Summary 39

5.12 Adjustment of PN-PEMS 41
6 PN-PEMS #2' (CPC) 45
6.1 Description 45
6.2 Calibration 45
6.3 Real time 46
6.4 Comparison to PMP-CVS 47
6.5 Comparison to PMP-TP 48
6.6 Particle size effect 49
6.7 Ambient temperature 49
6.8 Challenge aerosol (motorcycles) 49
6.9 Volatile removal efficiency 50
6.10 Regeneration 50
6.11 Summary 50
7 PN-PEMS #2' (DC) 53
7.1 Description 53
7.2 Calibration 53
7.3 Real time 54
7.4 Comparison to PMP-CVS 54
7.5 Comparison to PMP-TP 55
7.6 Particle size effect 55
7.7 Ambient temperature 56
7.8 Challenge aerosol (motorcycles) 56
7.9 Volatile removal efficiency 58
7.10 Summary 58
8 PN-PEMS #3 (PN) 59
8.1 Description 59
8.2 Calibration 59
8.3 Estimated mean size and real time PN 60
8.4 Comparison to reference PMP 62
8.5 Regeneration 64
8.6 Summary 64
8.7 On-road evaluation 65
9 PN-PEMS #3 (LDSA) 66
9.1 Calibration 66
9.2 Real time 68
9.3 Comparison to PMP-CVS 69

9.4 Comparison to PMP-TP 69
9.5 Particle size effect 70
9.6 Ambient temperature 70
9.7 Challenge aerosol (motorcycles) 70
9.8 Volatile removal efficiency 71
9.9 Regeneration 72
9.10 Summary 72
9.11 Adjustment of PN-PEMS 74
10 PN-PEMS #4 76
10.1 Description 76
10.2 Real time 76
10.3 Comparison to PMP-CVS 77
10.4 Comparison to PMP-TP 78
10.5 Particle size effect 78
10.6 Ambient temperature 78
10.7 Challenge aerosol (motorcycles) 80
10.8 Volatile removal efficiency 81
10.9 Summary 81
10.10 Adjustment of PN-PEMS 83
11 PN-PEMS #5' 85
11.1 Description 85
11.2 Real time 85
11.3 Comparison to PMP-CVS 87
11.4 (Ambient) Temperature effect 88
11.5 Particle size effect 89
11.6 Challenge aerosol (motorcycles) 90
11.7 Volatile removal efficiency 91
11.8 Summary 91
11.9 Adjustment of PN-PEMS 93
11.10 CPC 95
12 PN-PEMS #6' 97
12.1 Description 97
12.2 Real time 97
12.3 Comparison to PMP-TP 99
12.4 Comparison to PMP-CVS 100
12.5 Particle size effect 101

12.6 Ambient temperature 101
12.7 Challenge aerosol (motorcycles) 101
12.8 Volatile removal efficiency 102
12.9 Summary 103
13 PN-PEMS #7' 106
13.1 Description 106
13.2 Calibration 106
13.3 Real time 107
13.4 Comparison to PMP-CVS 109
13.5 Comparison to PMP-TP 110
13.6 Particle size effect 110
13.7 Ambient temperature 111
13.8 Challenge aerosol (motorcycles) 111
13.9 Volatile removal efficiency 112
13.10 DPF Regeneration 113
13.11 Summary 114
14 Overview 117
14.1 Phase I results 117
14.2 Examined emissions levels and technologies 118
14.3 PMP-CVS 119
14.4 Summary of PN-PEMS 119
14.4.1 PASS/FAIL 119
14.4.2 Accuracy (bias and precision) 121
14.4.3 Cut-off size 122
14.4.4 Volatile removal efficiency 122
14.5 Specific comments for PN-PEMS 123
14.5.1 PN-PEMS #1' 123
14.5.2 PN-PEMS #2 (CPC) 123
14.5.3 PN-PEMS #2' (DC) 124
14.5.4 PN-PEMS #3 124
14.5.5 PN-PEMS #4 125
14.5.6 PN-PEMS #5' 125
14.5.7 PN-PEMS #6' 125
14.5.8 PN-PEMS #7' 126
14.6 Calibration in the lab 126
14.7 Calibration with exhaust particles 128

14.8 Key messages 129
15 References 132
16 Annex A: Detailed measurement protocol 134
17 Annex B: Comparison of measurements at the tailpipe and the dilution tunnel 136
17.1 Effect of extracted flow on absolute levels 136
17.2 Thermophoretic losses 136
17.3 Condensation 137
17.4 Coagulation 137
17.5 Exhaust flow 138
17.6 Time alignment 139
18 Annex C: Volatile Removal Efficiency (VRE) 142
19 Annex D: Further evaluation of PN-PEMS 146

Abbreviations

CPC	Condensation Particle Counter
CS	Catalytic Stripper
CVS	Constant Volume Sampler
DC	Diffusion Charger
DF	Dilution Factor
DPF	Diesel Particulate Filter
E	Efficiency
EC	European Commission
EEPS	Engine Exhaust Particle Sizer
EO	Emery Oil
ET	Evaporation Tube
GDI	Gasoline Direct Injection
GMD	Geometric Mean Diameter (from EEPS unless specified)
I	Current
LDSA	Lung Deposited Surface Area
NEDC	New European Driving Cycle
NTE	Not-To-Exceed
PCRF	Particle number Concentration Reduction Factor
PEMS	Portable Emission Measurement System
PFI	Port Fuel Injection
PMP	Particle Measurement Program
PN	Particle Number
R	Reading
RDE	Real Driving Emissions
SMPS	Scanning Mobility Particle Sizer
TP	Tailpipe
US	United States
VELA	Vehicle Emissions Laboratory
VRE	Volatile Removal Efficiency
WLTC	World Harmonized Light duty Transient Cycle

1 Introduction

The newest Euro 6 cars meet stringent emission limits for regulated pollutants. However, these emission limits are evaluated with a standard test performed under predefined conditions in a chassis dynamometer laboratory (Franco et al. 2013). There is evidence that the actual on-road emissions are higher compared to the laboratory test.

On-road emission measurements can be conducted with Portable Emission Measurement Systems (PEMS). PEMS are relatively simple and inexpensive to purchase and maintain in comparison to a full dynamometer test cell, and they have thus become a popular tool for scientific studies. In recent years, they have also been applied for regulatory purposes. US authorities have introduced additional emissions requirements based upon PEMS testing and the "not to exceed" (NTE) concept, whereby emissions averaged over a time window must not exceed specified values for regulated pollutants while the engine is operating within a control area under the torque curve (U.S. EPA 2005). In Europe, PEMS are being used to verify the in-service conformity of Euro V and Euro VI heavy-duty vehicles with the applicable emissions standards (EC 2011, 2012), and the European Commission is working with stakeholders in the Real Driving Emissions (RDE) from light-duty vehicles group to include PEMS testing as part of the type-approval process of Euro 6 passenger cars (Weiss et al. 2013). The RDE procedure was approved in May 2015 as part of the Euro 6 legislation, Appendix IIIA of 692/2008. The use of PEMS and the introduction of the 'not-to exceed' regulatory concept is based on Regulation 715/2007 where it was stated that revisions may be necessary to ensure that real world emissions correspond to those measured at type approval. According to Regulation 459/2011 attention should be given to the particle emissions of positive ignition vehicles under real driving conditions and the development of respective test procedures. The Commission should develop and introduce corresponding measurement procedures at the latest three years after the entry into force of Euro 6.

PEMS typically measure instantaneous raw exhaust emissions of CO_2, CO, NO_x, and total hydrocarbons. Portable particle mass analysers have recently become commercially available after extensive testing (Mamakos et al. 2011). Portable particle number (PN) analysers (PN-PEMS) are under investigation. At the moment there are no systems compliant to the requirements of the legislation for on-board usage. First of all, there can be no full dilution tunnel for on-board testing. Nevertheless, preliminary investigations showed that measuring raw exhaust gives similar results to the tests from the dilution tunnel (Cavina et al. 2013). However, the main concern is the robustness of the condensation particle counters (CPCs) when used in the car. For this reason another principle was evaluated recently (i.e. diffusion chargers DC). In November 2012 the interest for PN-PEMS was announced and in April 2013 the kick-off meeting took place.

In a preliminary study (Giechaskiel et al. 2014) a theoretical evaluation was conducted and showed that DCs are an acceptable alternative. However, due to their size dependency an extra uncertainty around 50% is introduced for typical size distributions with geometric mean diameters (GMD) of 40-90 nm. Tests with laboratory soot confirmed the findings, but some DCs showed higher uncertainty due to their higher dependency on size and/or calibration uncertainties of the DC and the dilution system. Based on the findings of that study, the response requirements of the DCs in function of size were drafted.

At a next step (end of 2013) various prototype PN-PEMS (based on DCs) were evaluated in a chassis dynamometer lab to assess and validate the application and performance of portable PN instrumentation (Riccobono et al. 2014). The systems were measuring from the tailpipe and were compared to reference PN systems at the tailpipe and the CVS. The results showed that the best performing PN-PEMS was within 60% compared to the reference system, while for the second best around 100%. Another important finding of the study was that the systems needed thermal pre-treatment of the sample in order to get rid of volatile nucleation mode particles. The minimum temperature requirement was 200°C until the sensor or the primary dilution.

Based on the findings of the previous studies, some technical requirements were drafted. In this report the evaluation of the second generation of PN-PEMS (which fulfils those) will be presented. Main targets are to confirm the findings of the first phase and finalise the technical requirements.

The topics that were examined for each PN-PEMS were:

- Calibration
- Real time signal
- Comparison with PMP systems
- Dependency on particle size
- Ambient temperature effect
- Challenge aerosol (solid sub-23 nm)
- Volatile removal efficiency (moped 2-stroke)
- Regeneration (DPF)
- Bias and precision
- PASS or FAIL success rate
- Calibration at the CVS

The main findings can be found in the next pages. A more detailed overview can be found at the last chapter.

1.1 Main findings

1.1.1 Lab calibration

In Phase I PN-PEMS were calibrated with monodisperse aerosol. Their normalized efficiency (response function) to 100 nm had to fulfil some requirements (<0.5 for 23 nm, <2.5 for 200 nm) (Table 1-1). Then an extra calibration factor was allowed to 'optimize' their performance for typical vehicle exhaust size distributions. In Phase II, based on the experimental data, this factor was found to be the (monodisperse) 70 nm calibration factor or the optimization with 55 nm polydisperse distribution (Chapter 14). The new normalized to 70 nm efficiency requirements are shown in Table 1-1. Check (not calibration) of the PN-PEMS in a chassis dynamometer with a hot WLTC was also shown to be possible, but not reliable enough to calibrate a system.

In Phase II there was one DC system (#3) and a multi-electrometer spectrometer (EEPS) that could fulfil more strict efficiencies due to the internal corrections of the size information they have (Table 1-1). Their real time performance was only marginally better than the well-calibrated DCs based systems, considering also the uncertainty that is introduced when tailpipe measurements are conducted. However, such efficiencies

minimize the size dependency of the DC based systems. Such efficiencies can only be achieved by DC systems with internal size info or flat size dependency. The CPC based systems fulfil them easily of course.

Table 1-1: Phase I, Phase II PN-PEMS efficiency *E* requirements. Future feasible requirements are also shown.

Size	23 nm	50 nm	70 nm	100 nm	200 nm	Extra
Phase I	<0.5	>0.4	-	1.0	<2.5	Yes
Phase II (new)	<0.6	>0.6	1	<1.6	<3.7	No
Phase II (to confirm)	<0.6	>0.6	0.7 – 1.3	0.7 – 1.3	<2.0	No

The volatile removal efficiency of the PN-PEMS was investigated with evaporation-condensation tetracontane particles and atomized emery oil. The systems that were examined (#2' (CPC), #3, #4) could handle orders of magnitude higher tetracontane mass than what is required in the legislation. The atomized oil tests showed that high mass of oil can only be handled by systems with catalytic stripper (15 mg/m^3) but much lower when only an evaporation tube exists (Annex C).

1.1.2 Chassis tests

In Phase II 7 GDI, 3 PFI and 2 DPF diesel vehicles were tested. In addition 1 moped and 3 motorcycles were used to challenge the PN-PEMS with extreme 'conditions' (Chapter 2, Annex A).

Initially two reference legislation compliant PN systems were compared to each other (one at the tailpipe and one at the dilution tunnel) (PMP-TP vs PMP-CVS) (Chapter 3). Mean differences up to 20% were found (with standard deviation of the differences of 15%) due to agglomeration (0-15%), thermophoresis (0-5%), exhaust flow estimation (±10) and time alignment issues (0-10%) (Annex B).

Then the PN-PEMS systems were compared with the reference system at the tailpipe (PMP-TP). The differences of the best performing systems (#1, #3, #2 (CPC)) were between -25% and +30% (with standard deviation lower than 20%). The CPC based system was even closer to the reference system, especially the second by second data.

At a next step the PN-PEMS were compared with the PMP-CVS. The differences of the best performing PN-PEMS were between -35% and +50% (with precision less than 25%). These values refer to differences from reference PMP systems at the CVS over a cycle (>10 min duration). These values include the tests with motorcycles and mopeds where the GMD was on the order of 25 nm. For GDIs the results were in general within 30% (20%). The second by second data have higher differences.

The sensitivity of PN-PEMS to smaller than 23 nm (solid) particles was assessed by measuring exhaust gas of motorcycles. The results showed that most CPC based PN-PEMS were only slightly affected. The DC based PN-PEMS actually were slightly underestimating the emissions.

The volatile particle removal efficiency was assessed by measuring exhaust aerosol of a 2-stroke moped. For the systems tested there was no indication of overestimation of emissions, thus the PMP-like thermal pre-treatment was found to be sufficient.

Regeneration of a DPF also was measured without any volatile artefact interference for all CPC and DC based PN-PEMS. However, the DC based system had higher deviations from the reference systems.

In general, the results showed that the PN-PEMS, with a few exceptions, had a high success rate (>90%) and were able to catch a PASS or FAIL at emission levels close to 6x10^11 p/km. When this was not the case, they had similar success rates with the PMP-TP (Chapters 4-13).

At the end of the campaign two PN-PEMS were further evaluated with 10 more vehicles, mostly from the dilution tunnel, confirming the previous findings: The DC based system had differences of ±40% to the reference systems (-35% to +15% with size estimated PN) and the CPC based ±15%. The CPC based system had very good comparability with the reference system regarding the second to second data (Annex D).

Finally it should be noted that some of the PN-PEMS had issues during the measurements (e.g. due to condensation, drift etc.). This resulted in underestimation of the emissions in the case of drift and underestimation in the case of malfunction of the thermal-pretreatment unit. This means that special attention should be given from the instrument manufacturers for the long term robustness of the systems for the 'aggressive' exhaust gas and the on-board application.

2 Experimental

The tests were conducted in the Vehicle Emission Laboratories (VELA) of the Joint Research Centre (JRC) in Ispra, Italy. VELA 1 is a single axis roller dynamometer used mainly for motorcycles. VELA 2 is a double axis roller dynamometer that was mainly used for the tests conducted in this report.

2.1 Instrumentation

In total 8 PN-PEMS were used. PN-PEMS #4 was the same (also same unit) that was used in Phase I. PN-PEMS #3 was the same (in terms of principles) as in Phase I, but a different unit. The rest PN-PEMS were second generation PN-PEMS (indicated with an ' after the number). Most of them were DC based, except PN-PEMS #7' (only CPC based), PN-PEMS #5' (both DC and CPC in the same unit), PN-PEMS #2' (two separate units one with DC, the other with CPC). Instrument manufacturers did the commissioning and training for their instruments which were then ran by JRC personnel. During the campaign they were free to join and check their instruments. This was the case for PN-PEMS #5' and PN-PEMS #7'. Details of the PN-PEMS can be found in the corresponding chapters.

Two PMP compliant systems were used: One was connected to the dilution tunnel of VELA 1 and the other of VELA 2 (APC 489 from AVL) (PCRF always 100x10) (from now on PMP-CVS). Another PMP system one was connected to the tailpipe (Nanomet from Matter Aerosol/Testo AG) (PCRF always 125x4) (from now on PMP-TP). An Engine Exhaust Particle Sizer (EEPS) from TSI downstream of a catalytic stripper (prototype from AVL) was used to measure solid size distributions from the CVS. Based on the size distribution the Geometric Mean Diameter (GMD) was calculated for every second. In real time figures, the 5 s moving average is plotted. In figures where aggregated results are plotted, the average of the whole cycle is plotted. The results presented here used the original inversion matrix of the instrument. The new fractal matrix was available only at the end of the campaign and was evaluated for a limited number of tests.

2.2 Setup

Initially the PN-PEMS were connected to the dilution tunnel for some first comparisons with the PMP system there (PMP-CVS). Then the PN-PEMS were connected to the tailpipe where another PMP system was also measuring (PMP-TP) (Figure 2-1). All systems were measuring from multi-hole probes spaced 7 cm and at an angle of 85° to each other to minimise any influence. Preliminary tests showed that there was no measurable effect between the different locations (Phase I).

The effect of the multi-hole probes on the absolute emission levels was not investigated, but it is expected to be similar to all instruments measuring at tailpipe.

2.3 Vehicles

In total 7 Gasoline Direct Injection (GDI) vehicles were tested, 2 Port Fuel Injection (PFIs), 2 diesel with Diesel Particulate Filter (DPF), 1 moped and 3 motorcycles. Five of the GDIs were certified as Euro 6 and one of the DPF equipped vehicles. The vehicles were selected such as to have emissions close to the Euro 5B diesel limit (6x10^11

p/km). Another 10 vehicles were used for the evaluation of two Pn-PEMS after the end of the campaign (Annex D).

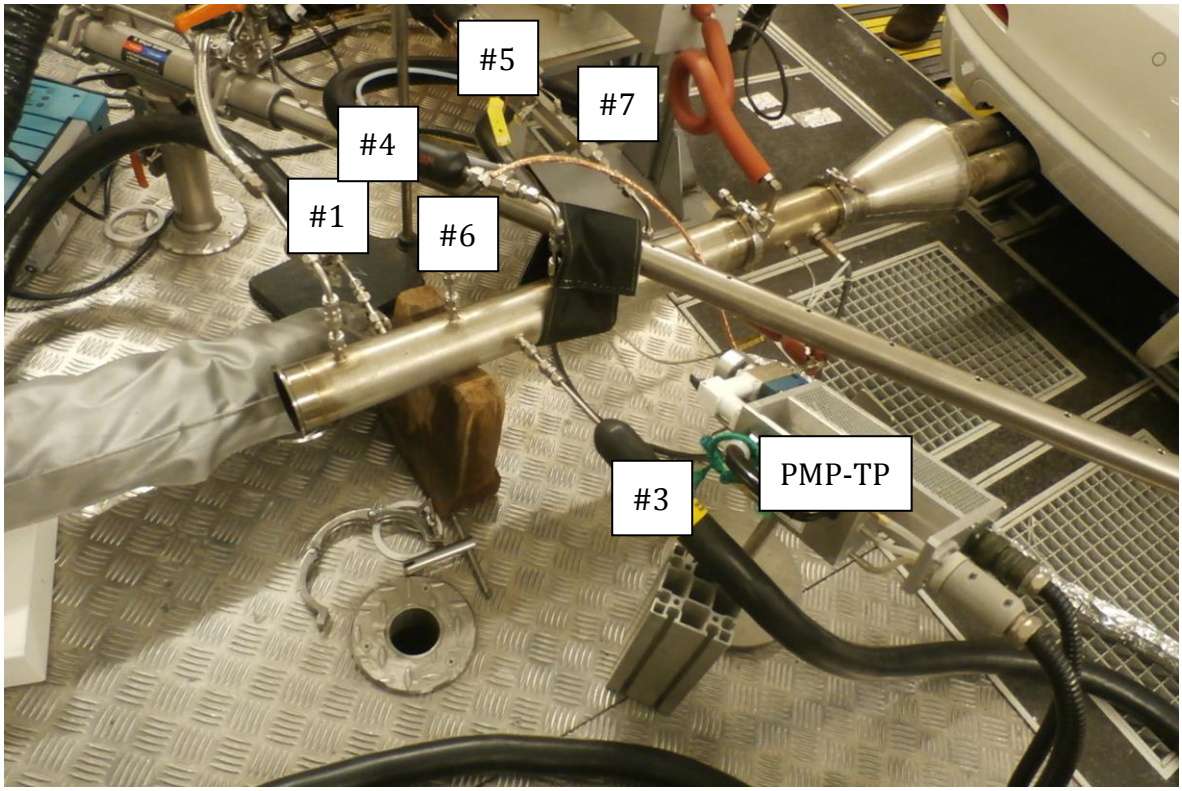

Figure 2-1: Example of PN-PEMS connected to the tailpipe.

2.4 Protocol

The protocol consisted of 3-5 tests per day with the total tests exceeding 130. The tests were either steady state speeds or cycles like the NEDC, WLTC, Artemis and Random Driving Cycles. Only the first test of the day was 'cold' start. The rest were relatively warm (typically the time between tests is around 20 min due to the bag analysis). Some tests were conducted at test cell temperature of 8°C, in order to investigate potential issues with the PEMS at relatively low temperatures (Table 2-1). The detailed protocol can be found in Annex A. There was a preparation / commissioning period, the main campaign and some extra evaluation period.

2.5 Calculations

For the systems at the CVS, the CVS flow rate and the distance travelled were used to calculate the emissions in p/km. For the systems at the tailpipe, the particle concentration was time aligned with the exhaust flow rate and then they were multiplied with each other. The sum was divided with the distance to give p/km. The exhaust flow in all tests presented was estimated from the difference of the total flow of the dilution tunnel minus the dilution air flow.

Table 2-1: Summary of tests conducted.

Code	EU	Dates	Lab	Testo	AVL	Horiba	Testo	Pegasor	Sensors	Shimadzu	Maha
		2014	**PMP-CVS**	**PMP-TP**	**#1'**	**#2'**	**#3**	**#4**	**#5'**	**#6'**	**#7'**
Preparation phase											
Moto #1	2	17/10	VELA 1	CVS				CVS			
PFI #1	5	6-7/8	VELA 2				CVS				
PFI #2	6	11-26/8	VELA 2				CVS				
GDI #1	6	28-29/10	VELA 2					CVS			CVS
Moto #2	3	30/10-4/11	VELA 1	CVS				TP	TP (issues)	TP	TP
GDI #2	6	05/11	VELA 2					TP	TP	TP	TP
Main campaign											
GDI #3	5	6-7/11	VELA 2 (8°C)	TP	TP			TP	TP*	TP	TP**
GDI #4	6	11-14/11	VELA 2 (8°C)	TP	TP		TP	TP	TP	TP	TP**
GDI #5	5	18-24/11	VELA 2		CVS						
PFI #3	5	18-24/11	VELA 2		CVS						
GDI #2	6	25-28/11	VELA 2 (8°C)	TP	TP		TP	TP	TP*	TP	TP
GDI #6	6	1-5/12	VELA 2	TP	TP	TP	TP	TP	TP*	CVS	TP***
Extra evaluation											
Moto #1	2	9-10/12	VELA 1		CVS	CVS	CVS			CVS	CVS
GDI #7	6	11-12/12	VELA 1		CVS	CVS				CVS	CVS
GDI #7	6	12-16/12	VELA 1	TP	TP	TP	TP			CVS	TP
Moto #3	2	17-18/12	VELA 1	TP	TP	TP	TP	TP	TP	CVS	TP
Moto #4	3	19-23/12	VELA 1	TP	TP	TP	TP	TP		CVS	TP
DPF #1	5	28-30/1/15	VELA 2	TP	TP						TP
DPF #2	6	15/3/15	VELA 2	CVS		CVS	CVS				CVS
On road evaluation											
GDI #3	5	17-24/11	On-road				Yes				Yes*

* issues CPC

** issues at 8°C

*** CPC replaced

3 PMP systems

Before the discussion for the PN-PEMS the behaviour of the PMP systems will be discussed.

3.1 Calibration of PMP systems

The PMP system at Vela 1 (APC 489, PMP-CVS) was recently calibrated by the manufacturer (AVL).

The PMP system at Vela 2 (APC 489, PMP-CVS) was only validated and was found within specifications: 2.5% (the VPR) and 8% the CPC. This PMP system was also used at Phase I (no modifications). During Phase I the wick from the CPC was exchanged to ensure the proper operation without any drift. The total efficiency of the PMP system versus a reference CPC (3025A) using spark discharge graphite particles can be seen in Figure 3-1. The results are in agreement with the validation results (i.e. the PMP is only slightly overestimating the emissions, <5%).

The PMP system that was connected at the tailpipe (Testo, PMP-TP) was validated with spark discharge graphite particles. The results are shown in Figure 3-1. The PMP efficiency reached slightly above than 90% for particles larger than 80 nm. Since the difference was lower than 10%, the calibration factor was not adjusted. By not correcting (and having systems from different manufacturers) the maximum differences between tailpipe and dilution tunnel are expected; other studies should have better agreement between tailpipe and dilution tunnel.

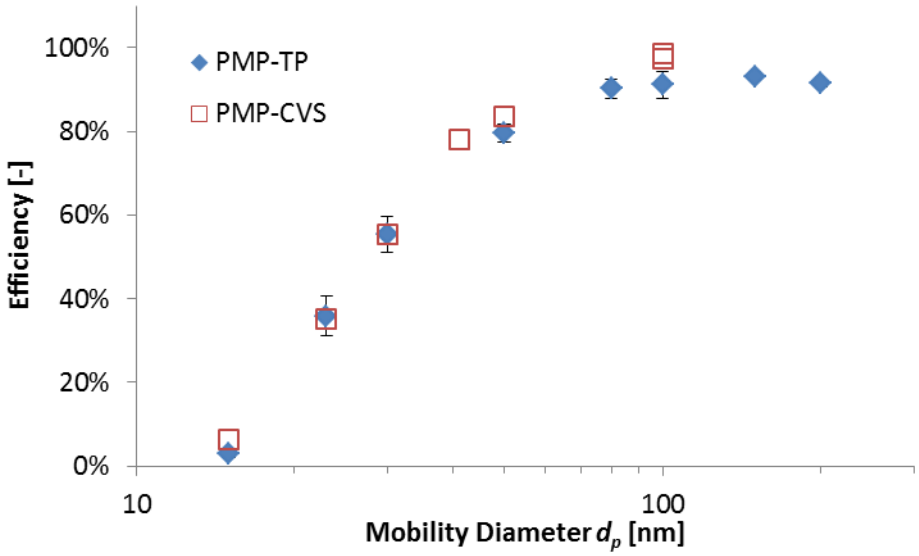

Figure 3-1: Efficiency of the PMP systems.

3.2 Real time (CVS)

A comparison of both PMP systems at the CVS can be seen in the Figure 3-2. Generally the agreement of the two systems was excellent.

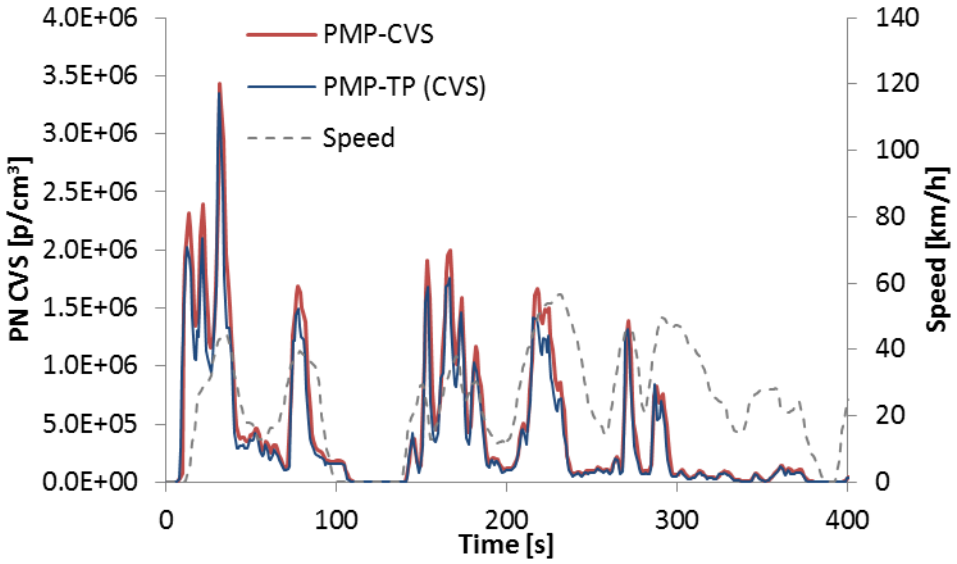

Figure 3-2: Comparison of PMP-systems connected at the dilution tunnel (20141205-01-WLTC cold, GDI #6).

3.3 Real time (TP)

The comparison of the PMP-CVS at the dilution tunnel and PMP-TP at the tailpipe can be seen in Figure 3-3. The PMP-CVS is corrected with the CVS flow rate, while the PMP-TP with the exhaust flow rate. The agreement is quite good. A closer look (see Figure 3-4) revels that the PMP-CVS is smoother and especially at the beginning of the cycles many particles are lost (e.g. to the cold walls).

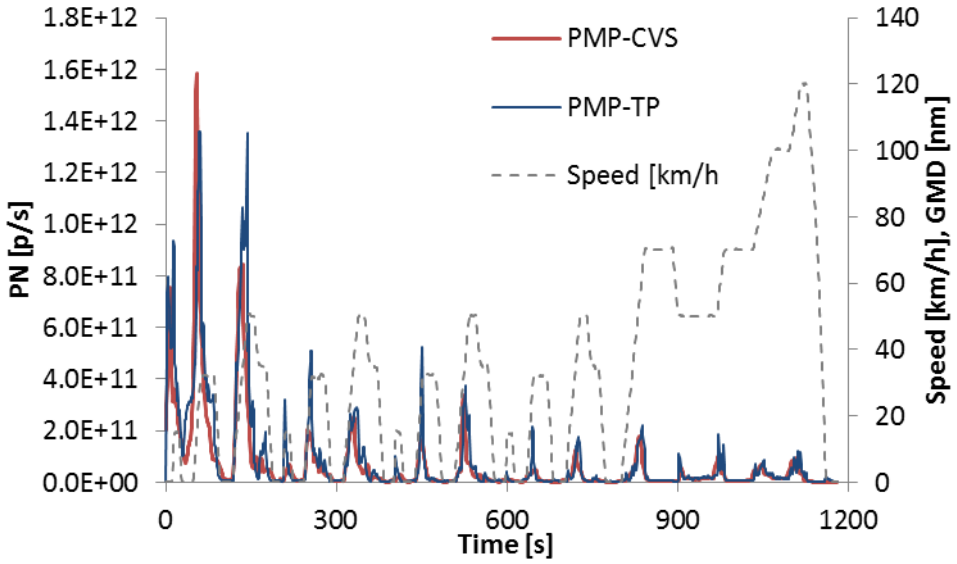

Figure 3-3: Comparison of PMP-CVS at the dilution tunnel with PMP-TP at the tailpipe (20141106-01-NEDC cold, GDI #3).

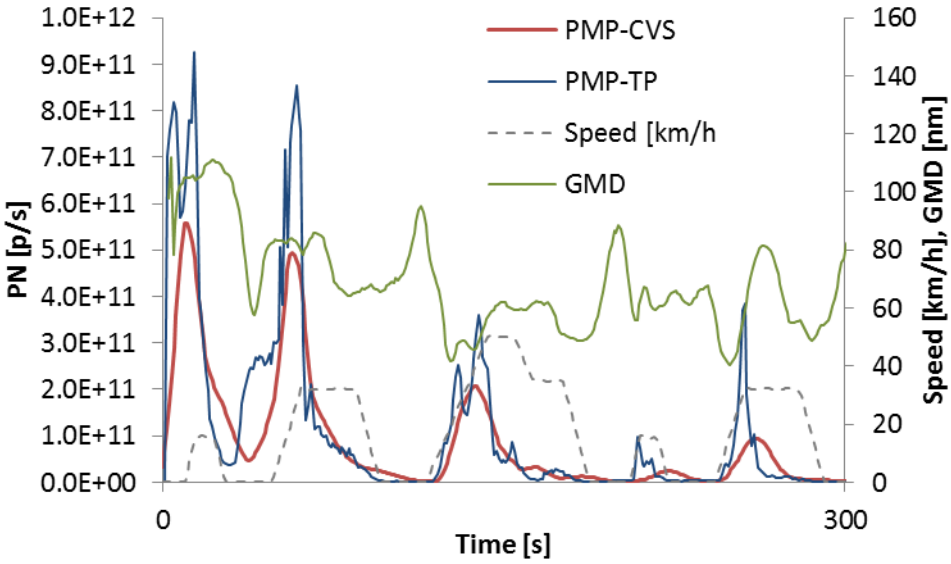

Figure 3-4: Detail of previous figure. GMD is a 5 s moving average.

The cross-correlation of the two PMP systems is medium (R^2=0.84) and the slope quite high (1.42) (Figure 3-5). Indeed, for the specific test the PMP-TP was 30% higher than the PMP-CVS. In any case, it is important to highlight that the cross-correlation cannot be used to assess a system at the tailpipe. Even two PMP systems cannot have an excellent correlation (i.e. >0.95). The main reason is the different location of the two systems which results in different emission profiles due to the different residence time of the exhaust gas in the tube in between (which depends on the vehicle exhaust flowrate). Differences in response times of the systems can amplify this effect.

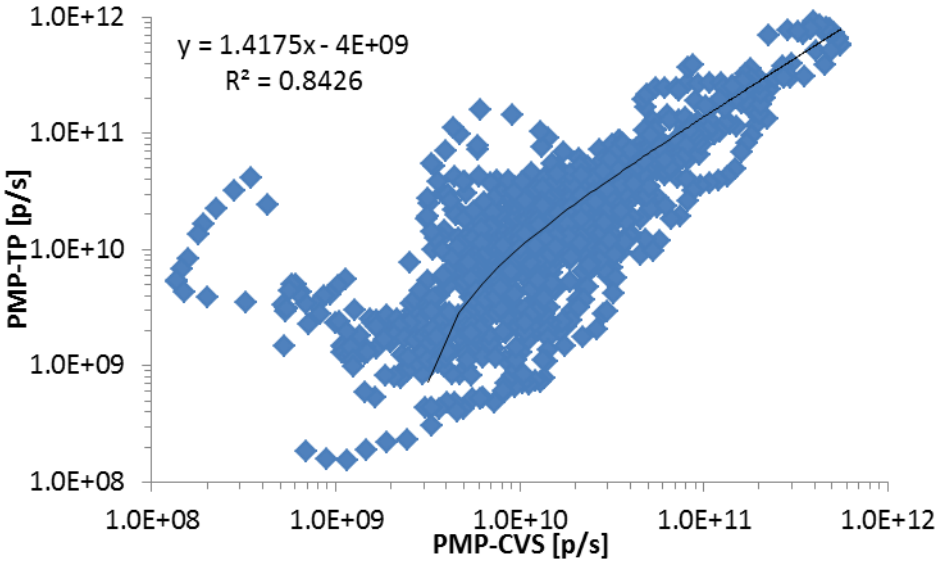

Figure 3-5: Cross correlation of PMP-CVS and PMP-TP for the test cycle of the previous figure.

3.4 Emission levels

The differences of the two PMP systems were also plotted in function of the emission levels when both measuring at the dilution tunnel (Figure 3-6) or one at the tailpipe and the other at the dilution tunnel (Figure 3-7). No clear tendency can be seen.

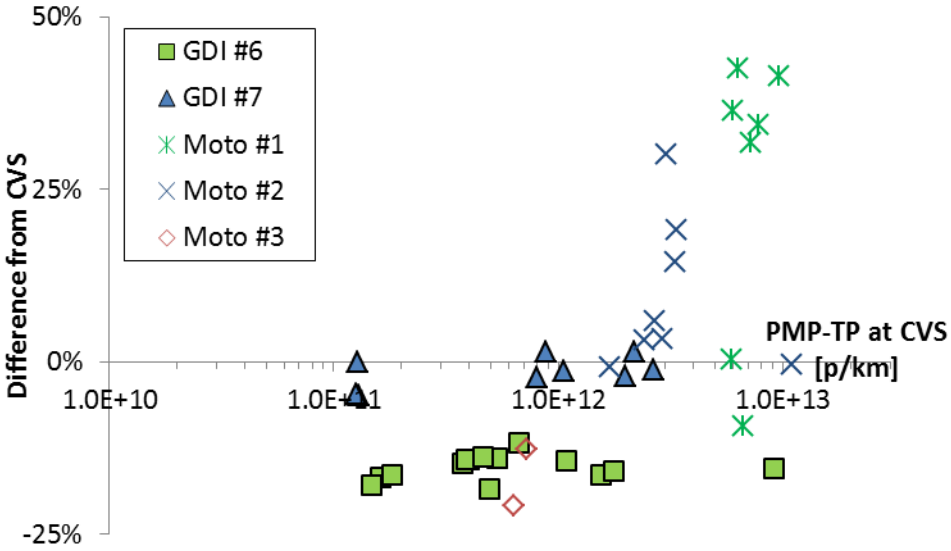

Figure 3-6: Differences of PMP systems (both at the dilution tunnel).

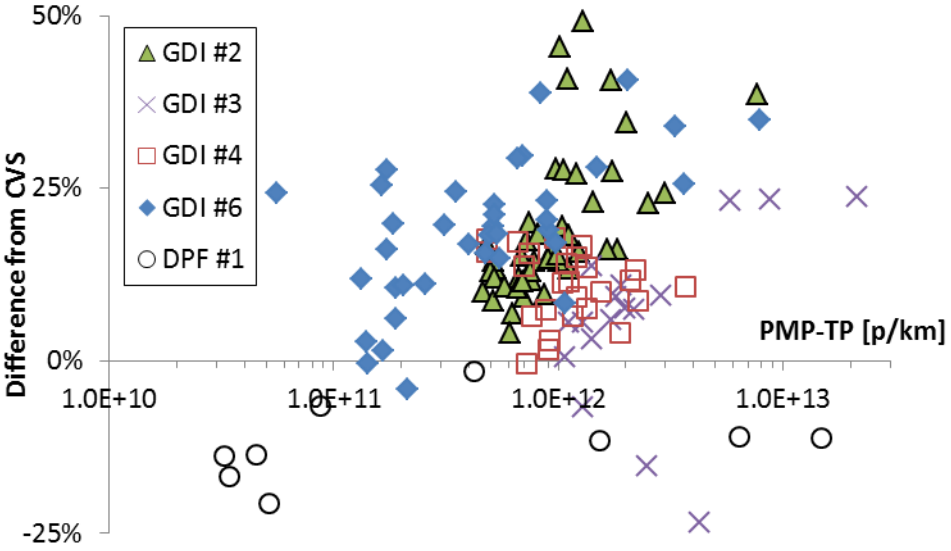

Figure 3-7: Differences of PMP systems.

Another way of evaluating the systems is by plotting the results of the PMP-TP vs the PMP-CVS. By setting the limit values one can visualize which tests would give a correct results (i.e. PASS when the PMP-CVS would give PASS or FAIL when the PMP-CVS system would give FAIL) or wrong (PASS for FAIL or FAIL for PASS). Figure 3-8 gives all results and Figure 3-9 focuses on the 6x10^11 p/km range. There are a few tests where the PMP-TP gave wrong result (FAIL instead of PASS) and as mentioned previously this had to do with the overestimation of the emissions when it was connected to the

tailpipe. The dotted lines contain almost all data and represent the 0.85x and 1.45x lines.

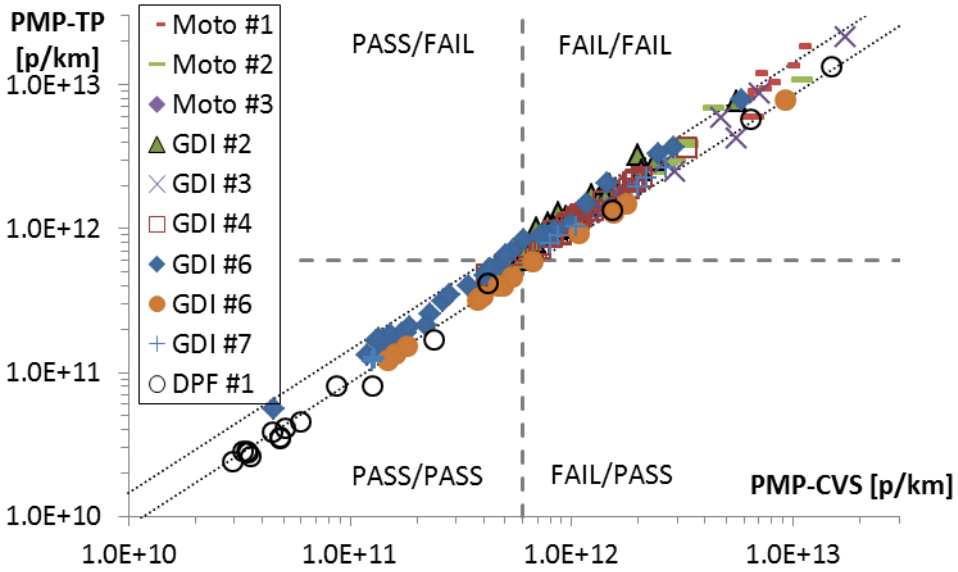

Figure 3-8: PASS/FAIL overview.

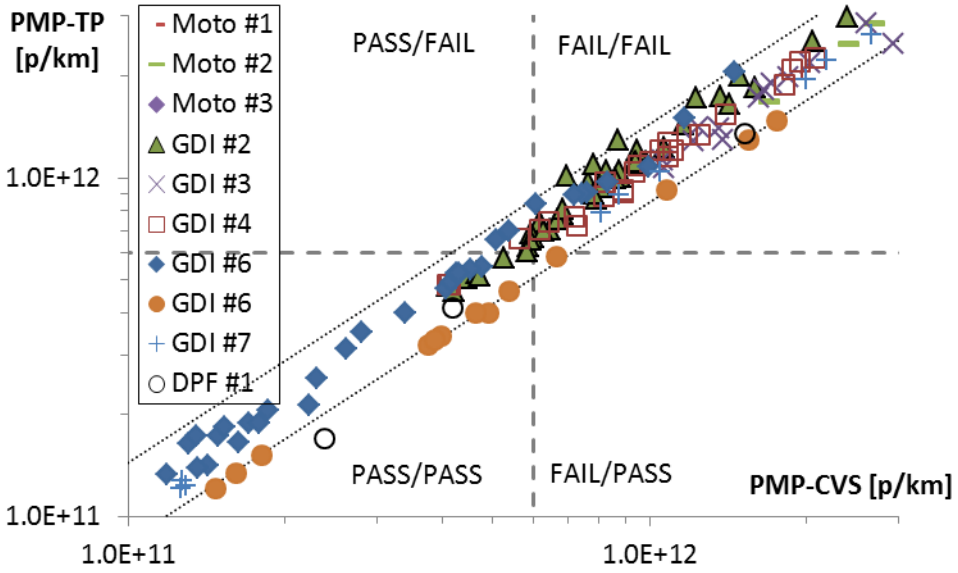

Figure 3-9: Detail of previous figure.

3.5 *Size dependency*

The differences of the two PMP systems were also plotted in function of the mean size (GMD) of each sub-cycle tested in Vela 2 (Figure 3-10). There is no size dependency or if any, it is covered by the scatter of the differences of the two systems.

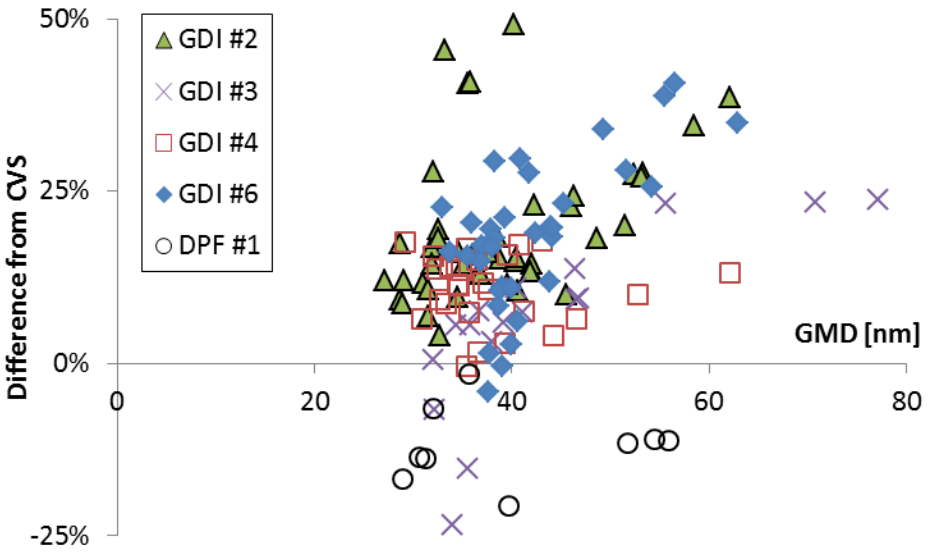

Figure 3-10: Differences of PMP systems in function of mean size of each sub-cycle (Vela 2).

3.6 Summary PMP

The differences between the PMP-TP and the PMP-CVS are summarized in Figure 3-11 (VELA 1) and Figure 3-12 (VELA 2).

In VELA 1 (Figure 3-11) no differences were observed. Generally the two PMP systems were within 20% when measuring at the same location (green points). This difference seems rather high but it has to do with the nature of the exhaust of motorcycles. There are many particles <23 nm, thus small differences in the cut-off size (=$d_{50\%}$ in this report) of the CPCs can have a big effect.

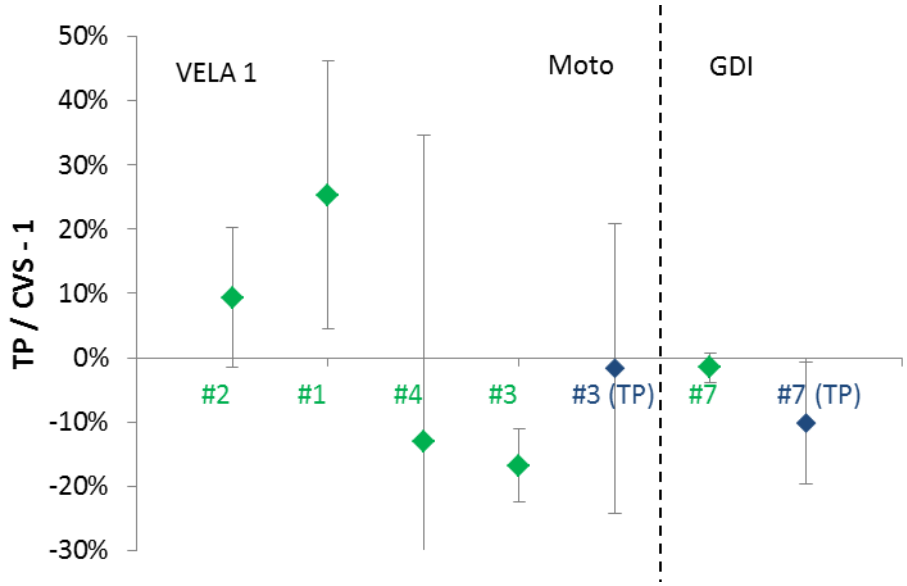

Figure 3-11: Comparison of PMP-CVS (VELA 1) with PMP-TP connected to the tailpipe (TP) or dilution tunnel (no brackets) for different vehicles.

For VELA 2 (Figure 3-12, green points), when both systems were connected at the dilution tunnel the PMP-TP system was underestimating the emissions approximately 15% in agreement with the calibration results (Figure 3-1). When the PMP-TP was connected to the tailpipe, it was overestimating the emissions 10-20% (Figure 3-12, blue points). This was attributed to the exhaust flow estimation, time alignment uncertainties, thermophoretic losses and coagulation until the CVS (Giechaskiel et al. 2010). A more detailed analysis can be found in Annex B. As the CO_2 results show, parts of the differences can be attributed to the exhaust flow rate uncertainty (tests with similar trends, see e.g. blue points for GDI #3 and DPF #1), but since the CO_2 tests with the PMP-TP system at the CVS were similar with the rest (see e.g. GDI #6 at the CVS and TP), the 20% difference has to do with uncertainties due to particle losses. In the following analysis the PN-PEMS will be compared to both the PMP-CVS and PMP-TP systems. In addition any comparison of the PN-PEMS with the PMP-CVS will be judged based on the differences of PMP-TP to the PMP-CVS for the same tests.

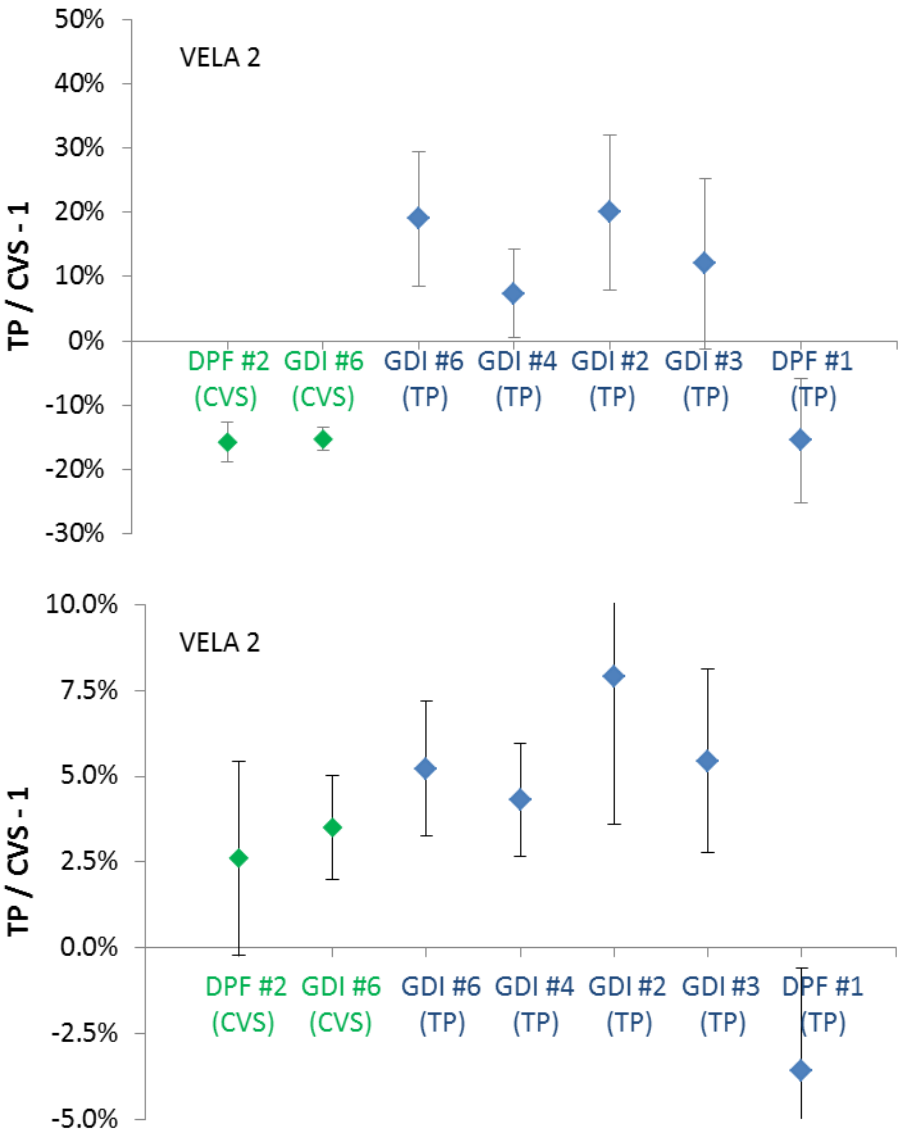

Figure 3-12: Top: Comparison of PMP-CVS (VELA 2) with PMP-TP connected to the tailpipe (TP) or dilution tunnel (CVS) for different vehicles. Bottom: The same tests comparing the real time CO_2 emissions from the tailpipe and dilution tunnel.

4 EEPS

An Engine Exhaust Particle Sizer (EEPS, TSI 3090) was used to measure size distribution in real time. It was always connected to the CVS via a catalytic stripper (CS) in order to remove volatile particles. Extra dilution (typically between 5-10) was conducted at the exit of the CS in order to reach the flow required by the EEPS.

To better understand the results of the EEPS, its size distributions were compared with a Scanning Mobility Particle Sizer (SMPS) using lab aerosol. The total concentration that was given by the EEPS (>23 nm) was also compared with the concentration given by the PMP system at the CVS. Finally the EEPS was evaluated as an 'advanced' DC-based PN-PEMS.

4.1 Monodisperse calibration

The EEPS was calibrated as a DC. Because the EEPS was always used in combination with a CS, the whole system was calibrated. The results for monodisperse aerosol can be seen in Figure 4-1 (total current of the device) and Figure 4-2 (PN as estimated by EEPS). The tests were conducted in the lab using soot particles from propane diffusion flame or graphite particles from spark discharge. For some tests a neutralizer was used downstream of the DMA. The normalized efficiencies using the total current fulfil the original PN-PEMS efficiency requirements (Table 4-1).

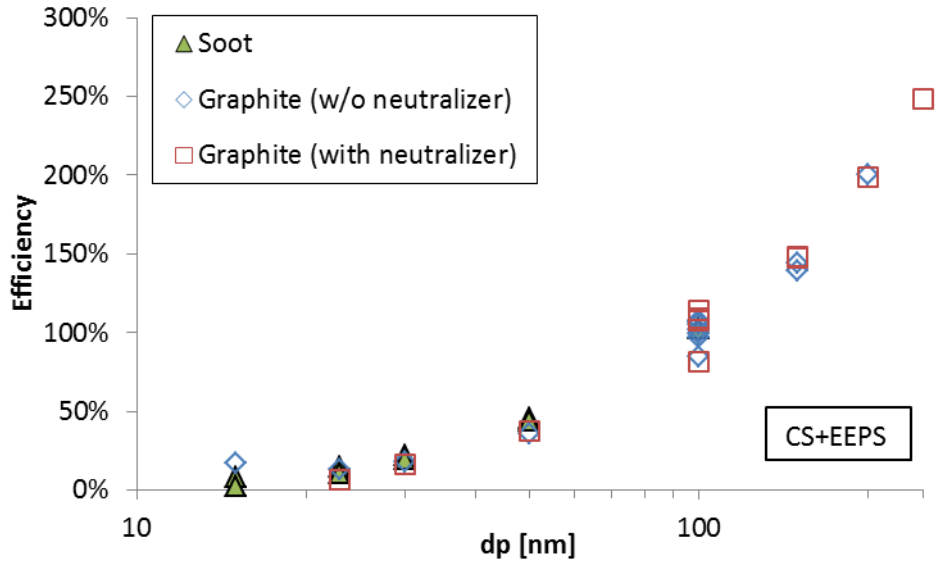

Figure 4-1: Normalized efficiency to 100 nm of total current (factors for graphite x5.5, for soot x 7).

Table 4-1: Normalized efficiencies of CS+EEPS

dp [nm]	23 nm	50 nm	100 nm	200 nm
$E_{Current}$	0.10	0.37	1.00	2.00
$E_{PN(original)}$	0.52	0.86	1.00	-
$E_{PN(fractal)}$	0.61	1.00	1.00	-

The efficiencies using the estimated PN from EEPS at big sizes are off, especially for the graphite (Figure 4-2b). The error is >100% at sizes >100 nm. Using the 'fractal matrix' (soot matrix called in the software of EEPS) the agreement is better, especially for soot. The graphite particles are still overestimated. Probably they acquire more charge due to their smaller primary size. It can be seen that for soot there is a 50% overestimation of the PN at big sizes. At smaller sizes the losses in the CS result in efficiencies smaller than 100%. The normalized efficiencies are given in Table 4-1. A correction factor of 1.5 was needed to normalize them to 100 nm.

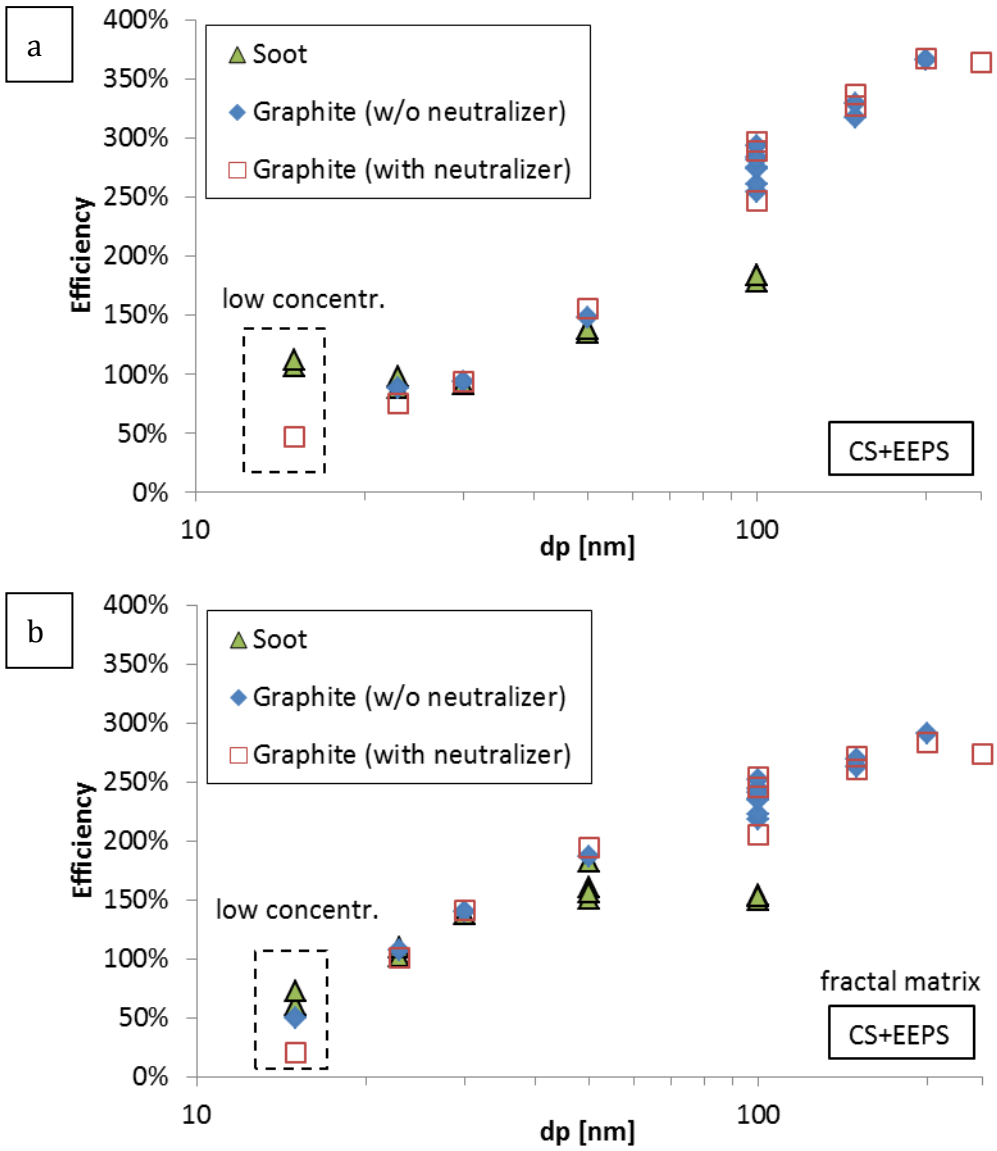

Figure 4-2: Efficiency of PN (estimated by EEPS) a) original matrix b) fractal matrix.

The size estimation can be seen in Figure 4-3. The set monodisperse diameter set at the DMA is plotted versus the EEPS GMD. Note that monodisperse particles will spread over 5 channels and will appear as polydisperse size distribution. The agreement of the set monodisperse size and the measured EEPS GMD is relatively good until 50 nm but

completely off at big sizes. The second panel plots the GMD as estimated by using the fractal matrix. There is a small improvement but the differences remain big at big sizes.

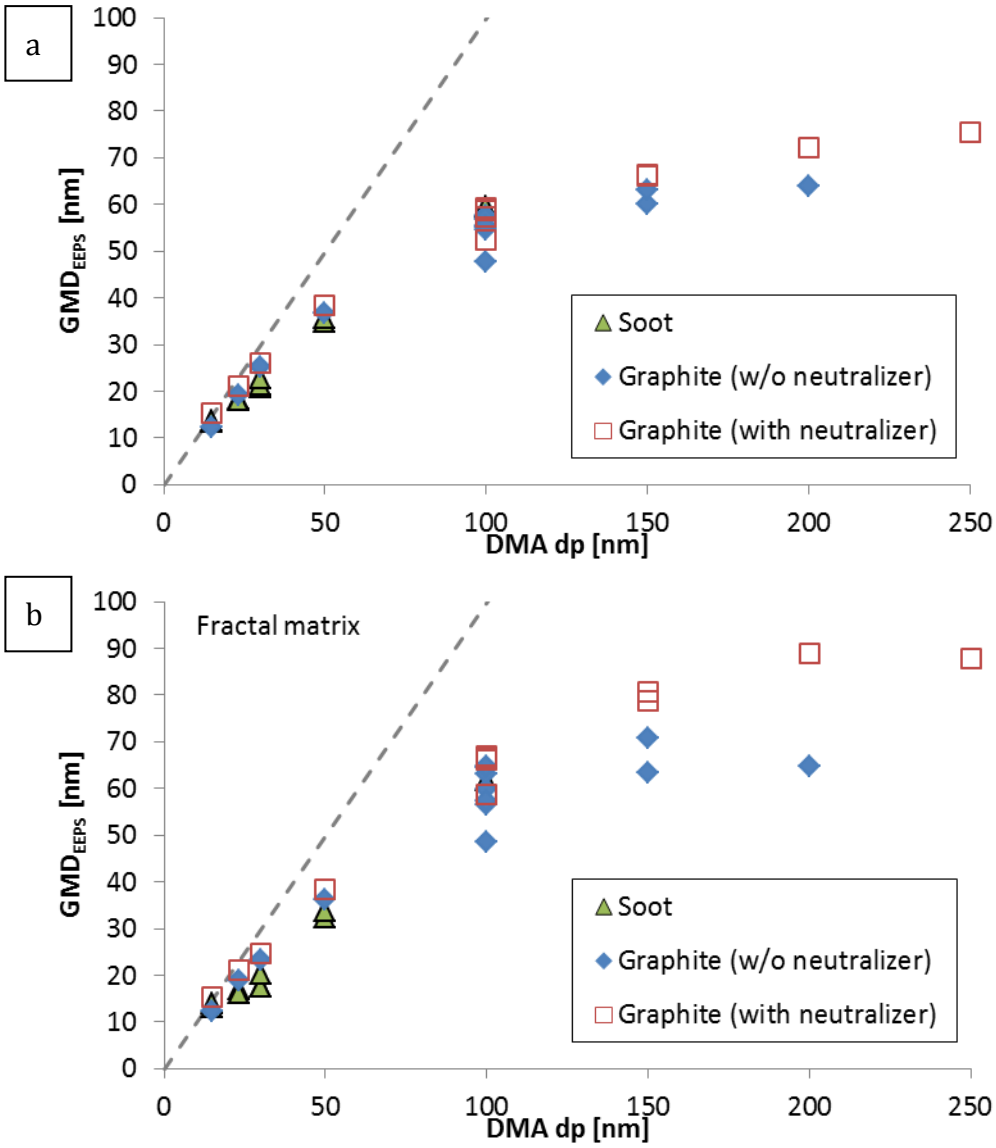

Figure 4-3: Estimated size from EEPS vs DMA set diameter a) original matrix b) fractal matrix.

4.2 Polydisperse comparisons

At a next step the EEPS was compared with an SMPS when measuring polydisperse aerosol (Figure 4-4). The geometric standard deviation (GSD) was 1.72±0.1. For soot particles the agreement is quite good for GMDs between 30 and 70 nm. At bigger sizes the difference remains <50%. It becomes better using the fractal matrix. For graphite particles the agreement is quite good only for sizes between 40 and 50 nm. The difference becomes >50% for sizes bigger than 60 nm. Using the fractal matrix the size effect becomes smaller.

The overestimation of the emissions of the EEPS should be also noted. It becomes more pronounced using the fractal matrix.

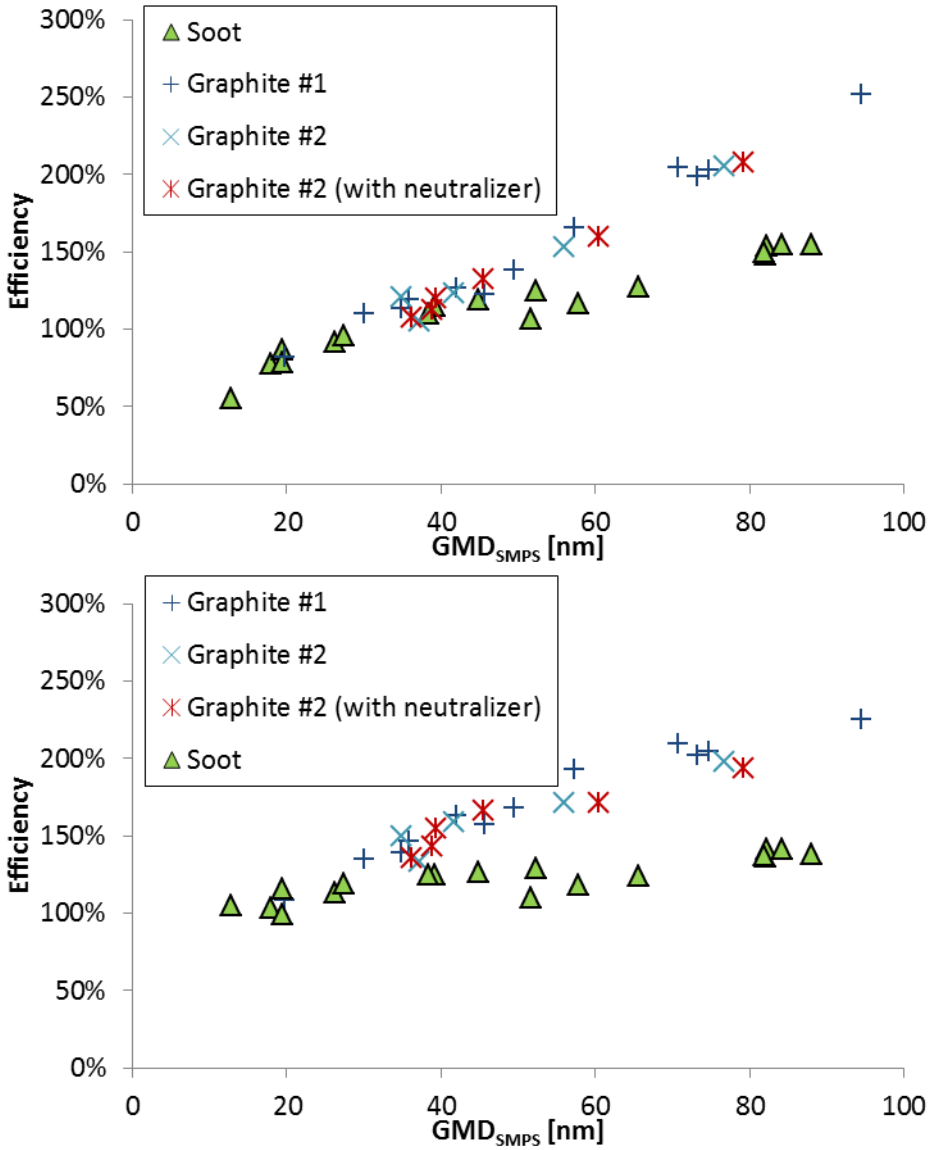

Figure 4-4: Comparison of EEPS with SMPS measuring polydisperse aerosol a) original matrix b) fractal matrix.

The comparison of the GMDs from the EEPS and the SMPS are compared in Figure 4-5. EEPS is underestimating the GMD for particles >45 nm and this underestimation becomes bigger with increasing size. Thus any diameter plotted in this report, which was based on the EEPS, is underestimating the true GMD. In addition any size dependency reported for the DCs is in reality smaller.

Using the fractal matrix the results become much better. Especially for soot particles the agreement is quite good even for bigger sizes.

To convert the GMD_{EEPS} to the GMD_{SMPS} the factors plotted in Figure 4-6 can be used. It can be assumed that the 'Soot' curve is the closest to the engine exhaust particles.

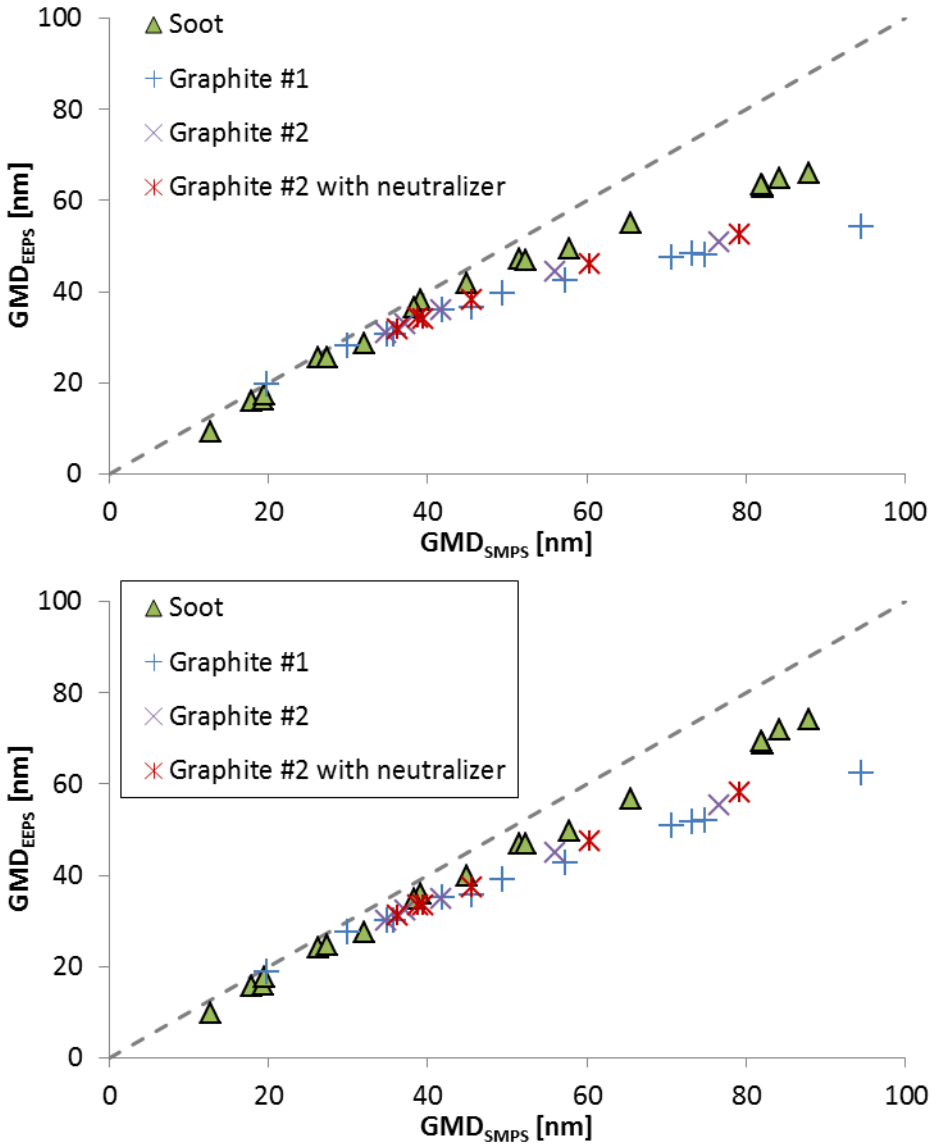

Figure 4-5: Comparison of SMPS with EEPS Geometric Mean Diameters (GMD)

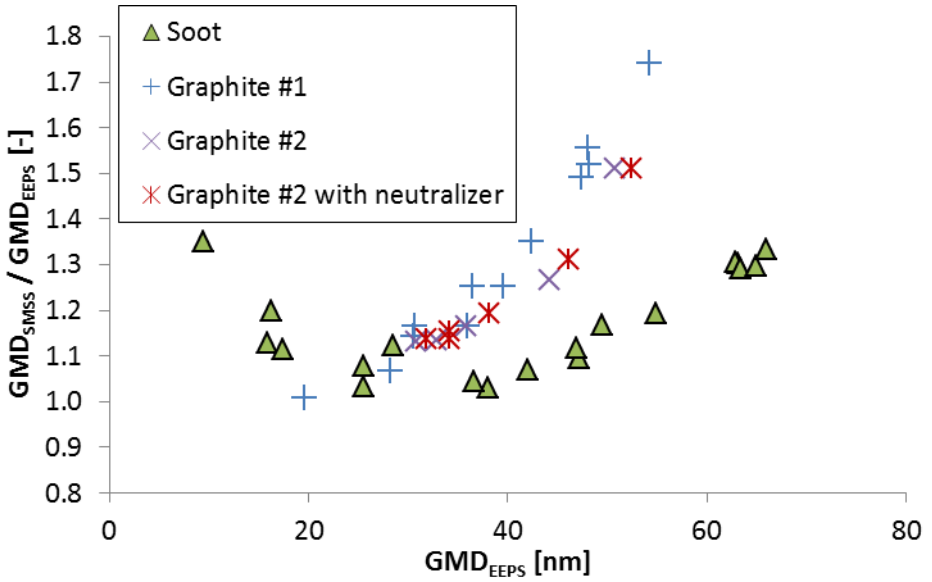

Figure 4-6: Relative difference between SMPS and EEPS GMDs.

4.3 Vehicle results

A real time plot can be seen in Figure 4-7. The agreement is quite good with small differences at the cold start.

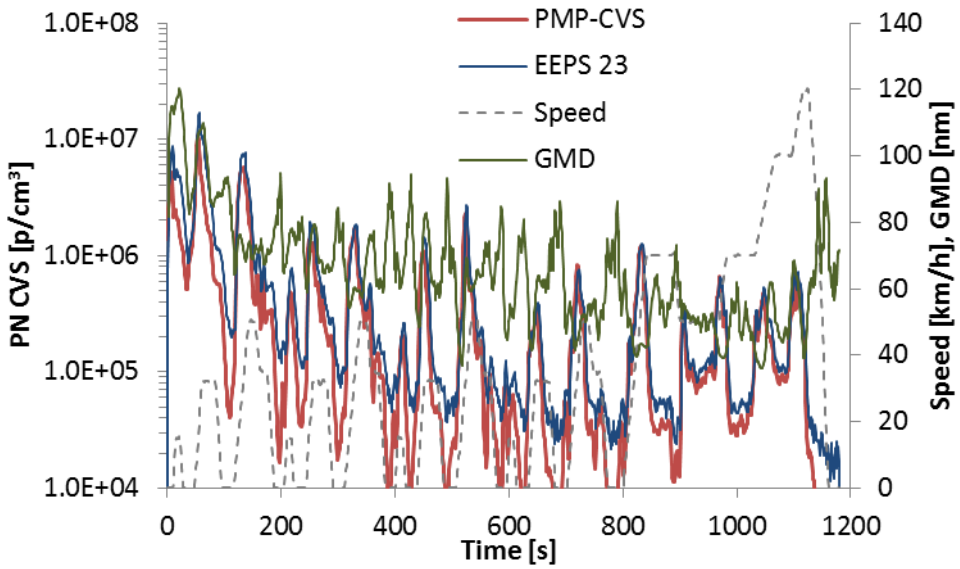

Figure 4-7: Real time signals (20141107-NEDC, GDI #3)

The summary of the comparisons of the EEPS >23 nm with the PMP-CVS can be seen in Figure 4-8 for the GDIs and the DPF and in Figure 4-9 for the motorcycles and the PFIs. Typically the EEPS was overestimating the PN concentration by 20-40% and the standard deviation of the differences was 15%. The good agreement of the EEPS with the PMP-CVS has to do with the GMDs of the vehicles tested: they were around 20-50 nm (average of a test cycle measured with EEPS). Using a 'PMP' size dependent penetration for the EEPS would further improve the results (approximately 5%). This could be done e.g. by the manufacturer in the future when PMP like measurements are done. However, using the fractal matrix would probably increase the difference as it was noted previously.

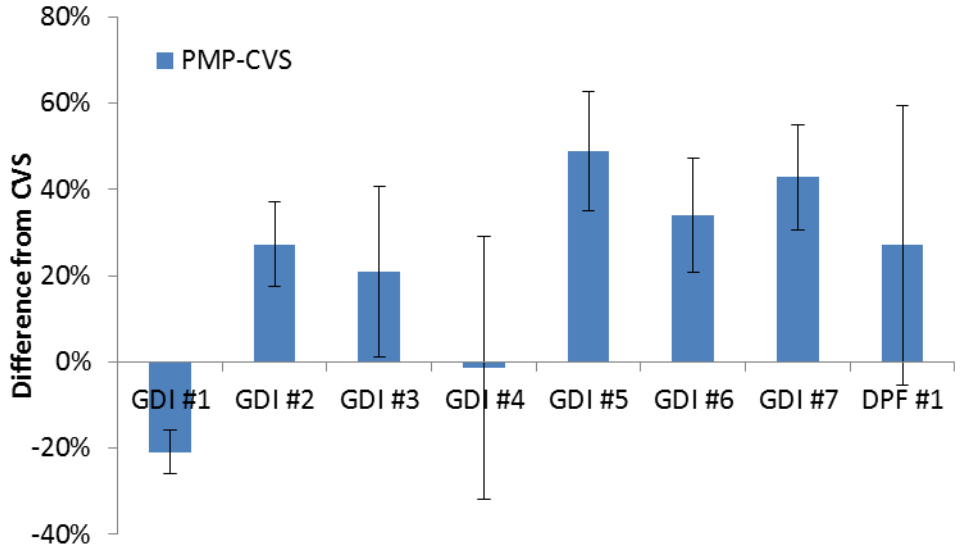

Figure 4-8: Difference of PN concentration by EEPS (>23 nm) from the PMP-CVS system.

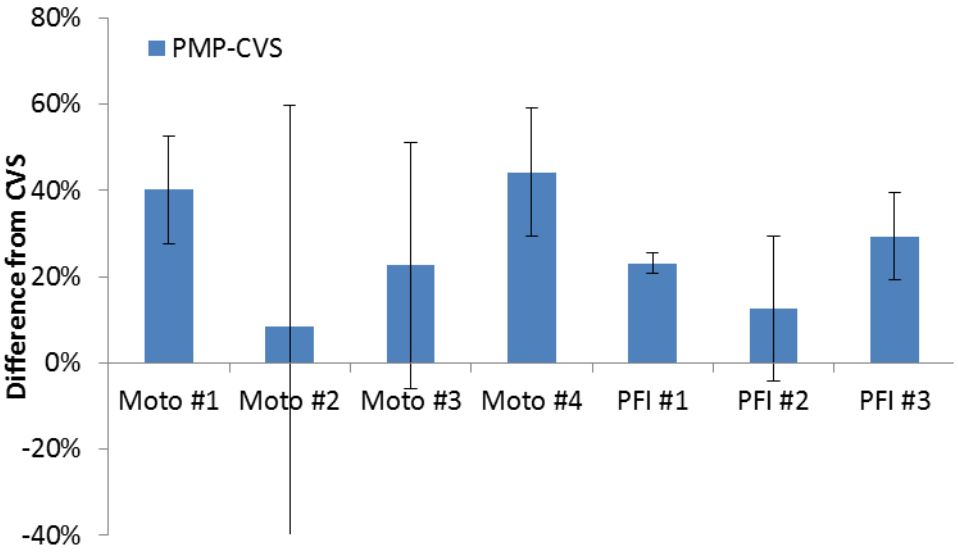

Figure 4-9: Difference of EEPS (>23 nm) from the PMP-CVS system.

Note that if the calibration procedures recommended in Phase I were followed a correction of 1.5 would be needed at the results and thus the EEPs results would be 10-30% lower than the reference systems.

All results in this report were with the original matrix of the EEPS and are presented without any corrections, unless otherwise specified.

The key message from this chapter is that a very 'advanced' DC based system gave results within 20% and 40% with standard deviation of differences of around 15%. Applying the calibration procedures, the differences would be -30% to -10%. These values give an indication of the maximum expectations for advanced DC based systems.

5 PN-PEMS #1'

5.1 Description

PN-PEMS #1' (AVL) consists of a VPR and a DC (modified particle detector, Partector, from Naneos). The VPR is connected to the tailpipe with a short (0.7 m) heated line at 150°C. The VPR consists of a two stage dilution with an evaporation tube and a catalytic stripper in between (both set at 300°C). The primary dilution is 2:1, and the secondary 5:1. For the upstream dilution the dilution air is heated at 150°C. The downstream dilution is performed with dilution air at 60°C, to minimize nucleation potential. The diluted sample is transferred to the DC in a 0.8 m heated line at 60°C. The VPR and the DC were calibrated separately by the manufacturer. The DC (Fierz et al. 2014) gives Lung Deposited Surface Area (*LDSA*) in $\mu m^2/cm^3$. A constant factor *C* of 300 was used to convert the LDSA to particle number (reading). This value, which was given by the manufacturer, was based on comparisons of the device with a PMP system for different vehicles, thus it should also account for the particle losses in the system. Thus the reading *R* of the instrument was:

$$R_{PN-PEMS} = C\ LDSA$$

5.2 Calibration

The PN-PEMS was calibrated at the end of the measurement campaign with monodisperse spark discharge graphite particles. For details see Giechaskiel et al. (2014). The results can be seen in Figure 5-1.

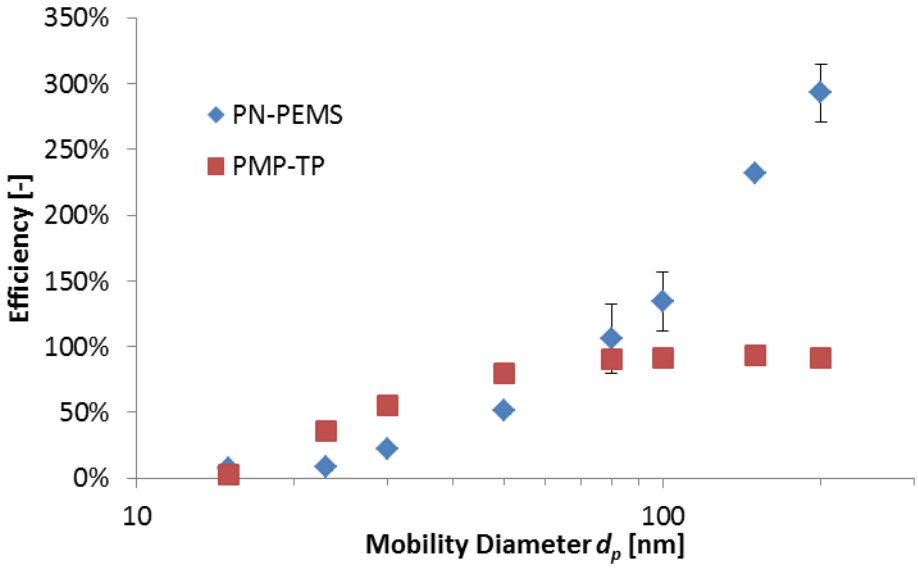

Figure 5-1: Efficiency of PN-PEMS with monodisperse spark-discharge graphite.

The ratios of the efficiencies with monodisperse aerosol were compared with the older units (Table 5-1). PN-PEMS #1 was the prototype of Phase 1, PN-PEMS #1b was the

prototype of Phase II and PN-PEMS #1' was the actual unit tested in Phase II. The results are quite similar and fulfil the draft requirements. The calibration factor of the manufacturer corresponds to approximately 75-80 nm monodisperse normalization which was acceptable, and thus was not adjusted (Figure 5-1).

It should be noted that applying the suggested calibration procedure (normalization at 100 nm and then applying an extra factor to optimize the 70 nm monodisperse size or a polydisperse distribution of 55 nm) would give very similar value with the one with the manufacturer (10% higher), thus the results with the correction factor will not be presented separately.

Table 5-1: Ratios of efficiencies of PN-PEMS. Units #1 and #1b were evaluated in Giechaskiel et al. (2014).

d_p [nm]	23	30	50	80	100	200
#1	0.07	0.15	0.40	0.77	1.00	2.24
#1b	0.17	0.24	0.47	0.79	1.00	2.11
#1'	0.06	0.17	0.38	0.79	1.00	2.17

Then the PN-PEMS was compared with the PMP system measuring polydisperse spark discharge graphite particles (Figure 5-2). One of the systems was the PMP-TP system, the other was the SMPS applying a theoretical counting efficiency of a PMP system (see Giechaskiel et al. 2014). The differences range from -40% to +100% for GMDs ranging from 30 to 105 nm. The difference to the PMP system is minimized at approximately 60 nm. In this size range differences among vehicles should be expected. The biggest contribution is the size dependency of the PN-PEMS; however differences between PMP systems can also contribute up to 20%. In the specific graph the reason of the big deviation between the PMP and SMPS 23 nm could be that the CPC that was used downstream of the SMPS was overestimating the emissions (the 3025A), or the PMP-TP was underestimating the emissions. By correcting the PMP with a factor that gives counting efficiency 100% at 100 nm (see Figure 5-1) the differences become very small.

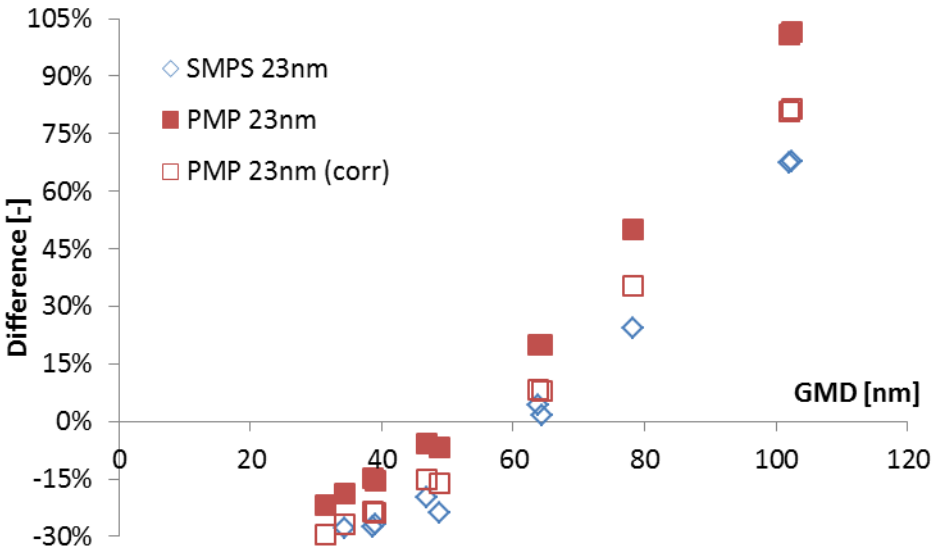

Figure 5-2: PN-PEMS and PMP systems comparisons with polydisperse aerosol.

5.3 Real time

Initially the PN-PEMS was connected to the CVS and was compared with the PMP-CVS system (Figure 5-3). The PN-PEMS follows the PMP-CVS system closely especially when the mean size is around 50 nm. At higher sizes the emissions are overestimated (after time 800 s, difference in response compared to PMP). In the real time figures the GMD is a moving average of 5 s.

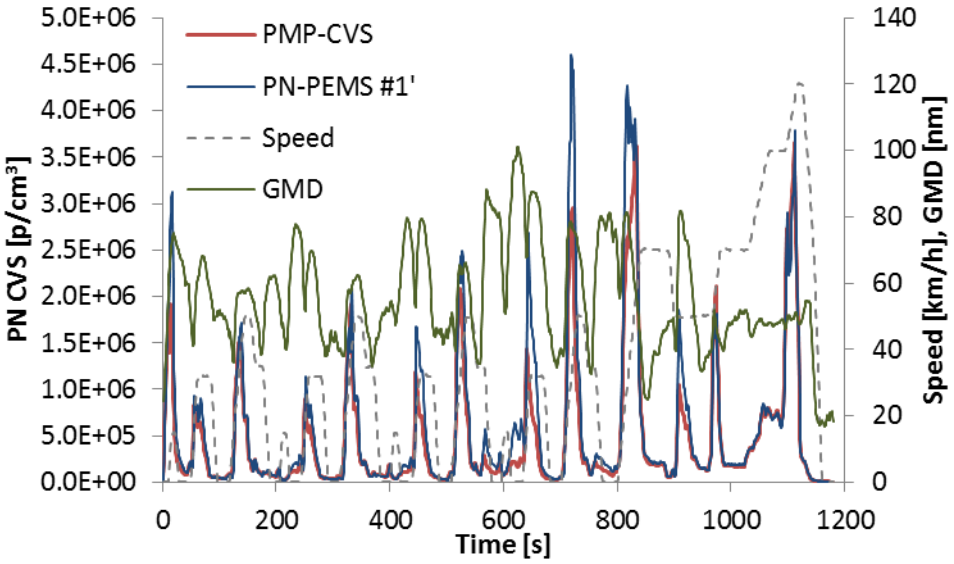

Figure 5-3: Comparison of PN-PEMS with PMP-CVS, both connected to the dilution tunnel (20141119-NEDC cold, GDI #5).

Similar behaviour was shown when the PN-PEMS was connected to the tailpipe (Figure 5-4) and with other GDIs (Figure 5-5):

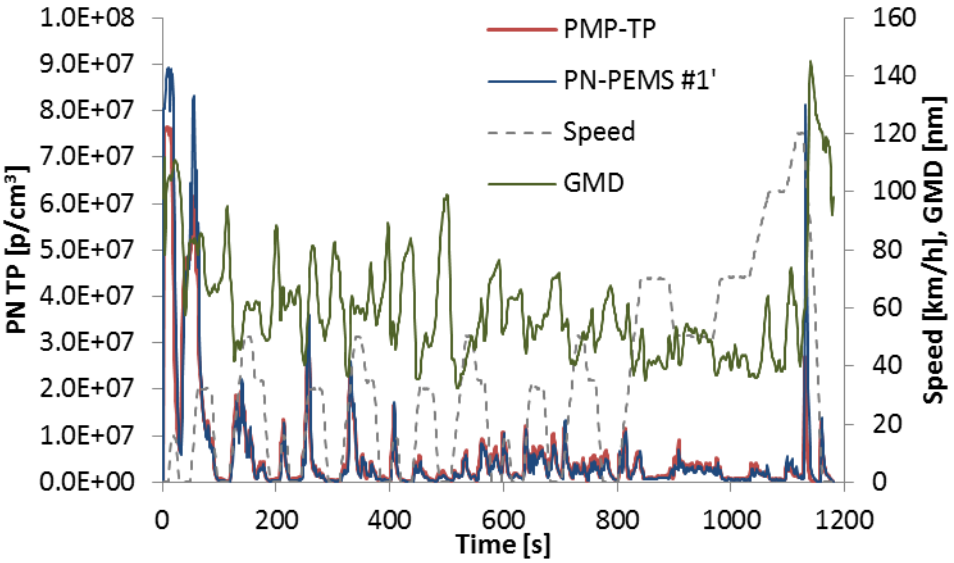

Figure 5-4: Comparison of PN-PEMS with PMP-TP, both connected to the tailpipe (20141106-01-NEDC cold, GDI #3).

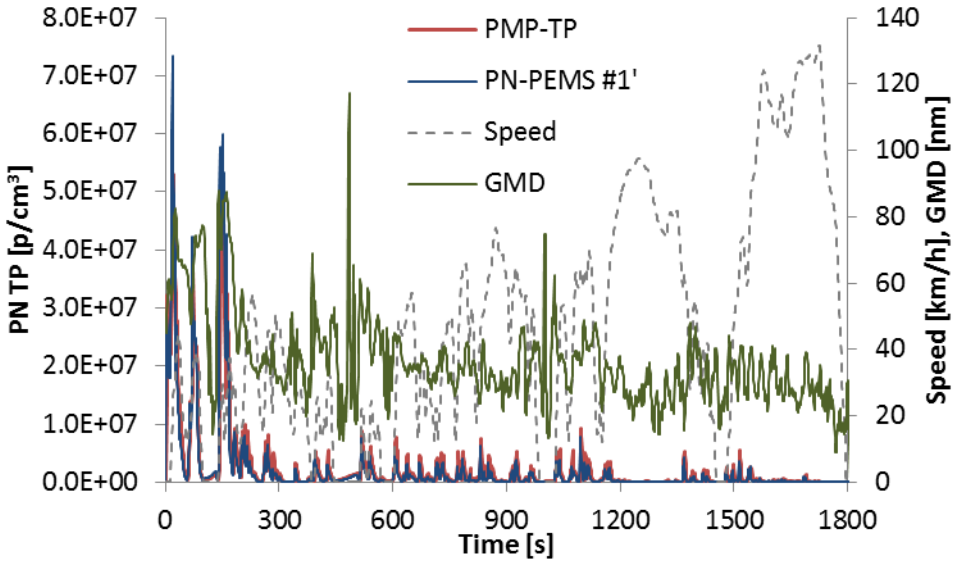

Figure 5-5: Comparison of PN-PEMS with PMP-TP, both connected to the tailpipe (20141203-01-WLTC, GDI #6).

5.4 Comparison to PMP-CVS

Figure 5-6 summarizes the results when the PN-PEMS was connected to the CVS. The differences are approximately from -25% to +40% for emissions spanning from less than 10^11 p/km to higher than 10^13 p/km.

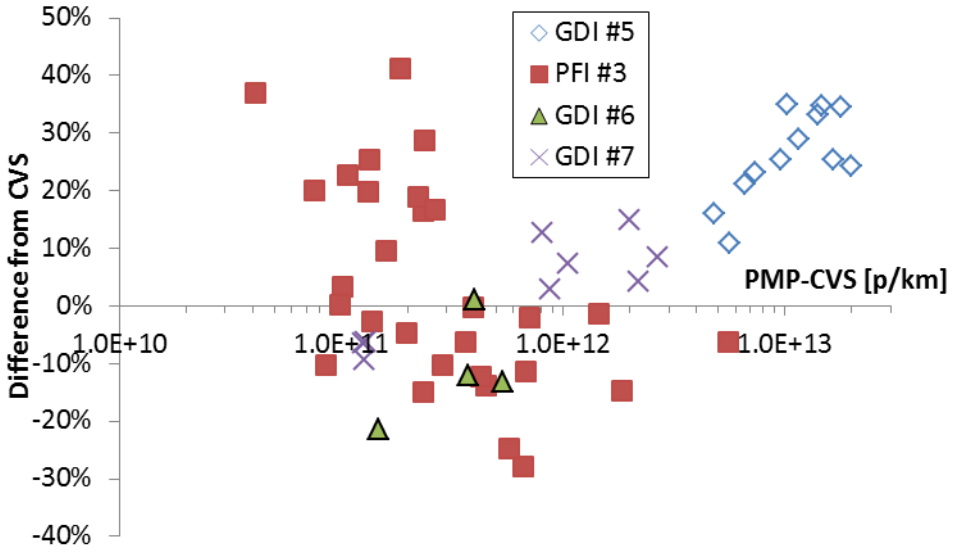

Figure 5-6: Comparison of PN-PEMS with PMP-CVS for different vehicles. The PN-PEMS was connected to the CVS.

Then the PN-PEMS was connected to the tailpipe for different vehicles. The comparison with the PMP system at the CVS (PMP-CVS) can be seen in Figure 5-7. The differences range approximately from -50% to +50% for different emission levels.

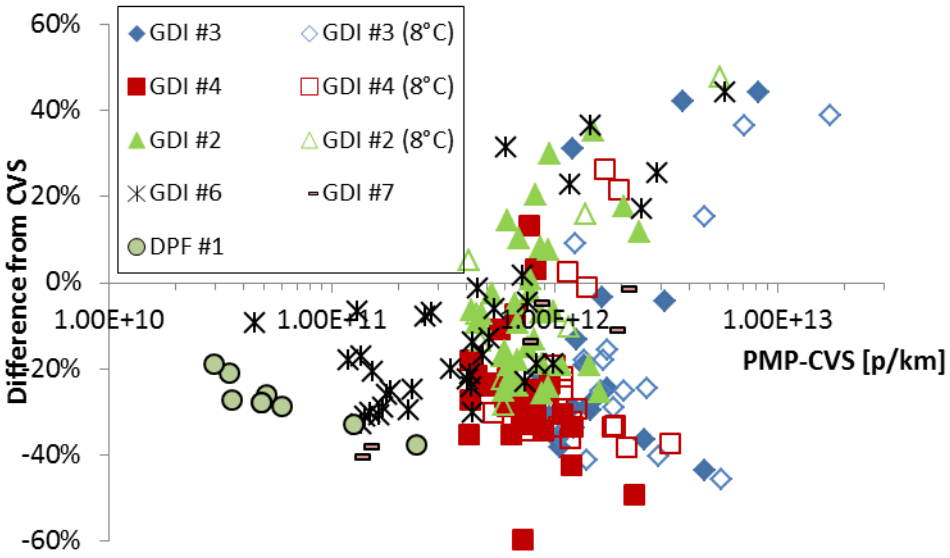

Figure 5-7: Comparison of PN-PEMS with PMP-CVS for different vehicles. The PN-PEMS was connected to the tailpipe.

5.5 Comparison to PMP-TP

The difference of the PN-PEMS from the PMP at the tailpipe (PMP-TP) can be seen in the Figure 5-8. The differences range from -45% up to +10%.

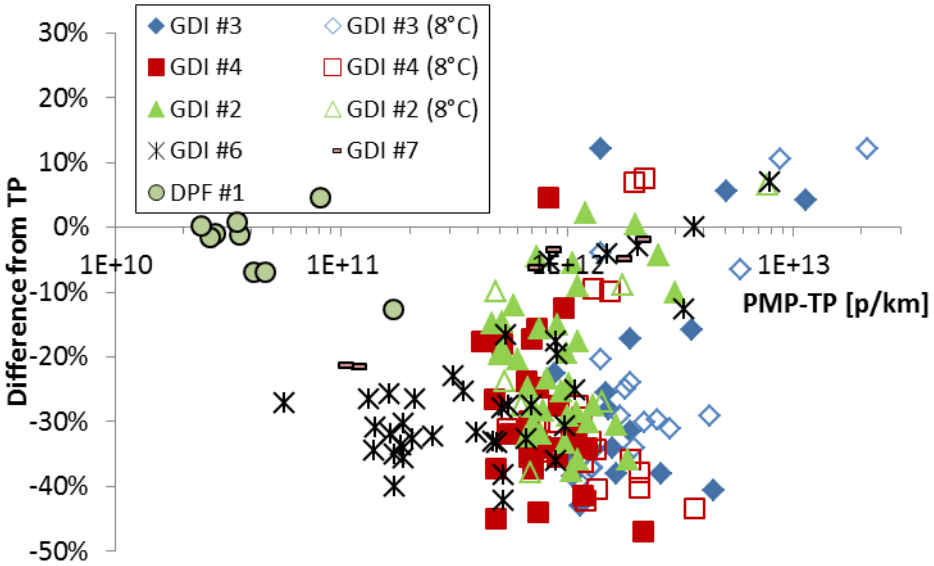

Figure 5-8: Comparison of PN-PEMS with PMP-TP for different vehicles. The PN-PEMS was connected to the tailpipe.

5.6 Particle size effect

The size dependency of the PN-PEMS response can be seen in Figure 5-9. The effect is <20% for a 10nm change of the particle size. Similar trend was observed comparing the

PN-PEMS with the PMP-TP (Figure 5-10). In these figures the GMD is average of the cycle.

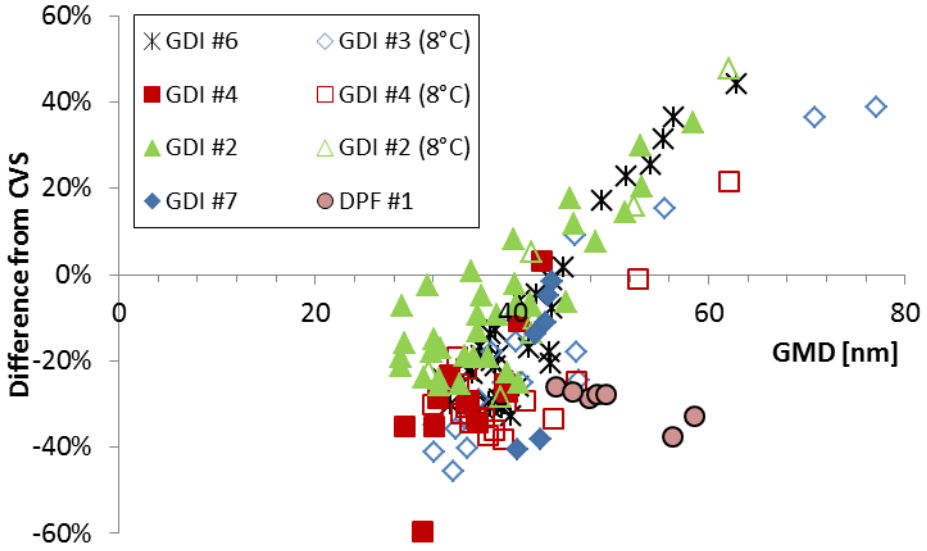

Figure 5-9: Particle size dependency of PN-PEMS. PN-PEMS was sampling from the tailpipe.

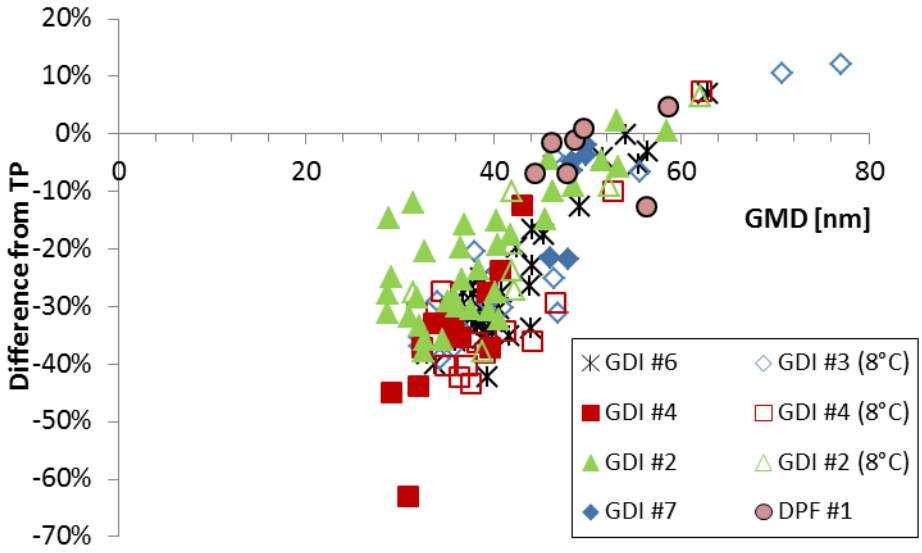

Figure 5-10: Particle size dependency of PN-PEMS. PN-PEMS was sampling from the tailpipe.

Combining the data of the PN-PEMS at tailpipe and CVS the trend is confirmed (Figure 5-11).

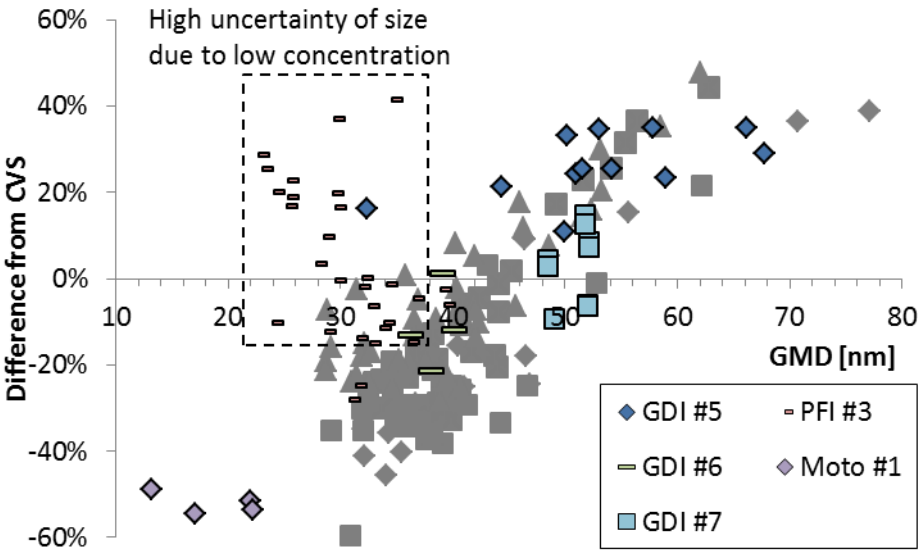

Figure 5-11: Summary of particle size dependency on PN-PEMS. Coloured symbols when PN-PEMS was connected at the dilution tunnel; grey refer to the tailpipe.

5.7 Ambient temperature

No effect of the ambient temperature down to 8°C was observed (Figure 5-12). The behaviour was the same as during the 23°C tests.

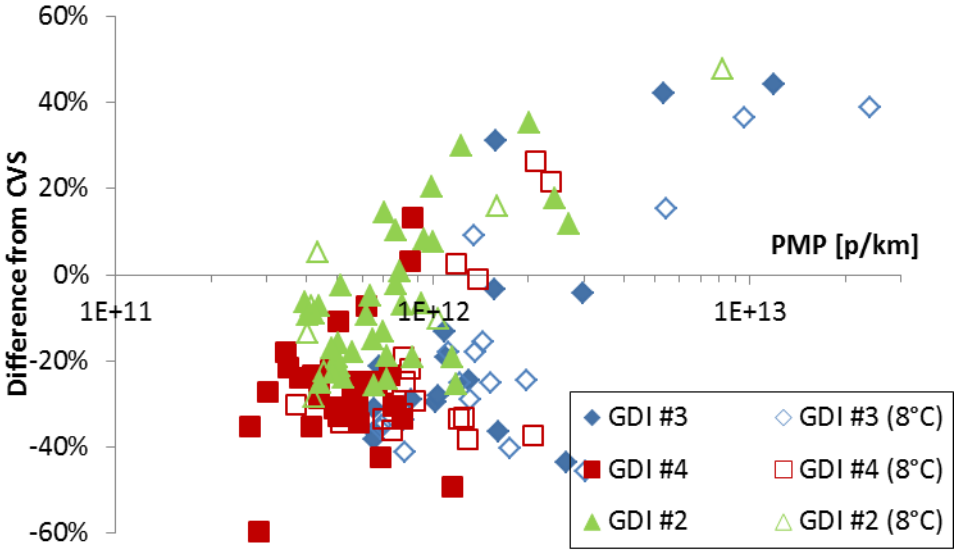

Figure 5-12: Ambient temperature effect on PN-PEMS.

5.8 Challenge aerosol (motorcycles)

The PN-PEMS was used also to measure exhaust aerosol of motorcycles. Moto #3 is a 4-stroke 50 cm^3 moped with max speed around 30 km/h (modified). Moto #4 is a 4-stroke 125 cm^3 motorcycle with max speed around 90 km/h. The specific motorcycles were producing particles with mean diameter smaller than 20 nm. Thus the PN-PEMS could overestimate the emissions (because it doesn't have counting efficiency 0 at small

sizes) or underestimate the emissions (because the response function decreases with size). Thus the differences could be large and in any direction. Nevertheless, the comparison of PN-PEMS with the PMP-TP gave differences of approximately -40% to +20% with a few exceptions (Figure 5-13).

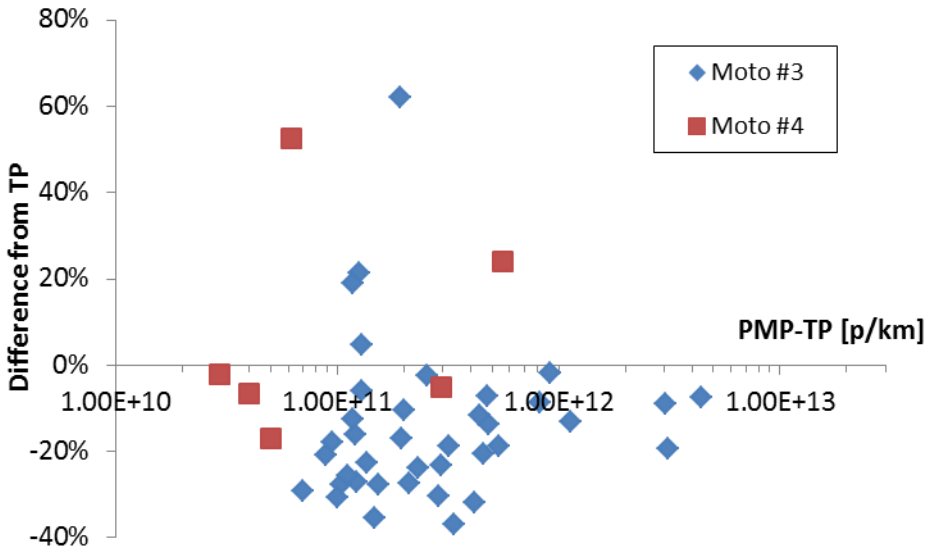

Figure 5-13: Behaviour of PN-PEMS with motorcycles aerosol.

The results were also plotted as a function of particle size (Figure 5-14). No clear size dependency could be observed at sub-30 nm sizes.

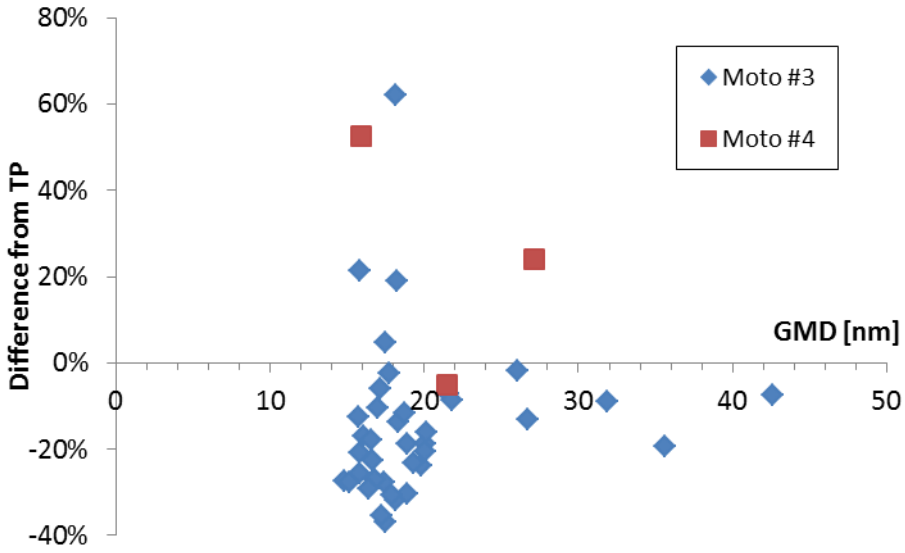

Figure 5-14: Behaviour of PN-PEMS with motorcycles aerosol.

5.9 Volatile removal efficiency

The volatile removal efficiency of the PN-PEMS was evaluated by measuring diluted aerosol from a 2-stroke 50 cm^3 moped (Moto #1) from the CVS. The size distribution at the CVS has a mean size around 90 nm. After thermal pre-treatment the mean size decreases to <20 nm. The results (with the previous motorcycles) are shown in Figure 5-15. The PN-PEMS measures 50% less than the PMP-CVS indicating that the size of the particles was efficiently decreased and there was no re-nucleation that could influence the results. The underestimation has to do with the small size of particles.

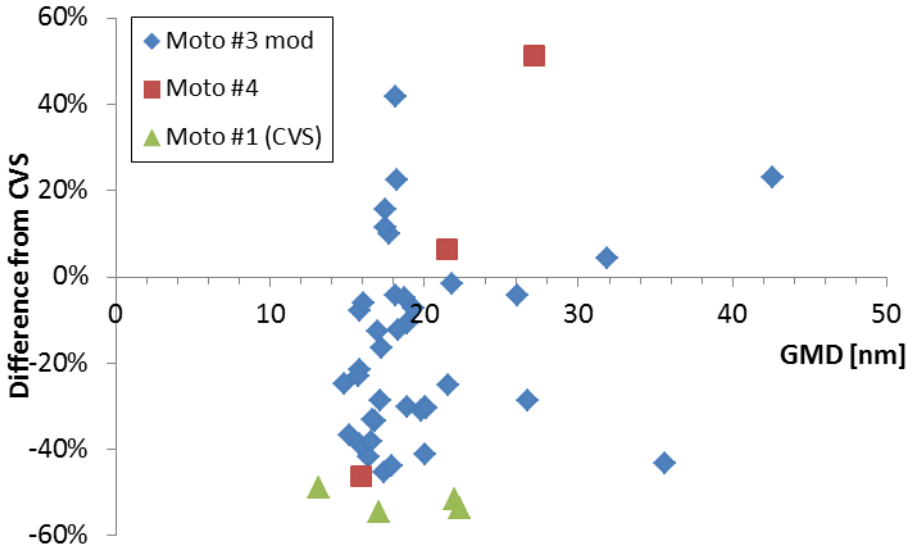

Figure 5-15: Behaviour of PN-PEMS with motorcycles aerosol.

5.10 DPF Regeneration

The PN-PEMS was connected to the tailpipe of a diesel vehicle equipped with a DPF (#1), in parallel with the PMP-TP system. An EEPS was measuring from the dilution tunnel. Figure 5-16 compares all systems, after correction with the dilution factor at the dilution tunnel. EEPS was measuring >10^8 p/cm^3. However, the GMD of the nucleation mode was around 12 nm, so only a small percentage is >23 nm. The two PMP systems were very close to each other. The PN-PEMS was measuring 40% lower than the PMP-TP. During normal cycles (e.g. Artemis or WLTC) the PN-PEMS was measuring similarly with the PMP system at TP for the specific vehicle. This indicates that either the soot particles that were emitted during the regeneration were smaller or that the catalytic stripper of the PN-PEMS oxidizes more efficiently some of the particles emitted during the regeneration that cannot be removed with the PMP protocol. As Figure 5-16 shows, different PCRFs of the PMP system didn't change the concentration indicating that these particles were really non-volatiles and not an artefact.

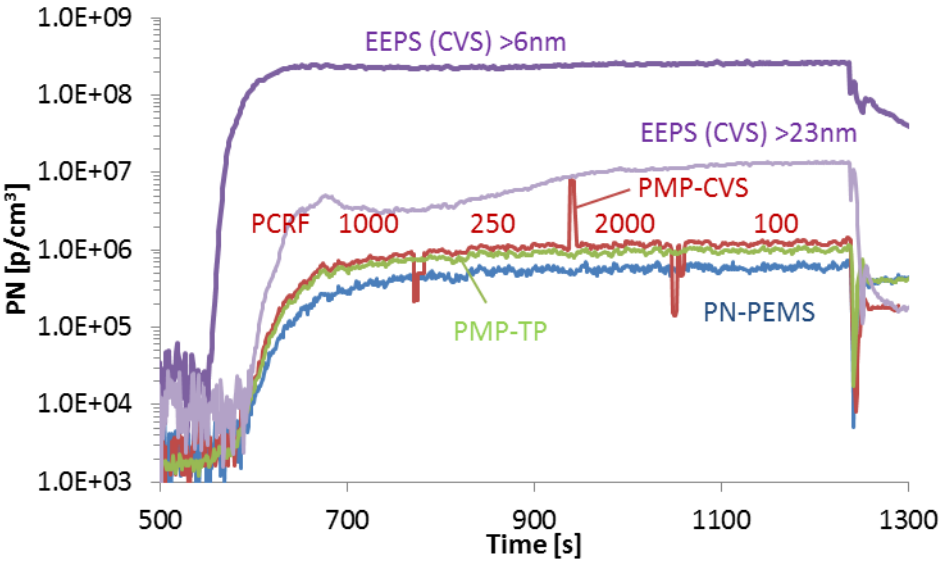

Figure 5-16: Regeneration tests with DPF #1.

5.11 Summary

Figure 5-17 summarizes the differences of the PN-PEMS from the PMP-CVS and PMP-TP for all GDI cases examined. Figure 5-18 examines the rest cases (PFI, DPF and motorcycles). For GDIs, when the PN-PEMS was measuring at the tailpipe, the mean differences are -25% to -5% with a variability (expressed as ±standard deviation) of ±20%. When the PN-PEMS was at the CVS, the differences ranged from +5% to +25%, but the variability was smaller (±10%) and this had to do with the higher mean size of particles from these cars. The DPF equipped vehicle and the motorcycles gave similar results with the PMP system, with the exception of Moto #1 (which was underestimated). Assuming that when the error bars cross the 0% the PN-PEMS is equivalent with the PMP-CVS, in most cases the PN-PEMS measures equivalently with the PMP-CVS.

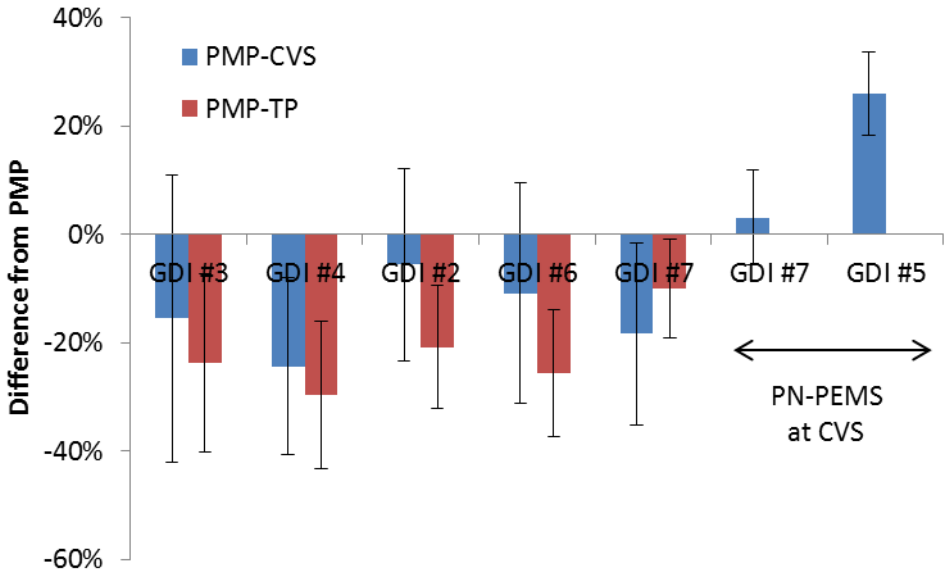

Figure 5-17: Overview of differences of PN-PEMS from the PMP-CVS. Error bars are one standard deviation.

Note that applying the correction factor according to the recommended calibration procedures would give 10% higher results and then they would be very close to the reference systems.

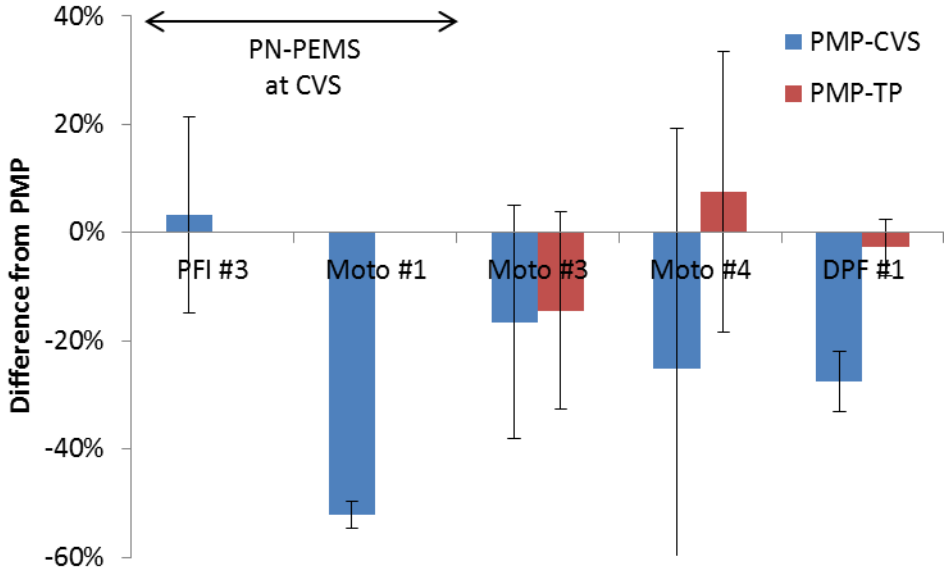

Figure 5-18: Overview of differences of PN-PEMS from the PMP-CVS. Error bars are one standard deviation.

Another way of evaluating the PN-PEMS is by plotting the results of the PN-PEMS vs the PMP-CVS. By setting the limit values one can visualize which tests would give a correct results (i.e. PASS when the PMP would give PASS or FAIL when the PMP system would give FAIL) or wrong (PASS for FAIL or FAIL for PASS). Figure 5-19 gives all results and Figure 5-20 focuses on the 6x10^11 p/km range. There are a few tests where the PN-PEMS gave wrong result (PASS instead of FAIL) and as mentioned previously this had to do with the calibration factor that was used and was underestimating the emissions.

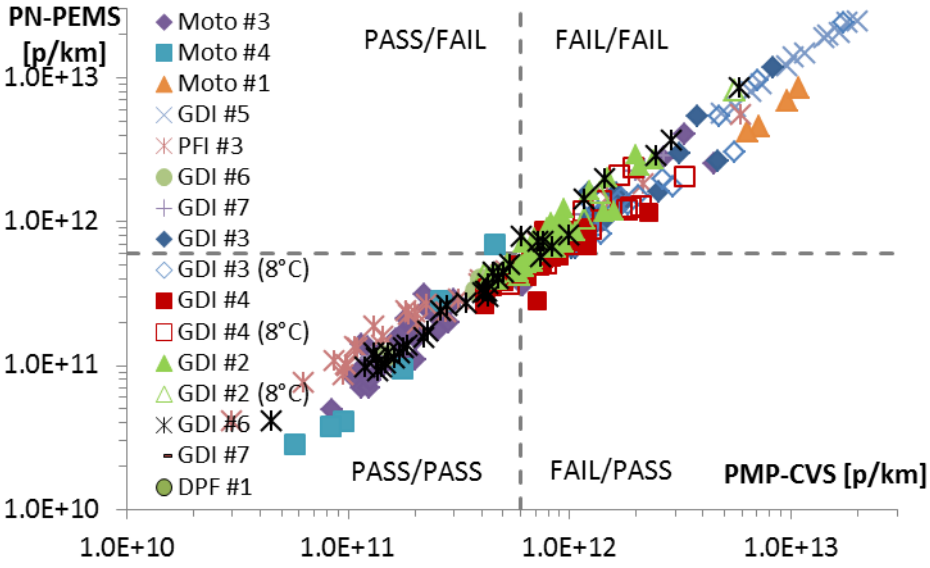

Figure 5-19: Overview of all PASS/FAIL results.

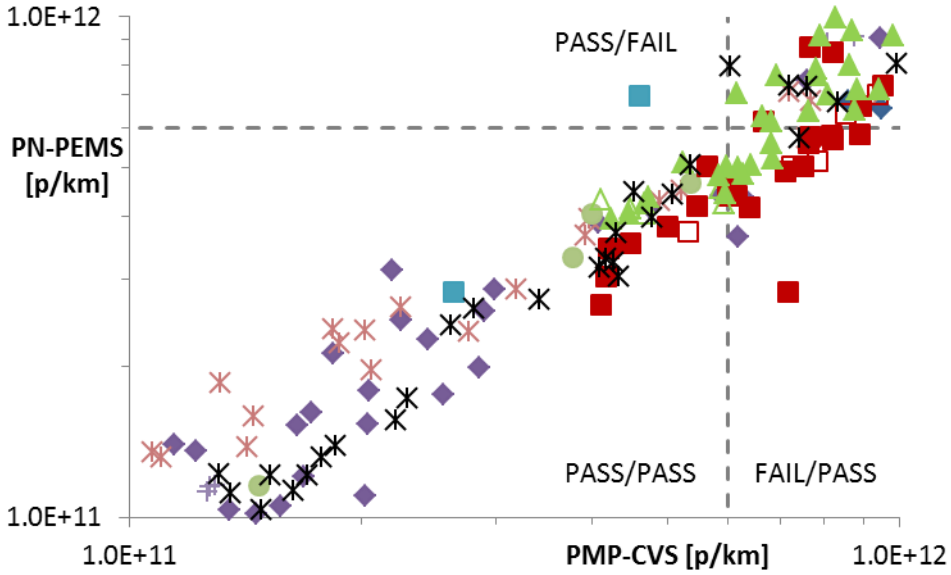

Figure 5-20: Detail of previous Figure.

Table 5-2 shows the PASS/FAIL results of the PMP-TP and the PN-PEMS compared to the PMP-CVS assuming a 6x10^11 p/km limit. The success rate (i.e. catching a FAIL as FAIL or a PASS as PASS) is very high and similar to the PMP-TP.

5.12 Adjustment of PN-PEMS

The PN-PEMS based on DCs have an inherent uncertainty due to their dependency on particles size. Even when calibrated it is possible to have a 'bias' for vehicles that emit particles in a different size range. The topic was investigated by conducting different cycles in one day and comparing the difference of the PN-PEMS to the PMP-CVS.

The results for all sub-cycles (each symbol is a sub-cycle) are presented in Figure 5-21. The specific vehicle emits particles with a high GMD at the beginning of the test. Thus, the PN-PEMS is overestimating the emissions >40% (first part of the WLTC). At the subsequent sub-cycles the PN-PEMS is underestimating around 20%. For the next WLTC in the afternoon a similar behaviour is observed. The next hot WLTC has even smaller effect of the initial start of the cycle. Excluding the 'cold' starts all cycles range from -30% to -15% approximately. The behaviour of the car on the road is expected more similar to the 'hot' sub-cycles. Thus a calibration with a 'hot' cycle would probably improve the 'bias'. However this assumption should be checked with the real behaviour of the car on the road. Note that using the 'cold' WLTC to 'calibrate' the PN-PEMS would give wrong calibration factor (+23% average of the cycle).

The same evaluation was followed for other vehicles. Similar behaviour was observed: The 'hot' emissions were approximately -15% to -30% (GDI #2) (Figure 5-22) or -40% (GDI#4) (Figure 5-23) or -50% (GDI #3) (Figure 5-24). The results are summarized in Figure 5-25. The mean correction factors are approximately -30% to -15%. An interesting observation is that the variability of the correction factor between the vehicles (15%) is not much higher than the variability of the correction of the different 'hot' cycles of the same car (8%).

Table 5-2: PASS/FAIL success rate. In red percentages <90%.

Vehicle	Lab	Category	# of tests	PMP-TP	PN-PEMS
GDI #3	VELA 2	PASS	0	-	-
	VELA 2	FAIL	34	100%	100%
GDI #4	VELA 2	PASS	9	78%	100%
	VELA 2	FAIL	41	100%	67%
GDI #2	VELA 2	PASS	13	62%	100%
	VELA 2	FAIL	31	100%	84%
GDI #6	VELA 2	PASS	26	92%	100%
	VELA 2	FAIL	12	92%	92%
GDI #7	VELA 1	PASS	2	100%	100%
	VELA 1	FAIL	4	100%	100%
GDI #7 (only CVS)	VELA 1	PASS	3	-	100%
	VELA 1	FAIL	6	-	100%
GDI #5 (only CVS)	VELA 2	PASS	0	-	100%
	VELA 2	FAIL	12	-	100%
PFI #3 (only CVS)	VELA 2	PASS	22	-	100%
	VELA 2	FAIL	7	-	86%
Moto #1 (only CVS)	VELA 1	PASS	0	-	-
	VELA 1	FAIL	4	-	100%
Moto #4	VELA 1	PASS	6	100%	83%
	VELA 1	FAIL	0	-	-
Moto #3	VELA 1	PASS	30	100%	100%
	VELA 1	FAIL	8	75%	75%
DPF #1	VELA 2	PASS	9	100%	100%
	VELA 2	FAIL	0	-	-

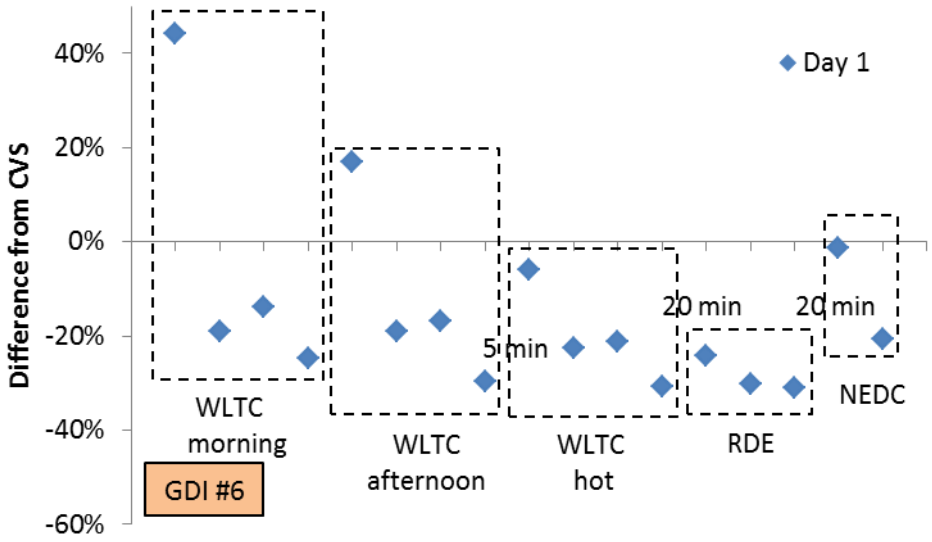

Figure 5-21: Differences of PN-PEMS and PMP-CVS over the day. Each symbol is a sub-cycle.

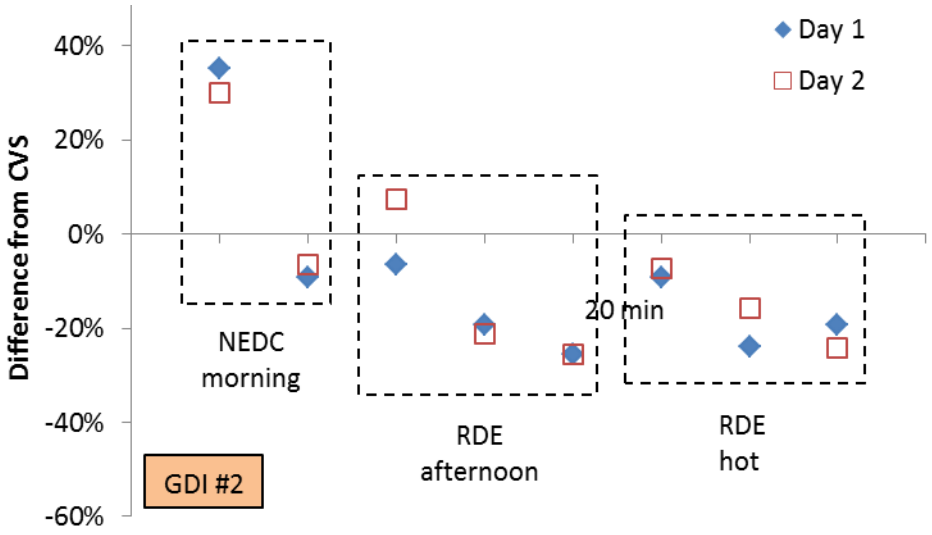

Figure 5-22: Differences of PN-PEMS and PMP-CVS over the day.

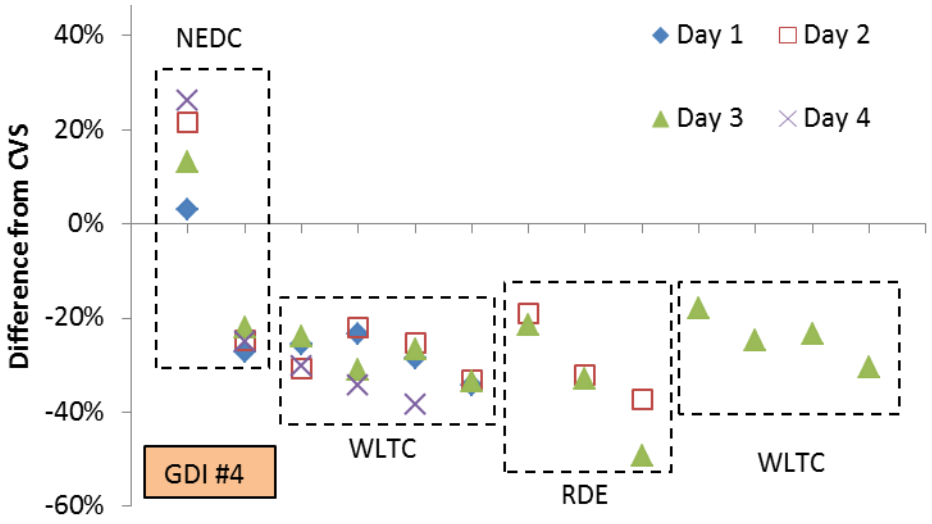

Figure 5-23: Differences of PN-PEMS and PMP-CVS over the day.

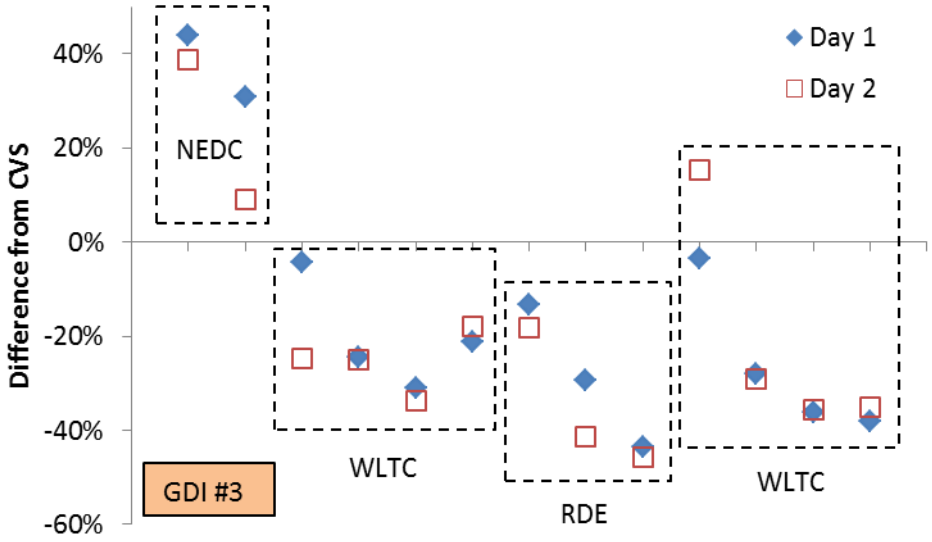

Figure 5-24: Differences of PN-PEMS and PMP-CVS over the day.

Comparing the factors from Figure 5-17 and Figure 5-25, similar factors can be seen. The reason is that the cold start effect is minimized by the big number of hot sub-cycles included.

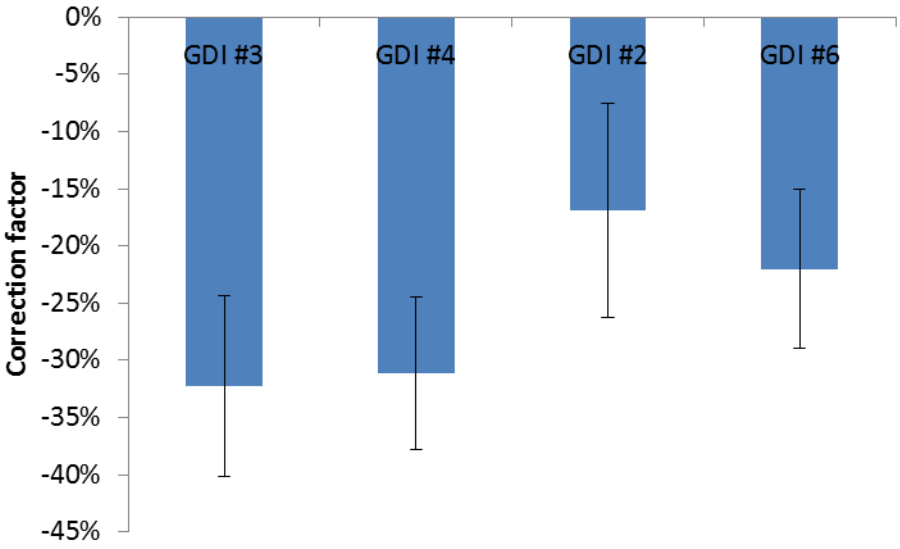

Figure 5-25: Summary of correction factors of PN-PEMS for hot cycles.

6 PN-PEMS #2' (CPC)

6.1 Description

PN-PEMS #2' (CPC) (modified TSI NPET) consists of a VPR and a CPC. The VPR consists of a cold dilution 10:1 at the tailpipe, a 3 m line that brings the diluted aerosol to the main cabinet, a catalytic stripper at 350°C in the main cabinet, a second cold dilution around 10:1, followed by an isopropanol-based CPC with 23 nm cut-off. The CPC was optimized for on-road measurements and has an environmental operating temperature ranging from -10°C to +40°C. The PN-PEMS was calibrated by the manufacturer with GDI particles comparing it with a CPC.

The system is compliant with the technical specifications only for ambient temperatures of 20°C (non-condensing aerosol). The system arrived only after the end of the measurement campaign, so it was evaluated only with a few tests. Nevertheless more tests were conducted after the end of the measurement campaign (Annex D).

6.2 Calibration

PN-PEMS #2' (CPC) was calibrated according to the procedures described in Giechaskiel et al. (2014) with monodisperse spark discharge graphite. The results, in comparison with the PMP system that was connected to the tailpipe (PMP-TP), can be seen in Figure 6-1. The counting efficiency is almost flat down to 80 nm, then it starts to decrease, and it is approximately 60% at 23 nm and 20% at 15 nm.

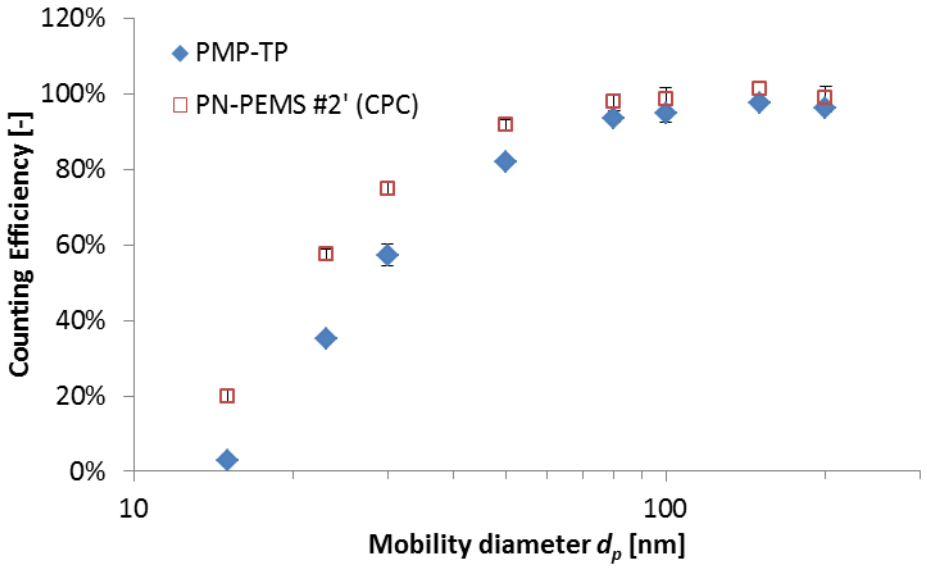

Figure 6-1: Calibration of PN-PEMS with monodisperse aerosol (spark discharge graphite).

Then the PN-PEMS was compared with other instruments measuring polydisperse aerosol (Figure 6-2). Compared to the PMP-TP (PMP 23 nm) the PN-PEMS is measuring 5-10% higher and the difference increases as the GMD decreases. Compared to a simulated PMP curve from the SMPS size distribution (see details in Giechaskiel et al.

2014) the trend is different but the difference is 5-10% less. Thus the PN-PEMS is expected to have differences between these two curves for most cases. In the same figure, the difference compared to a 10 nm CPC is shown. As the GMD decreases, the difference decreases, confirming that the PN-PEMS has a 50% counting efficiency lower than 23 nm but higher than 10 nm.

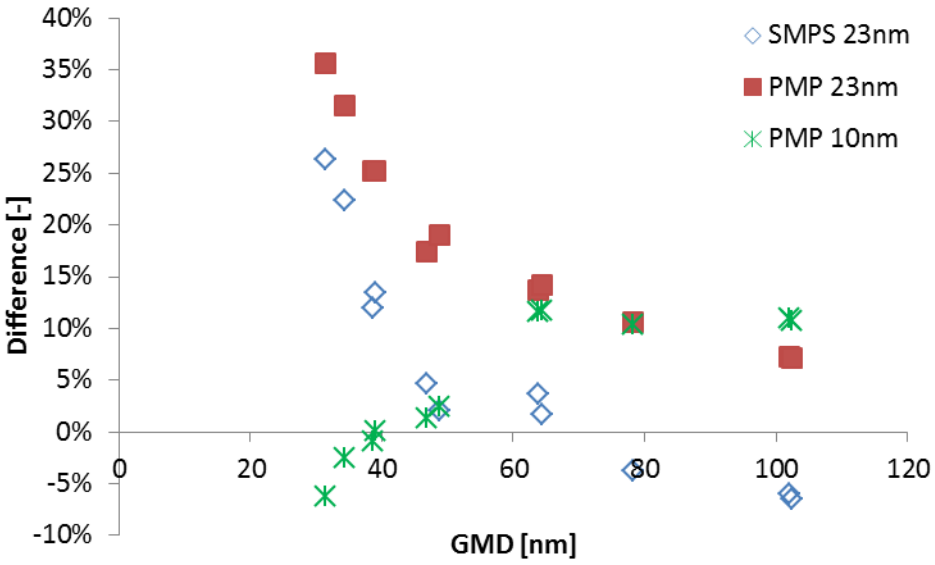

Figure 6-2: Difference in counting efficiency between PN-PEMS and other instruments measuring polydisperse aerosol (spark-discharge graphite) as a function of the GMD of the particles.

6.3 Real time

Initially the PN-PEMS was connected to the CVS and was compared with the PMP-CVS system (Figure 6-3). The PN-PEMS follows the PMP-CVS system closely.

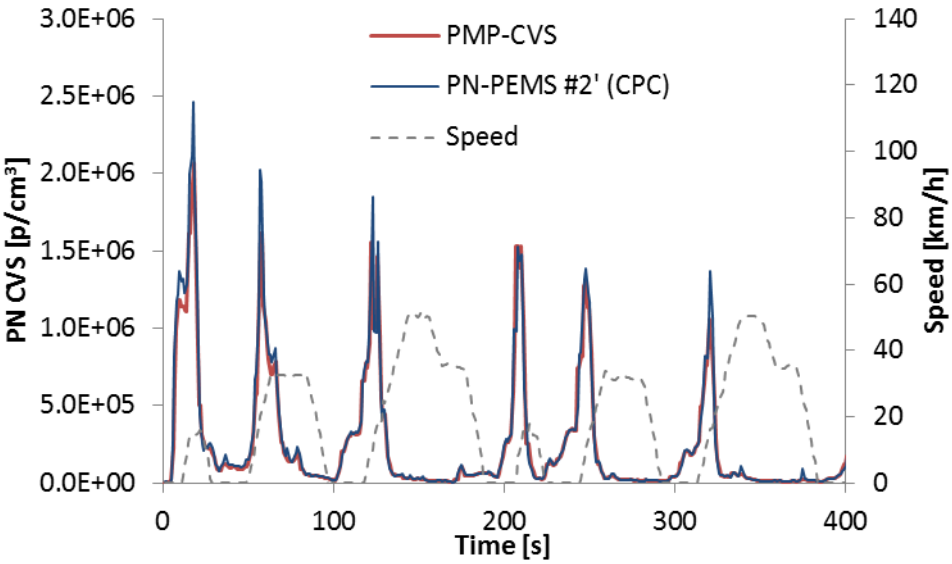

Figure 6-3: Comparison of PN-PEMS with PMP-CVS. Both instruments at the dilution tunnel (20141211-01-NEDC cold, GDI #7).

Similar behaviour was shown when the PN-PEMS was connected to the tailpipe (Figure 6-4). The GMD is the 5s moving average for the real time figures.

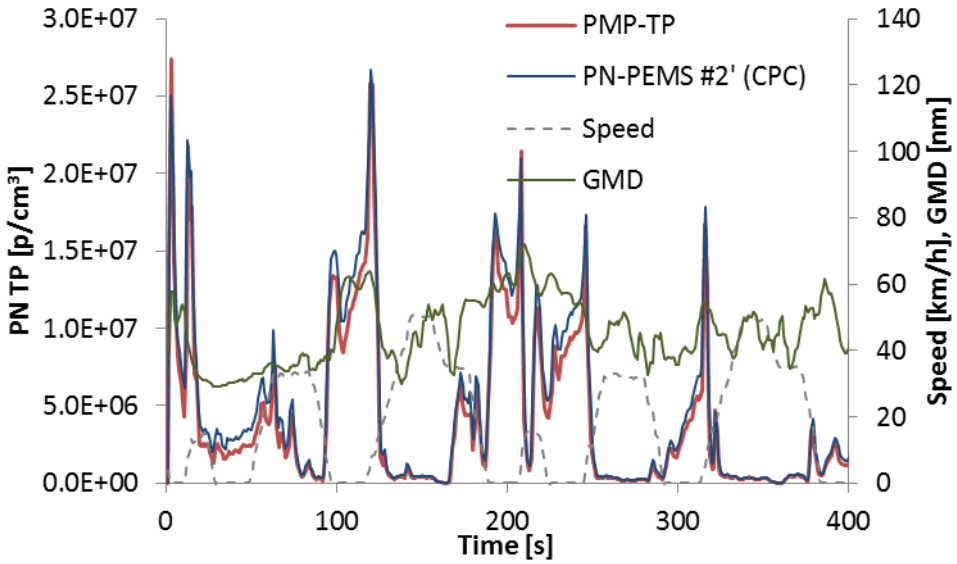

Figure 6-4: Comparison of PN-PEMS with PMP-TP. Both instruments connected to the tailpipe (20141215-03 NEDC, GDI #7).

6.4 Comparison to PMP-CVS

Figure 6-5 summarizes the results when the PN-PEMS was connected to the CVS. The differences are around 10% for GDI #7. The Moto #1 will be discussed in section 5.9.

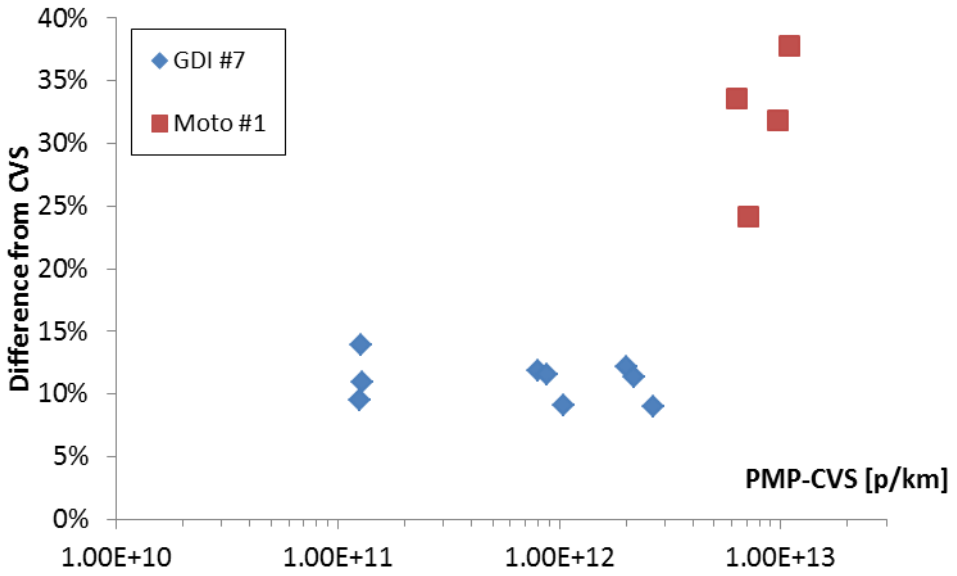

Figure 6-5: Summary of results of PN-PEMS vs PMP-CVS when connected to the dilution tunnel.

Then the PN-PEMS was connected to the tailpipe for different vehicles. The comparison with the PMP system at the CVS (PMP-CVS) can be seen in Figure 6-6. The differences range approximately from -20% to +50% for different emission levels.

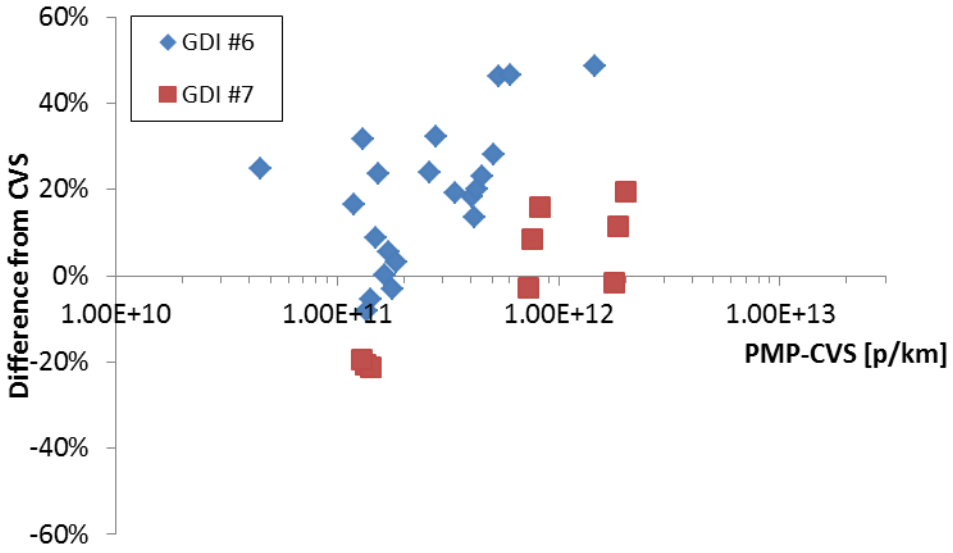

Figure 6-6: Summary of results of PN-PEMS vs PMP-CVS. PN-PEMS was connected to the tailpipe.

6.5 Comparison to PMP-TP

The difference of the PN-PEMS from the PMP at the tailpipe (PMP-TP) can be seen in Figure 6-7. The differences range from -10% up to +20%.

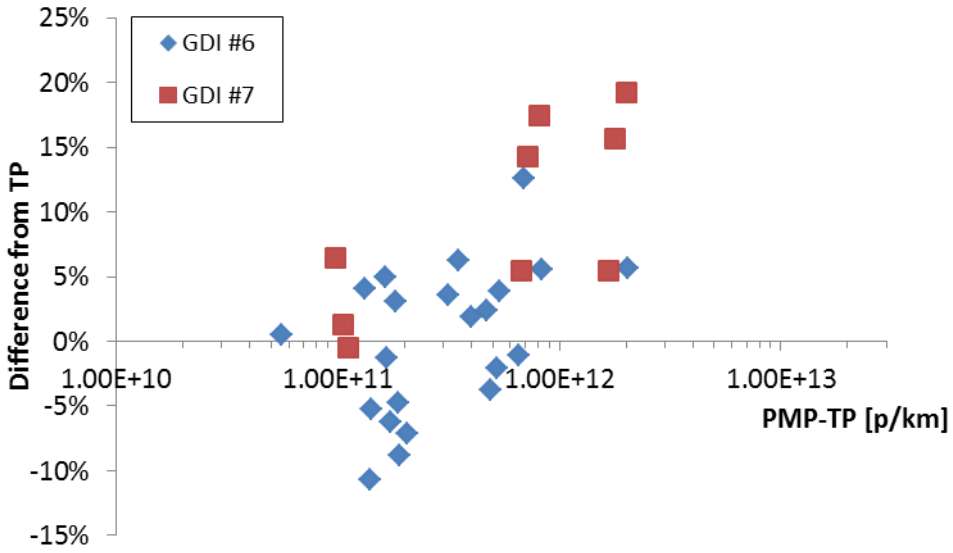

Figure 6-7: Summary of results of PN-PEMS vs PMP-TP. Both connected to the tailpipe.

6.6 Particle size effect

No size dependency of the PN-PEMS is expected. Indeed, when the differences of the PN-PEMS from the PMP-CVS were plotted in function of mean particle size (Figure 6-8), no size dependency could be seen. At sizes <20 nm the variability increases because these sizes are lower than the cut-off of the CPCs at both the PN-PEMS and the PMP-CVS. In this figure the GMD is the average of cycle.

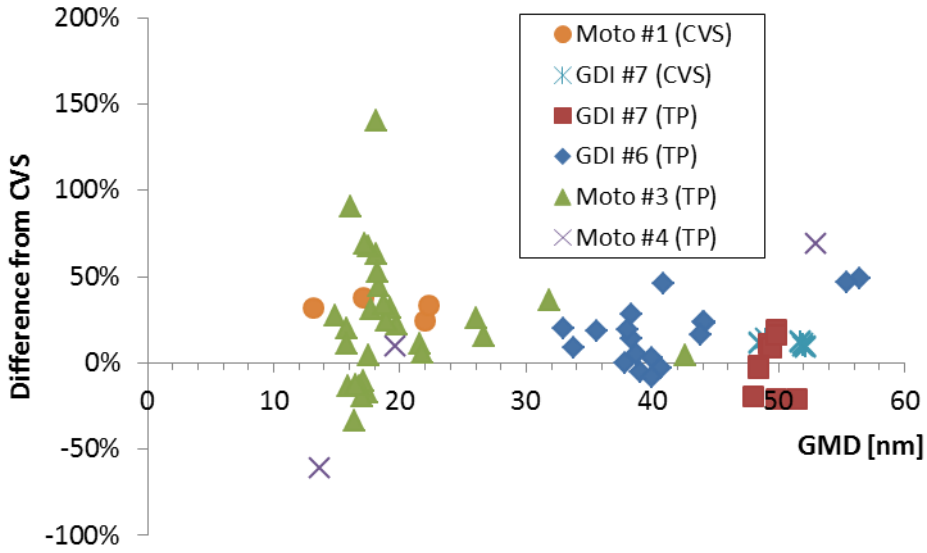

Figure 6-8: Particle size dependency of PN-PEMS.

6.7 Ambient temperature

Not investigated.

6.8 Challenge aerosol (motorcycles)

The PN-PEMS was used also to measure exhaust aerosol of motorcycles. Moto #3 is a 4-stroke 50 cm^3 moped with max speed around 30 km/h (modified). Moto #4 is a 4-stroke 125 cm^3 motorcycle with max speed around 90 km/h. The specific motorcycles were producing particles with mean around 20 nm. Thus the PN-PEMS could give wrong results due to differences in the cut-off size of the CPC. The PN-PEMS compared to the PMP-TP can be seen in Figure 6-9. The differences are within 20% for sizes >30 nm. There are a few tests where the PN-PEMS measured 40-80% higher. As it can be seen in Figure 6-9, these were tests where the GMD was around 15-20 nm. In this size range there is high uncertainty for both the PN-PEMS and the PMP. Above 30 nm no size dependency could be observed.

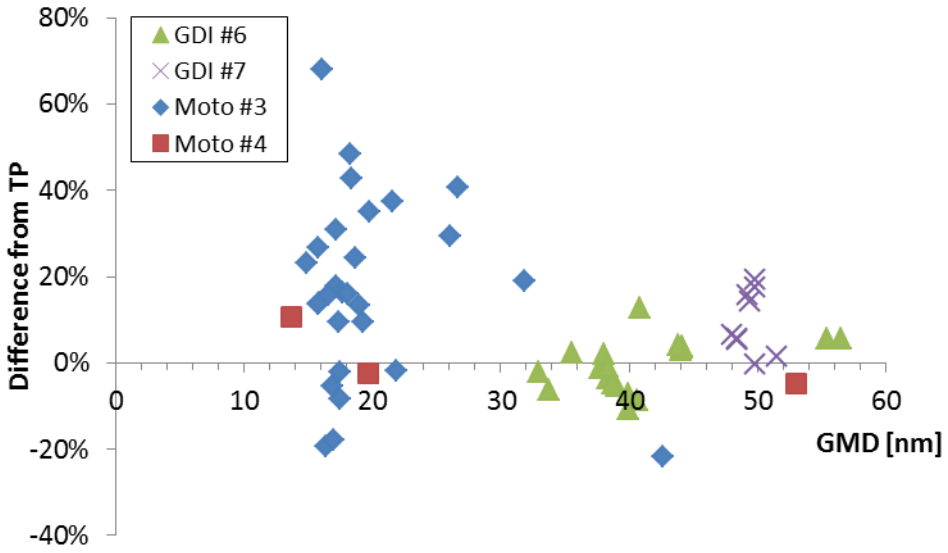

Figure 6-9: Size dependency of PN-PEMS

6.9 Volatile removal efficiency

The volatile removal efficiency of the PN-PEMS was evaluated by measuring from the CVS diluted aerosol from a 2-stroke 50 cm^3 moped (Moto #1). The size distribution at the CVS has a mean around 90 nm. After thermal pre-treatment the mean decreases to <20 nm. The results (with the previous motorcycles) are shown in Figure 6-5 and Figure 6-8. The PN-PEMS measures 35% more than the PMP-CVS indicating that the size of the particles were efficiently decreased and there was no significant re-nucleation and growth that could influence the results. It measures a little higher than the GDIs (35% vs 10%) probably due to the slightly higher counting efficiency at 23 nm.

6.10 Regeneration

The PN-PEMS was connected to the dilution tunnel and was measuring in parallel with the PMP-CVS the emissions of a diesel vehicle equipped with a DPF (#2). An EEPS was measuring from the dilution tunnel. Figure 6-10 compares all systems. EEPS was measuring >10^7 p/cm^3. The PN-PEMS was within 10% of the PMP-TP. During normal cycles (e.g. 3xEUDC) the PN-PEMS was measuring similarly with the PMP systems (within 10%). This indicates that the PN-PEMS was not affected by the regeneration.

6.11 Summary

Figure 6-11 summarizes the differences of the PN-PEMS from the PMP-CVS and PMP-TP for all cases examined. For GDIs, the mean differences are 0% to +20% with a variability (expressed as ±standard deviation) of ±15%. For the motorcycles, the mean differences range from -15% to +30% with higher variability (±30%). Assuming that when the error bars cross the 0% the PN-PEMS is equivalent with the PMP-CVS, in most cases the PN-PEMS measures equivalently with the PMP-CVS.

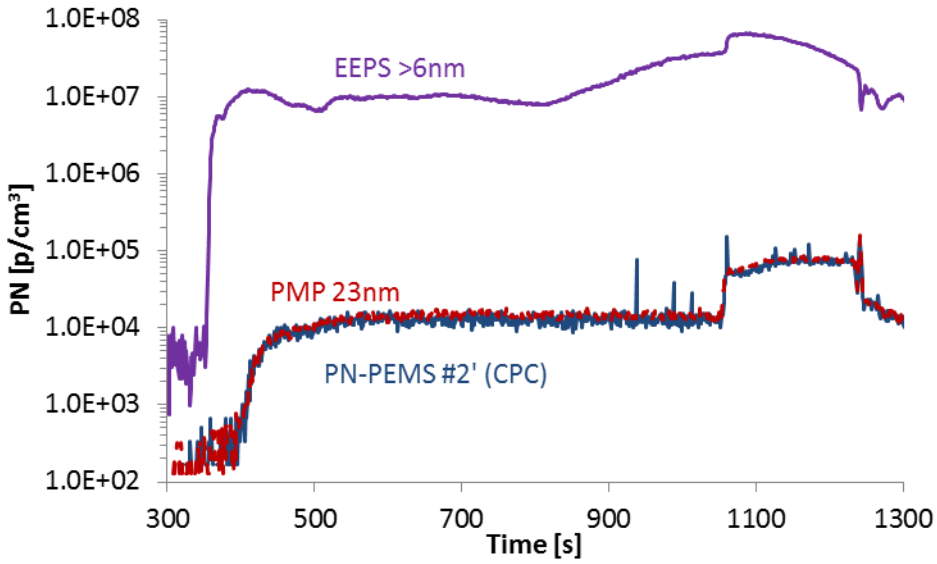

Figure 6-10: Regeneration tests with DPF #2.

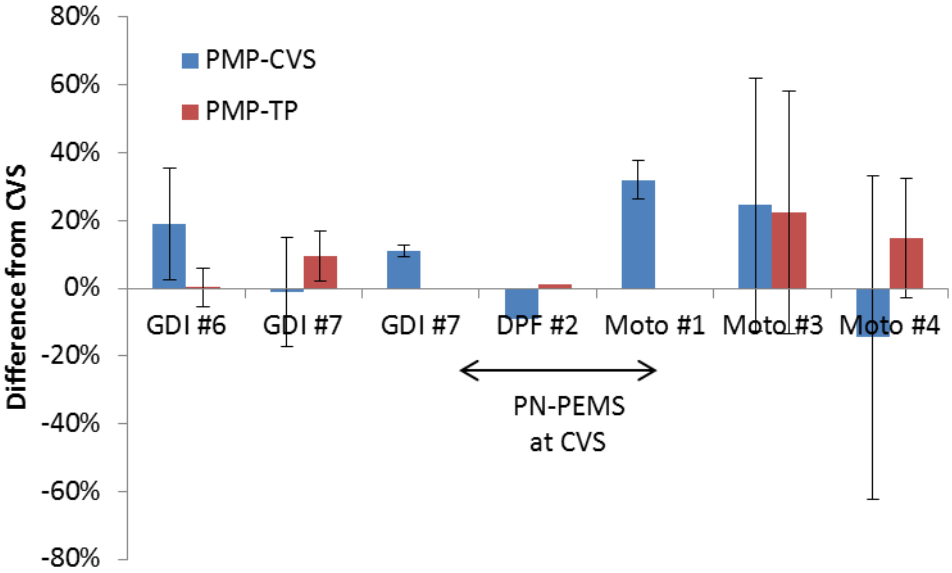

Figure 6-11: Overview of differences of PN-PEMS from the PMP-CVS and PMP-TP. Error bars are one standard deviation.

Another way of evaluating the PN-PEMS is by plotting the results of the PN-PEMS vs the PMP-CVS. By setting the limit values one can visualize which tests would give a correct results (i.e. PASS when the PMP would give PASS or FAIL when the PMP system would give FAIL) or wrong (PASS for FAIL or FAIL for PASS). Figure 6-12 gives all results. There are a few tests where the PN-PEMS gave wrong result (FAIL instead of PASS) and as mentioned previously this had to do with the differences between tailpipe and dilution tunnel results.

Table 6-1 shows the PASS/FAIL results of the PMP-TP and the PN-PEMS compared to the PMP-CVS assuming a 6x10^11 p/km limit. The success rate (i.e. catching a FAIL as FAIL or a PASS as PASS) is very high and similar to the PMP-TP.

Table 6-1: PASS/FAIL success rate.

Vehicle	Lab	Category	# of tests	PMP-TP	PN-PEMS
GDI #6	VELA 2	PASS	20	90%	90%
	VELA 2	FAIL	2	100%	100%
GDI #7	VELA 1	PASS	3	100%	100%
	VELA 1	FAIL	6	100%	100%
GDI #7 (CVS)	VELA 1	PASS	3	-	100%
	VELA 1	FAIL	6	-	100%
Moto #4	VELA 1	PASS	6	83%	83%
	VELA 1	FAIL	0	-	-
Moto #3	VELA 1	PASS	24	100%	92%
	VELA 1	FAIL	5	100%	100%
Moto #1 (CVS)	VELA 1	PASS	0	-	-
	VELA 1	FAIL	4	-	100%
DPF #2 (CVS)	VELA 2	PASS	1	-	100%
	VELA 2	FAIL	1	-	100%

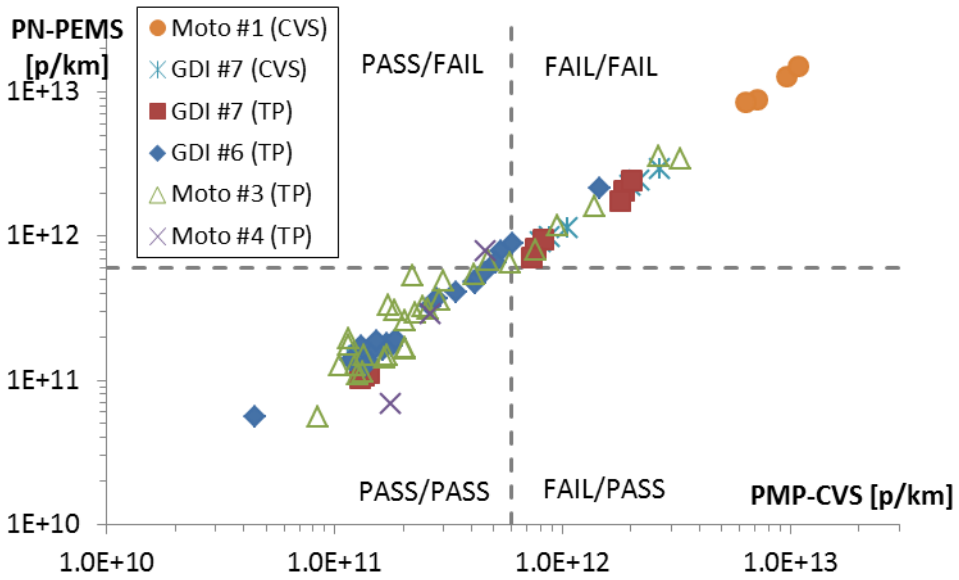

Figure 6-12: Overview of all PASS/FAIL results.

7 PN-PEMS #2' (DC)

7.1 Description

The PN-PEMS #2' (DC) (Horiba OBS-PM) consists of a VPR and a DC. The VPR consists of an evaporation tube at 350°C, a cold dilution 10:1 at the tailpipe, and a 3 m heated line (47°C) that brings the diluted aerosol to the main cabinet. The DC (DCS-100 from TSI) was used with diffusion screens to reduce the sensitivity to sub-23 nm particles. The DC gives 'aerosol length' L [mm/cm^3]. A constant factor C of 361344 was used to convert the length to particle number. This value, which was given by the manufacturer (and includes dilution and particle losses), was based on comparisons of the device with a CPC both measuring GDI particles in parallel.

The system is not fully compliant with the technical specifications because of the cold dilution (condensing aerosol). The system arrived only at the end of the measurement campaign, so it was evaluated only for a few tests.

7.2 Calibration

The PN-PEMS was calibrated at the end of the measurement campaign with monodisperse spark discharge graphite. For details see Giechaskiel et al. (2014). The results can be seen in Figure 7-1.

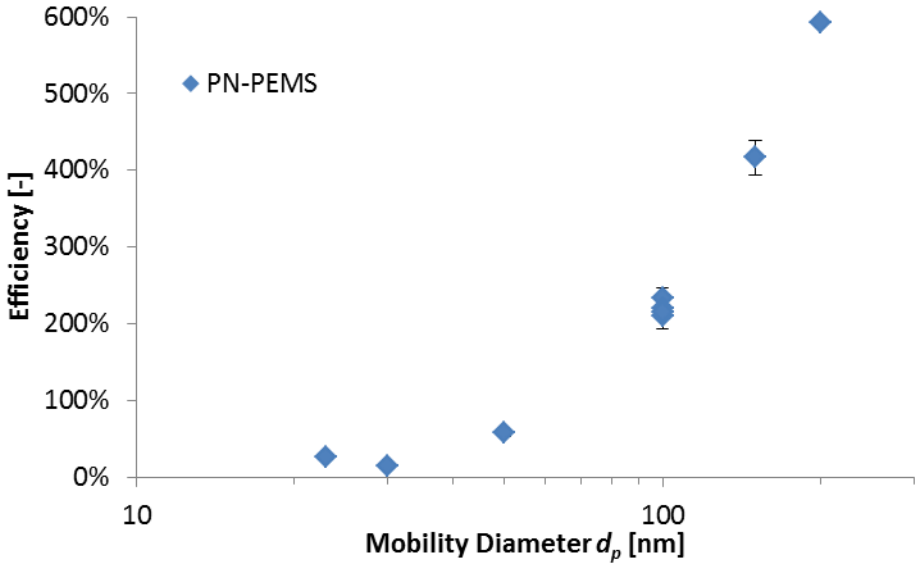

Figure 7-1: Efficiency of PN-PEMS with spark-discharge graphite.

The ratios of the efficiencies were compared with the older units (Table 7-1). PN-PEMS #2 was the prototype of Phase 1, PN-PEMS #2' (CPC) is the other unit used in Phase II and PN-PEMS #2' (DC) is the unit tested in Phase II. The results are quite similar but with slightly higher ratio of 200 nm, indicating a size dependency. The calibration factor of the manufacturer (i.e. where the 100% efficiency is) corresponds to approximately

60 nm monodisperse (70 nm recommended) normalization which will probably overestimate the emissions.

Applying the recommended procedures (correction factor to normalize at 70 nm or polydisperse distribution of 55 nm) a correction factor of 0.65 would be needed for the results.

Table 7-1: Ratios of efficiencies of PN-PEMS. Unit #2 from Phase I was evaluated in Giechaskiel et al. (2014).

d_p [nm]	23	30	50	100	200
#2	0.00	0.07	0.36	1.06	2.50
#2' (DC)	0.12	0.06	0.26	1.00	2.69
#2' (CPC)	0.57	0.75	0.92	0.99	0.99

7.3 Real time

The comparison of the PN-PEMS with the PMP-TP can be seen in Figure 7-2. Although the PN-PEMS follows the same emissions pattern as the PMP-TP, there is a big difference at the cold start, where the mean particle size is bigger. In the real time figures the GMD is the 5s moving average.

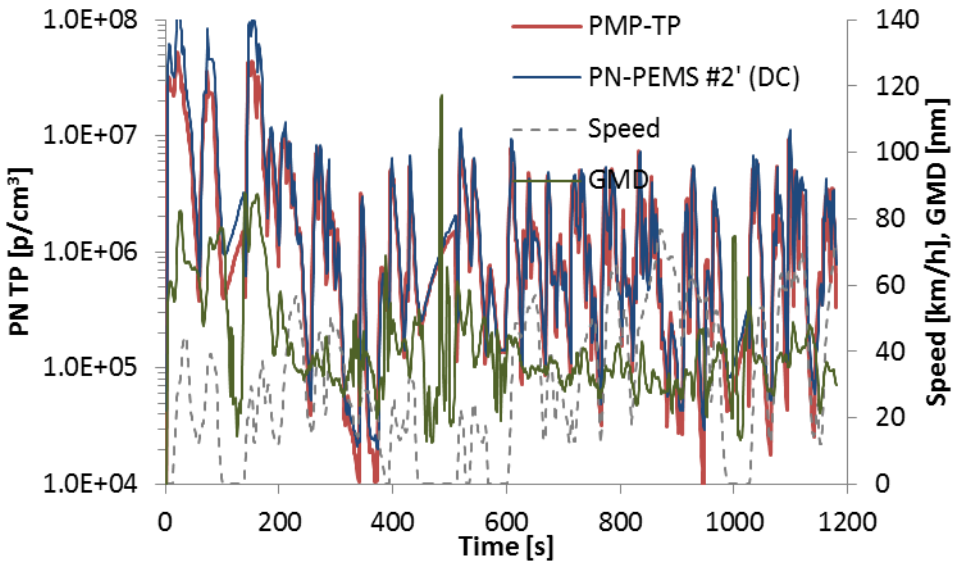

Figure 7-2: Comparison of PN-PEMS with PMP-TP, both connected to the tailpipe.

7.4 Comparison to PMP-CVS

Figure 7-3 summarizes the differences of the PN-PEMS from the PMP-CVS when the PN-PEMS was connected to the tailpipe. The differences range from10% to 150%. The results of GDI #7 are not presented because the dilution air was not connected.

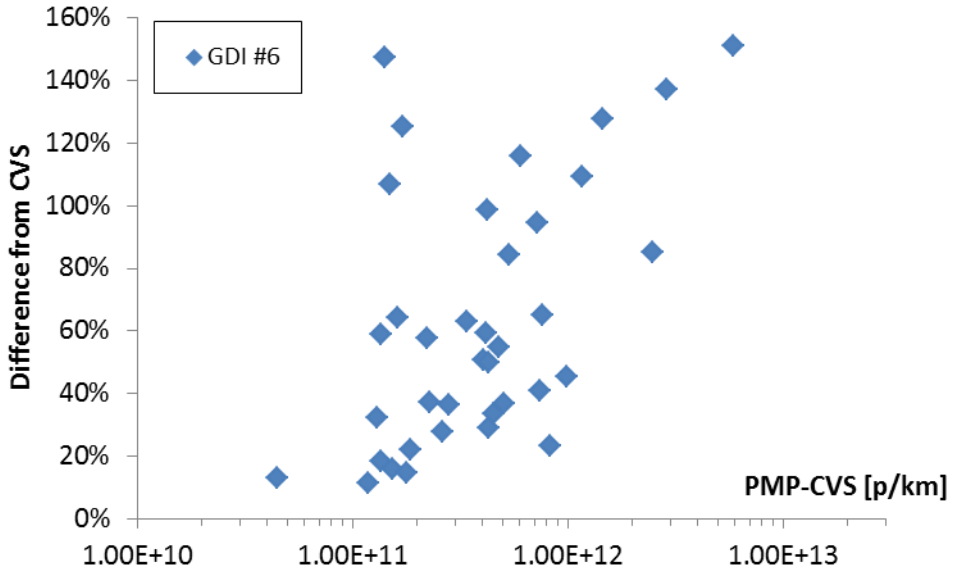

Figure 7-3: Summary of comparisons of PN-PEMS to the PMP-CVS. PN-PEMS was connected to the tailpipe.

7.5 Comparison to PMP-TP

The difference of the PN-PEMS from the PMP at the tailpipe (PMP-TP) can be seen in Figure 7-4. The differences range from -10% up to +150%.

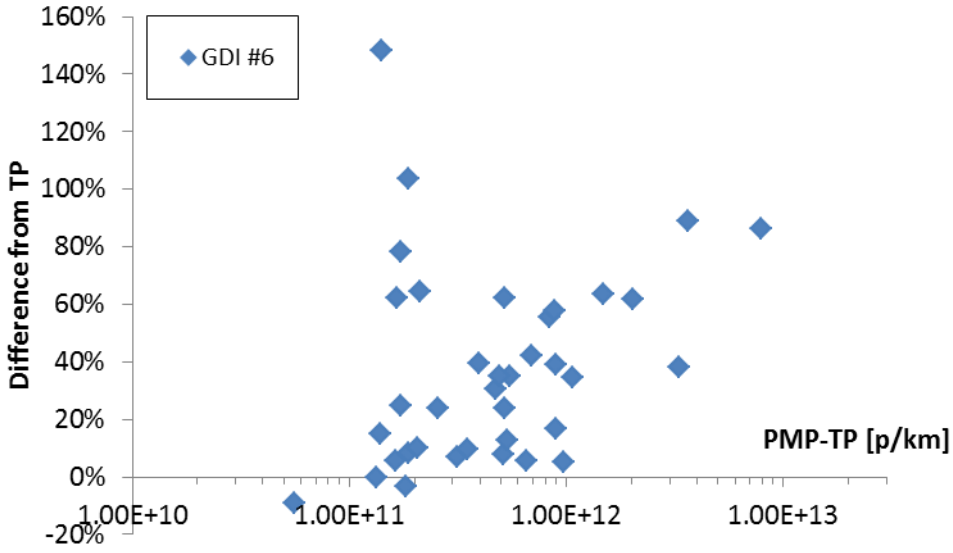

Figure 7-4: Summary of comparisons of PN-PEMS to the PMP-TP, both connected to the tailpipe.

7.6 Particle size effect

No size dependency could be observed for the PN-PEMS (Figure 7-5). Probably the limited number of tests and the high variability of the tests masked the size dependency. In these figures the GMD is the average of cycle.

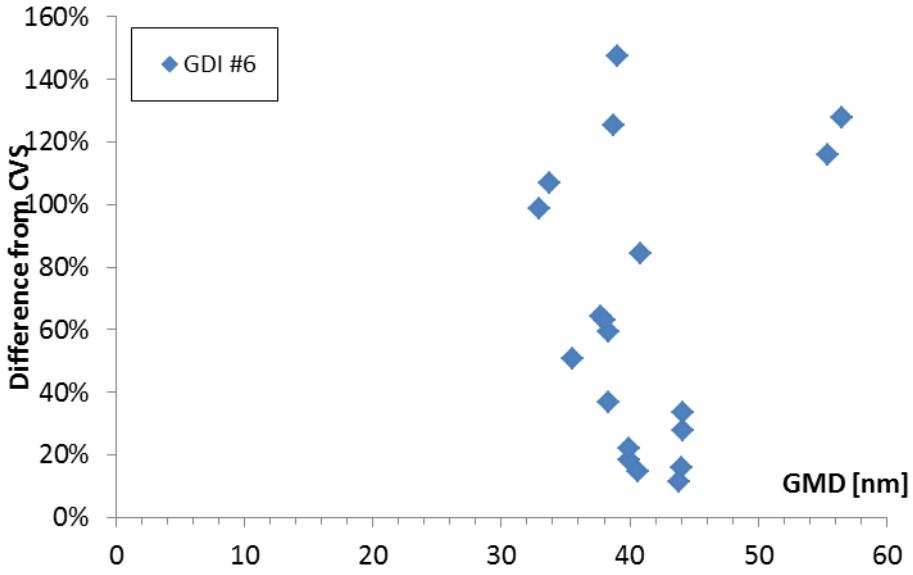

Figure 7-5: Size dependency of PN-PEMS.

7.7 Ambient temperature

Not investigated.

7.8 Challenge aerosol (motorcycles)

The PN-PEMS was used also to measure exhaust aerosol of motorcycles. Moto #3 is a 4-stroke 50 cm^3 moped with max speed around 30 km/h (modified). Moto #4 is a 4-stroke 125 cm^3 motorcycle with max speed around 90 km/h. The specific motorcycles were producing particles with mean around 20 nm. Thus the PN-PEMS could overestimate the emissions (because it doesn't have counting efficiency 0 at small sizes) or underestimate the emissions (because the response function decreases with size). The PN-PEMS compared to the PMP-TP (GDIs also included) can be seen in Figure 7-6.

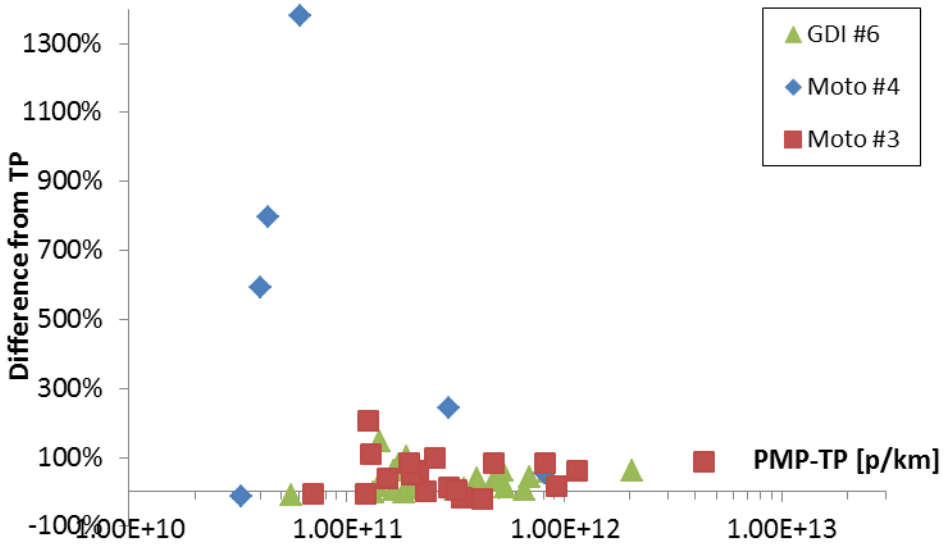

Figure 7-6: Behaviour of PN-PEMS when measuring motorcycles exhaust.

The results were also plotted as a function of mean particle size (Figure 7-7). The differences are within 150% for sizes >30 nm. There are a few tests where the PN-PEMS measured 14 times higher. As it can be seen in the figure, these were tests where the GMD was <20 nm. Actually these particles were solids around 10 nm (Figure not shown) as identified with other CPCs downstream of PMP systems. Figure 7-8 shows that these particles were measured at the high speed part of the cycle. Thus either the volatiles were not completely removed (i.e. particles were bigger when measured by the DC) or the DC is still sensitive to these small particles.

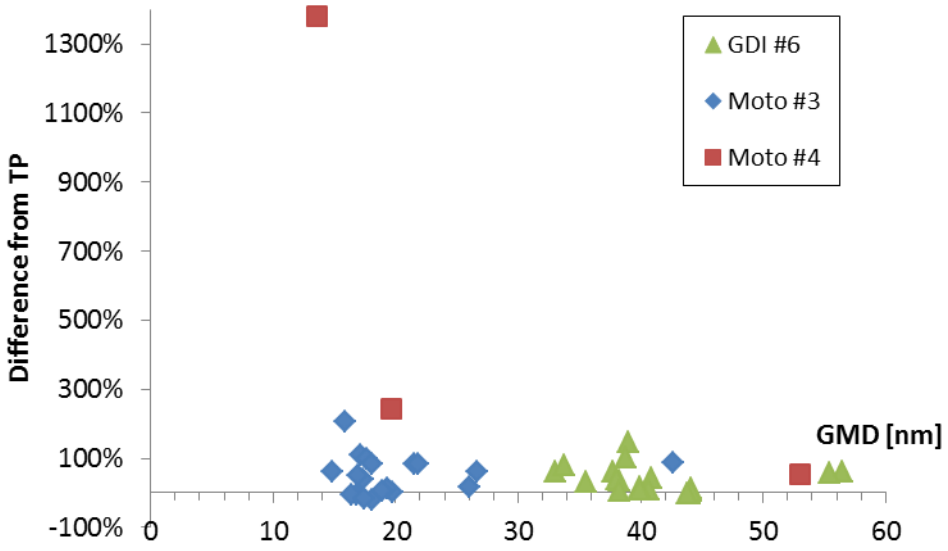

Figure 7-7: Size dependency of PN-PEMS when measuring motorcycles exhaust.

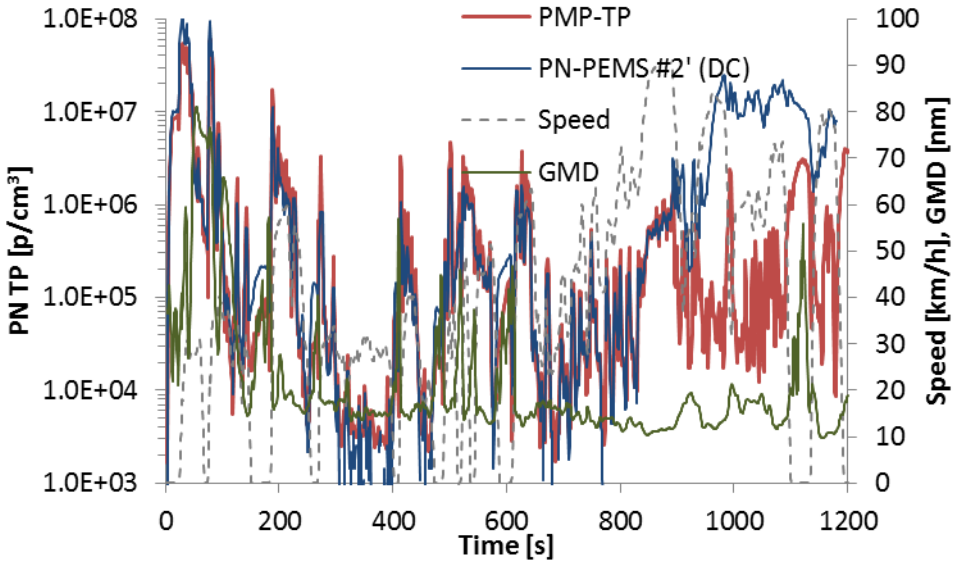

Figure 7-8: Comparison of PN-PEMS with PMP-TP when measuring motorcycles exhaust (20141219-01-WMTC, Moto #4).

7.9 Volatile removal efficiency

Not evaluated.

7.10 Summary

Figure 7-9 summarizes the differences of the PN-PEMS from the PMP-CVS and PMP-TP for all cases examined. For the GDI, the mean differences are around +60% with a variability (expressed as ±standard deviation) of ±40%. For the motorcycles, the mean differences range from +50% to +230% with higher variability (>50%). Note that applying the correction factor that was found following the suggested calibration procedures (0.65) the differences would be very close to 0%.

Table 7-2 shows the PASS/FAIL results of the PMP-TP and the PN-PEMS compared to the PMP-CVS assuming a 6x10^11 p/km limit. The success rate (i.e. catching a FAIL as FAIL or a PASS as PASS) is not very high but close to the PMP-TP for the GDIs, but not for the motorcycles.

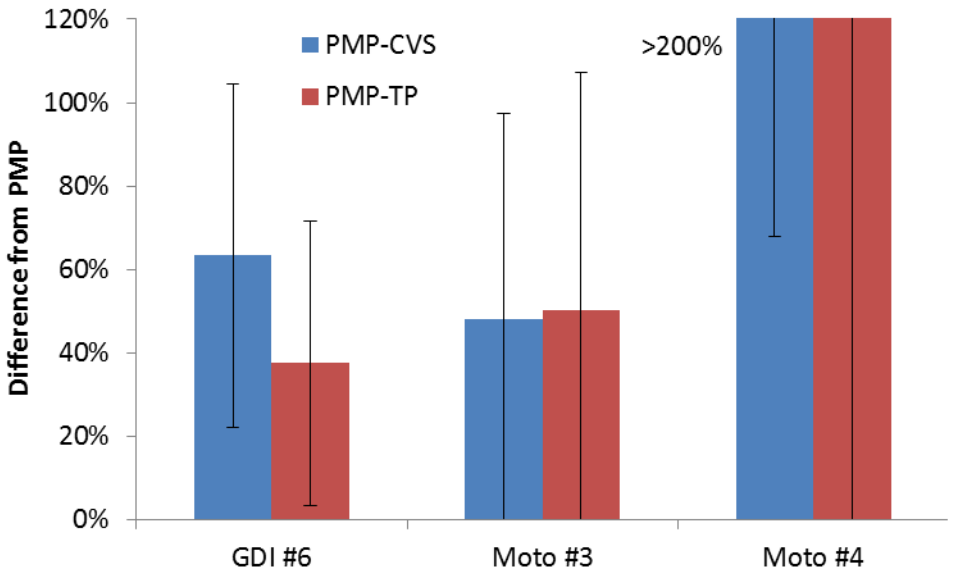

Figure 7-9: Overview of differences of PN-PEMS from the PMP-CVS and PMP-TP. Error bars are one standard deviation.

Table 7-2: PASS/FAIL success rate.

Vehicle	Lab	Category	# of tests	PMP-TP	PN-PEMS
GDI #6	VELA 2	PASS	26	92%	69%
	VELA 2	FAIL	11	100%	100%
Moto #4	VELA 1	PASS	6	83%	50%
	VELA 1	FAIL	0	-	-
Moto #3	VELA 1	PASS	15	100%	100%
	VELA 1	FAIL	4	100%	100%

8 PN-PEMS #3 (PN)

8.1 Description

PN-PEMS #3 (Nanomet 3-PS, Testo AG) consists of a VPR and a DC (Diffusion Size Classifier miniature, DiSC mini). The VPR consists of a heated sampling line at 100°C, a heated rotating disk diluter (*PCRF* used in this campaign around 100), and an evaporation tube at 300°C. A unique characteristic of the device is that the DC has two electrometers and can estimate a mean particle size based on their ratio (Fierz et al. 2008, 2011). The charged particles first flow through a diffusion stage. Some of the particles are captured in this stage and generate a current I_{diff}, while the remaining particles flow into a second stage that is equipped with a HEPA filter. Here, all particles are captured, and a current I_{filter} is measured with an electrometer. The ratio I_{filter}/I_{diff} is a measure of the average particle size, because smaller particles undergo larger Brownian motion, and are therefore more likely to be captured in the diffusion stage. The instrument gives particle number concentration based on the currents it measures and an estimated mean particle size. This approach will be examined in the following sections. Further evaluation after the end of the campaign can be found in Annex D.

8.2 Calibration

Figure 8-1 shows the comparison of the diameter set at the electrostatic classifier (DMA) and the one estimated by the PN-PEMS. The results are quite close especially at the range of interest (<100nm).

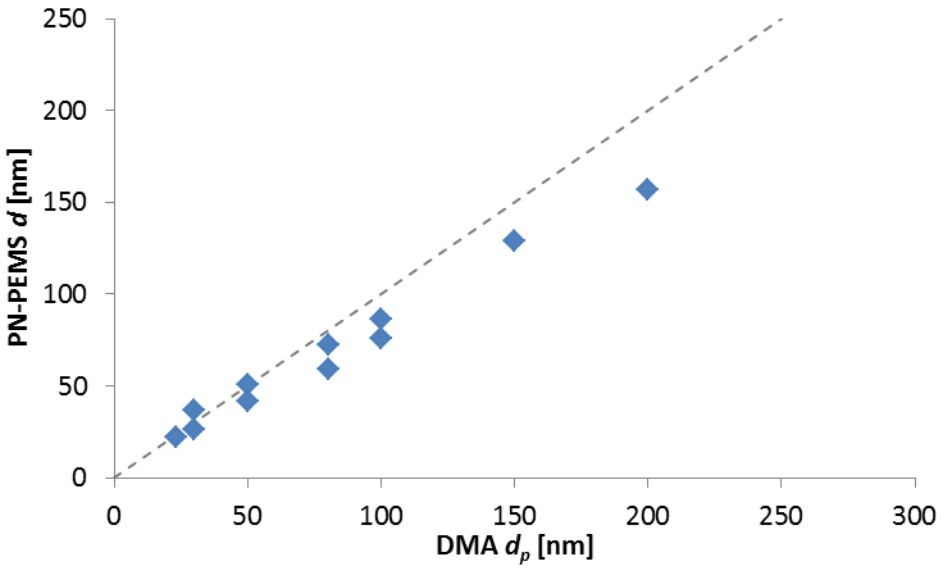

Figure 8-1: Comparison of (monodisperse) diameter set at the electrostatic classifier (DMA) and the one estimated by the PN-PEMS. The dashed line is the 1:1 line.

The efficiency of the PN PEMS is shown in Figure 8-2. The results are very encouraging for DC based PN-PEMS: <50% for 23 nm and >70% for 50 nm, and almost no size

dependency for bigger sizes. An efficiency corrected for an assumed PMP penetration is also plotted.

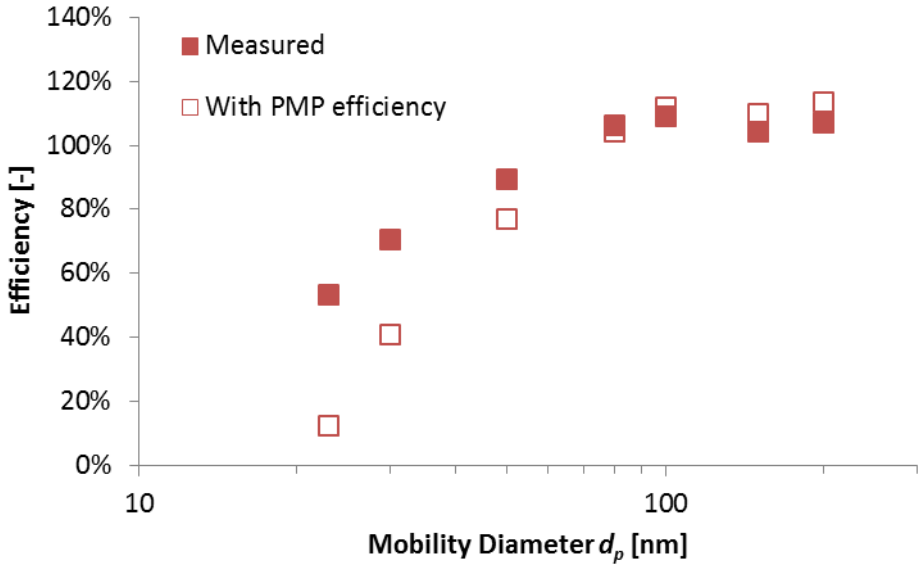

Figure 8-2: Efficiency of PN-PEMS. A corrected efficiency using a typical penetration curve of a PMP system and the estimated diameter of the PN-PEMS is also shown.

8.3 Estimated mean size and real time PN

The size information was also evaluated in the lab with polydisperse spark discharge graphite aerosol. The mean size is underestimated, in agreement with the results in Giechaskiel et al (2014) and the references therein (Figure 8-3).

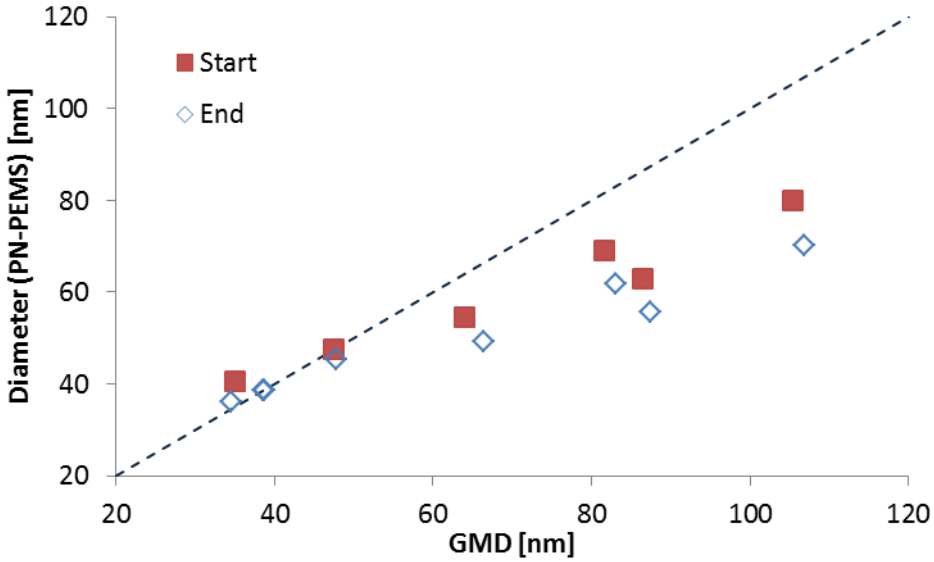

Figure 8-3: Estimated size from the PN-PEMS compared to the GMD measured by the SMPS.

It should be noted that this is the static instrument response, and it does not ensure that the system will behave similarly in the transient operation. Real time GMDs (moving averages of 5 s) are shown in Figure 8-4 for GDI #2 and Figure 8-5 for GDI #6. It can be seen that the estimated diameter is not in good agreement with the measured from the EEPS. The disagreement was very often also at concentrations much above the zero levels indicating that that the methods with size info have to be better evaluated for transient operations.

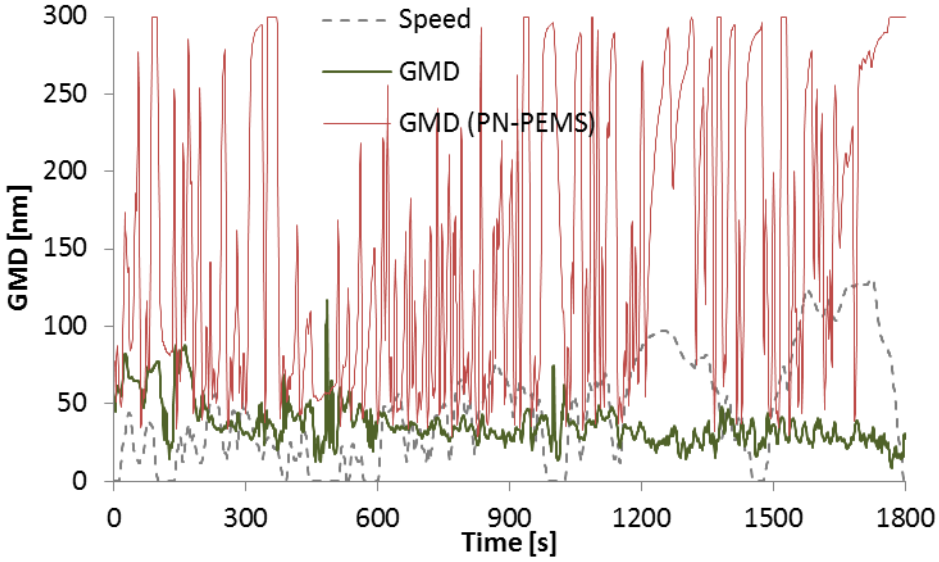

Figure 8-4: Comparison of GMDs measured by the PN-PEMS and the EEPS for GDI #6.

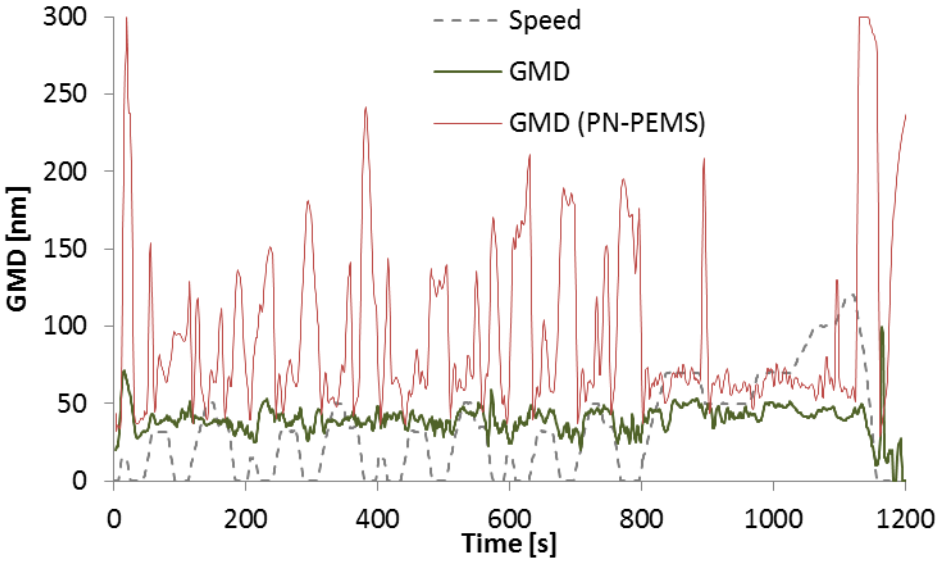

Figure 8-5: Comparison of GMDs measured by the PN-PEMS and the EEPS for GDI #2

Nevertheless, the calculated PN seems to be in good agreement with the PMP-TP (Figure 8-6 and Figure 8-7). This is due to the relatively small effect (<20%) of the size info on the estimated PN (Fierz et al. 2011).

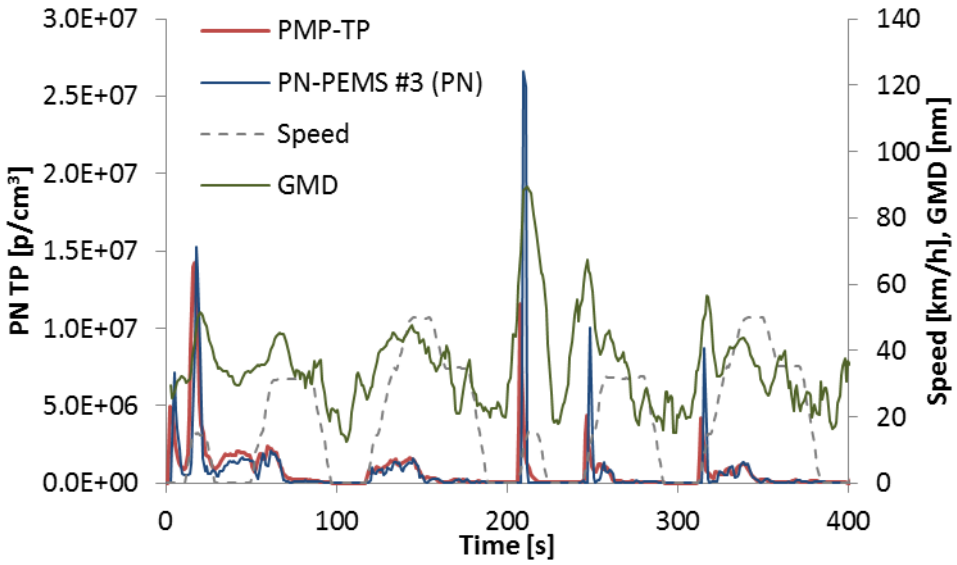

Figure 8-6: Comparison of PN-PEMS (PN) to the PMP-TP, both connected to the tailpipe.

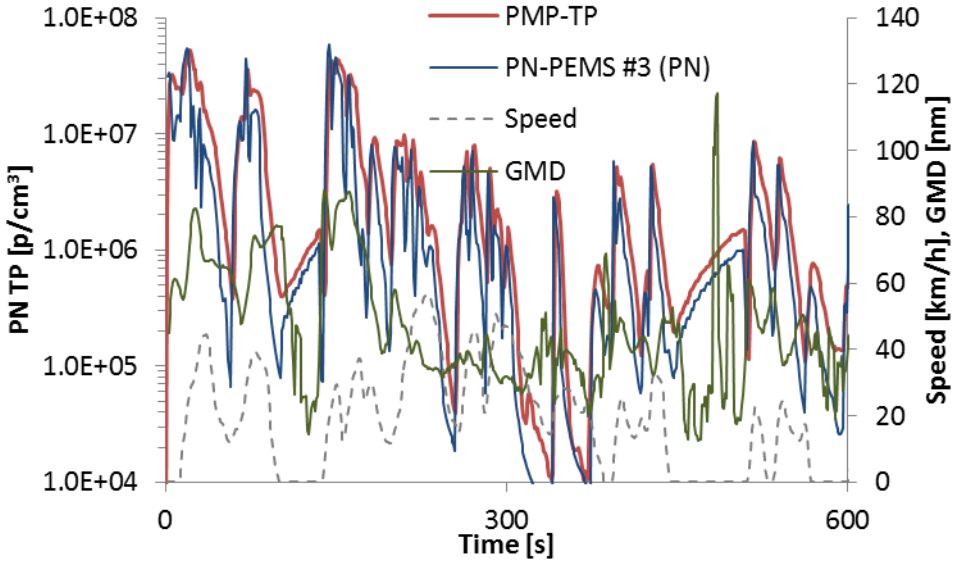

Figure 8-7: Comparison of PN-PEMS (PN) to the PMP-TP, both connected to the tailpipe.

8.4 Comparison to reference PMP

Figure 8-8 summarizes all results. The differences for the GDIs lie between -35% and +40%. Higher differences were found in some cases for motorcycles. This could be due to the existence of small particles that are measured by the PN-PEMS (Figure 8-9). Using a theoretical cut-off at 23 nm probably would improve the correlation for the motorcycles.

Figure 8-10 summarizes all results compared to the PMP-CVS. With a few exceptions the differences to the PMP-CVS lie between -35% and +40%.

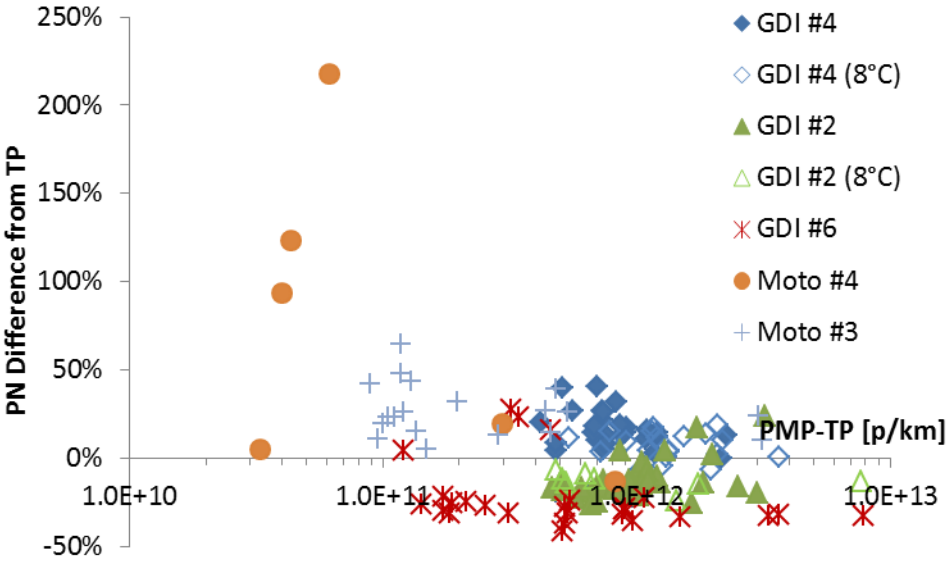

Figure 8-8: Summary of comparisons of PN-PEMS to PMP-TP, both connected to the tailpipe.

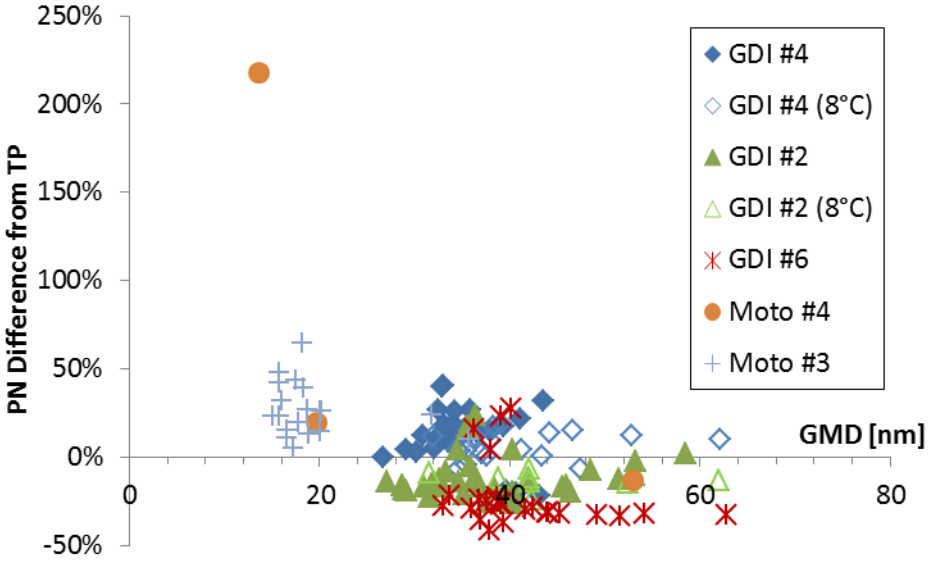

Figure 8-9: Size dependency of PN-PEMS.

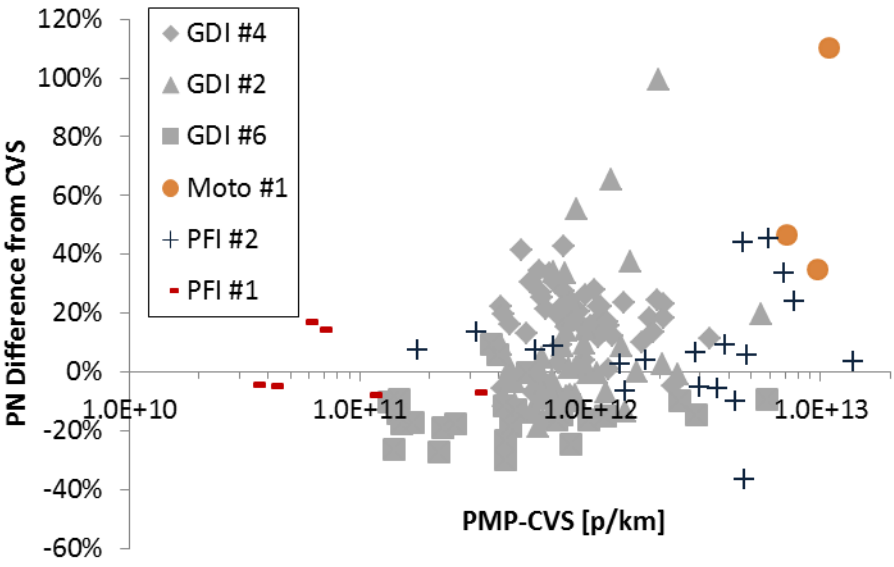

Figure 8-10: Summary of comparisons of PN-PEMS to the PMP-CVS

8.5 Regeneration

The PN-PEMS was connected to the tailpipe and was measuring in parallel with the PMP-TP the emissions of a diesel vehicle equipped with a DPF (#2). Figure 8-11 compares the systems. The PN-PEMS is underestimating the emissions by 40%.

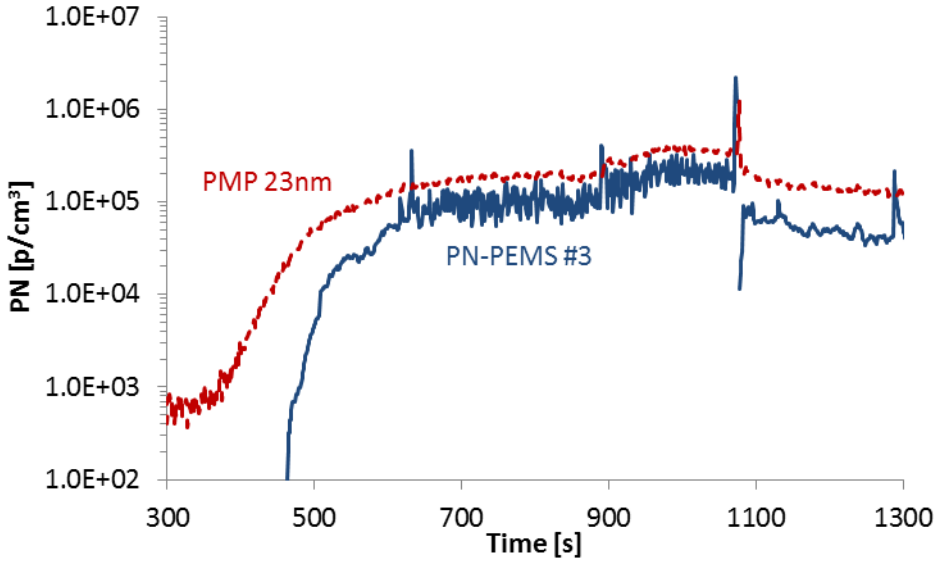

Figure 8-11: Regeneration of DPF #2. Measurements from tailpipe.

8.6 Summary

Figure 8-12 gives the overview: the agreement of the estimated PN is very good (<25%) for the GDIs, however for the motorcycles higher differences are observed (25%-70%).

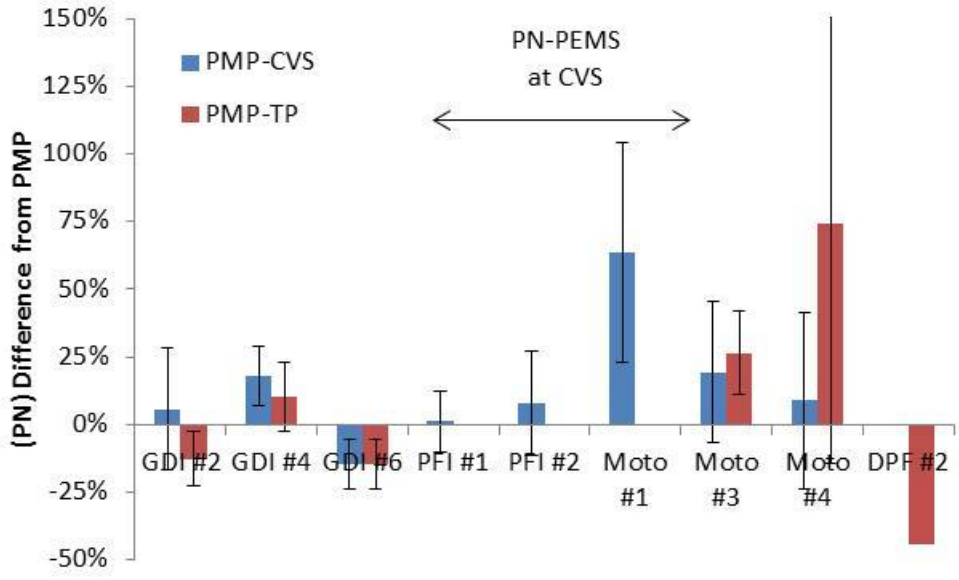

Figure 8-12: Overview of differences of PN-PEMS (based on the estimated PN) from the PMP-CVS and PMP-TP. Error bars are one standard deviation

Another way of evaluating the PN-PEMS is by plotting the results of the PN-PEMS vs the PMP-CVS. By setting the limit values one can visualize which tests would give a correct results (i.e. PASS when the PMP would give PASS or FAIL when the PMP system would give FAIL) or wrong (PASS for FAIL or FAIL for PASS). Figure 8-13 gives all results and Figure 8-14 focuses on the 6x10^11 p/km range. There are only a few tests where the PN-PEMS gave wrong result (PASS instead of FAIL).

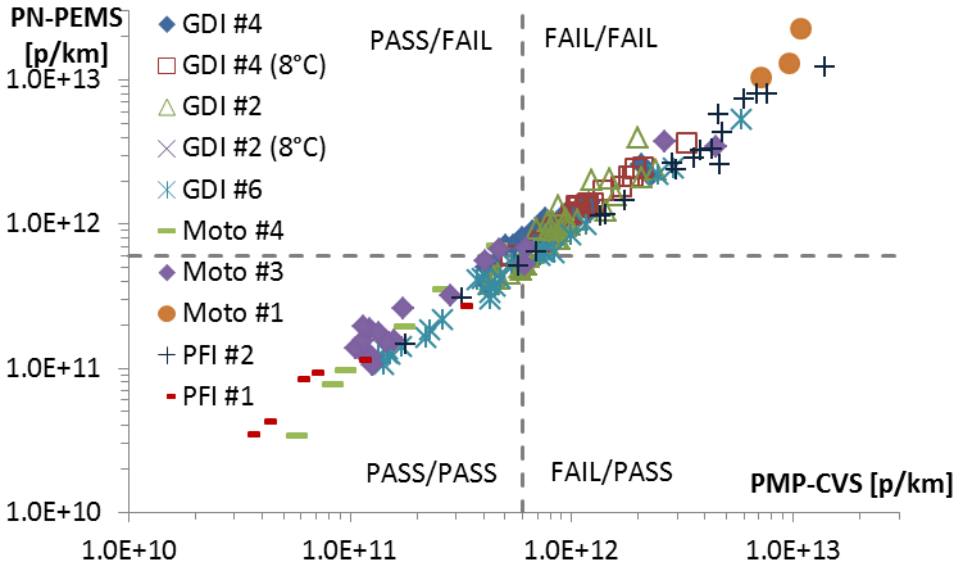

Figure 8-13: Overview of PMP vs PN-PEMS.

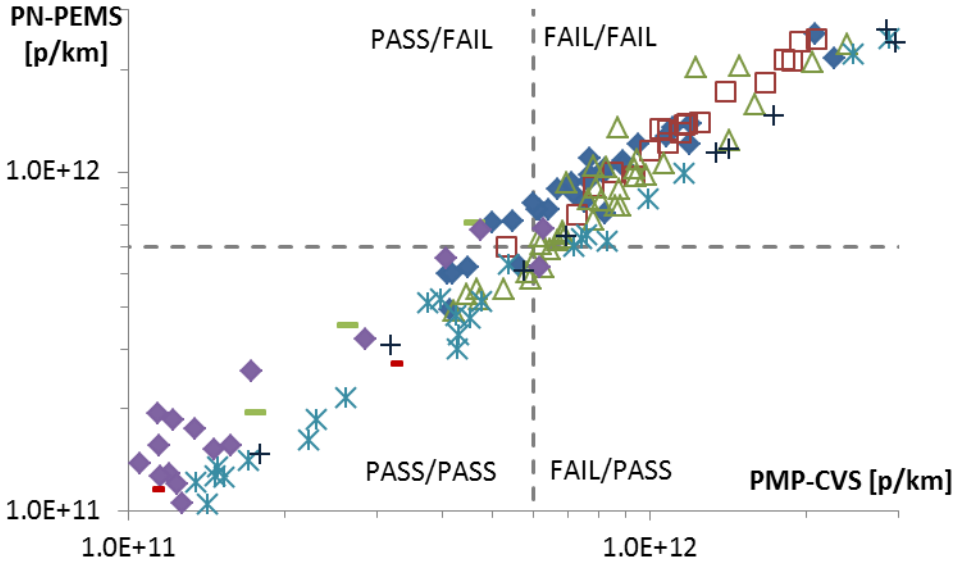

Figure 8-14: Detail of previous Figure.

8.7 On-road evaluation

The PN-PEMS was used to measure the PN emissions of a GDI #3 on the road. The ambient temperature was around 14°C. The tests were conducted successfully without any particular issue.

9 PN-PEMS #3 (LDSA)

The DC (Fierz et al. 2011) of PN-PEMS #3 gives Lung Deposited Surface Area (LDSA) in $\mu m^2/cm^3$. A constant factor C of 335 was also included to convert the $LDSA$ to particle number (reading). This value was based on the calibration conducted at JRC (see below). Thus the reading R of the instrument was:

$$R_{PN-PEMS} = C\ LDSA\ PCRF$$

The following results refer to the $LDSA$ value of the device. Further evaluation after the end of the campaign can be found in Annex D.

9.1 Calibration

The PN-PEMS was calibrated at the beginning and at the end of the measurement campaign with monodisperse aerosol from a spark-discharge graphite generator. Details can be found in Giechaskiel et al. (2014). The ratios of the efficiencies to the 100 nm efficiency can be seen in Table 9-1. They are almost identical and comply with the draft requirements. In the same table the efficiencies of the manufacturer only for the DC are shown (normalized to 100 nm).

Table 9-1: Ratios of efficiencies.

Dp [nm]	23	30	50	80	100	150	200
Start	10%	15%	34%	68%	100%	160%	223%
End	8%	16%	35%	69%	100%	165%	221%
Manuf	21%	27%	47%	79%	100%	155%	211%

At a next step the calibration factor was calculated. The procedure hasn't been decided yet, but the suggestions are normalization at:

1. d_p=100 nm (monodisperse) (i.e. no extra correction)
2. d_p=70 nm (monodisperse) (i.e. with extra correction)
3. GMD=75 nm (polydisperse) (i.e. no extra correction)
4. GMD=55 nm (polydisperse) (i.e. with extra correction)

For simplicity reasons the second option was chosen (factor 335). Figure 9-1 shows the efficiencies with calibration factor optimizing the chassis tests. The two repetitions were in relatively good agreement (differences within 15%) and one of them is almost identical with the manufacturer's data. Note that the manufacturer's curve is only the DC and doesn't include the VPR which would decrease the efficiency of small particles due to diffusion losses.

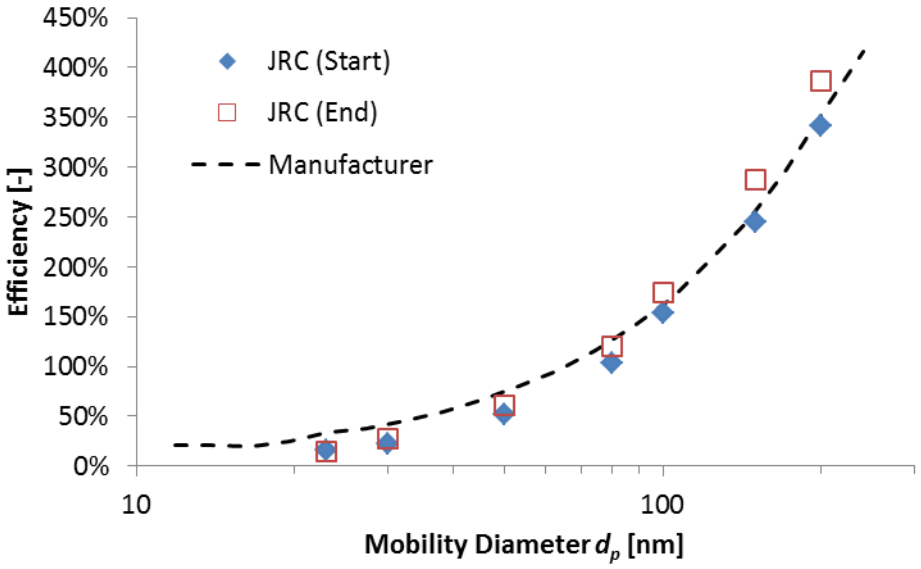

Figure 9-1: Results of monodisperse calibration of PN-PEMS at the beginning and end of the measurement campaign. The calibration factor is included.

Then the response of the PN-PEMS was compared with a PMP system or a simulated PMP system (using a SMPS and applying the theoretical efficiencies of a PMP system). The results can be seen in Figure 9-2. The scatter is quite high but probably it includes most cases that will be encountered in real working conditions. The differences range from -40% at GMD 30 nm to +100% at 110 nm. The main reason of the scatter is the size dependency of the PN-PEMS. However a 15% uncertainty comes from the calibration and a 10% offset comes from the PMP system.

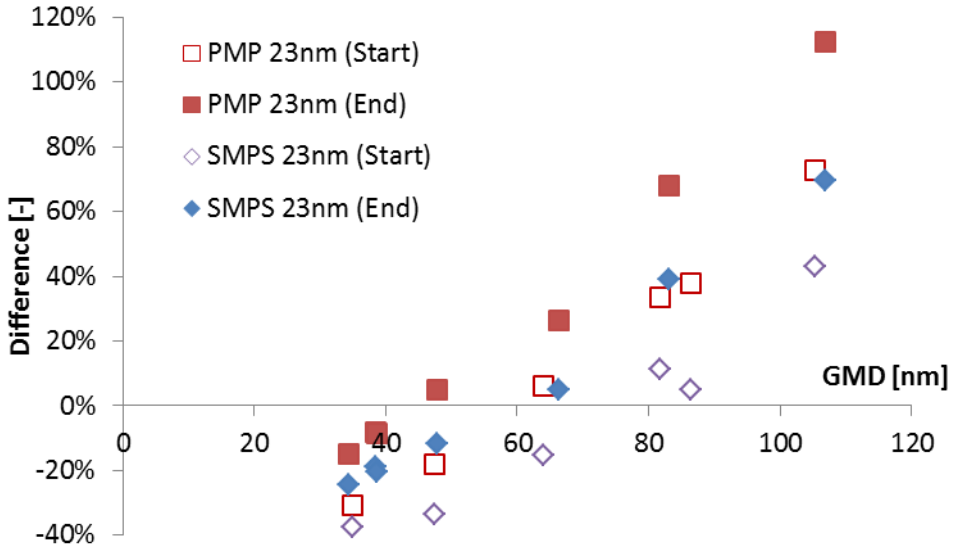

Figure 9-2: Comparison of PN-PEMS with PMP systems.

9.2 Real time

Figure 9-3 compares the PN-PEMS connected to the tailpipe with the PMP-TP. The PN-PEMS follows the PMP-TP system closely. In the real time figures the GMD is the 5s moving average.

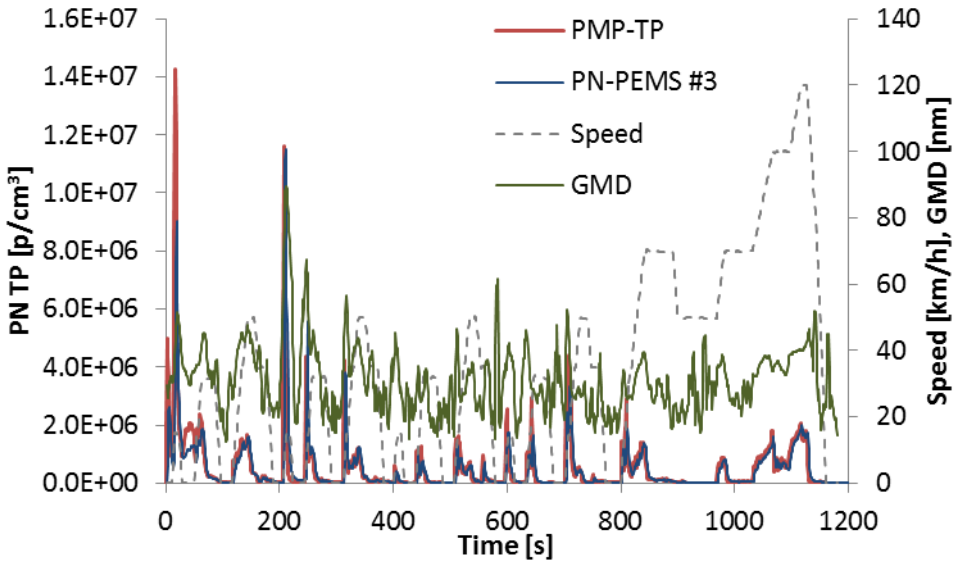

Figure 9-3: Comparison of PN-PEMS to the PMP-TP, both connected to the tailpipe (20141111-01-NEDC cold, GDI #4).

Similar behaviour was shown with other GDI vehicles (Figure 9-4):

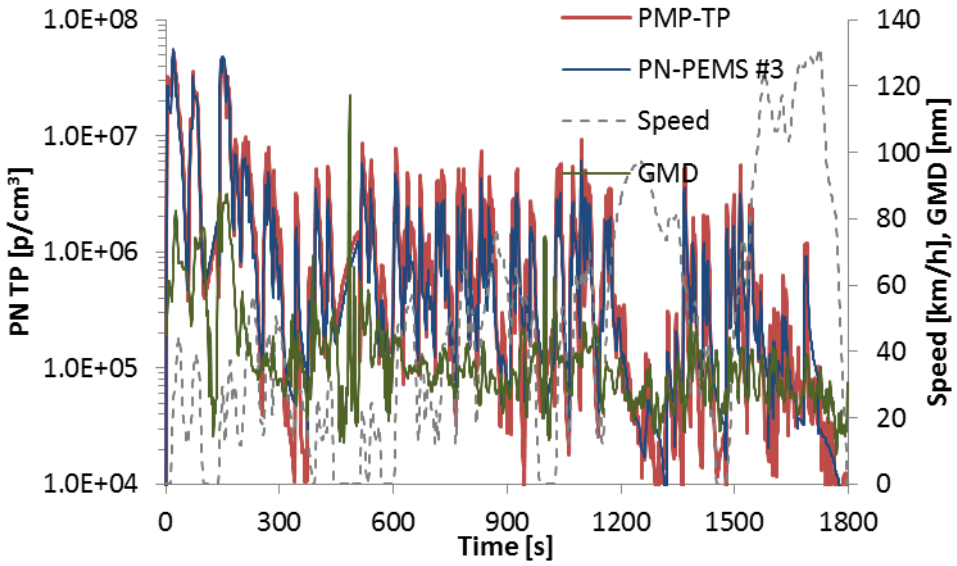

Figure 9-4: Comparison of PN-PEMS to the PMP-TP, both connected to the tailpipe (20141203-01-WLTC cold, GDI #6).

9.3 Comparison to PMP-CVS

The PN-PEMS was connected to the tailpipe for different GDI vehicles. The comparison with the PMP system at the CVS (PMP-CVS) can be seen in Figure 9-5. The differences range approximately from -30% to +35% for different emission levels.

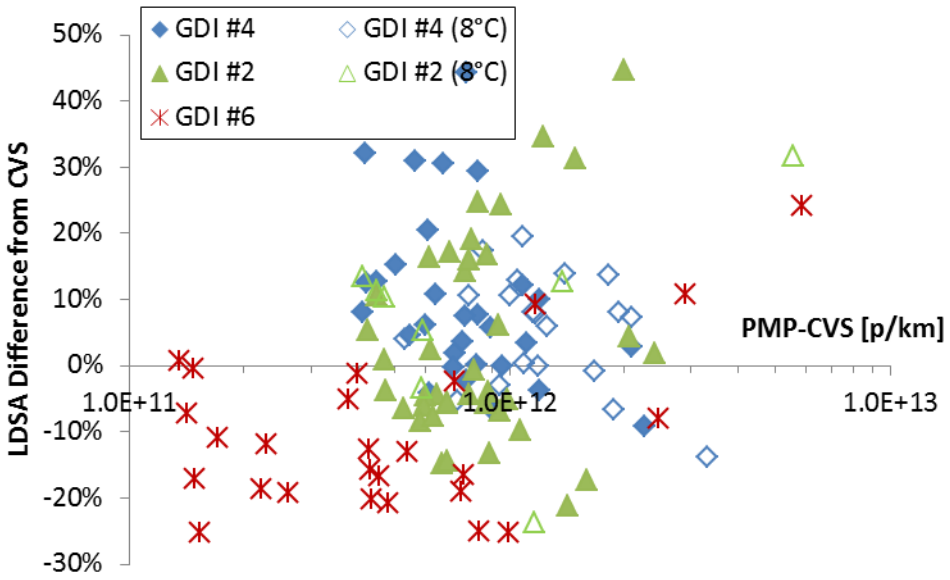

Figure 9-5: Summary of comparisons between PN-PEMS and PMP-CVS. PN-PEMS connected to the tailpipe.

9.4 Comparison to PMP-TP

The difference of the PN-PEMS from the PMP at the tailpipe (PMP-TP) can be seen in Figure 9-6. The differences range from -40% up to +20%.

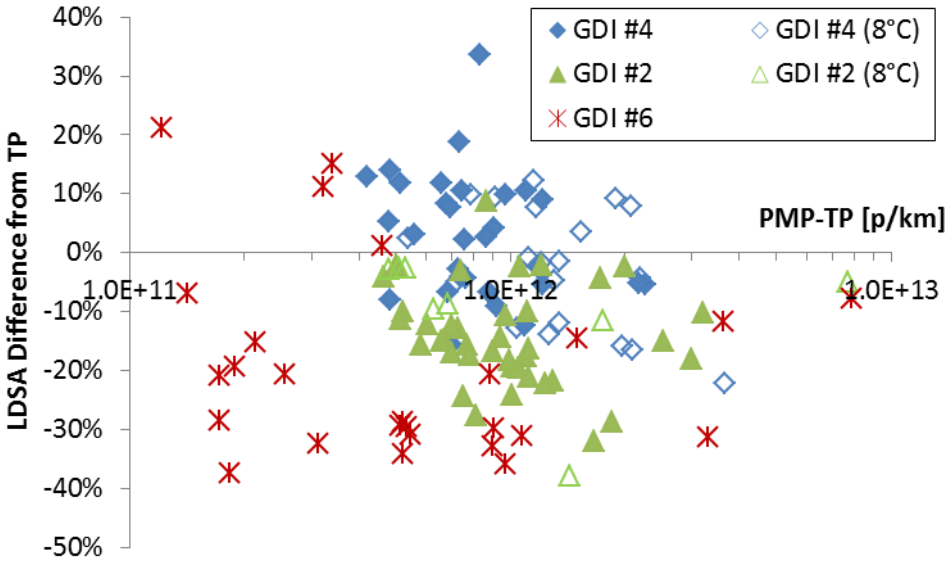

Figure 9-6: Summary of comparisons between PN-PEMS and PMP-TP. Both connected to the tailpipe.

9.5 Particle size effect

The difference of the PN-PEMS from the PMP-CVS was plotted in function of cycle mean particle size (Figure 9-7). There is no clear size dependency trend, or the small tendency is masked by the measurement variability between the different vehicles. In these figures GMD is the average of cycle.

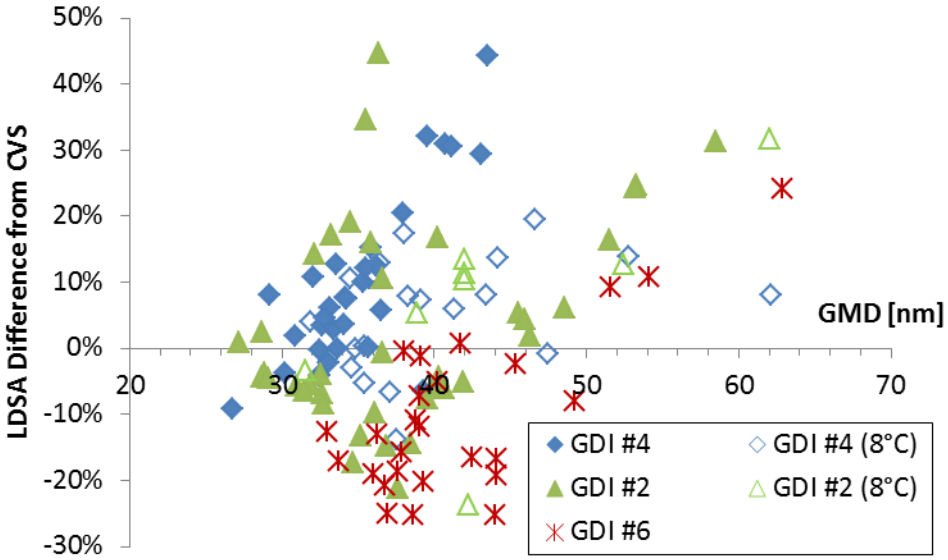

Figure 9-7: Size dependency of PN-PEMS.

9.6 Ambient temperature

No effect of the ambient temperature down to 8°C was observed (see previous figures). The behaviour was the same as during the 23°C tests.

9.7 Challenge aerosol (motorcycles)

The PN-PEMS was used also to measure exhaust aerosol of motorcycles. Moto #3 is a 4-stroke 50 cm^3 moped with max speed around 30 km/h (modified). Moto #4 is a 4-stroke 125 cm^3 motorcycle with max speed around 90 km/h. The specific motorcycles were producing particles with mean less than 20 nm. Thus the PN-PEMS could overestimate the emissions (because it doesn't have counting efficiency 0 at small sizes) or underestimate the emissions (because the response function decreases with size).

The PN-PEMS compared to the PMP-TP can be seen in Figure 9-8 in function of the mean cycle size. The differences are approximately -50% to -5%. No clear size dependence could be observed at these sub-30 nm sizes.

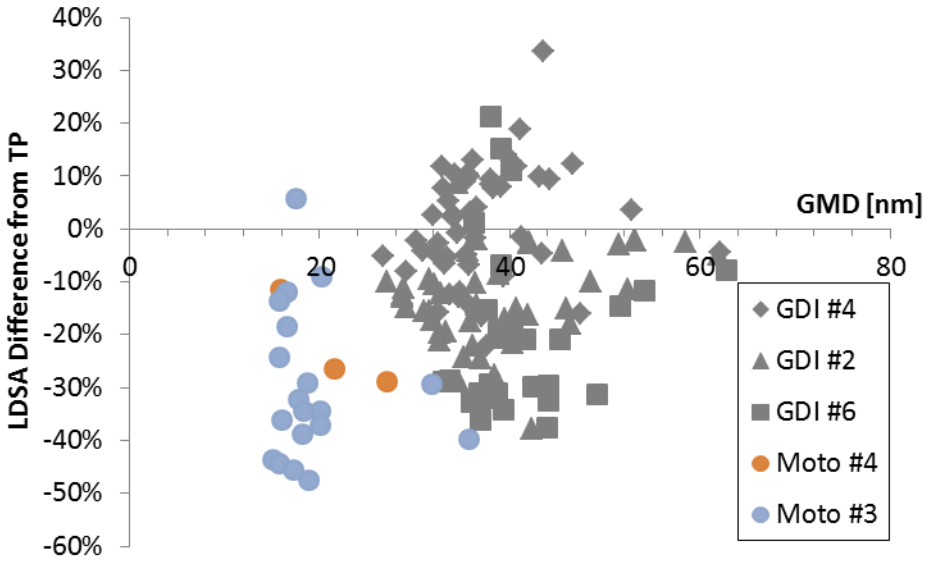

Figure 9-8: Size dependency of PN-PEMS when measuring motorcycles' exhaust.

9.8 Volatile removal efficiency

The volatile removal efficiency of the PN-PEMS was evaluated by measuring from the CVS diluted aerosol of a 2-stroke 50 cm^3 moped (Moto #1). The size distribution at the CVS has a mean around 90 nm. After thermal pre-treatment the mean decreases to <20 nm. The results (with the previous motorcycles) are shown in Figure 9-9. The PN-PEMS measures 40% less than the PMP-CVS indicating that the size of the particles were efficiently decreased and there was no re-nucleation that could influence the results.

In the same figure some tests with PFIs are shown. For these vehicles the differences range from -10% up to +70%, slightly higher compared to the GDIs. However the highest differences are observed for the tests where the emissions were much lower than 1x10^11 p/km. The PN-PEMS was used at the CVS, thus it was measuring close to its detection limit.

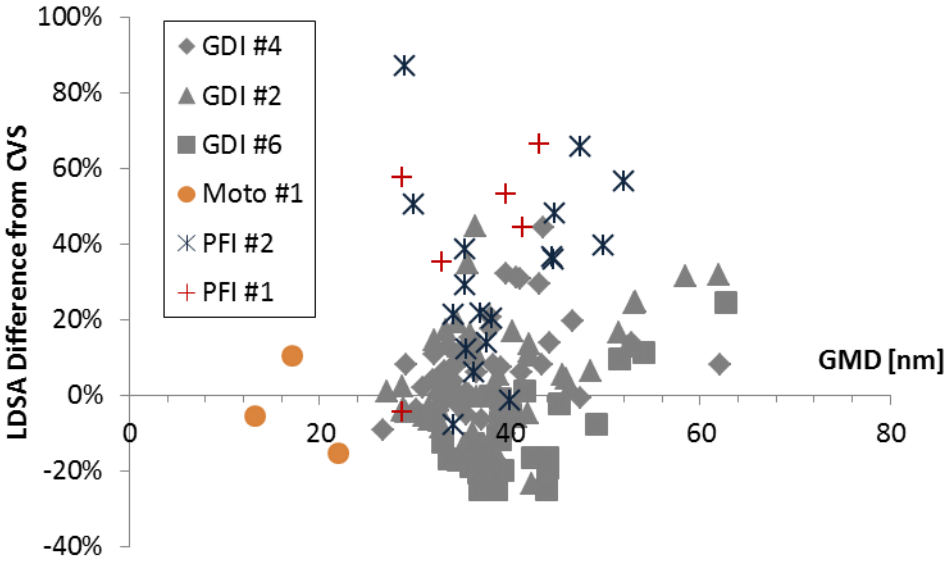

Figure 9-9: Behaviour of PN-PEMS when measuring moped's exhaust.

9.9 Regeneration

The PN-PEMS was connected to the tailpipe and was measuring in parallel with the PMP-TP the emissions of a diesel vehicle equipped with a DPF (#2). Figure 9-10 compares the systems. The PN-PEMS is overestimating the emissions 44%. Based on the PN-PEMS size information the mean diameter was 140 nm; for this reason the current was higher. This indicates that only an evaporation tube might not be enough to completely remove the volatiles.

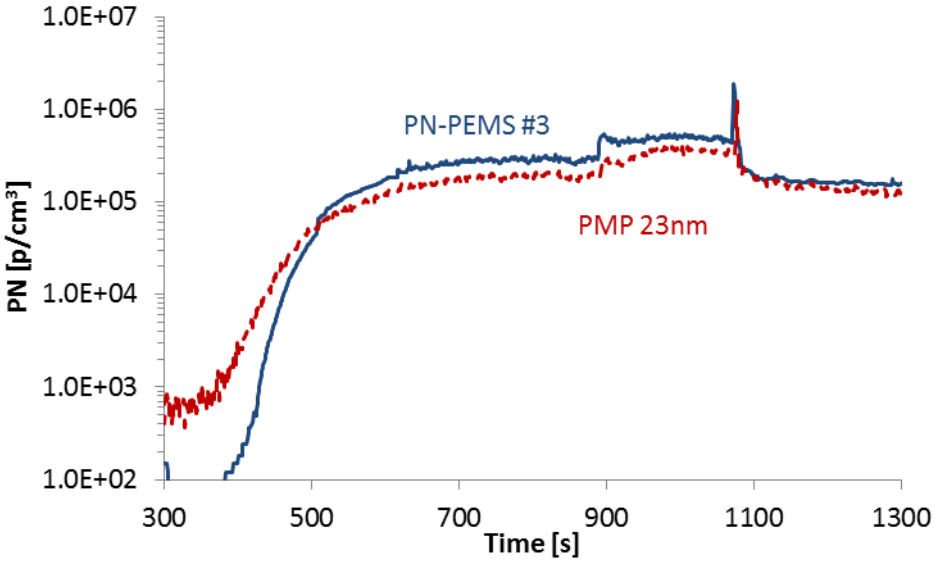

Figure 9-10: Regeneration of DPF #2. Measurements from tailpipe.

9.10 Summary

Figure 9-11 summarizes the differences of the PN-PEMS from the PMP-CVS and PMP-TP for all cases examined. For GDIs, the mean differences are -20% to 10% with a variability (expressed as ±standard deviation) of ±10%. For the PFIs, which were measured with the PM-PEMS at the CVS, the differences are +0% to +40% with higher variability in one case (±20%). For the motorcycles, the mean differences are around -30%. Assuming that when the error bars cross the 0% the PN-PEMS is equivalent with the PMP-CVS, in most cases the PN-PEMS measures equivalently with the PMP-CVS.

Table 9-2 shows the PASS/FAIL results of the PMP-TP and the PN-PEMS compared to the PMP-CVS assuming a 6x10^11 p/km limit. The success rate (i.e. catching a FAIL as FAIL or a PASS as PASS) is very high and similar to the PMP-TP

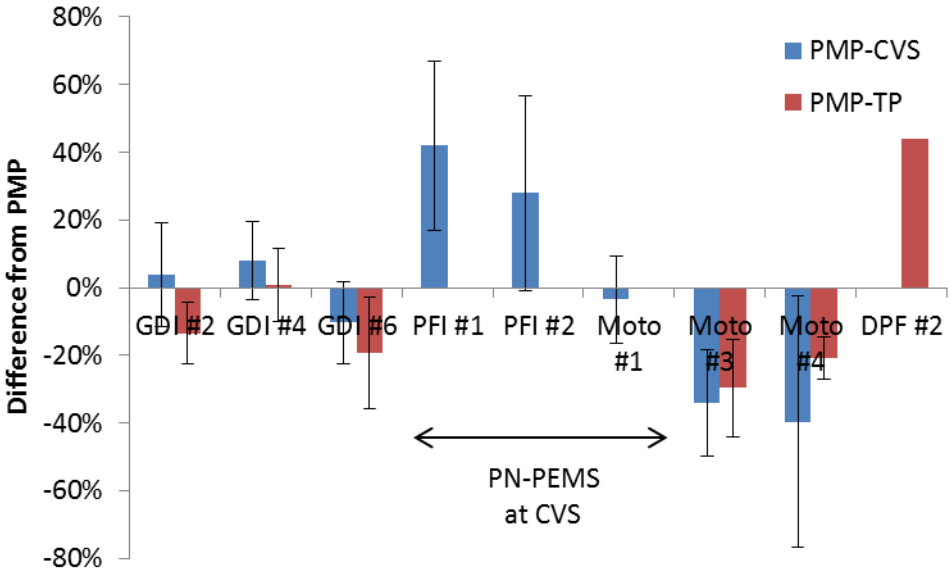

Figure 9-11: Overview of differences of PN-PEMS from the PMP-CVS. Error bars are one standard deviation.

Table 9-2: PASS/FAIL success rate.

Vehicle	Lab	Category	# of tests	PMP-TP	PN-PEMS
GDI #4	VELA 2	PASS	9	78%	78%
	VELA 2	FAIL	41	100%	98%
GDI #2	VELA 2	PASS	13	62%	92%
	VELA 2	FAIL	41	100%	91%
GDI #6	VELA 2	PASS	13	100%	100%
	VELA 2	FAIL	9	100%	100%
Moto #4	VELA 1	PASS	6	83%%	100%
	VELA 1	FAIL	0	-	-
Moto #3	VELA 1	PASS	15	100%	100%
	VELA 1	FAIL	4	50%	50%
Moto #1 (CVS)	VELA 1	PASS	0	-	-
	VELA 1	FAIL	3	-	100%
PFI #1 (CVS)	VELA 1	PASS	6	-	100%
	VELA 1	FAIL	0	-	-
PFI #2 (CVS)	VELA 1	PASS	3	-	67%
	VELA 1	FAIL	16	-	100%
DPF #2 (CVS)	VELA 2	PASS	2	-	100%
	VELA 2	FAIL	1	-	100%

9.11 Adjustment of PN-PEMS

The PN-PEMS based on DCs have an inherent uncertainty due to their dependency on particles size. Even when calibrated it is possible to have a 'bias' for vehicles that emit particles in a different size range. The topic was investigated by conducting different cycles in one day and comparing the difference of the PN-PEMS to the PMP-CVS.

The results for all sub-cycles are presented in Figure 9-12. The specific vehicle emits particles with a high mean at the beginning of the test. Thus, the PN-PEMS is overestimating the emissions by 30% (first part of the NEDC). At the subsequent part the PN-PEMS is measuring close to the PMP-CVS. The next hot RDEs show similar differences to the PMP-CVS (around -10%). Next day the 'hot' sub-cycles ranged from -25% to -10%. Excluding the 'cold' starts all cycles range from -20% to +5% approximately. The behaviour of the car on the road is expected more similar to the 'hot' sub-cycles. Thus a calibration with a 'hot' cycle would probably improve the 'bias'. However this should be checked with the real behaviour of the car on the road. Note that using the 'cold' WLTC to 'calibrate' the PN-PEMS could give wrong calibration factor (+17% average of the cycle).

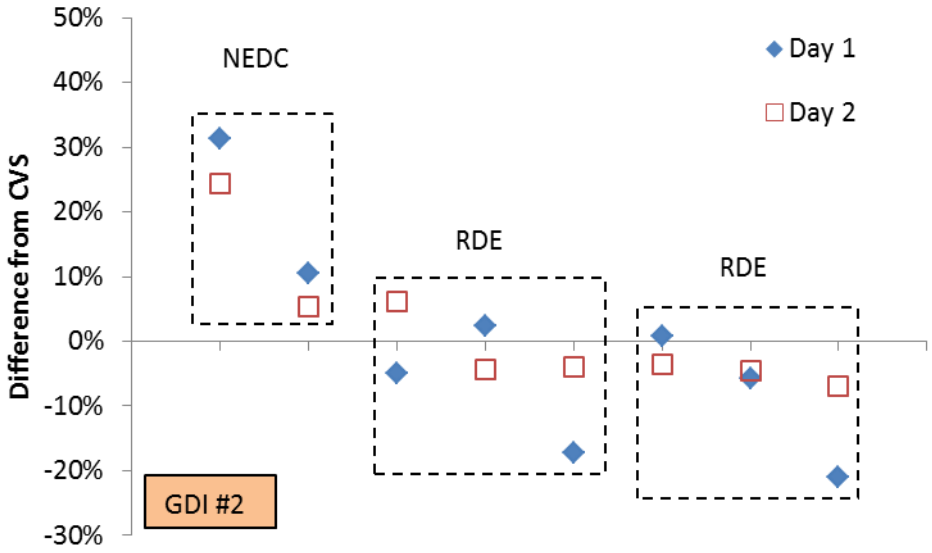

Figure 9-12: PN-PEMS behaviour over the day.

The same evaluation was followed for other vehicles (Figure 9-13). Similar behaviour was observed: The 'hot' emissions were approximately -15% to +10%.

Figure 9-14 summarizes the correction factors of the hot cycles. They are from -15% to -2%. An interesting observation is that the variability of the correction factor between the vehicles (17%) is not much higher than the variability of the correction of the different 'hot' cycles of the same car (15%). These correction factors are also very close to those of Figure 9-11. The reason is that the ratio of hot to cold cycles is high, so any cold start influence is minimized.

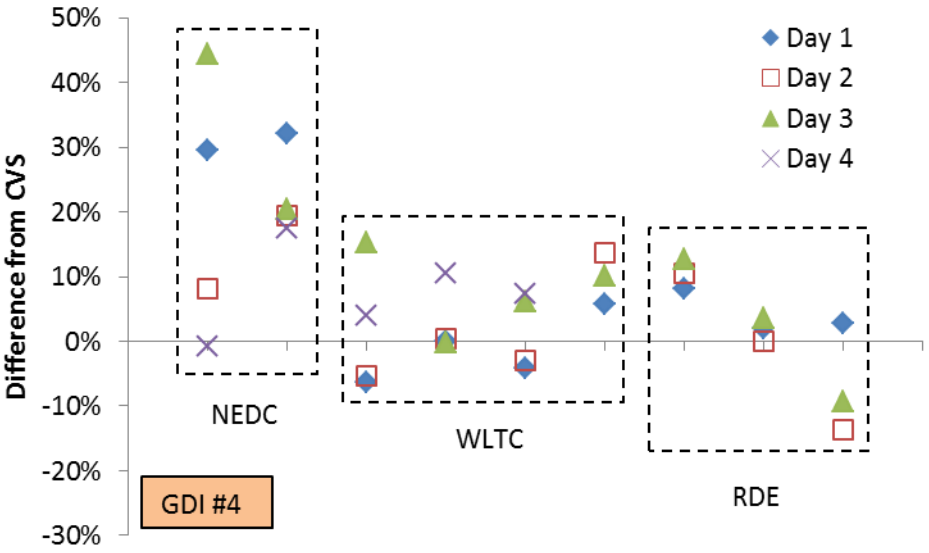

Figure 9-13: PN-PEMS behaviour over the day

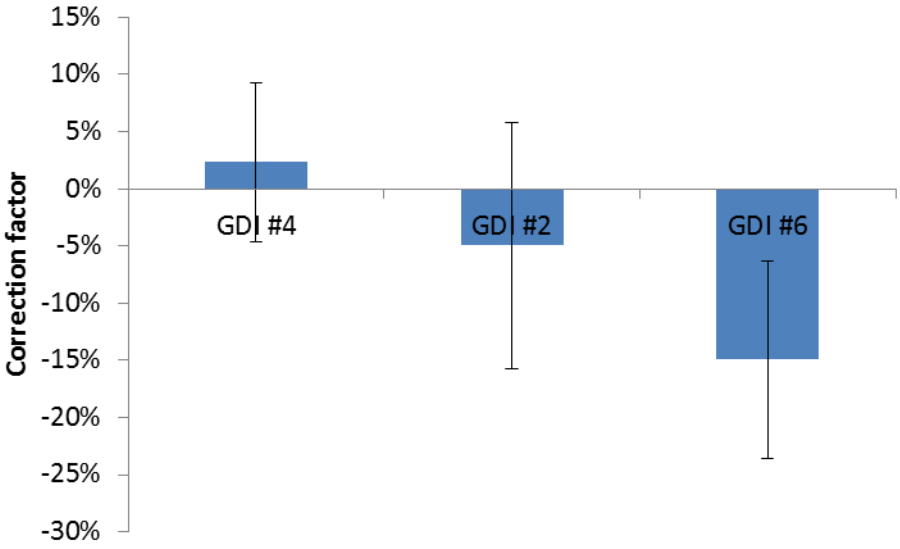

Figure 9-14: Summary of PN-PEMS calibration factor with hot cycles.

10 PN-PEMS #4

10.1 Description

PN-PEMS #4 (PPS, Pegasor) consists of a VPR and DC at the same unit. The sample is drawn through a 2 m heated line (200°C) by an ejector pump. The sample line and the whole unit with the DC are heated at 200°C. The PN-PEMS gives a current I [pA] which is proportional to the active surface of the particles. Based on the flow rate of the device Q [lpm], the current can be converted to particle number concentration. Thus the reading of the instrument is (see Ntziachristos et al. 2013):

$$R_{PN-PEMS} = C\,I$$

The constant C is a function of the inlet DC flow Q [lpm]. For trap voltage 400 V (see Ntziachristos et al. 2013).

$$C = \frac{288000}{Q}$$

A flow of 5.5 lpm was measured giving a value of C=52400. This calibration was based on light-duty vehicles with GMD around 50 nm which is in agreement with a monodisperse aerosol of 70 nm (or polydisperse of 55 nm), thus no other modification was applied. Detailed description can be found elsewhere (e.g. Rostedt et al. 2014).

10.2 Real time

Initially the PN-PEMS was connected to the CVS and was compared with the PMP-CVS system (Figure 10-1).

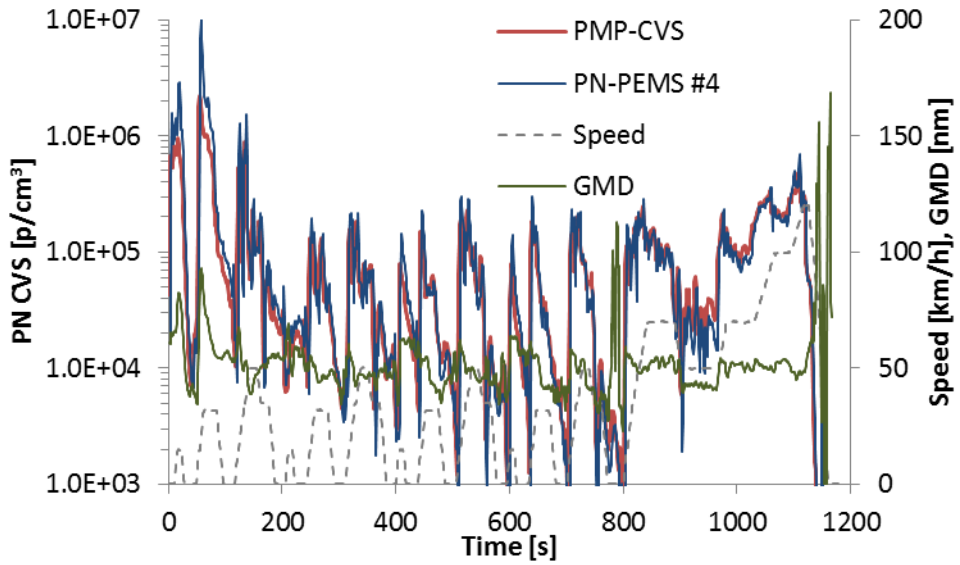

Figure 10-1: Comparison of PN-PEMS to PMP-CVS, both connected to the CVS (20141029-01-NEDC cold, GDI #1).

The PN-PEMS follows the PMP-CVS system closely especially when the mean size is <50 nm. At higher sizes the emissions are overestimated and probably the cold start increases the difference (maybe insufficient temperature at PN-PEMS to remove the volatile particles). In the real time figures GMD is 5s moving average. Similar behaviour was shown when the PN-PEMS was connected to the tailpipe (Figure 10-2):

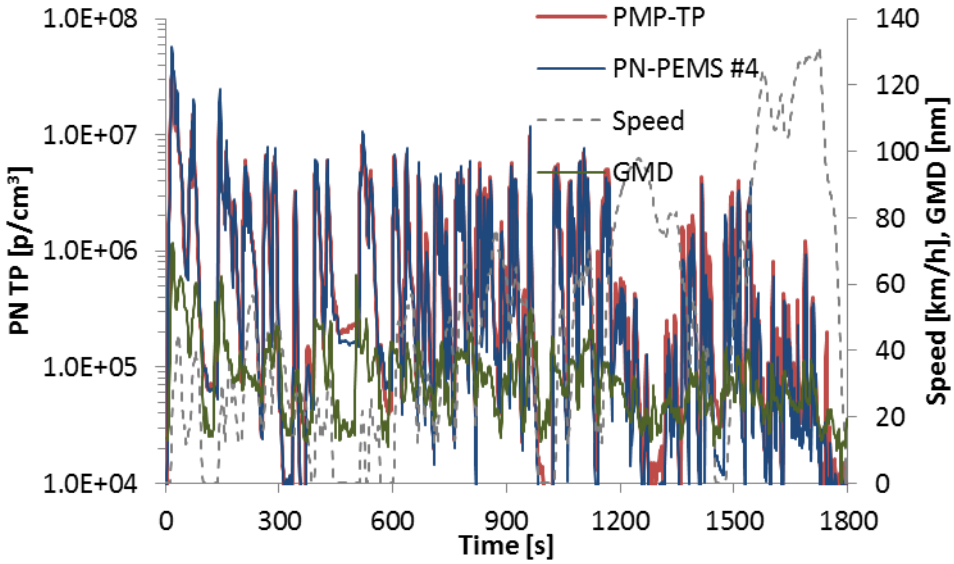

Figure 10-2: Comparison of PN-PEMS to the PMP-TP, both connected at the tailpipe.

10.3 Comparison to PMP-CVS

The PN-PEMS was connected to the tailpipe for different vehicles. The comparison with the PMP system at the CVS (PMP-CVS) can be seen in Figure 10-3.

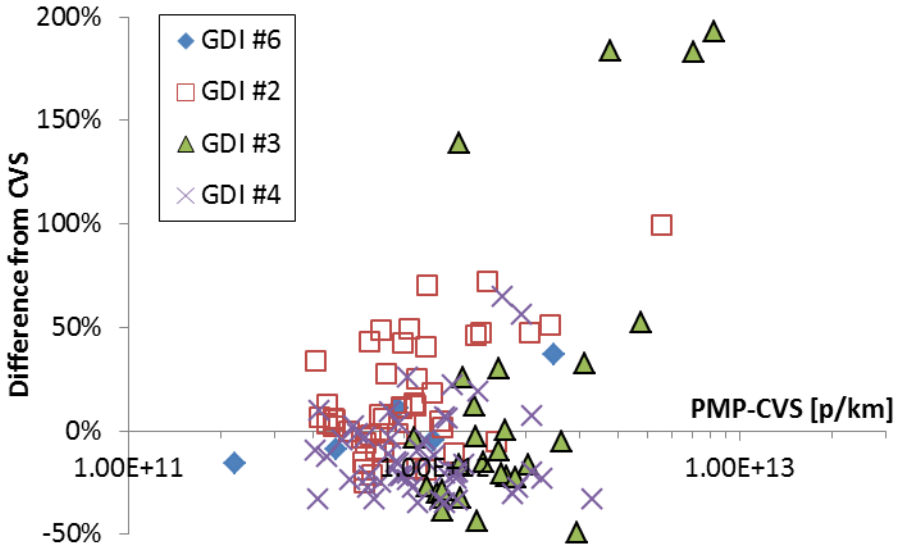

Figure 10-3: Summary of comparison of PN-PEMS to PMP-CVS.

The differences range from -50% to +100% approximately for different emission levels (with a few exceptions that will be discussed later). Figure 10-3 also shows the results for the vehicle that the PN-PEMS was connected to the CVS (GDI #1). The difference to the PMP-CVS is on the same order.

10.4 Comparison to PMP-TP

The difference of the PN-PEMS from the PMP at the tailpipe (PMP-TP) can be seen in Figure 10-4. The differences range from -50% up to +50% (with a few exceptions). There are some cases with differences of +100%. As it will be discussed later these are cold start emissions.

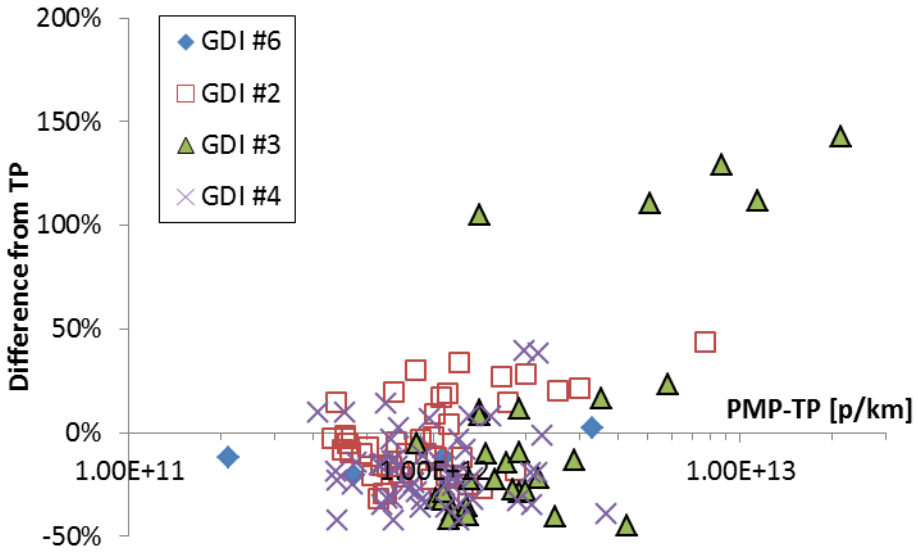

Figure 10-4: Summary of comparison of PN-PEMS to PMP-TP.

10.5 Particle size effect

The size dependency of the PN-PEMS response can be seen in Figure 10-5. The effect is <40% for a 10 nm change of the particle size. Similar trend was observed comparing the PN-PEMS with the PMP-TP (but smaller size effect) (Figure 10-6). In these figures GMD is the average of a cycle.

10.6 Ambient temperature

No effect of the ambient temperature down to 8°C was observed (Figure 10-7). The behaviour was the same as during the 23°C tests.

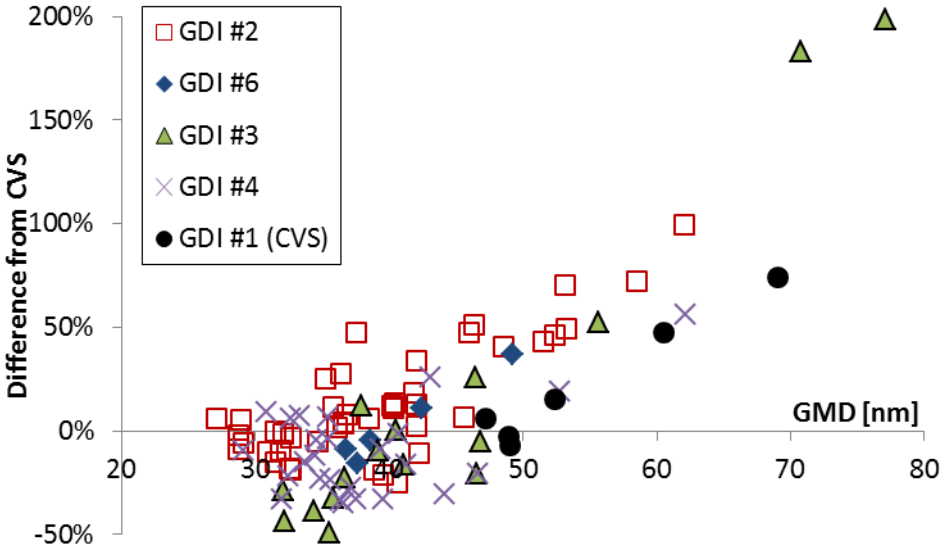

Figure 10-5: Size dependency of PN-PEMS.

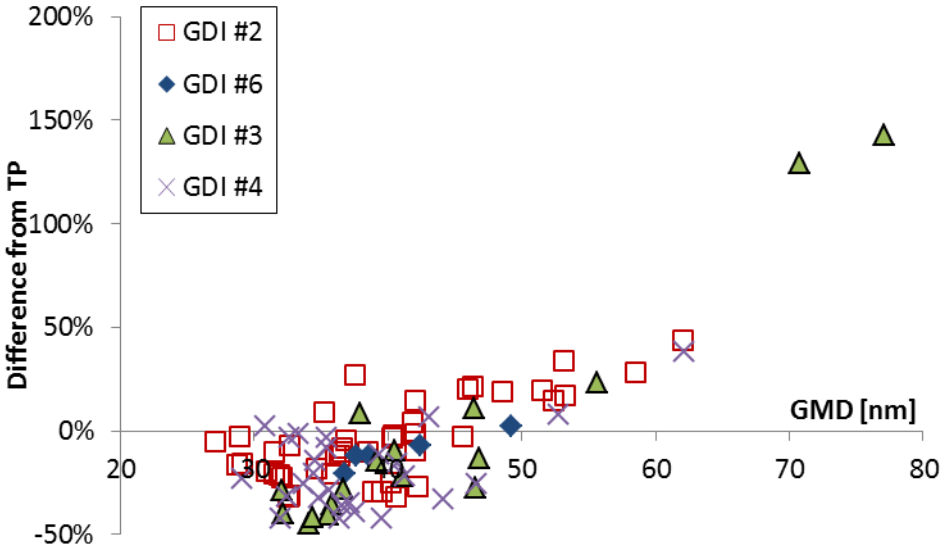

Figure 10-6: Size dependency of PN-PEMS.

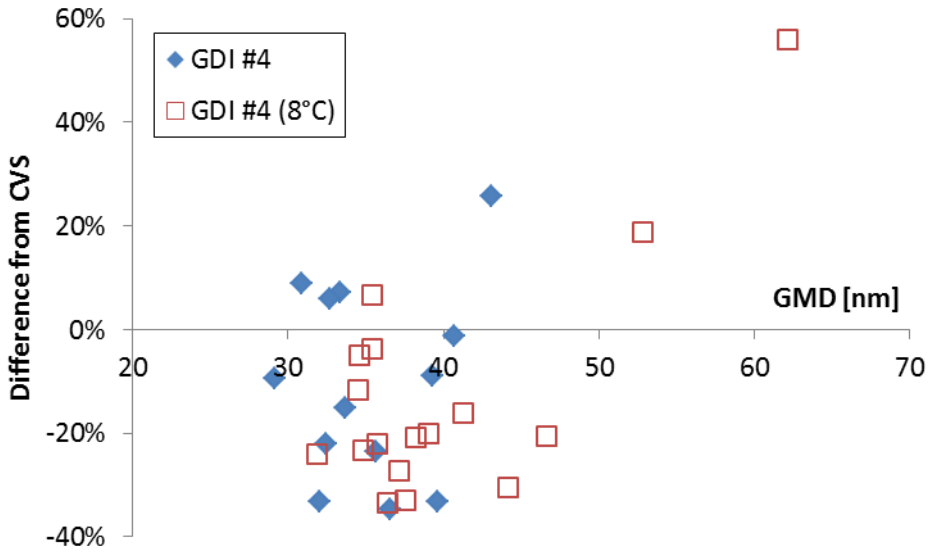

Figure 10-7: Ambient temperature effect on PN-PEMS.

10.7 Challenge aerosol (motorcycles)

The PN-PEMS was used also to measure exhaust aerosol of motorcycles. Moto #3 is a 4-stroke 50 cm^3 moped with max speed around 30 km/h (modified). Moto #4 is a 4-stroke 125 cm^3 motorcycle with max speed around 90 km/h. Moto #2 is a 4-stroke 400 cm^3 motorcycle. The motorcycles #3 and #4 were producing particles with mean less than 20 nm, while #2 around 35 nm. Thus the PN-PEMS could overestimate the emissions (because it doesn't have counting efficiency 0 at small sizes) or underestimate the emissions (because the response function decreases with size). The PN-PEMS compared to the PMP-CVS can be seen in Figure 10-8. The differences are approximately -60% to +60% for Moto #3 and #4. However for Moto #2 much higher differences are observed. This motorcycle had high percentage of sub-23 nm particles and it seems that the PN-PEMS is sensitive to particles smaller than 23 nm or the 200°C thermal pre-treatment is not sufficient to decrease the size of particles enough thus they are producing high current. Figure 10-9 shows the results in function of size.

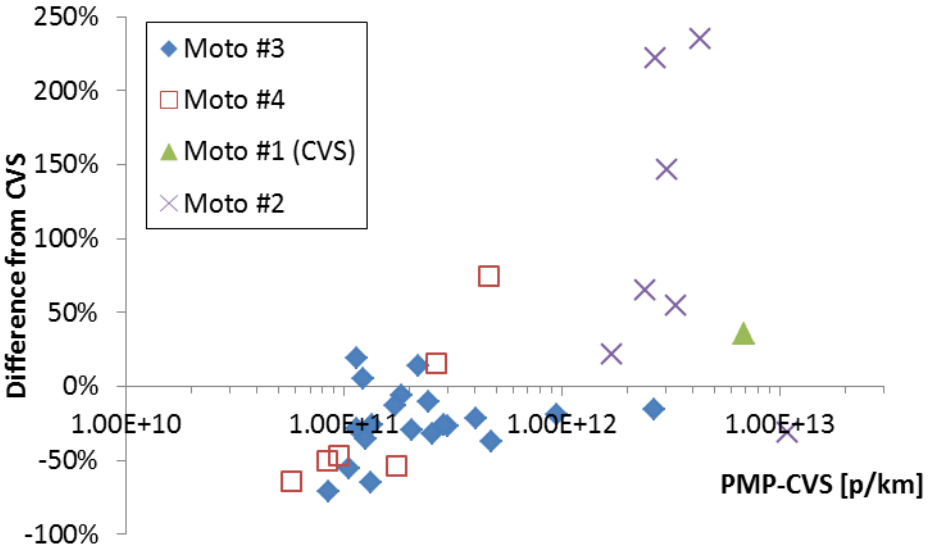

Figure 10-8: Behaviour of PN-PEMS with motorcycles exhaust.

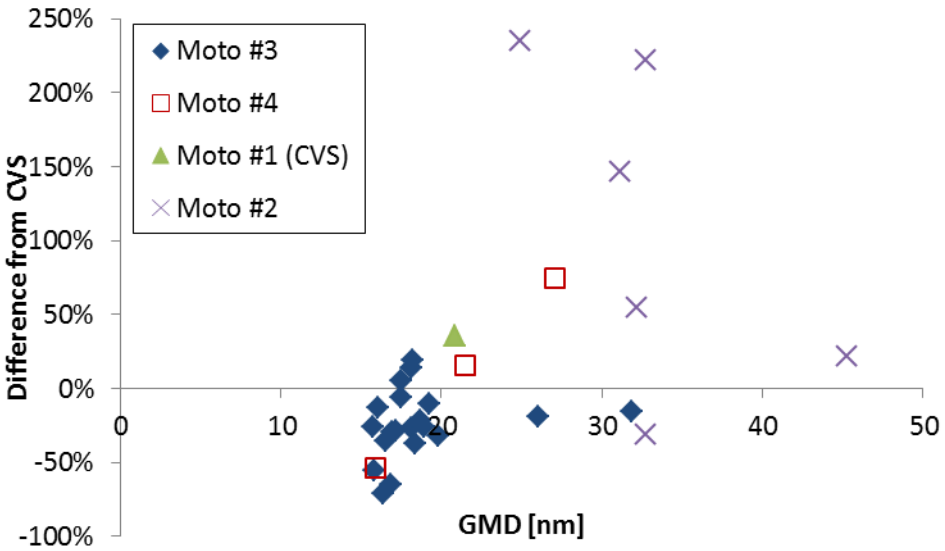

Figure 10-9: Size dependency of PN-PEMs when measuring motorcycles exhaust.

10.8 Volatile removal efficiency

The volatile removal efficiency of the PN-PEMS was evaluated by measuring from the CVS diluted aerosol from a 2-stroke 50 cm^3 moped (Moto #1). The size distribution at the CVS has a mean around 90 nm. After thermal pre-treatment the mean decreases to <20 nm. The results (with the previous motorcycles) are shown in Figure 10-8 and Figure 10-9. The PN-PEMS measures 60% more than the PMP-CVS which is quite similar to the difference of the rest motorcycles. Thus it seems that the size of the particles was efficiently decreased and there was no re-nucleation that could influence the results, or at least it's not at the size range that will affect the signal of the PN-PEMS significantly.

10.9 Summary

Figure 10-10 summarizes the differences of the PN-PEMS from the PMP-CVS and PMP-TP for all GDI cases examined. Figure 10-11 examines the rest cases (Motorcycles).

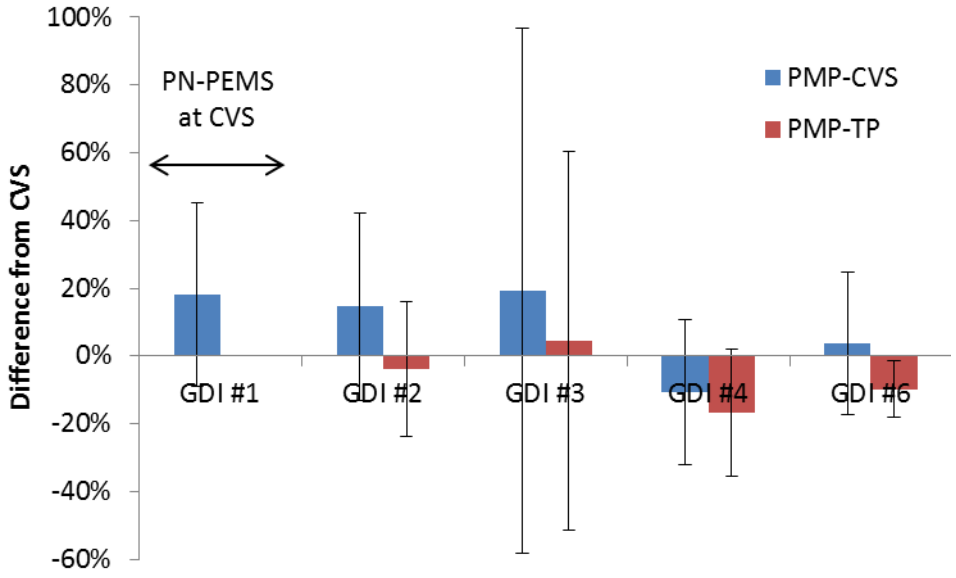

Figure 10-10: Overview of differences of PN-PEMS from the PMP-CVS. Error bars are one standard deviation.

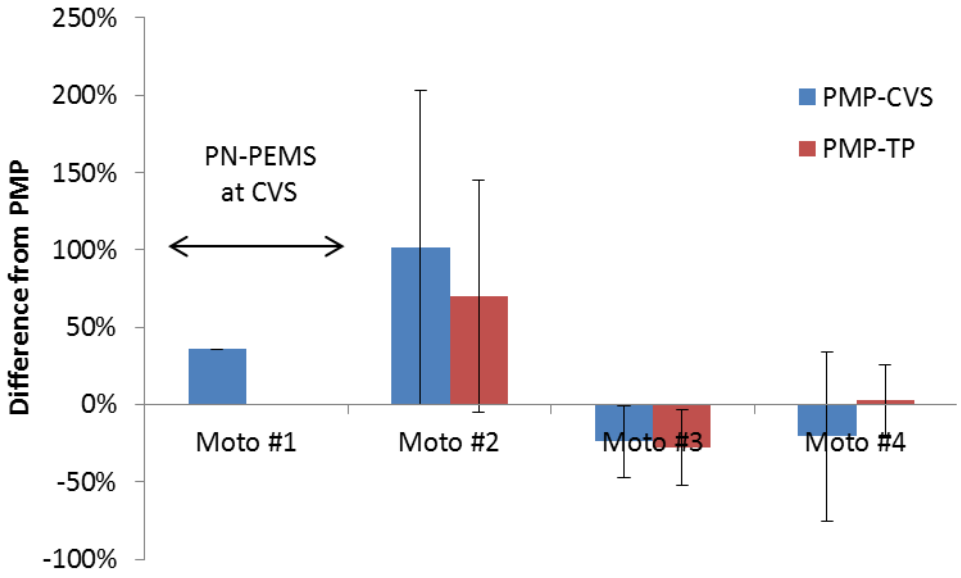

Figure 10-11: Overview of differences of PN-PEMS from the PMP-CVS. Error bars are one standard deviation.

For GDIs, the mean differences are -20% to +20% with a variability (expressed as ±standard deviation) of ±30% (or higher in one case). Three of the motorcycles had small differences from the PMP-CVS, but one had mean differences >50%. Assuming that when the error bars cross the 0% the PN-PEMS is equivalent with the PMP-CVS, in most cases the PN-PEMS measures equivalently with the PMP-CVS.

Another way of evaluating the PN-PEMS is by plotting the results of the PN-PEMS vs the PMP-CVS. By setting the limit values one can visualize which tests would give a correct results (i.e. PASS when the PMP would give PASS or FAIL when the PMP system would give FAIL) or wrong (PASS for FAIL or FAIL for PASS). Figure 10-12 gives all results and Figure 10-13 focuses on the 6x10^11 p/km range. There are a few tests where the PN-PEMS gave wrong result (PASS instead of FAIL) and as mentioned previously this had to do with the relatively high scatter of the results.

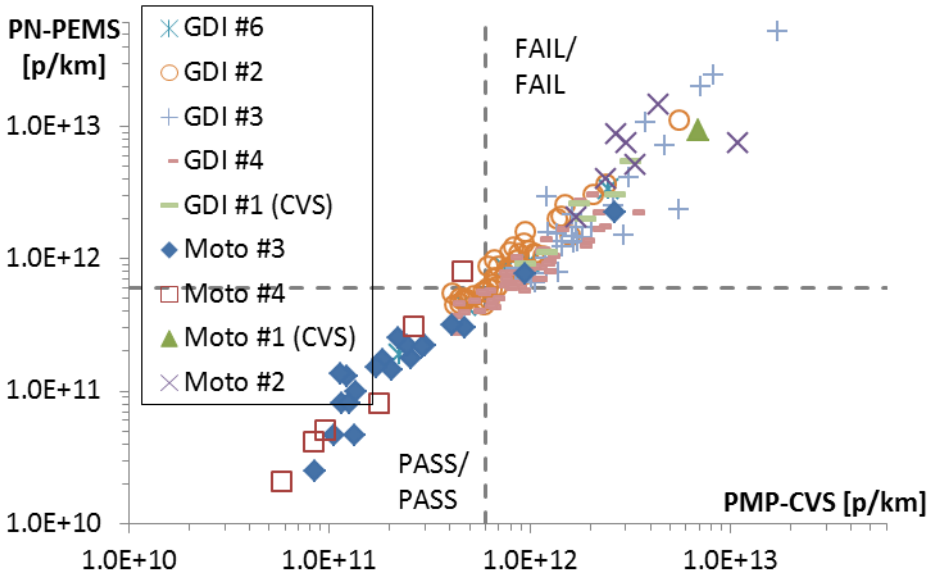

Figure 10-12: Overview of PASS/FAIL results

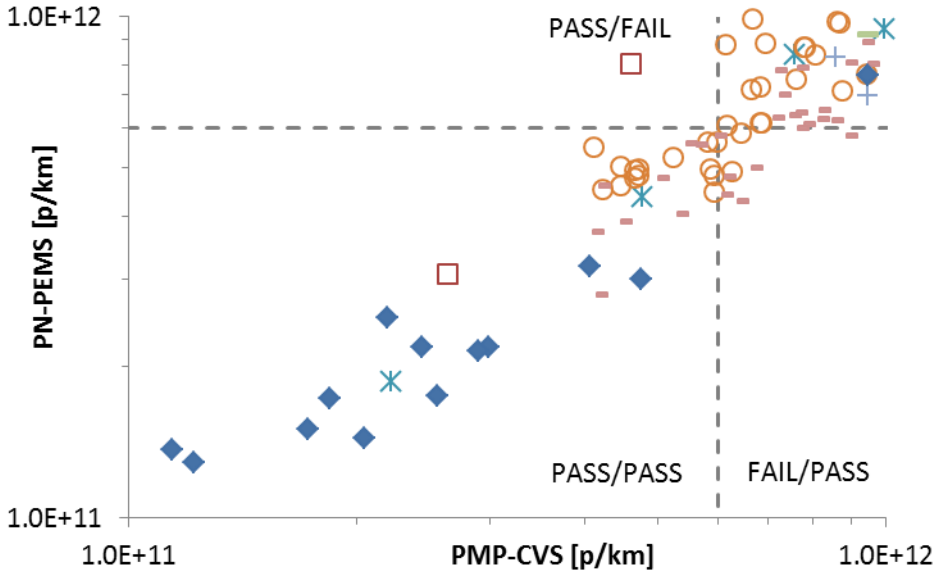

Figure 10-13: Detail of previous figure.

Table 10-1 shows the PASS/FAIL results of the PMP-TP and the PN-PEMS compared to the PMP-CVS assuming a 6x10^11 p/km limit. The success rate (i.e. catching a FAIL as FAIL or a PASS as PASS) is quite similar to the PMP-TP, but in some cases wrong results can occur (probably due to the high scatter of the results).

Table 10-1: PASS/FAIL success rate.

Vehicle	Lab	Category	# of tests	PMP-TP	PN-PEMS
GDI #3	VELA 2	PASS	0	-	-
	VELA 2	FAIL	30	100%	100%
GDI #4	VELA 2	PASS	9	78%	100%
	VELA 2	FAIL	41	100%	85%
GDI #2	VELA 2	PASS	13	62%	100%
	VELA 2	FAIL	32	100%	94%
GDI #6	VELA 2	PASS	2	100%	100%
	VELA 2	FAIL	3	100%	100%
GDI #1 (CVS)	VELA 2	PASS	0	-	-
	VELA 2	FAIL	9	-	100%
Moto #1 (CVS)	VELA 2	PASS	0	-	-
	VELA 2	FAIL	1	-	100%
Moto #4	VELA 2	PASS	6	83%	83%
	VELA 2	FAIL	0	-	-
Moto #3	VELA 2	PASS	18	100%	100%
	VELA 2	FAIL	2	100%	100%

10.10 Adjustment of PN-PEMS

The PN-PEMS based on DCs have an inherent uncertainty due to their dependency on particles size. Even when calibrated it is possible to have a 'bias' for vehicles that emit particles in a different size range. The topic was investigated by conducting different cycles in one day and comparing the difference of the PN-PEMS to the PMP-CVS.

The results for all sub-cycles are presented in Figure 10-14. The specific vehicle emits particles with a high mean size at the beginning of the test. Thus, the PN-PEMS is overestimating the emissions 70% (first part of the NEDC). At the subsequent part the PN-PEMS is similar to the PMP. For the next Random Driving Cycle a similar behaviour is observed. The next hot cycle has even smaller effect of the initial start of the cycle. Excluding the 'cold' starts all cycles range from -20% to +5% approximately. Next day the 'hot' sub-cycles ranged in the same range. The behaviour of the car on the road is expected more similar to the 'hot' sub-cycles. Thus a calibration with a 'hot' cycle would

probably improve the 'bias'. However this should be checked with the real behaviour of the car on the road. Note that using the 'cold' NEDC to 'calibrate' the PN-PEMS would give wrong calibration factor (+45% average of the cycle).

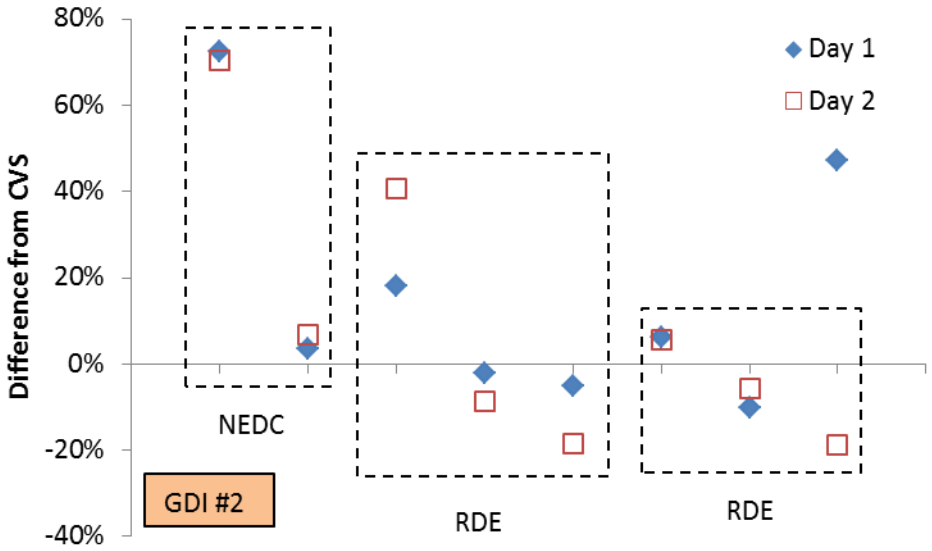

Figure 10-14: Behaviour of PN-PEMS over a day. Each point is a sub-cycle.

The same evaluation was followed for other vehicles (Figure 10-15). Similar behaviour was observed: The 'hot' emissions were approximately within 30% of the PMP-CVS.

An interesting observation is that the variability of the correction factor between the vehicles (20%: From -25% to -5%) is not much higher than the variability of the correction of the different 'hot' cycles for the same car (25%).

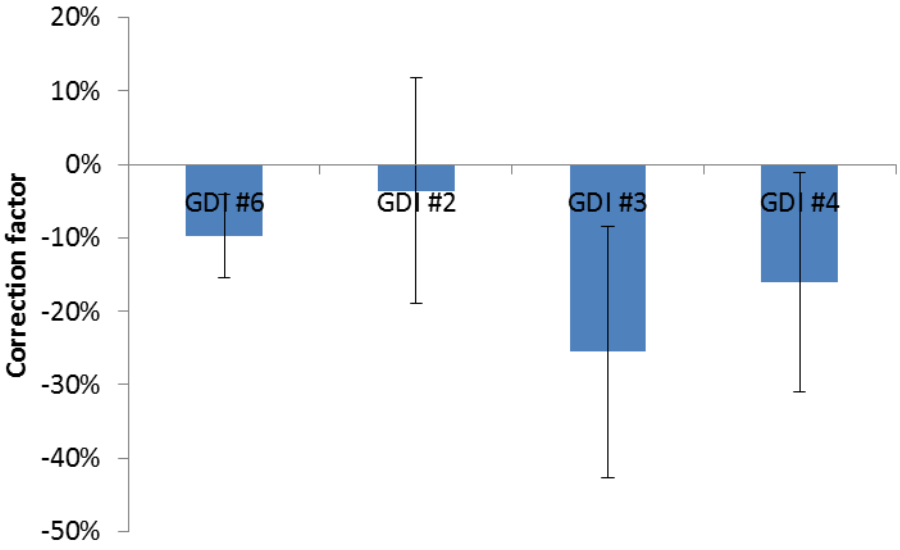

Figure 10-15: Summary of PN-PEMs correction factor based on hot cycles.

11 PN-PEMS #5'

11.1 Description

PN-PEMS #5' (Ecostar, Sensors) consists of a VPR and a DC (PPS from Pegasor). The VPR consists of a capillary diluter at 150°C, a heated line at 150°C and a catalytic stripper heated to 300°C. The hot aerosol was cooled down in a spiral coil before entering the DC. The primary dilution was estimated by the measured flows by the manufacturer and the dilution factor *DF* was typically 15-20. The particle losses for a similar system were measured at JRC so a factor of 1.3 was applied. The DC primarily measures the escaping current *I* which is proportional to the active surface (see Ntziachristos et al. 2013). The PN-PEMS converts the escaping current to particle number concentration with an internal constant *C*. Thus the reading *R* of the instrument was:

$$R_{PN-PEMS} = C\ I\ DF$$

The constant *C* is a function of the inlet DC flow *Q* [lpm] (see Ntziachristos et al. 2013). For a trap voltage of 400 V holds:

$$C = \frac{288000}{Q}$$

For the flowrate *Q* in the device (4.5 lpm) *C*=64000 and with the 1.3 loss correction *C*=83200, very close to the manufacturer's default value (80000). The calibration of the DC was based on optimization with light-duty particles (GMD 50 nm) which is close to the recommended monodisperse 70 nm recommendation (or 55 polydisperse). Thus no other correction was applied.

This device was also provided with a prototype CPC downstream of a venturi diluter (dilution around 150) downstream of the VPR. The CPC is a mixing type CPC with a cut-off size around 6 nm (as estimated by JRC). This CPC will be evaluated separately at the end of the chapter.

11.2 Real time

The PN-PEMS followed the signal of the PMP system at the tailpipe (Figure 11-1). When the mean size of the emitted particles was high, the PN-PEMS overestimated the emissions. Since there is a hot dilution and a catalytic stripper this overestimation is due to the size of particles and not due to incomplete removal of volatiles.

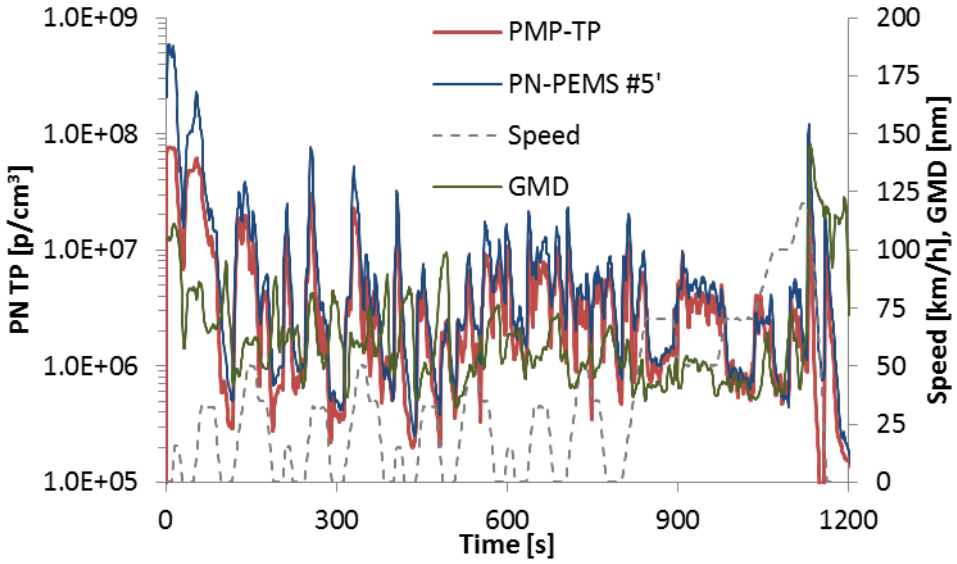

Figure 11-1: Comparison of PN-PEMS with PMP-CVS. PN-PEMS was connected to the tailpipe (20141106-01-NEDC cold, GDI #3).

Comparison of the signal of the DC (corrected for the dilution factor and the losses) with another PN-PEMS using the same sensor (PN-PEMS #4) showed good agreement (Figure 11-2).

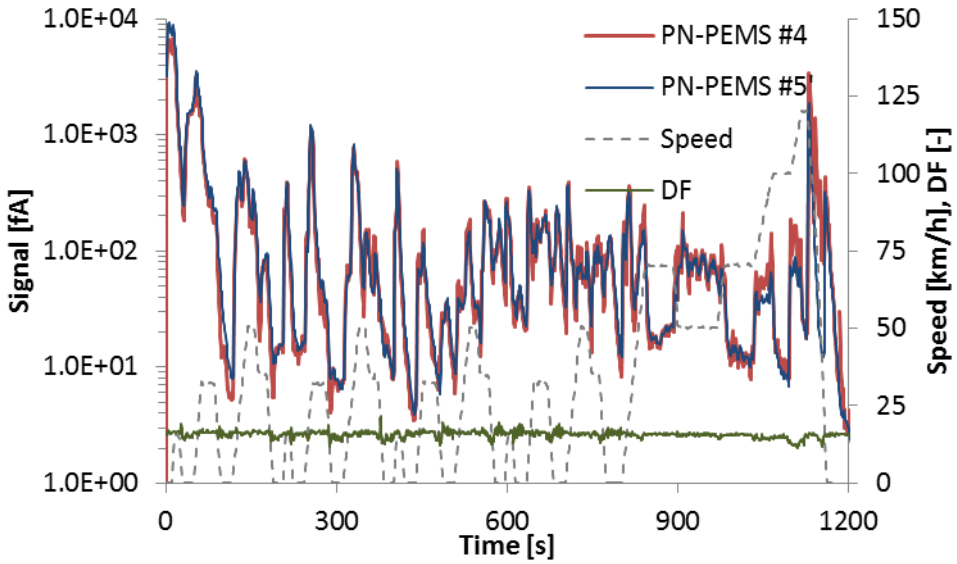

Figure 11-2: Comparison of two PN-PEMS.

Similar trends were observed with another vehicle (Figure 11-3, Figure 11-4). However there is a concern that at high speeds the emissions could be underestimated (probably an effect of the high flow, temperature or pressure) (see seconds 1700-1800).

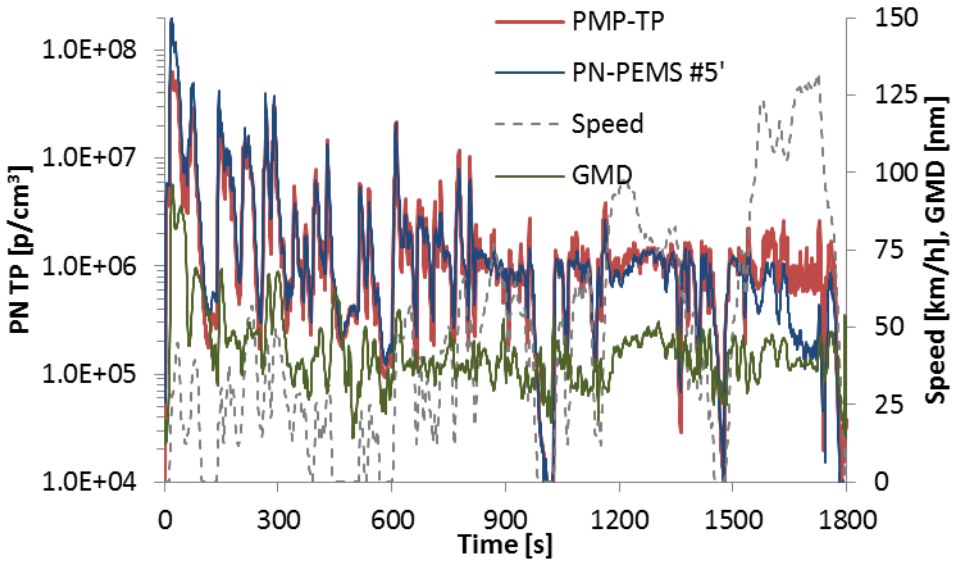

Figure 11-3: Comparison of PN-PEMS with PMP-TP (20141125-03-WLTC 8°C, GDI #2).

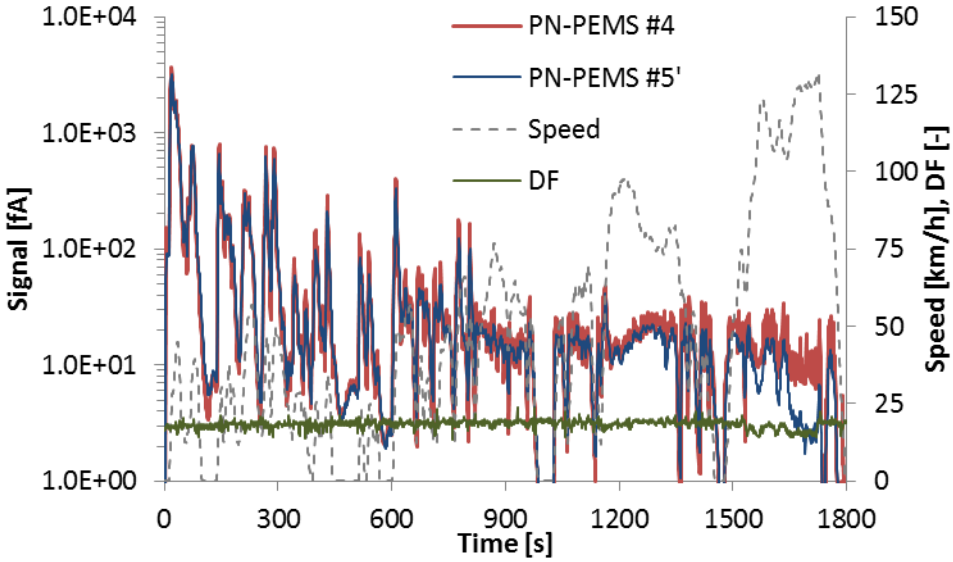

Figure 11-4: Comparison of two PN-PEMS.

11.3 Comparison to PMP-CVS

PN-PEMS #5' was always connected to the tailpipe. For the available tests, the difference to the PMP system at the CVS (PMP-CVS) is shown in Figure 11-5. The differences range from -50% to +150%. In some cases higher differences can be observed.

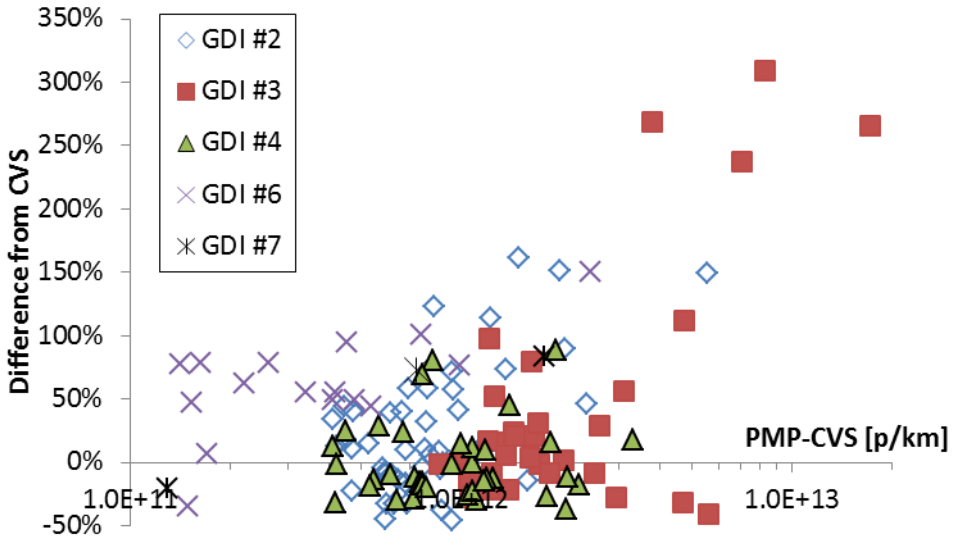

Figure 11-5: Summary of comparisons between PN-PEMS and PMP-CVS. The PN-PEMS was always connected to the tailpipe.

The same tests were plotted in function of the PMP system at the tailpipe (PMP-TP) (Figure 11-6). The difference ranges from -55% to +100% for most cycles with a few exceptions.

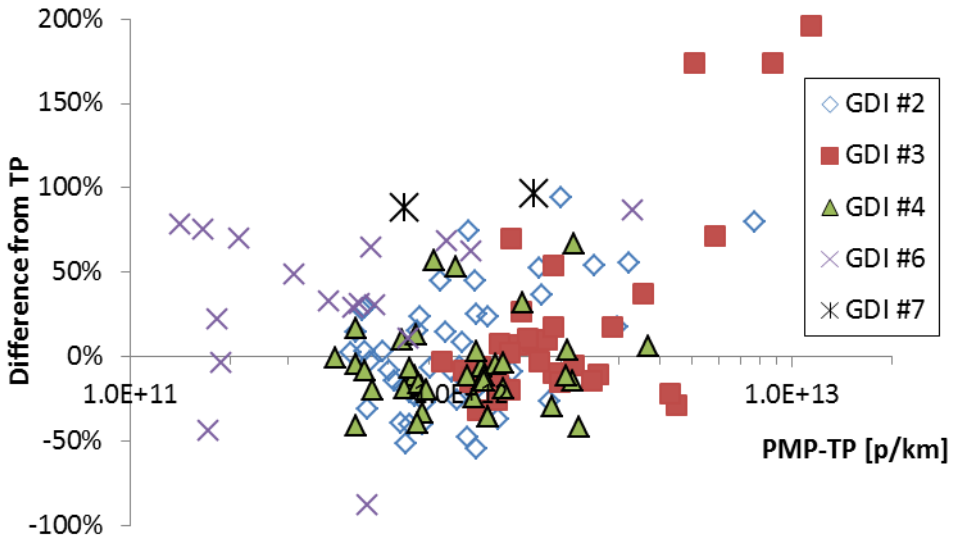

Figure 11-6: Summary of comparisons between PN-PEMS and PMP-TP. Both were connected to the tailpipe.

11.4 (Ambient) Temperature effect

Some tests were conducted at 8°C. Figure 11-7 shows that there was no particular effect on the PN-PEMS and it behaved as during the 23°C ambient (test cell) temperature tests.

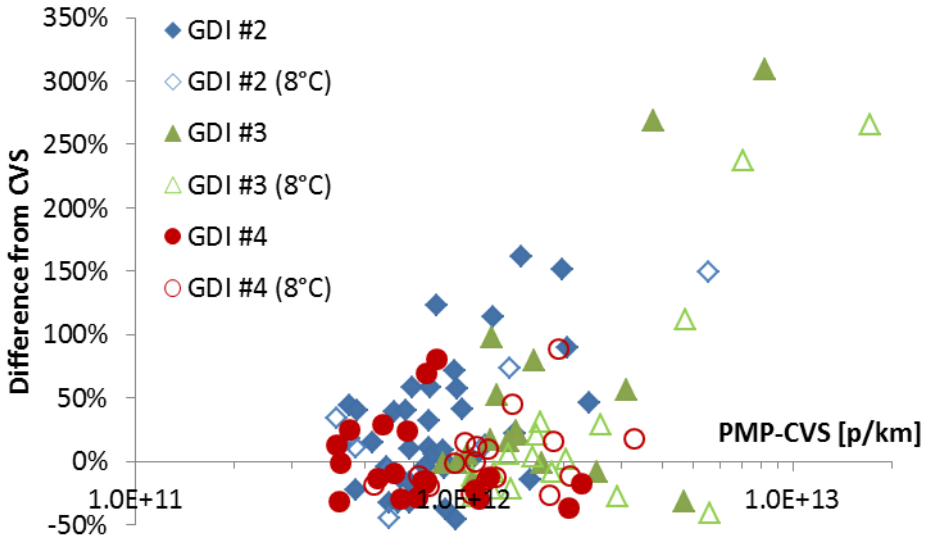

Figure 11-7: Effect of ambient temperature on PN-PEMS.

11.5 Particle size effect

Plotting the results in function of the mean particle size of the cycle, it can be observed that there is a small size dependency of the difference of the PN-PEMS to the PMP-CVS (Figure 11-8). The size dependency of DCs has been discussed elsewhere. Here it can be seen that a 10 nm increase of the size results on approximately 60% higher result. It can also be observed that the system was optimised for sizes between 30 and 45 nm.

Similar results gave the comparison with the PMP-TP (Figure 11-9). In this case a 10 nm size increase resulted in 50% effect on the results. However in both cases the scatter of the differences for a specific size is around ±50% thus masking small size changes (<20 nm).

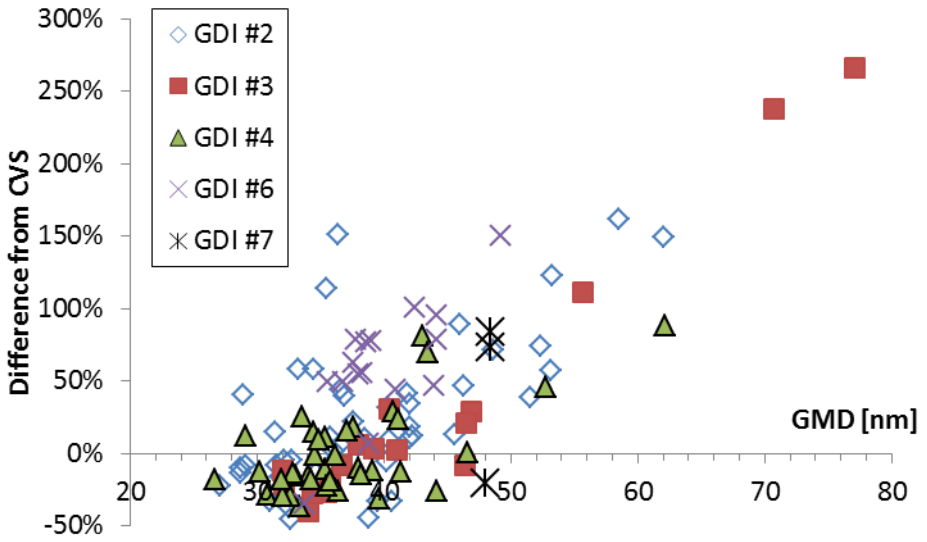

Figure 11-8: Size dependency of PN-PEMS.

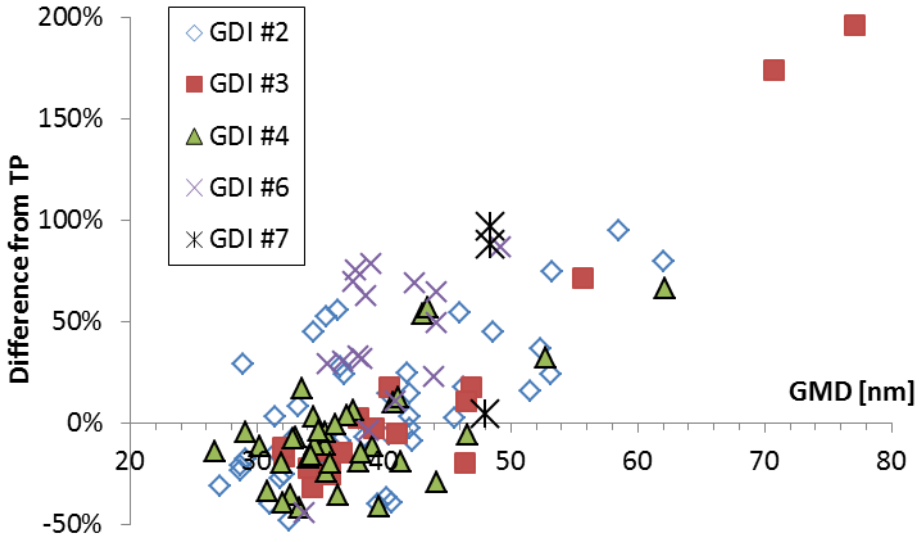

Figure 11-9: Size dependency of PN-PEMS.

11.6 Challenge aerosol (motorcycles)

The PN-PEMS was used also to measure exhaust aerosol of motorcycles. With Moto #2 (beginning of measurement campaign) there were some issues with the PN-PEMS and no data are presented. Thus, only results from Moto #3 will be presented. Moto #3 is a 4-stroke 50 cm^3 moped with max speed around 30 km/h (modified), that was producing particles with mean size smaller than 20 nm. Thus the PN-PEMS could overestimate the emissions (because it doesn't have counting efficiency 0 at small sizes) or underestimate the emissions (because the response function decreases with size). The PN-PEMS compared to the PMP-TP can be seen in Figure 11-10. The differences are approximately -50% to +30%, very close to the results of the GDI vehicles.

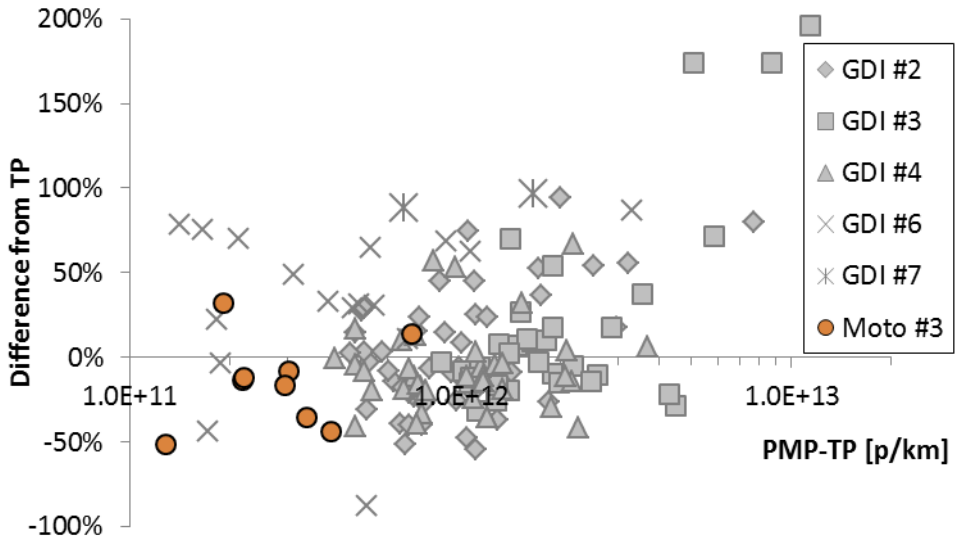

Figure 11-10: Comparison of PN-PEMS with PMP-TP when measuring motorcycles exhaust.

The results were also plotted in function of size (Figure 11-11). No clear size dependence could be observed at these sub-30 nm sizes.

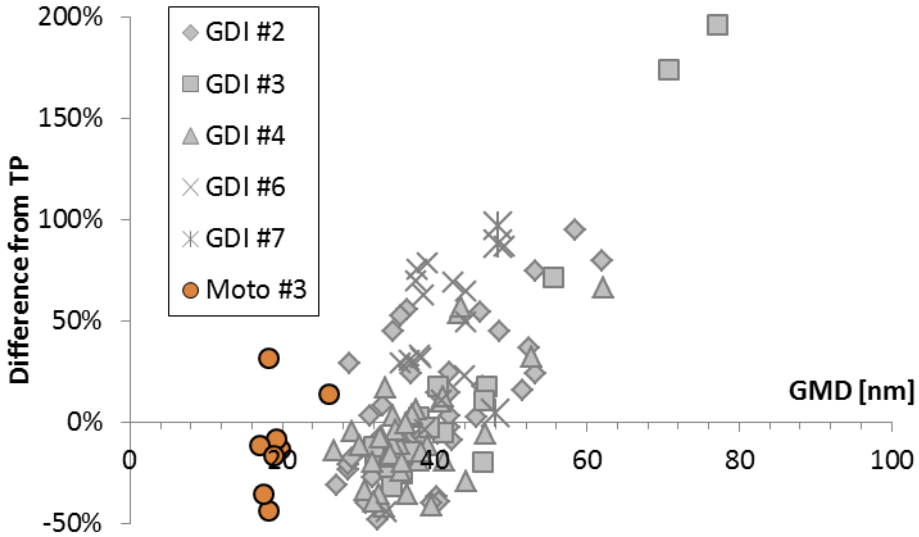

Figure 11-11: Size dependency of PN-PEMS when measuring motorcycles exhaust.

11.7 Volatile removal efficiency

The PN-PEMS has been evaluated in the lab and has shown excellent removal efficiency of tetracontane (see Giechaskiel et al. 2014). No volatile removal efficiency of engine exhaust could be evaluated because the system was not measuring when the instruments were challenged with a 2-stroke moped.

11.8 Summary

Figure 11-12 summarizes the differences of the PN-PEMS from the PMP-CVS and PMP-TP for all cases examined. The mean differences are 0% to +50% with a variability (expressed as ±standard deviation) of higher than ±50%.

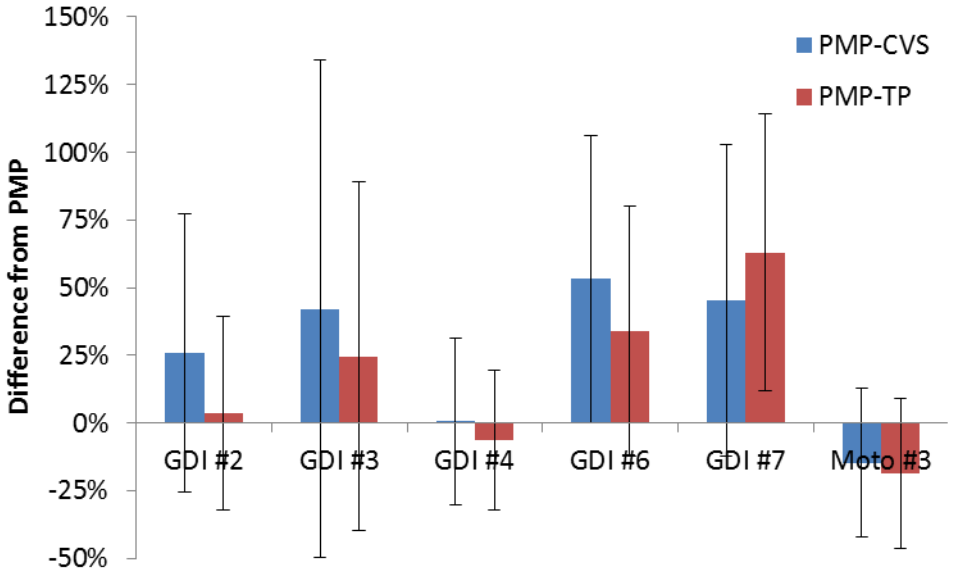

Figure 11-12: Overview of differences of PN-PEMS from the PMP-CVS and PMP-TP. Error bars are one standard deviation.

Table 11-1 shows the PASS/FAIL results of the PMP-TP and the PN-PEMS compared to the PMP-CVS assuming a 6x10^11 p/km limit. The success rate (i.e. catching a FAIL as FAIL or a PASS as PASS) is quite similar to the PMP-TP with one exception (GDI #6). One explanation could be the low emission levels of this car and the relatively small mean size of the particles.

Table 11-1: PASS/FAIL success rate.

Vehicle	Lab	Category	# of tests	PMP-TP	PN-PEMS
GDI #2	VELA 2	PASS	14	57%	79%
	VELA 2	FAIL	31	97%	80%
GDI #3	VELA 2	PASS	0	-	-
	VELA 2	FAIL	34	100%	100%
GDI #4	VELA 2	PASS	7	86%	86%
	VELA 2	FAIL	30	100%	90%
GDI #6	VELA 2	PASS	14	93%	64%
	VELA 2	FAIL	3	100%	100%
GDI #7	VELA 2	PASS	1	100%	100%
	VELA 2	FAIL	2	100%	100%
Moto #3	VELA 2	PASS	9	100%	100%
	VELA 2	FAIL	1	100%	100%

11.9 Adjustment of PN-PEMS

The PN-PEMS based on DCs have an inherent uncertainty due to their dependency on particles size. Even when calibrated it is possible to have a 'bias' for vehicles that emit particles in a different size range. The topic was investigated by conducting different cycles in one day and comparing the difference of the PN-PEMS to the PMP-CVS.

The results for all sub-cycles are presented in Figure 11-13. The specific vehicle emits particles with a large mean size at the beginning of the test. Thus, the PN-PEMS is overestimating the emissions >150% (first part of the NEDC). At the subsequent part the PN-PEMS is overestimating around 50%. For the next hot cycle (after 20 min) the first part is +50% but then for the next parts of the cycle the differences become 0%.

For the next WLTC in the afternoon a similar behaviour is observed: High differences at the cold start that reach 0% when the engine is warm. Next day was also similar. The behaviour of the car on the road is expected more similar to the 'hot' sub-cycles. Thus a calibration with a 'hot' cycle would probably improve the 'bias'. Note that using the 'cold' WLTC to 'calibrate' the PN-PEMS would give a wrong calibration factor (+114% average of the cycle). However, it is interesting to note that the original calibration was correct (the differences close to 0%).

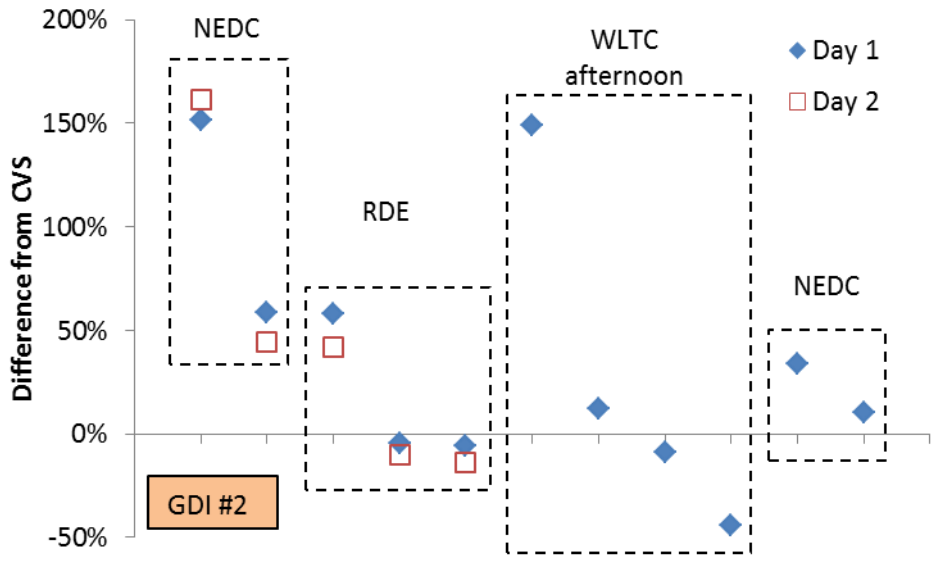

Figure 11-13: Difference of PN-PEMS from PMP-CVS over the day. Each point is a sub-cycle.

For the other vehicles the behaviour was similar (e.g. GDI #3, Figure 11-14): High differences at the 'cold' starts which were minimised over time, as the engine was getting hotter (and the mean size of the particles smaller).

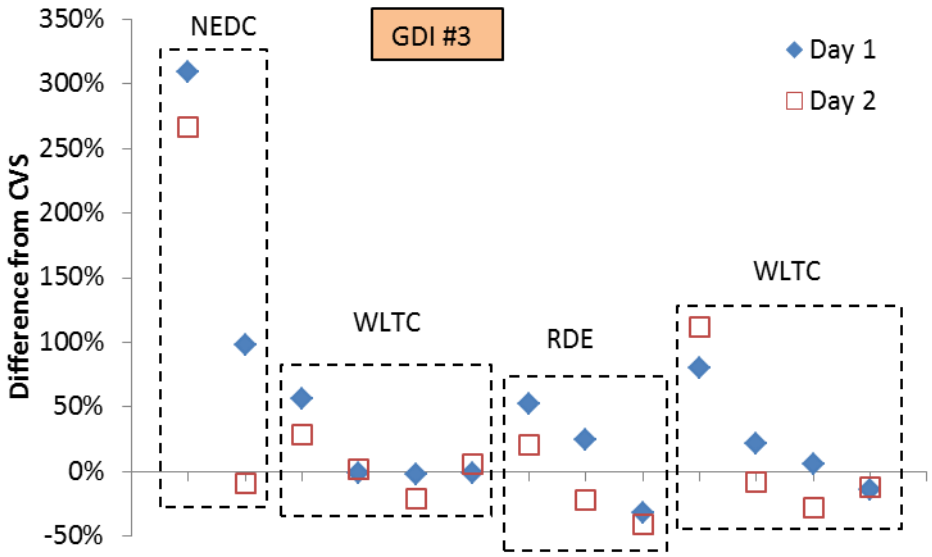

Figure 11-14: Difference of PN-PEMS from PMP-CVS over the day

Figure 11-15 summarises the correction factors for the different vehicles based on the 'hot' sub-cycles. The corrections were from -9% to -21% with one exception and the variability for each car ranged approximately 15-25%. One car showed a completely different correction factor (+54%). There is no clear explanation for this behaviour; probably because the specific car emitted smaller particles. Nevertheless, it indicates that there could be cases where a calibration of the PN-PEMS with a hot test could be advantageous.

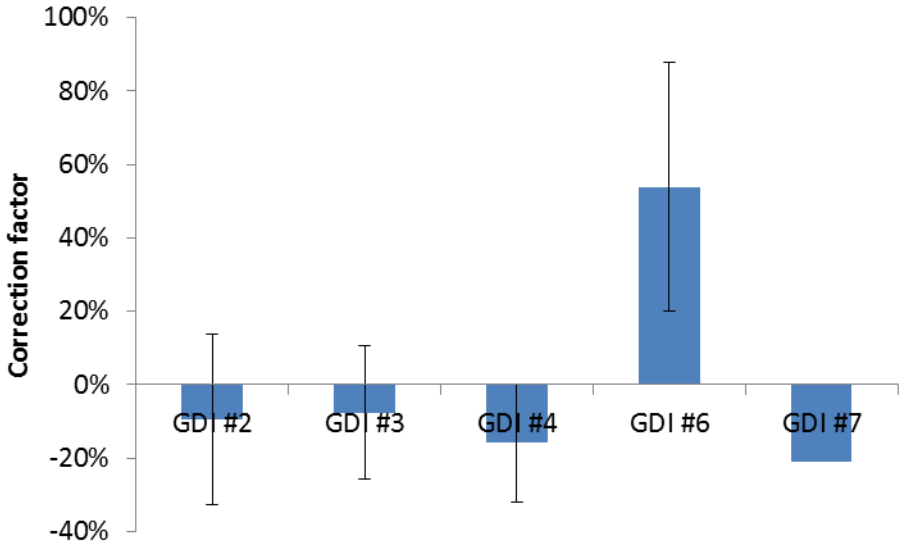

Figure 11-15: Summary of calibration factor for hot cycles for different vehicles.

11.10 CPC

PN-PEMS #5' was provided with a prototype CPC, which will be evaluated in this section. The cut-off size couldn't be determined due to the low concentration of spark discharge graphite particles generated at sizes smaller than 10 nm. Based on the calibration at larger sizes (not shown) and extrapolation, the 50% cut-off size is expected at 6 nm. This could create some issues when particles <23 nm exist. This is plotted in Figure 11-16 where the CPC of the PN-PEMS shows higher emissions than the PMP-TP at many parts of the cycle. The specific Motorcycle (#3) had high solid emissions <23 nm.

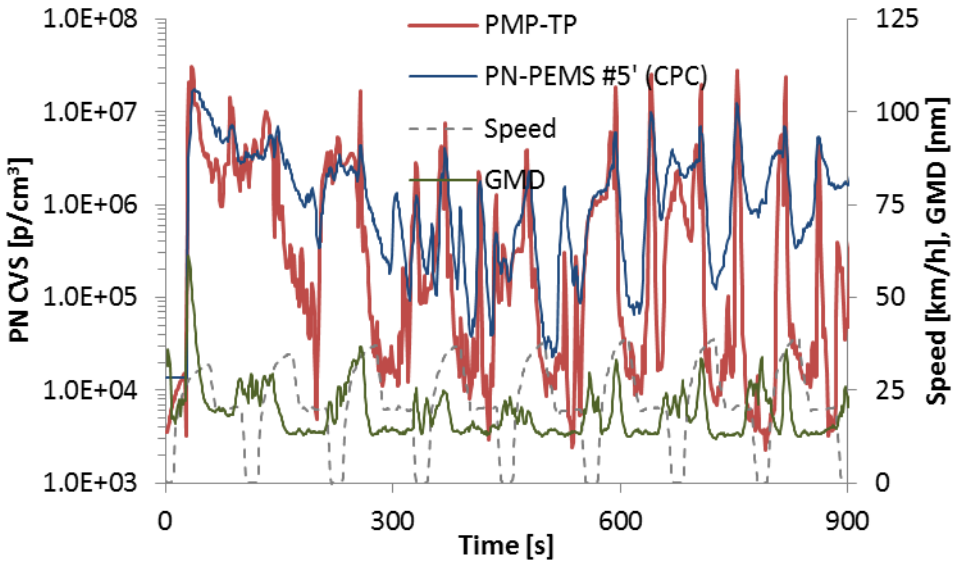

Figure 11-16: Comparison of PN-PEMS (CPC) with PMP-CVS. The PN-PEMS was connected to the tailpipe.

When no sub-23 nm particles existed (or their concentration was low), the real time behaviour of the CPC was good, as it can be seen in Figure 11-17.

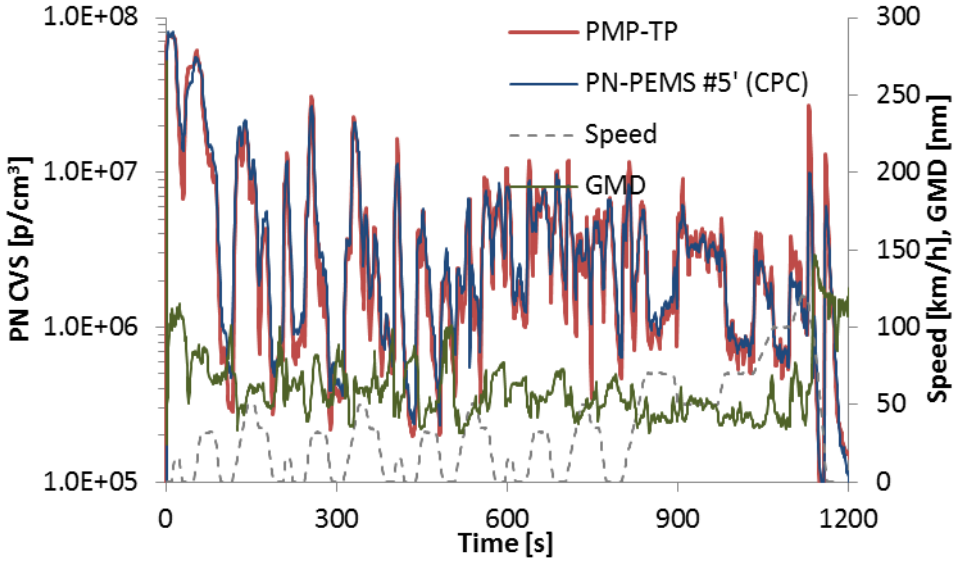

Figure 11-17: Comparison of PN-PEMS (CPC) with PMP-CVS. The PN-PEMS was connected to the tailpipe.

However there was a strange behaviour of the system for many tests. For example a test with an 'offset' is shown below (Figure 11-18). It was found out by the manufacturer that the fan was disconnected and the temperatures of the CPC increased. Although this was fixed, then it was found that there was a leak upstream of the venturi diluter of the CPC that also affected its results.

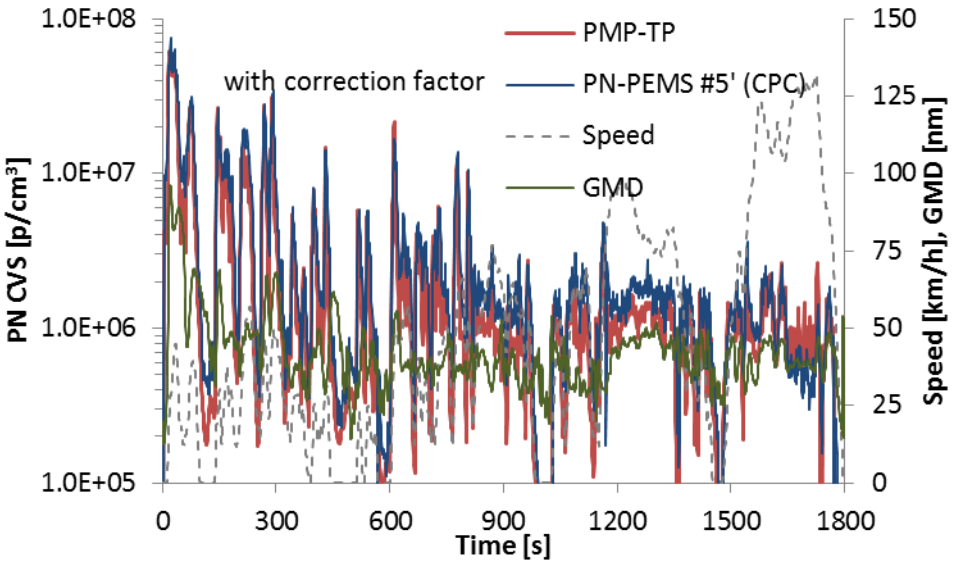

Figure 11-18: Comparison of PN-PEMS (CPC) with PMP-CVS. The PN-PEMS was connected to the tailpipe. A correction factor was applied.

The comparison to the PMP-CVS is plotted in Figure 11-19. Given the strong deviations from the PMP-CVS, the CPC was not further evaluated.

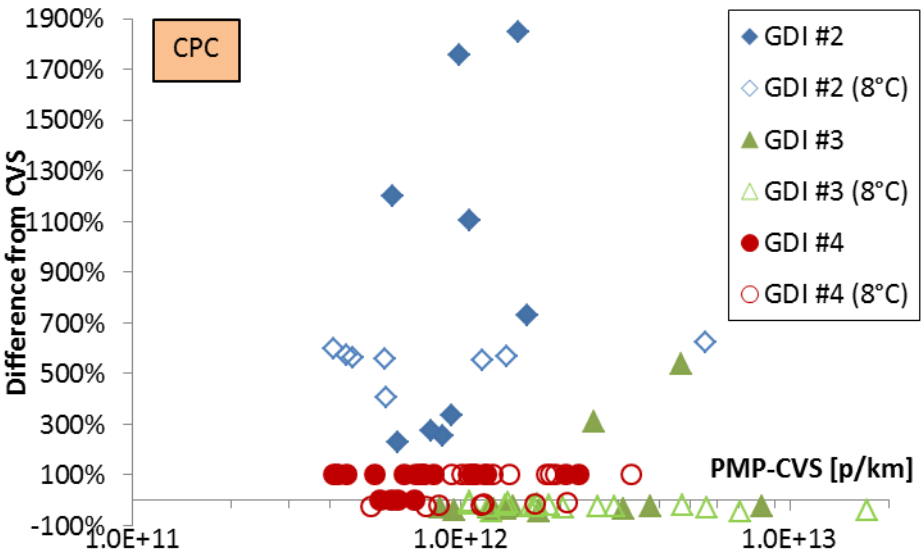

Figure 11-19: Summary of comparisons of PN-PEMS (CPC) with PMP-CVS.

12 PN-PEMS #6'

12.1 Description

PN-PEMS #6' (Nano Aerosol Monitor: NAM, Shimadzu) is a 6 stage electro mobility analyser without sheath flow. The cut-off size is 23 nm. For the tailpipe tests, the sample was drawn through a heated line (190°C) and diluted 10 times (*DF*=10). For the CVS tests a different heated line was used (50°C) without any dilution (*DF*=1). The instrument has the possibility to switch between three full-scale values that cover three different ranges of particle concentration; for all tests the mid-scale was used (*Sr*=756450). The total concentration [p/cm³] was given as the difference between the last and first electrometers (*AE*):

$$R_{PN-PEMS} = (AE_{6th} - AE_{1st})\ DF\ Sr$$

12.2 Real time

Figure 12-1 compares the PN-PEMS connected to the tailpipe with the PMP-TP. The PN-PEMS follows the PMP-TP system closely. In these real time figures the GMD is a 5s moving average.

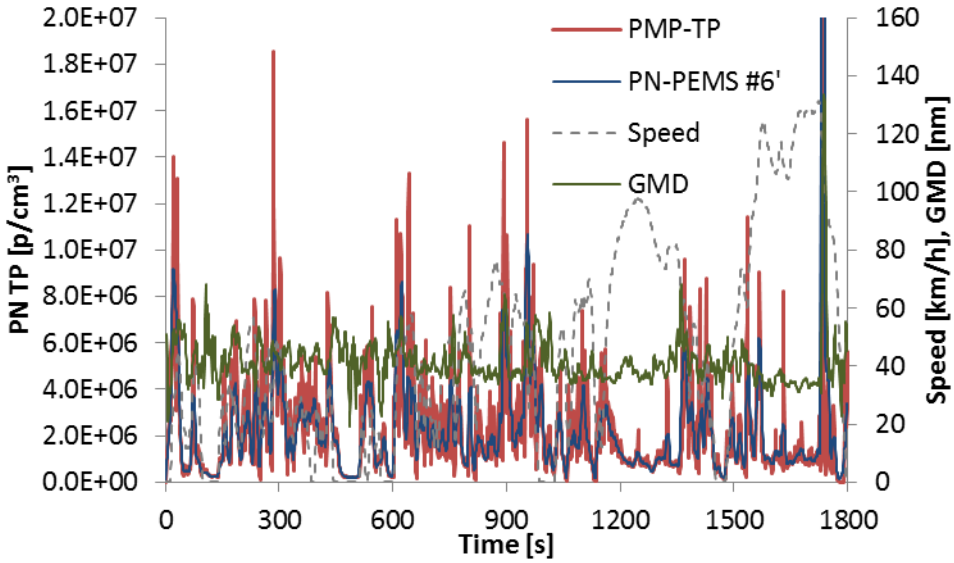

Figure 12-1: Comparison of PN-PEMS with PMP-TP, both connected to the tailpipe (20141107-02-WLTC 8°C, GDI #3).

Similar behaviour was shown with other GDIs (Figure 12-2):

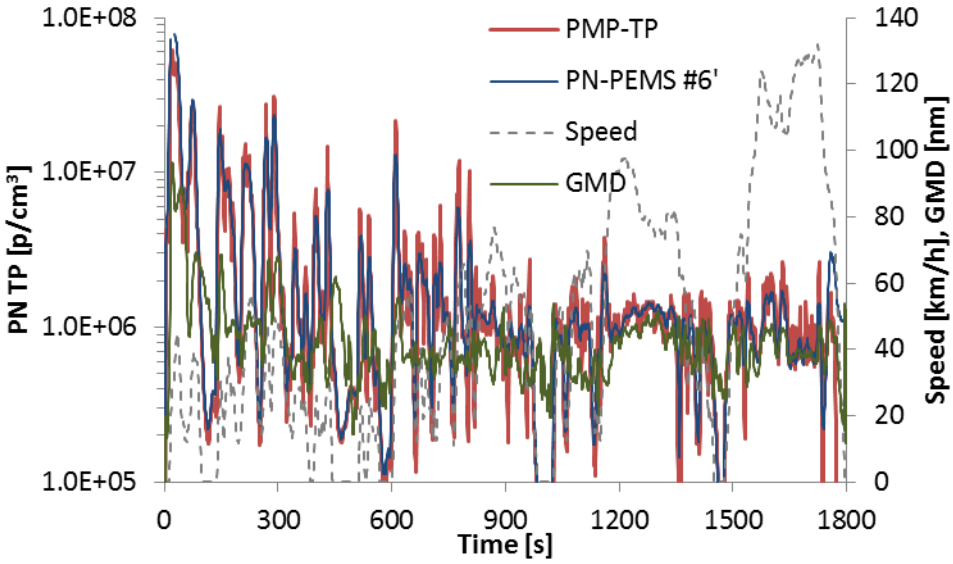

Figure 12-2: Comparison of PN-PEMS with PMP-TP, both connected to the tailpipe (20141125-03-WMTC, GDI #2).

However, at a certain point during the measurement campaign an unexpected behaviour was observed (Figure 12-3). One explanation could be condensation of exhaust gas or non-efficient removal of volatiles. After the measurement campaign the manufacturer checked the device and he found out that the capability of the adsorbent in the filtration unit of the dilution air was used up, and this could have been one of the reasons of this behaviour after GDI #6. These tests were disregarded from the following analysis.

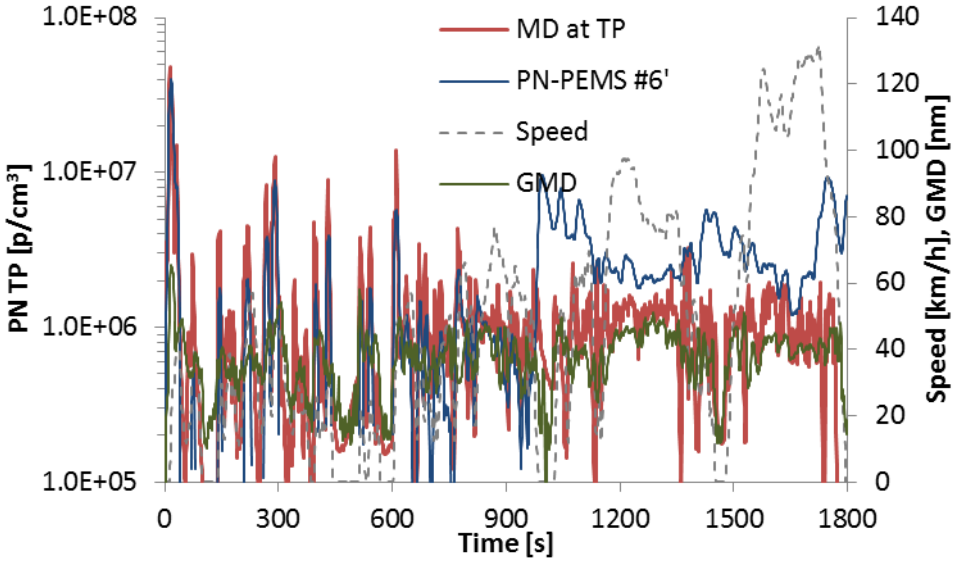

Figure 12-3: Comparison of PN-PEMS with PMP-TP, both connected to the tailpipe (20141128-02-WLTC, GDI #2).

The PN-PEMS was connected to the CVS for the following tests. Although the behaviour was better, there are still some concerns for the last part of the cycles (Figure 12-4, Figure 12-5).

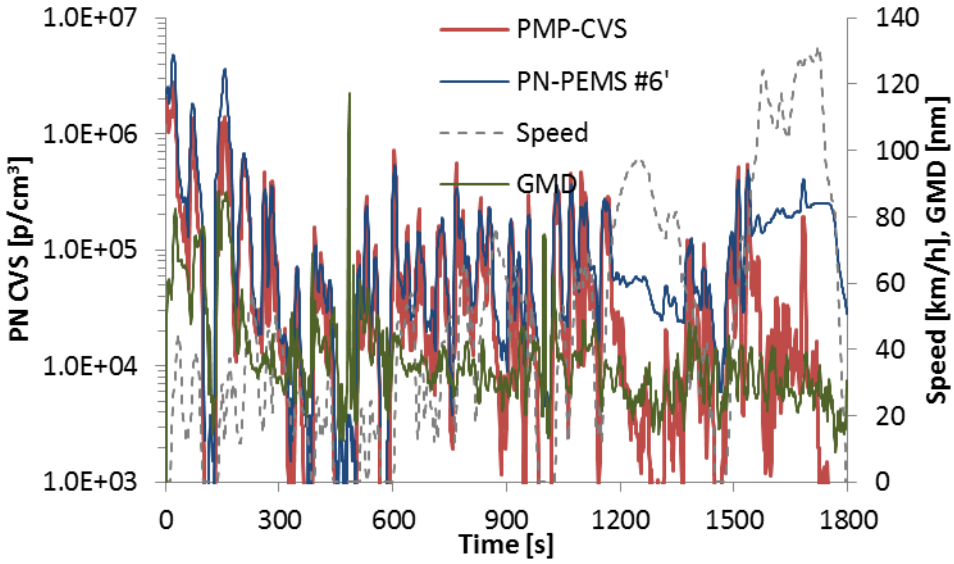

Figure 12-4: Comparison of PN-PEMS with PMP-CVS, both connected to the dilution tunnel (20141203-01-WLTC cold, GDI #6).

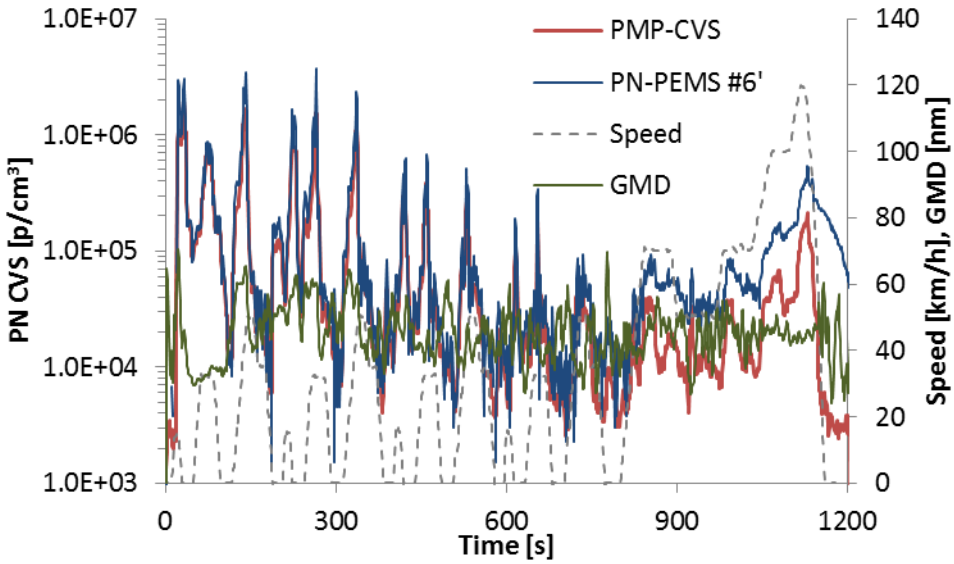

Figure 12-5: Comparison of PN-PEMS with PMP-CVS, both connected to the dilution tunnel (20141216-01-NEDC cold, GDI #7).

12.3 Comparison to PMP-TP

The summary of differences of the PN-PEMS from the PMP at the tailpipe (PMP-TP) can be seen in Figure 12-6. The differences range from -40% up to +30% in most cases. As mentioned previously the tests with GDI #2 that had differences >100% after a specific day were not considered.

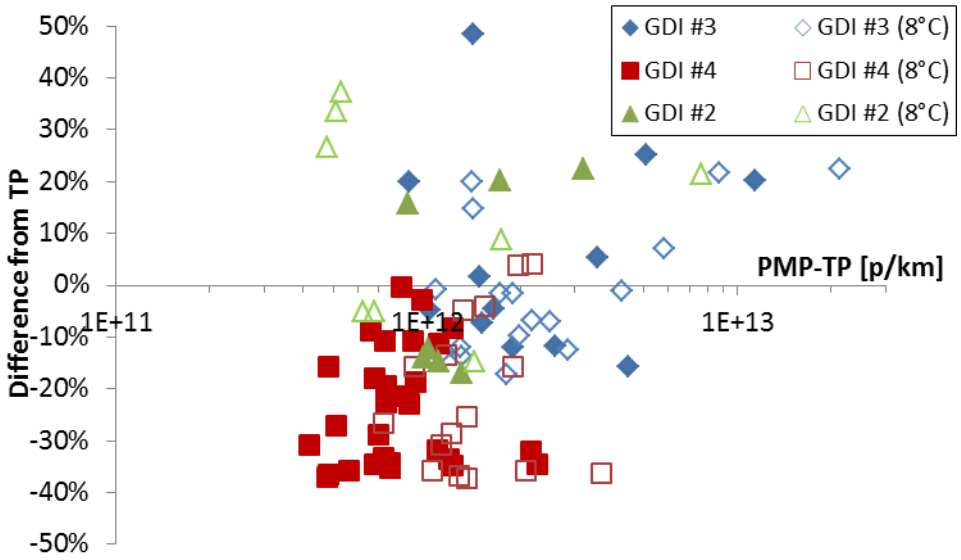

Figure 12-6: Summary of comparisons between PN-PEMS and PMP-TP, both connected to the tailpipe.

12.4 Comparison to PMP-CVS

The PN-PEMS was connected to the CVS for different vehicles. The comparison with the PMP system at the CVS (PMP-CVS) can be seen in Figure 12-7. The differences range from around 0% to +150% in most cases. However there is a cloud of points with differences >200%. These are the last parts of the cycles with high speeds. These could be volatile particles not efficiently removed. They are not solid particles because a CPC with cut-off size at 3 nm measured close to the 23 nm CPC.

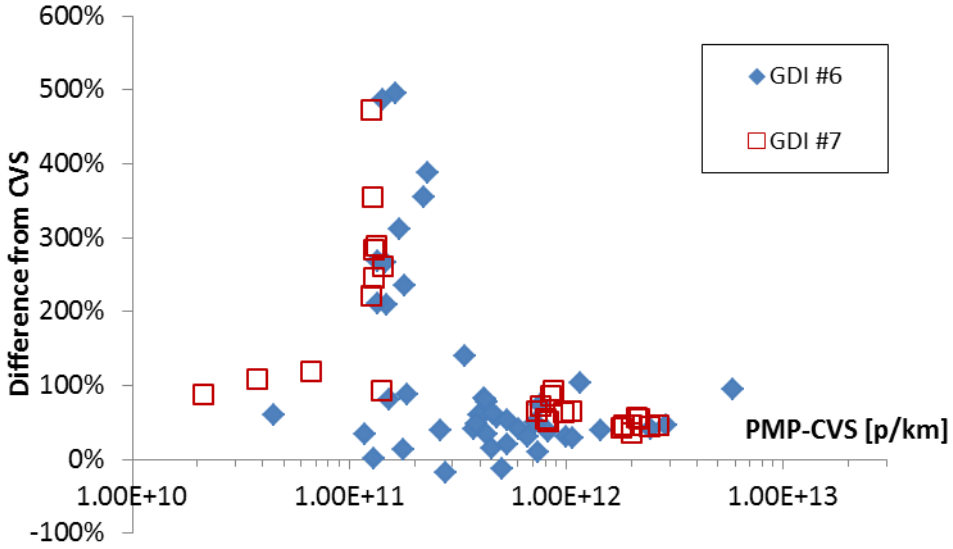

Figure 12-7: Summary of comparisons between PN-PEMS and PMP-CVS, both connected to the dilution tunnel.

12.5 Particle size effect

The differences of the PN-PEMS from the PMP-TP were plotted in function of cycle mean particle size (Figure 12-8). There is no clear size dependency trend, or the small tendency is masked by the measurement variability between the different vehicles. In these figures GMD is the average of cycle. The PN-PEMS vs PMP-CVS results were not plotted due to the high differences that were measured (see Figure 12-7).

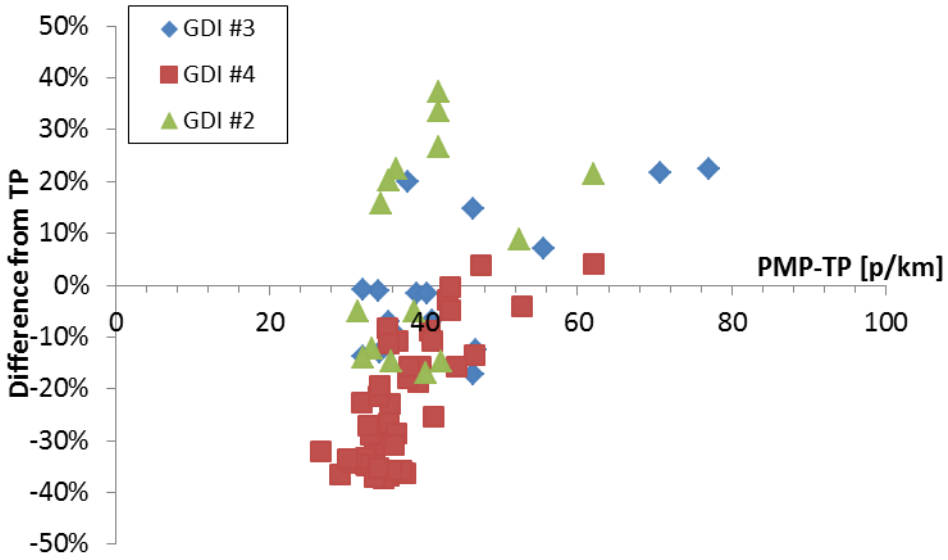

Figure 12-8: Ambient temperature effect on PN-PEMS.

12.6 Ambient temperature

No effect of the ambient temperature down to 8°C was observed. The behaviour was the same as during the 23°C tests (see Figure 12-6).

12.7 Challenge aerosol (motorcycles)

The PN-PEMS was used also to measure exhaust aerosol of motorcycles. Moto #2 is a 4-stroke 400 cm^3 motorcycle and was producing particles around 30 nm. Moto #3 is a 4-stroke 50 cm^3 moped with max speed around 30 km/h (modified). Moto #4 is a 4-stroke 125 cm^3 motorcycle with max speed around 90 km/h. The specific motorcycles were producing particles with means less than 20 nm. The PN-PEMS compared to the PMP-CVS can be seen in Figure 12-9 in function of the emission levels and in Figure 12-10 in function of the mean cycle size. The differences are very high and are increasing inversely proportionally to both emission levels and particle size. One possible explanation is that the particles do not shrink enough in the PN-PEMS and they are counted as >23 nm particles. These tests confirm that 50°C thermal pre-treatment is not enough. It would be interesting to examine whether the 190°C heated line would have the same issues.

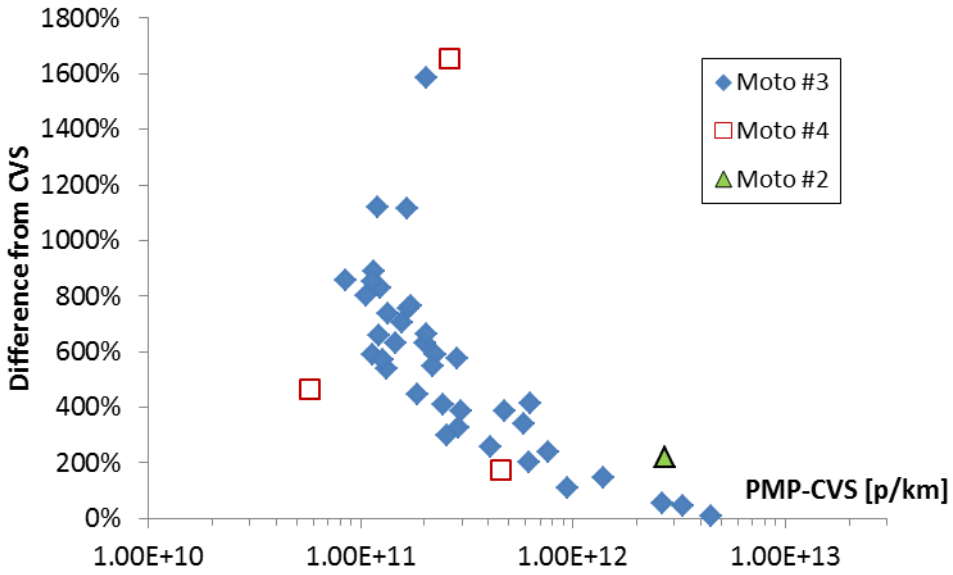

Figure 12-9: Difference of PN-PEMS from PMP-CVS in function of emission levels for motorcycles when both sampling from the dilution tunnel.

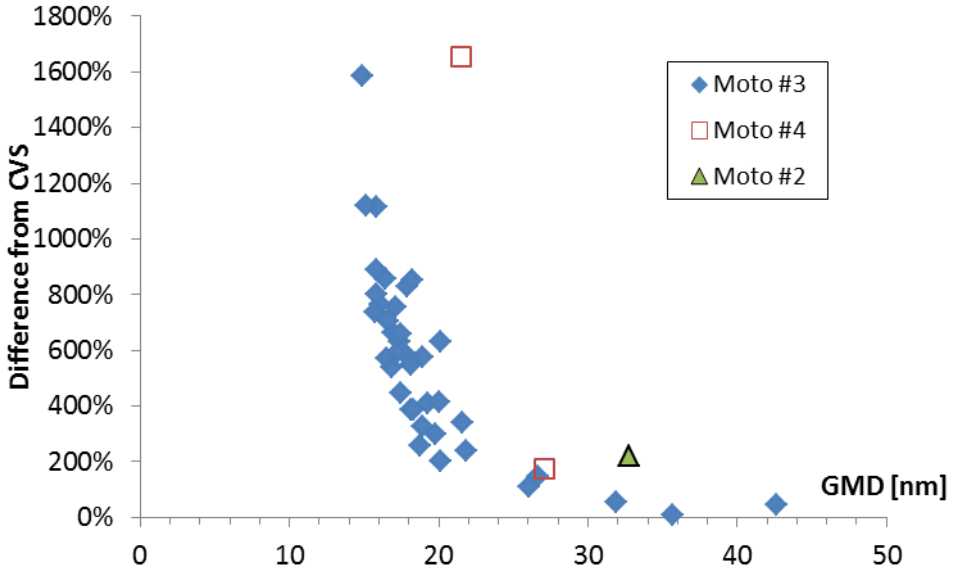

Figure 12-10: Difference of PN-PEMS from PMP-CVS in function of mean size for motorcycles when both sampling from the dilution tunnel.

12.8 Volatile removal efficiency

The volatile removal efficiency of the PN-PEMS was evaluated by measuring from the CVS diluted aerosol from a 2-stroke 50 cm^3 moped (Moto #1). The size distribution at the CVS has a mean around 90 nm. After thermal pre-treatment the mean size decreases to less than 20 nm. A real time pattern is shown in Figure 12-11. The PN-PEMS measured >100% (higher than the PMP-CVS) indicating that there was not effective volatile removal or the cut off size is less than 23 nm. This moped showed high concentration of sub-23 nm solid particles. Since the PN-PEMS was used at 50°C, the most likely explanation is that the particles remained >23 nm.

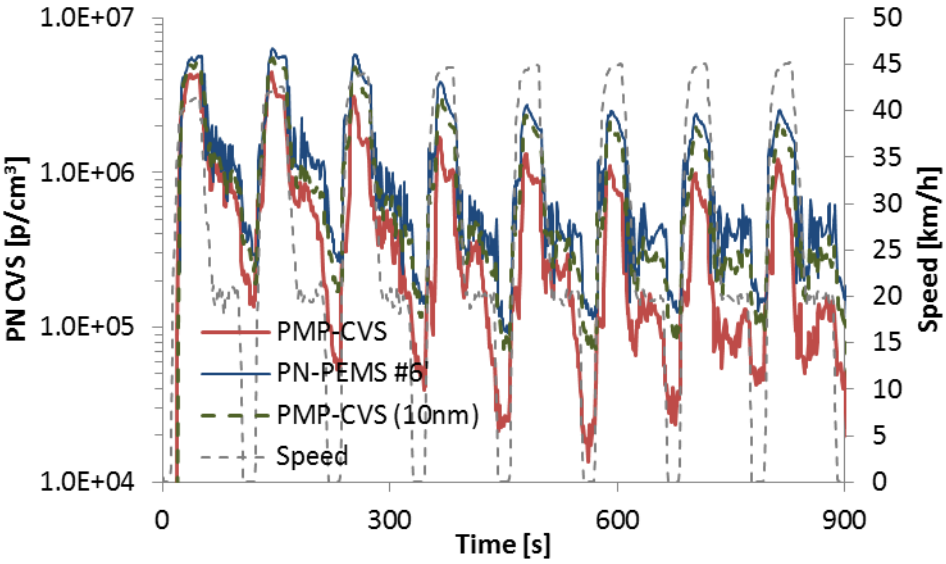

Figure 12-11: Comparison of PN-PEMS with PMP-CVS when measuring moped's exhaust. Both connected to the dilution tunnel.

12.9 Summary

Figure 12-12 summarizes the differences of the PN-PEMS from the PMP-CVS and PMP-TP for all GDI vehicles examined. Figure 12-13 shows the results for the tested motorcycles. For GDIs, when the PN-PEMS was measuring at the tailpipe, the mean differences are -20% to +35% with a variability (expressed as ±standard deviation) of ±30% (excluding some tests with unexpected behaviour). When the PN-PEMS was at the CVS, the difference was >100% and even higher for motorcycles showing higher variability. However the tests at CVS were conducted without thermal pre-treatment. In addition for most of them there was a concern for the proper operation of the unit.

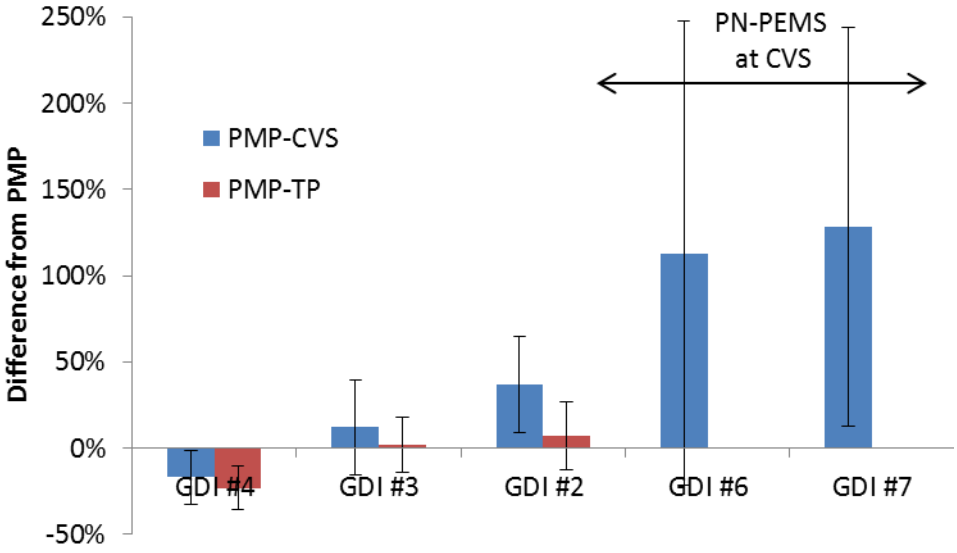

Figure 12-12: Overview of differences of PN-PEMS from the PMP-CVS and PMP-TP. Error bars are one standard deviation.

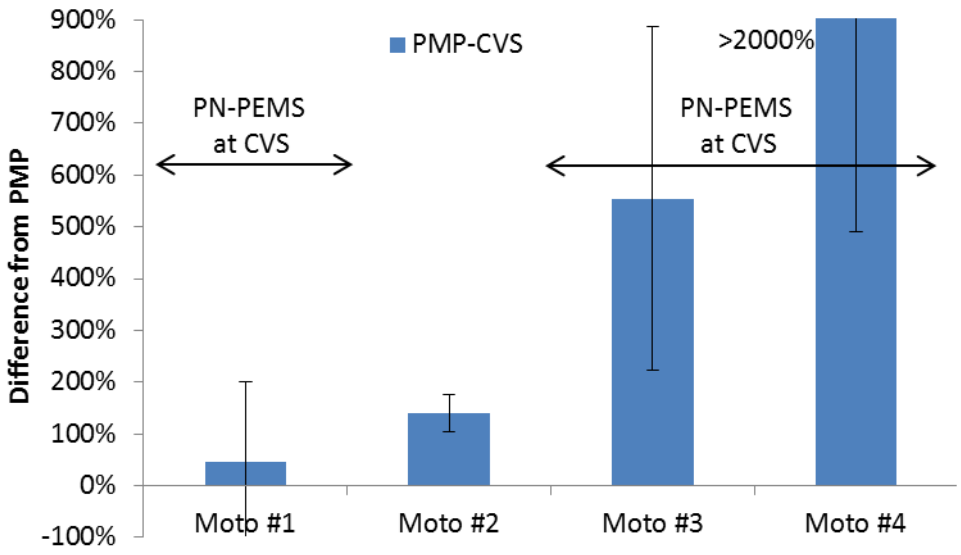

Figure 12-13: Overview of differences of PN-PEMS from the PMP-CVS and PMP-TP. Error bars are one standard deviation.

Table 12-1: PASS/FAIL success rate (* no thermal pre-treatment when used at CVS (heated line at 50°C)).

Vehicle	Lab	Category	# of tests	PMP-TP	PN-PEMS
GDI #2	VELA 2	PASS	5	60%	80%
	VELA 2	FAIL	10	100%	100%
GDI #3	VELA 2	PASS	0	-	-
	VELA 2	FAIL	29	100%	100%
GDI #4	VELA 2	PASS	8	75%	88%
	VELA 2	FAIL	38	100%	82%
GDI #6 (CVS)*	VELA 1	PASS	34	-	50%
	VELA 1	FAIL	11	-	100%
GDI #7 (CVS)*	VELA 1	PASS	11	-	91%
	VELA 1	FAIL	16	-	100%
Moto #1 (CVS)*	VELA 1	PASS	0	-	-
	VELA 1	FAIL	4	-	100%
Moto #4 (CVS)*	VELA 1	PASS	6	-	17%
	VELA 1	FAIL	0	-	-
Moto #3 (CVS)*	VELA 1	PASS	30	-	0%
	VELA 1	FAIL	7	-	100%
Moto #2	VELA 1	PASS	0	-	-
	VELA 1	FAIL	3	-	100%

Table 12-1 shows the PASS/FAIL results of the PMP-TP and the PN-PEMS compared to the PMP-CVS assuming a 6x10^11 p/km limit. The success rate (i.e. catching a FAIL as FAIL or a PASS as PASS) is not satisfactory especially for motorcycles.

13 PN-PEMS #7'

13.1 Description

The PN-PEMS #7' (MAHA-AIP GmbH & Co.) consists of a VPR and a CPC, thus is basically a portable PMP system. It has a short sampling line (0.5m) heated at 100°C. The primary diluter is a rotating disk also heated at 100°C, with a dilution of approximately 100. The evaporation tube is kept at 300°C, then a secondary dilution follows at ambient temperature (dilution approximately 10:1). The CPC is a 3007 TSI CPC with saturator and condenser temperatures adjusted to obtain a cut-off at 23 nm. The system was calibrated by the manufacturer (like a PMP system) and this calibration factor was used in this report.

At the beginning of December (from GDI #6) the CPC was replaced because of the long heat up time. The 0.5 m heated line was replaced with a flexible 2 m heated line and the inlet flow was increased (from 0.7 lpm to 4.5 lpm) to keep the sampling losses low.

13.2 Calibration

The PN-PEMS was evaluated conducting a long time comparison with a reference CPC and a PMP system that were both already warmed up measuring in parallel 100 nm monodisperse spark discharge graphite particles. The wick of the PN-PEMS was exchanged, then the unit was switched on and the recording was initiated. The overview of the experiment can be seen in Figure 13-1:

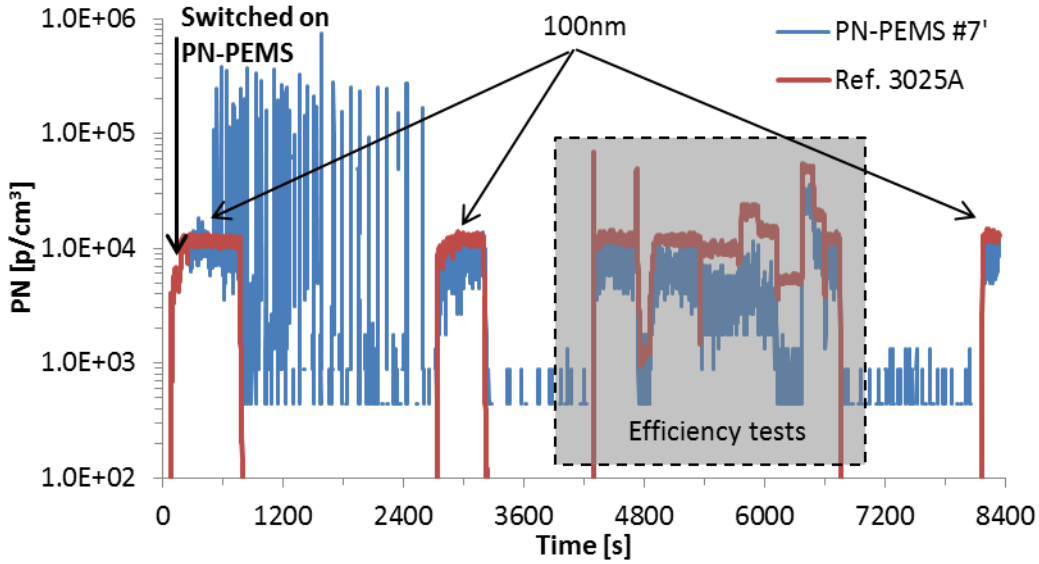

Figure 13-1: Long duration evaluation of PN-PEMS.

Initially strange spikes appeared probably due to liquid (iso-propanol) in the wick. This behaviour is not typical. Most of the times the system is counting 0 at the beginning. Nevertheless, the PN-PEMS was ready after 45 min and remained stable at least until the end of the experiment (8400 s, another 1.5 h).

The counting efficiency is shown in the second Figure 13-2. The PMP-CVS counting efficiency is also shown for comparison. There is a 35% underestimation of the emissions. Partly it could be due to the levels that were measured (10.000 p/cm^3), but similar results were found with a few test at 40.000 p/cm^3.

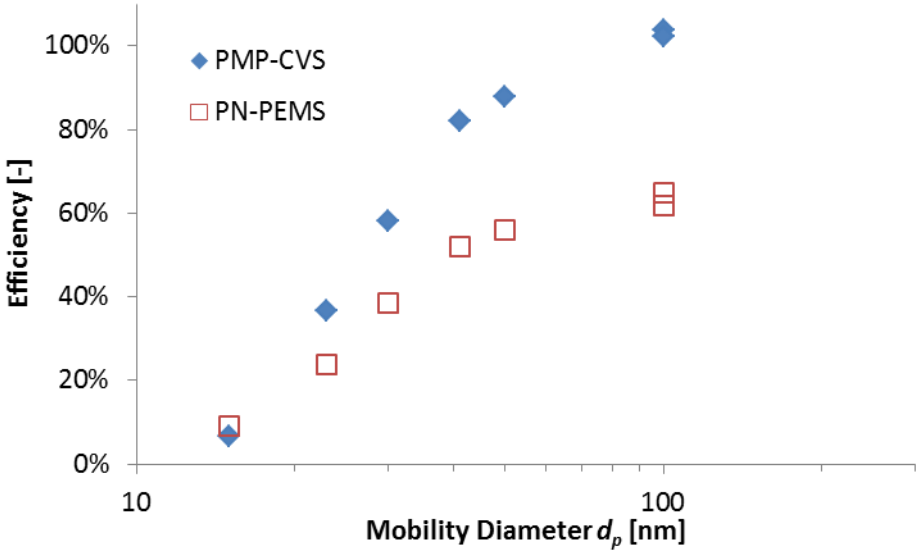

Figure 13-2: Efficiency of PN-PEMS and PMP-CVS (VELA 2).

13.3 Real time

Initially the PN-PEMS was connected to the CVS and was compared with the PMP-CVS system (Figure 13-3). The PN-PEMS follows the PMP-CVS system closely but a correction factor of 3 was needed. It is possible that the CPC did not reach its temperatures internally. In the real time figures GMD is a 5 s moving average.

The behaviour was similar with the replaced CPC (Figure 13-4).

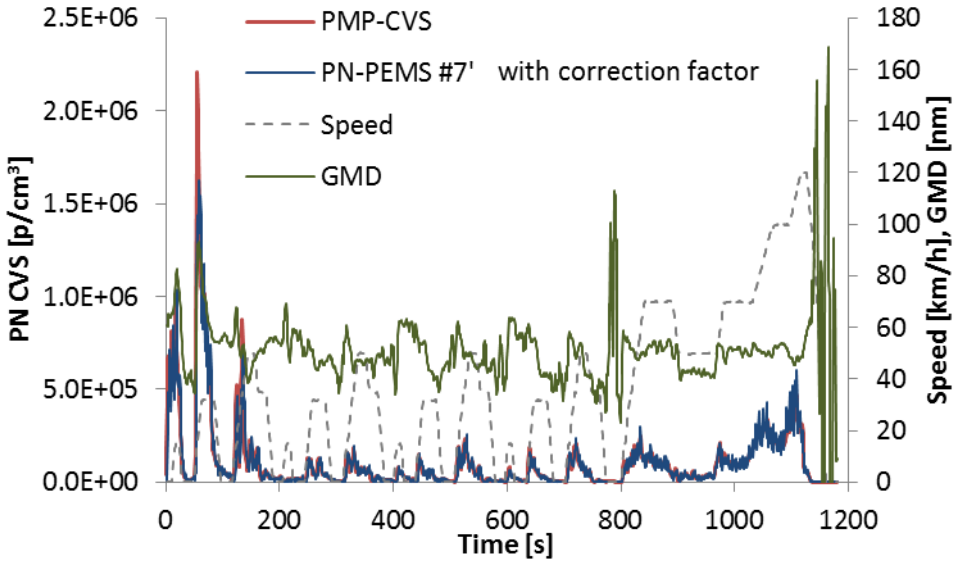

Figure 13-3: Comparison of PN-PEMS with PMP-CVS, both connected to the CVS (20141029-01-NEDC cold, GDI #1).

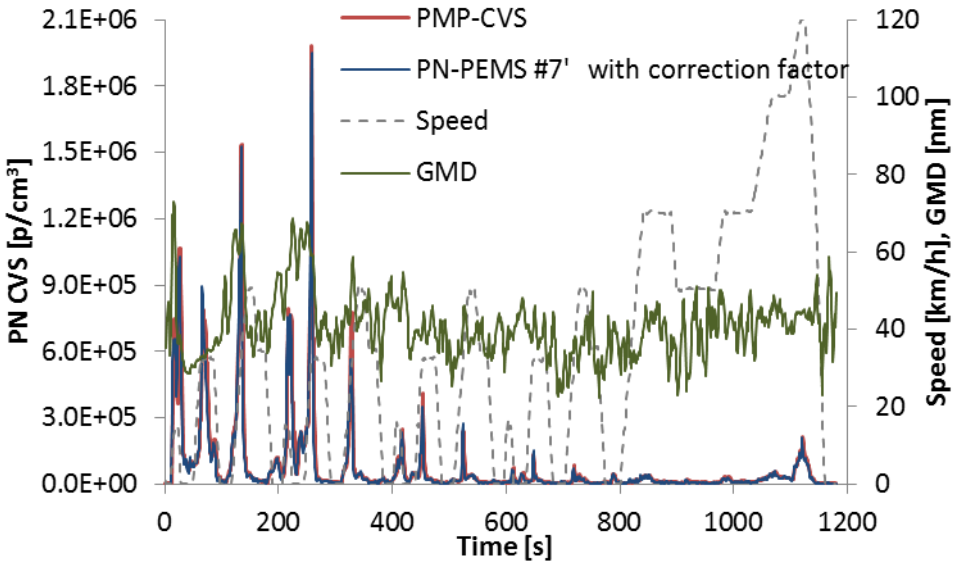

Figure 13-4: Comparison of PN-PEMS with PMP-CVS, both connected to the CVS (20141211-02-NEDC, GDI #7).

When the PN-PEMS was connected to the tailpipe the agreement with the PMP-TP was better. Special attention was also given to the warm up time: >1.5h for the 1st CPC, but after replacing the defective device warm up time was about 45 min. The differences were <30% (Figure 13-5). The real time behaviour was excellent in all cases, i.e. it followed the PMP-TP system closely (see Figure 13-6).

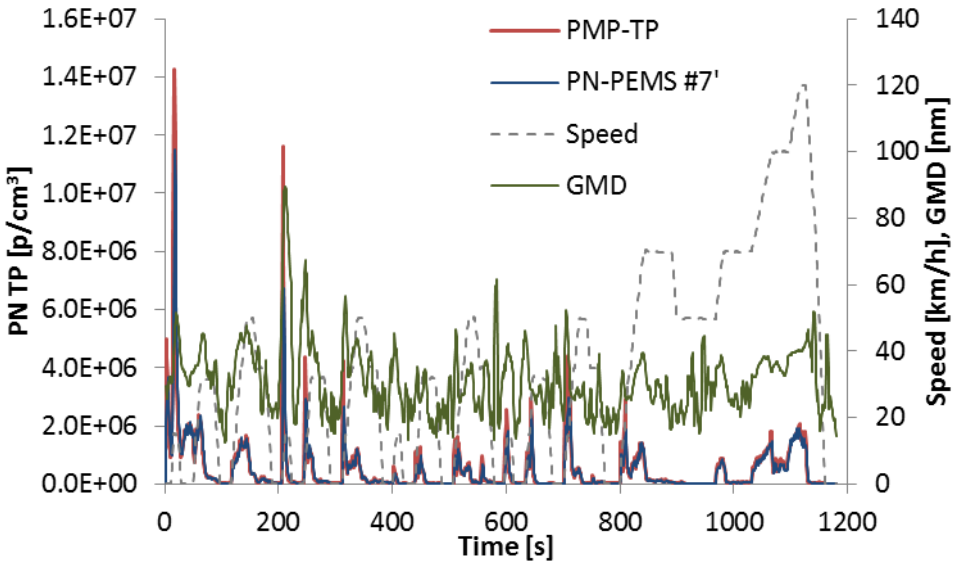

Figure 13-5: Comparison of PN-PEMS with PMP-TP, both connected to the tailpipe.

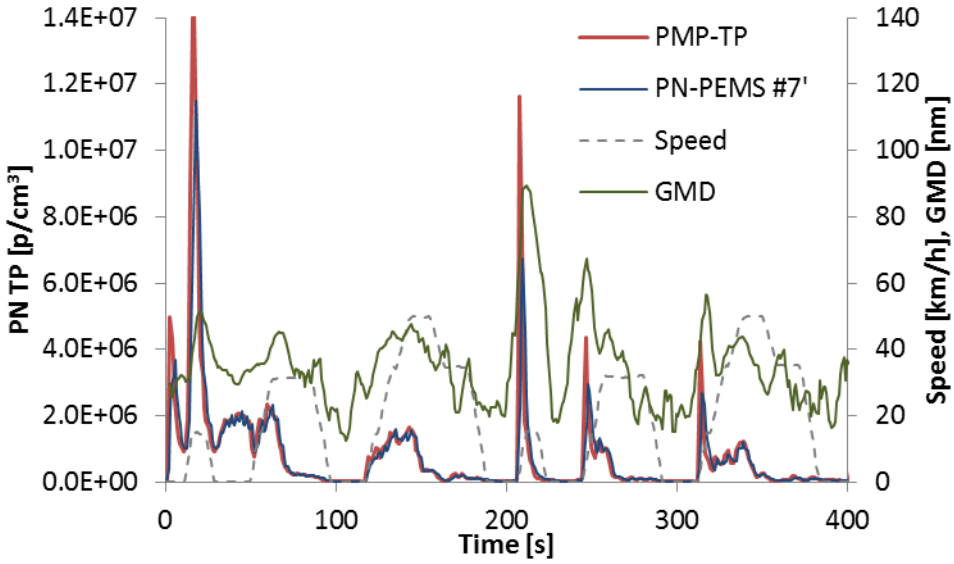

Figure 13-6: Detail of previous figure.

13.4 Comparison to PMP-CVS

Figure 13-7 summarizes the results when PN-PEMS was connected to the CVS. As discussed previously, the differences are from -70% to -60% approximately and in some cases -20% to -30%. The assumption is that the big differences are due to non-adequate warm up time especially for the 1st CPC. However, other reasons like drift of the CPC efficiency cannot be excluded.

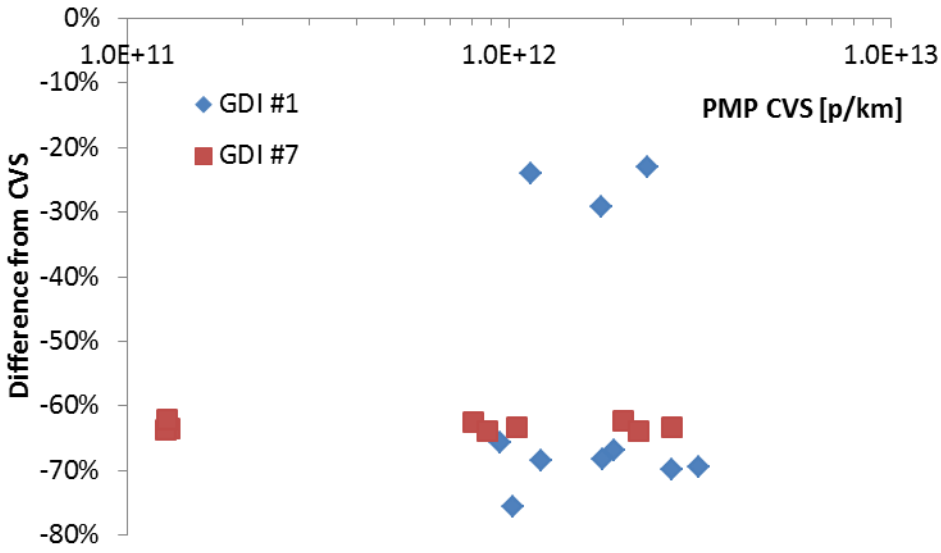

Figure 13-7: Summary of comparisons of PN-PEMS with PMP-CVS. Both connected to the dilution tunnel.

Then the PN-PEMS was connected to the tailpipe for different vehicles. The comparison with the PMP system at the CVS (PMP-CVS) can be seen in Figure 13-8. The differences range from -30% to +30% for the GDIs. GDI #7 seems to have higher differences, but this vehicle was tested in VELA 1 (with another PMP-CVS system).

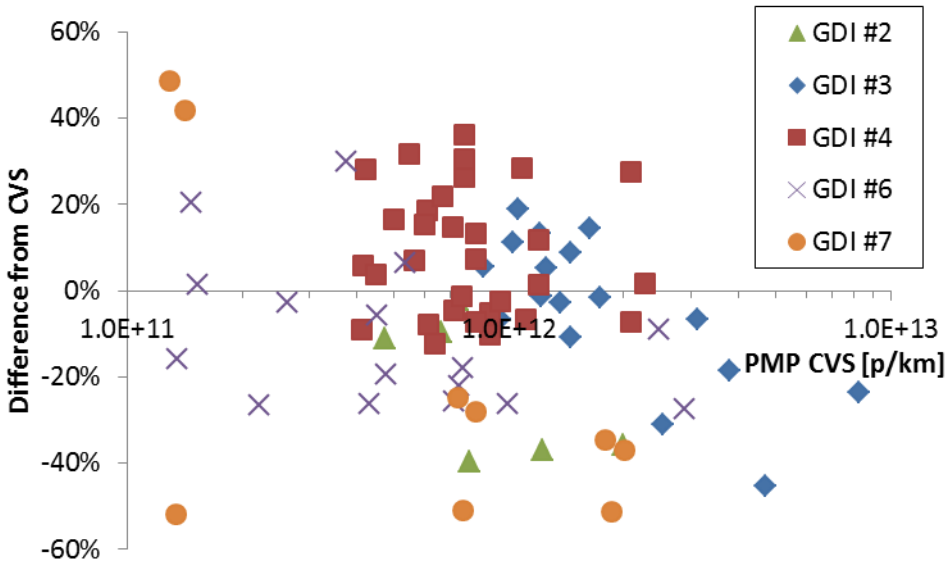

Figure 13-8: Summary of comparisons of PN-PEMS with PMP-CVS. PN-PEMS connected to the tailpipe.

13.5 Comparison to PMP-TP

The difference of the PN-PEMS from the PMP at the tailpipe (PMP-TP) can be seen in Figure 13-9. The differences range from -60% up to +60%.

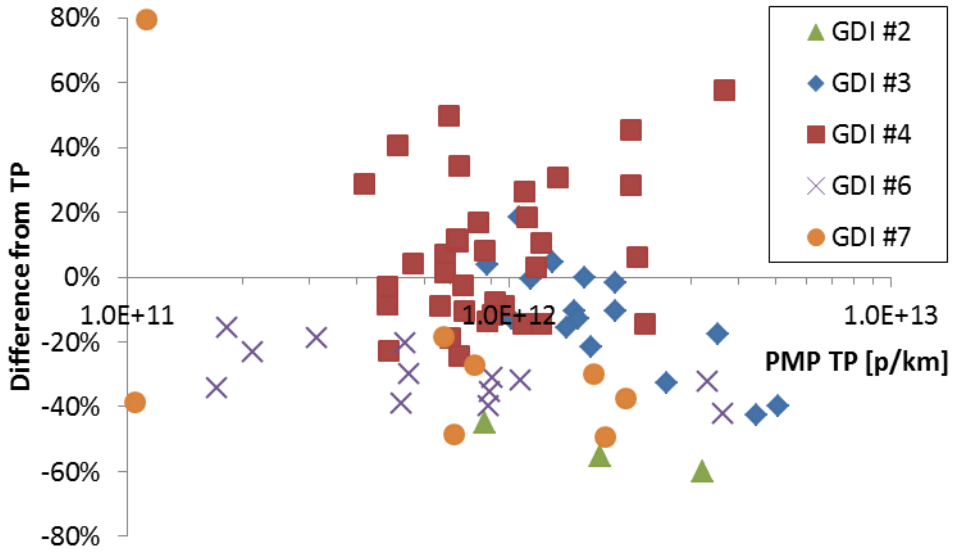

Figure 13-9: Summary of comparisons of PN-PEMS with PMP-TP. Both connected to the tailpipe.

13.6 Particle size effect

The size dependency of the PN-PEMS response can be seen in Figure 13-10. As expected, there is no effect of particle size on the difference between PN-PEMS and PMP-CVS. In these figures GMD is the average of a cycle.

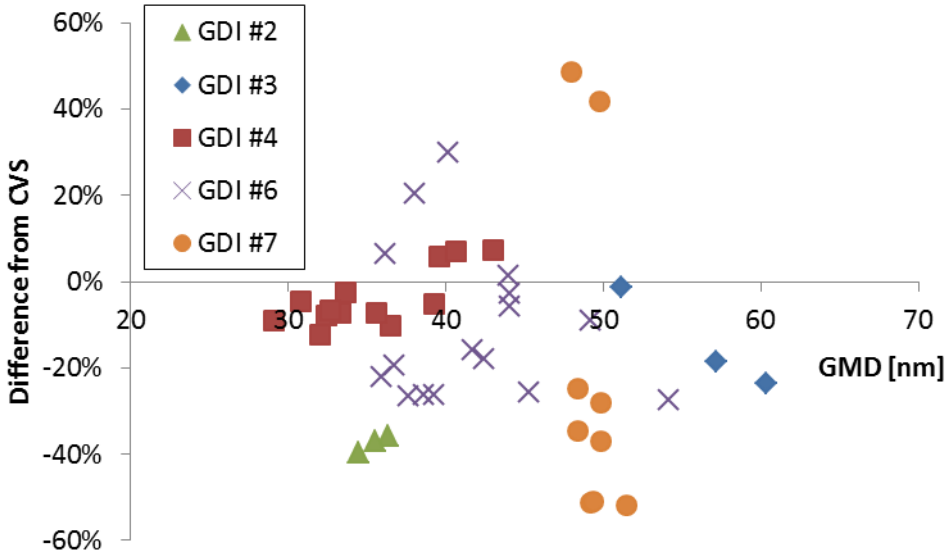

Figure 13-10: Particle size dependency of PN-PEMS.

13.7 Ambient temperature

The PN-PEMS couldn't measure at low temperatures (e.g. at 14°C during the on-road test and at 8°C during the test cell tests). This might be due to a defect of the first CPC. With the second CPC probably this issue wouldn't occur.

13.8 Challenge aerosol (motorcycles)

The PN-PEMS was used also to measure exhaust aerosol of motorcycles. Moto #3 is a 4-stroke 50 cm^3 moped with max speed around 30 km/h (modified). Moto #4 is a 4-stroke 125 cm^3 motorcycle with max speed around 90 km/h. Moto #2 is a 4-stroke 400 cm^3 motorcycle. The specific motorcycles were producing particles with mean size of 20-30 nm. Thus the PN-PEMS could give wrong results due to differences in the cut-off size of the CPC. The PN-PEMS compared to the PMP-TP can be seen in Figure 13-11. The differences are approximately -50% to 0%. There are a few tests where the PN-PEMS measured 40-80% higher. As it can be seen in Figure 13-12, these were tests where the GMD was around 15 nm. In this size range there is high uncertainty on the measured concentration of both the PN-PEMS and the PMP. Above 20 nm no size dependency could be observed.

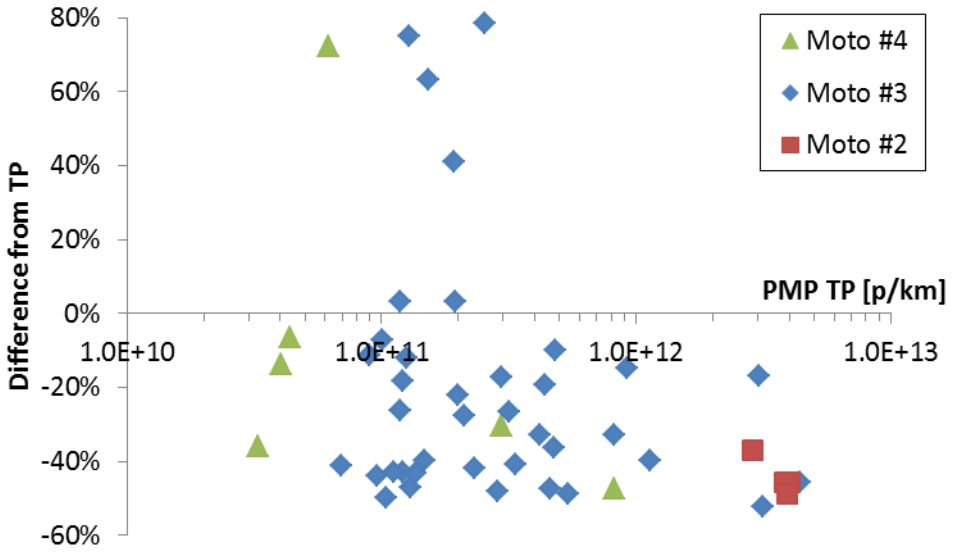

Figure 13-11: Comparison of PN-PEMs with PMP-TP when measuring motorcycles exhaust.

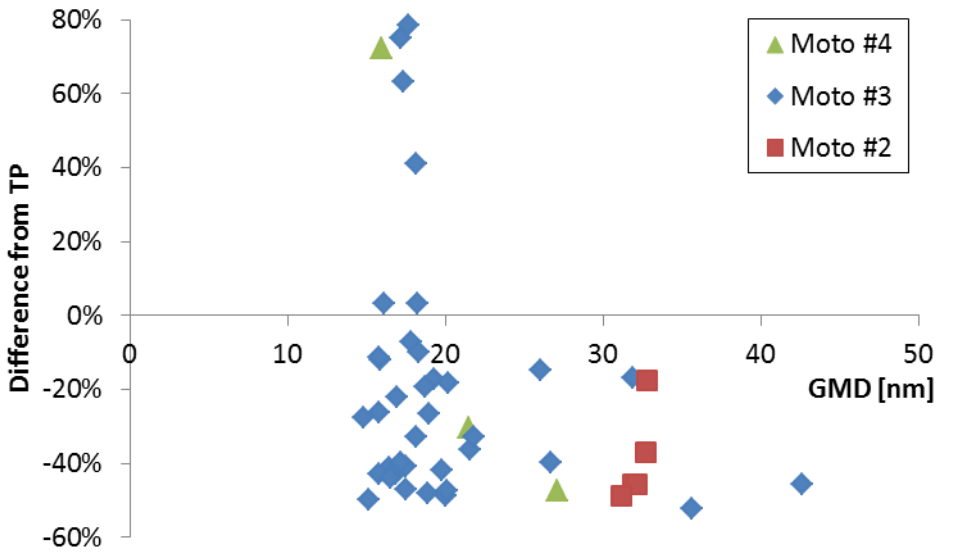

Figure 13-12: Size dependency of PN-PEMS for motorcycles particles.

13.9 Volatile removal efficiency

The volatile removal efficiency of the PN-PEMS was evaluated by sampling from the CVS diluted aerosol from a 2-stroke 50 cm^3 moped (Moto #1). The size distribution at the CVS has a mean around 90 nm. After thermal pre-treatment the mean decreases to <20 nm. The PN-PEMS was connected to the CVS. The results (with the previous GDIs) are shown in Figure 13-13. The PN-PEMS measures 50-70% less than the PMP-CVS indicating that the size of the particles was efficiently decreased and there was no re-nucleation that could influence the results (same behaviour compared to the results shown in Figure 13-7). Similar differences were seen with the GDIs.

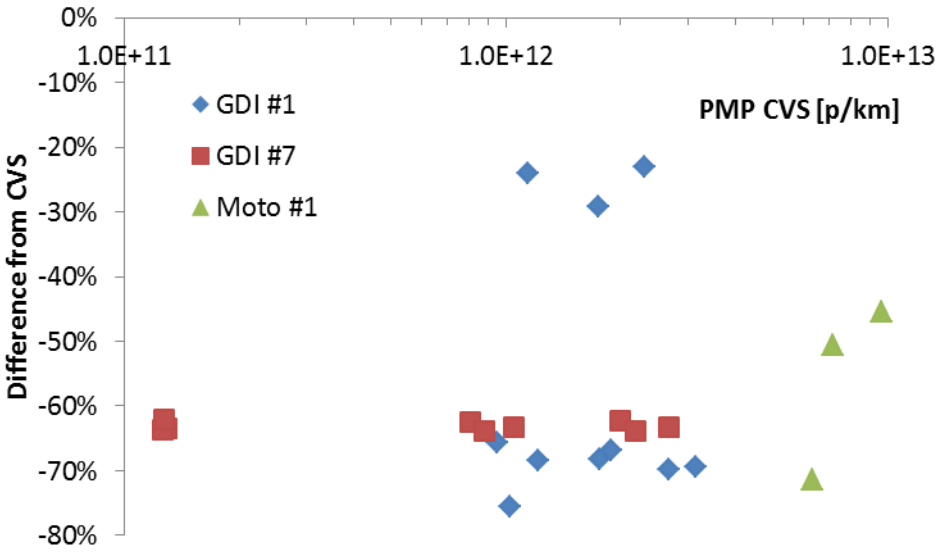

Figure 13-13: Behaviour of PN-PEMS when measuring moped's exhaust.

13.10 DPF Regeneration

The PN-PEMS was connected to the tailpipe of a diesel vehicle equipped with a DPF (#1), in parallel with the PMP-TP system. An EEPS was measuring from the dilution tunnel. Figure 13-14 compares all systems, after correction with the dilution factor at the dilution tunnel. EEPS was measuring >10^8 p/cm^3. However, the GMD of the nucleation mode was around 12 nm, so only a small percentage is >23 nm. The two PMP systems were very close to each other. The PN-PEMS was measuring 30% lower than the PMP-TP. During normal cycles (e.g. Artemis or WLTC) the PN-PEMS was also measuring 30% indicating that the PN-PEMS was not affected by the regeneration.

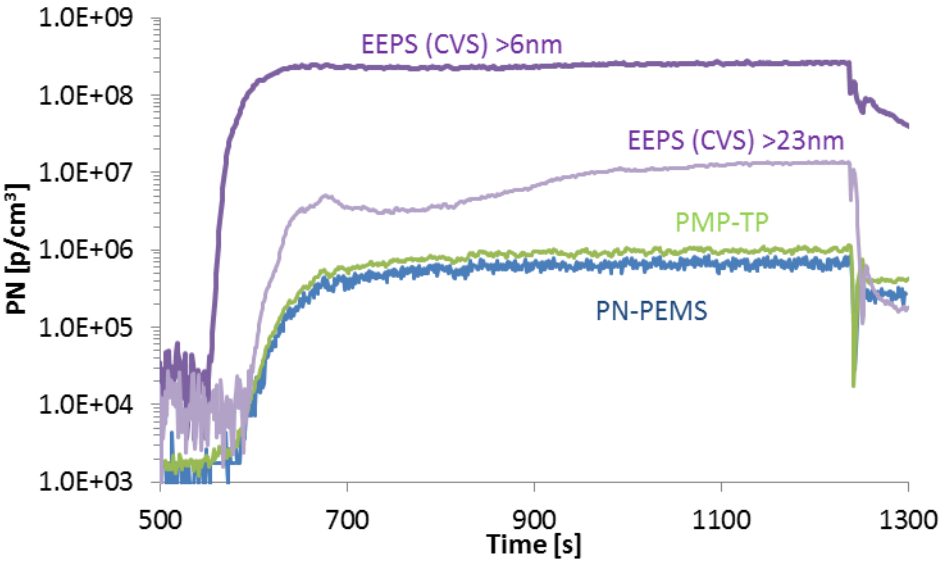

Figure 13-14: Regeneration tests with DPF #1. PN-PEMS connected to the tailpipe.

The PN-PEMS was connected to the dilution tunnel and was measuring in parallel with the PMP-CVS the emissions of a diesel vehicle equipped with a DPF (#2). An EEPS was measuring from the dilution tunnel. Figure 13-15 compares all systems. EEPS was measuring >10^7 p/cm³. The PN-PEMS was measuring 57% less than the PMP-CVS. Similar behaviour showed the PN-PEMS when connected to the CVS.

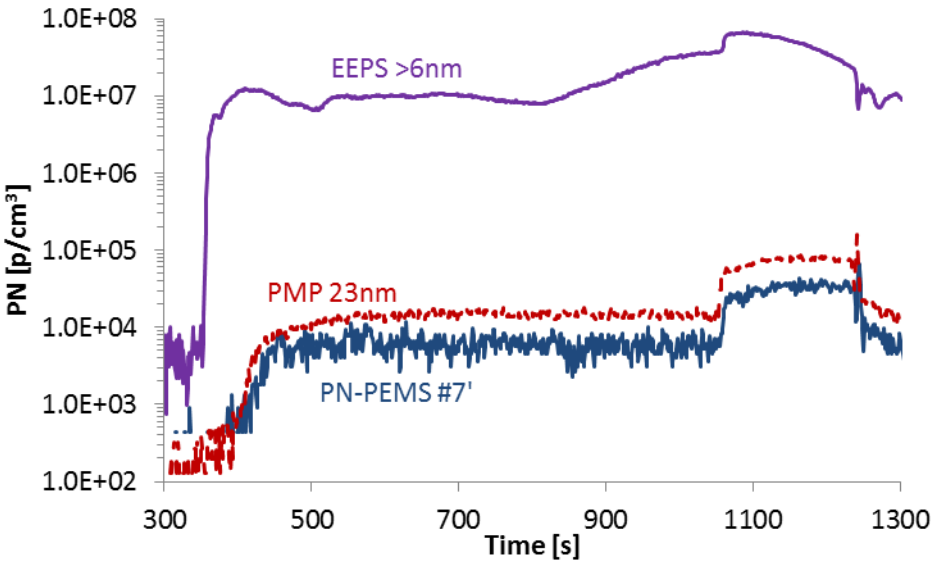

Figure 13-15: Regeneration tests with DPF #2. All systems connected to the dilution tunnel.

13.11 Summary

Figure 13-16 summarizes the differences of the PN-PEMS from the PMP-CVS and PMP-TP for all GDI cases examined. Figure 13-17 examines the motorcycles and the DPF equipped diesel vehicle.

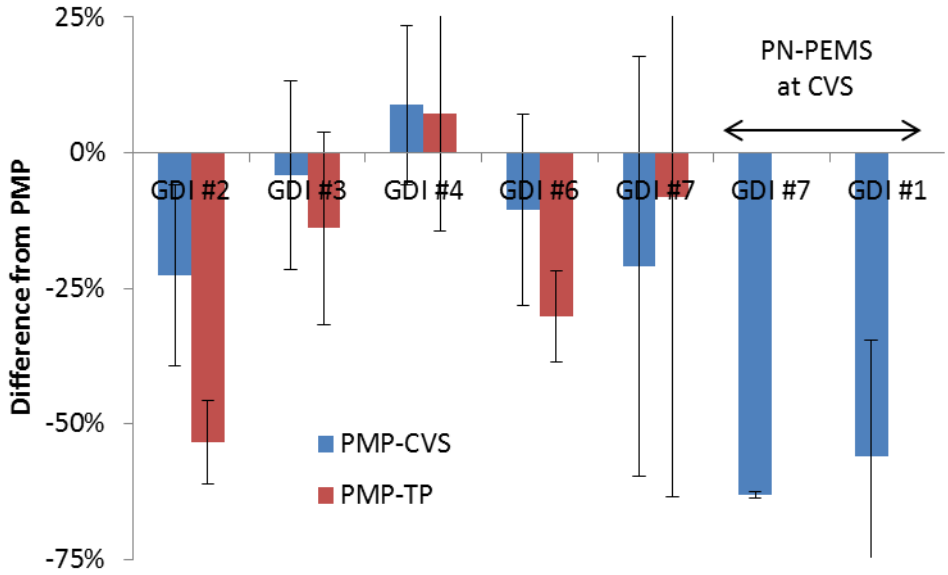

Figure 13-16: Overview of differences of PN-PEMS from the PMP-CVS and PMP-TP. Error bars are one standard deviation.

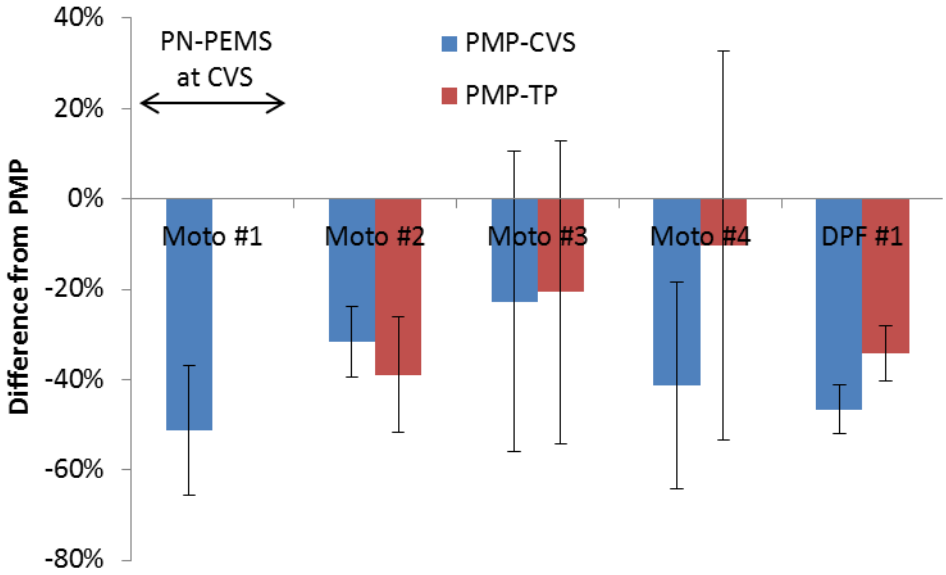

Figure 13-17: Overview of differences of PN-PEMS from the PMP-CVS and PMP-TP. Error bars are one standard deviation.

For GDIs, when the PN-PEMS was measuring at the tailpipe, the mean differences are -20% to +10% with a variability (expressed as ±standard deviation) of ±20%. When the PN-PEMS was at the CVS, the difference was around -50%. For motorcycles the differences ranged from -50% to -25%, with a variability of 20% or higher. Assuming that when the error bars cross the 0% the PN-PEMS is equivalent with the PMP-CVS, in most GDI cases the PN-PEMS (connected to the tailpipe) measured equivalently with the PMP-CVS.

Table 13-1 shows the PASS/FAIL results of the PMP-TP and the PN-PEMS compared to the PMP-CVS assuming a 6x10^11 p/km limit. The success rate (i.e. catching a FAIL as FAIL or a PASS as PASS) is not very high because the PN-PEMS was usually under-estimating the emissions.

Table 13-1: PASS/FAIL success rate.

Vehicle	Lab	Category	# of tests	PMP-TP	PN-PEMS
GDI #2	VELA 2	PASS	1		100%
	VELA 2	FAIL	5	100%	80%
GDI #3	VELA 2	PASS	0	-	-
	VELA 2	FAIL	17	100%	100%
GDI #4	VELA 2	PASS	8	75%	63%
	VELA 2	FAIL	27	100%	93%
GDI #6	VELA 2	PASS	10	100%	100%
	VELA 2	FAIL	6	100%	67%
GDI #7	VELA 1	PASS	3	100%	100%
	VELA 1	FAIL	6	100%	50%
GDI #1 (CVS)	VELA 2	PASS	0	-	-
	VELA 2	FAIL	10	-	60%
GDI #7 (CVS)	VELA 1	PASS	3	-	100%
	VELA 1	FAIL	6	-	50%
Moto #1 (CVS)	VELA 1	PASS	0	-	-
	VELA 1	FAIL	4	-	100%
Moto #4	VELA 1	PASS	6	83%	100%
	VELA 1	FAIL	0	-	-
Moto #3	VELA 1	PASS	30	100%	100%
	VELA 1	FAIL	0	75%	63%
Moto #2	VELA 1	PASS	0	-	-
	VELA 1	FAIL	5	100%	100%
DPF #1	VELA 2	PASS	14	100%	100%
	VELA 2	FAIL	3	100%	100%
DPF #2	VELA 2	PASS	2	100%	100%
	VELA 2	FAIL	1	100%	0%

14 Overview

At the moment a vehicle is certified in the laboratory with a specific test cycle (e.g. for light duty vehicles NEDC). However, the emissions measured during the certification process do not always represent the emissions in real operation of the vehicle. Revisions are under evaluation to ensure that real world emissions correspond to those measured at type approval (EC 2007). The use of portable emission measurement systems (PEMS) and the introduction of the 'not-to exceed' regulatory concept was decided for 2017+. However, the Particle Number (PN) systems are still under development and evaluation.

14.1 Phase I results

In 2013 a first campaign was conducted with various prototype PN-PEMS systems (Phase I). All of them were DC based. Based on the results of that campaign the following conclusions were drawn (Riccobono et al. 2014):

- DC based PN-PEMS is a feasible option for on-board measurements.
- At least one of the PN-PEMS showed good agreement with the reference PMP system (#3). A second one (#4) also had very good behaviour, but higher scatter.
- Thermal pre-treatment of the exhaust gas is necessary. A minimum temperature of 200°C was shown to be necessary and without nucleation/condensation at any point in the instrument.
- The 23 nm cut-off size was important to minimize any effect of re-nucleation or small solid particles.

A parallel work was also done to investigate how the new systems (based on DCs) could be calibrated. The main conclusions of that work were (Giechaskiel et al. 2014):

- PN-PEMS can be calibrated as a whole unit or separately (e.g. the VPR and the DC).
- The normalized efficiencies (to 100 nm) using soot should be less than 2.5 for 200 nm, and less than 0.5 for 23 nm. This normalization corresponds with a calibration with polydisperse aerosol of geometric mean diameter (GMD) of 75 nm and geometric standard deviation (GSD) of approximately 1.8.
- Using the 100 nm normalization calibration factor it was shown theoretically that the PN-PEMS can measure aerosol with particles having a GMD between 30 and 110 nm within -35% and +50%.
- However for real applications the DC measured emissions were always lower than the true (as measured with a reference PN system). For this reason an extra calibration factor was allowed until a final decision.

Phase II extended the previous findings. More specifically more vehicles were tested. Based on the new measurements the final calibration procedure was finalised. And the technical requirements were re-evaluated. Finally more accurate estimates of measurement uncertainty were given. The main findings are summarized below.

14.2 Examined emissions levels and technologies

In Phase II 7 GDI, 3 PFI and 2 DPF diesel vehicles were tested. In addition 1 moped and 3 motorcycles were used to challenge the PN-PEMS with extreme 'conditions' (Chapter 2, Annex A).

The GDIs had emissions that spanned from lower than 1x10^11 p/km up to 3x10^13 p/km. Special attention was given to the emission levels close to the 6x10^11 (current PN limit for diesel vehicles) because small differences there could result in a wrong PASS or FAIL result of the vehicle. For most GDIs the real time GMDs ranged typically from 40 to 100 nm (as measured with an EEPS downstream of a catalytic stripper at the CVS). However, there was a case that the size ranged from 20 to 80 nm. There was also a clear decreasing tendency of the GMD over the test cycle as the engine was getting warmer. This helped to investigate the size dependency of DC based PN-PEMS.

The cycle-mean GMDs as measured by the EEPS (corrected to match the SMPS, see Figure 4-6) are shown in Figure 14-1. They range from 40 to 65 nm. Note that the modes were in general 10-15 nm bigger. In the literature modes between 55 and 75 nm are found for GDI vehicles (Hall and Dickens 1999, Khalek et al. 2010, Maricq et al. 1999, 2011, Mohr et al., 2000, 2003, Ntziachristos et al. 2004), although most of the studies are relatively old. This means that the results of this study are similar or at the low edge of the reported sizes. A few studies with GDI engines have found wider range (25-110 nm) (Szybist et al. 2011, Hedge et al. 2011, Johansson et al. 2013). The Geometric Standard deviation (GSD) typically ranged from 1.6 to 2.0.

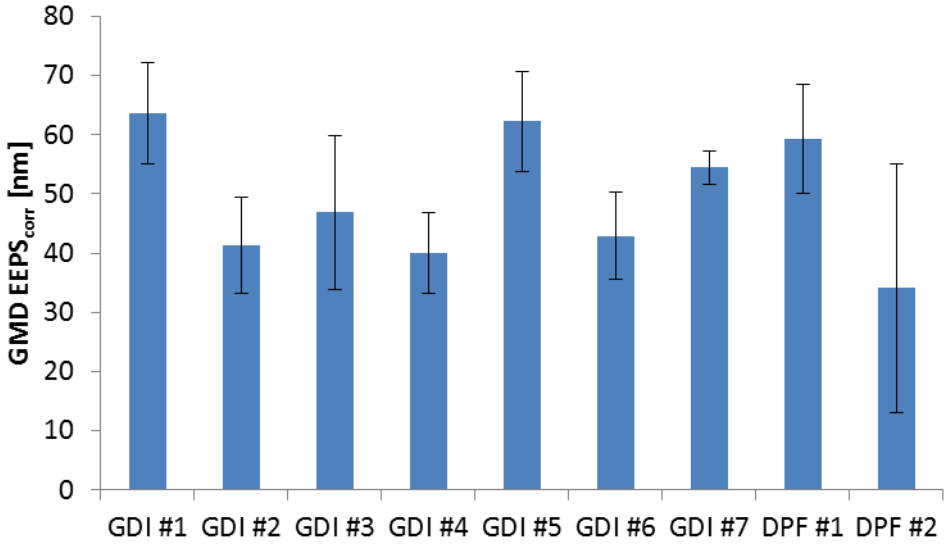

Figure 14-1: GMDs of GDIs and DPFs.

The PFIs were mainly tested to see how the PN-PEMS behave at relatively low emission levels (<1x10^11 p/km). In these technologies the emissions came mainly from accelerations.

The motorcycles were tested in order to challenge the PN-PEMS at their lower size range. Most of the motorcycles had high percentage of solid particles <23 nm. One moped was 2-stroke and high percentage of volatiles; thus the volatile removal efficiency of PN-PEMS was evaluated.

The GMDs of these technologies can be seen in Figure 14-2. The GSDs ranged from 1.55 to 1.85.

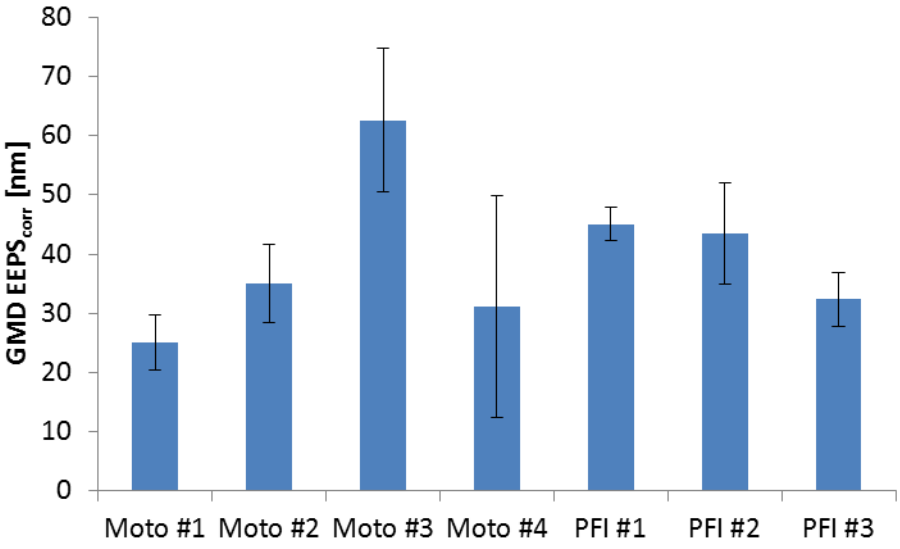

Figure 14-2: GMDs of motorcycles and PFIs.

14.3 PMP-CVS

The tests were conducted having almost always PMP systems both at the tailpipe and the CVS. One important finding was that the results between CVS and tailpipe had differences in many cases (Chapter 3). The mean differences spanned on average between 10% and 20% (tailpipe measuring higher) with a standard deviation of the differences 15%. The differences were attributed to coagulation, thermophoresis, exhaust flow accuracy and time alignment issues (Annex B). Coagulation could have an effect up to 20% for the highest emitting vehicle (4x10^12 p/km), but for most cases it should be <10%. Thermophoresis had low effect for the cold cycles but could reach up to 10% at the hot aggressive cycles. The time (mis)alignment of a few seconds could affect 5-15% the results; the effect was similar for both fast response time DCs and slower response time CPCs. The absolute level of the exhaust flow could affect the emissions up to 10%. Due to these differences, the evaluation of the PN-PEMS was always based on both PMP systems. Some of these phenomena affect only particle measurements (coagulation, thermophoresis), while others are common to the gas measurement too (exhaust flow accuracy, misalignment).

14.4 Summary of PN-PEMS

The results for each system were presented in Chapters 4-13.

14.4.1 PASS/FAIL

One way to evaluate the PN-PEMS was to investigate how many times they gave correct or wrong result compared to the PMP systems at the CVS (Table 14-1).

Percentages of 'correct' results below 90% were noted in red (this value was chosen arbitrarily). Since this evaluation includes the changes that happen between tailpipe and dilution tunnel the same evaluation for the PMP system at the tailpipe (PMP-TP)

was included. This way it can be ensured that a low score for a PN-PEMS is due to the system itself and not due to the particles evolution in the exhuast lines after the tailpipe. The main conclusions are:

Table 14-1: Summary of success rates (for PASS or FAIL) for the PN-PEMS and the PMP-TP. Comparisons are versus the PMP at the dilution tunnel (PMP-CVS). The number of tests that were available and considered for the success rate is also shown. In red success rates <90%. All systems calibrated by the manufacturers except #3 (LDSA) which was calibrated by JRC.

		PMP-TP	#1'	#2' (CPC)	#2' (DC)	#3	#3 (LDSA)	#4	#5'	#6'	#7'
GDI #1	PASS							0 -			0 -
(CVS)	FAIL							9 100%			10 60%
GDI #2	PASS	61%	13 100%			13 92%^	13 92%^	13 100%	14 79%	5 80%	1 100%
(TP)	FAIL	100%	31 84%			41 94%	41 91%	32 94%	31 80%	10 100%	5 80%
GDI #3	PASS	-	0 -					0 -	0 -	0 -	0 -
(TP)	FAIL	100%	34 100%					30 100%	34 100%	29 100%	17 100%
GDI #4	PASS	79%	9 100%			9 67%	9 78%^	9 100%	7 86%	8 88%	8 63%
(TP)	FAIL	100%	41 67%			41 100%	41 98%	41 85%	30 90%	38 82%	27 93%
GDI #5	PASS	-	0 100%								
(CVS)	FAIL	-	12 100%								
GDI #6	PASS	81%	26 100%	20 90%	26 69%	13 100%	13 100%	2 100%	14 64%	34 50%	10 100%
(TP)	FAIL	100%	12 92%	2 100%	11 100%	9 100%	9 100%	3 100%	3 100%	11 100%	6 67%
GDI #7	PASS	100%	2 100%	3 100%		2 100%			1 100%		3 100%
(TP)	FAIL	100%	4 100%	6 100%		4 100%			2 100%		6 50%
GDI #7	PASS	-	3 100%	3 100%						11 91%	3 100%
(CVS)	FAIL	-	6 100%	6 100%						16 100%	6 50%
PFI #1	PASS	-				6 100%	6 100%				
(CVS)	FAIL	-				0 -	0 -				
PFI #2	PASS	-				3 100%	3 67%				
(CVS)	FAIL	-				16 100%	16 100%				
PFI #3	PASS	-	22 100%								
(CVS)	FAIL	-	7 86%								
Moto #1	PASS	-	0 -	0 -		0 -	0 -	0 -		0 -	0 -
(CVS)	FAIL	-	4 100%	4 100%		3 100%	3 100%	1 100%		4 100%	4 100%
Moto #2	PASS	-								0 -	0 -
(TP)	FAIL	100%								3 100%	5 100%
Moto #3	PASS	100%	30 100%	24 92%	15 100%	15 93%	15 100%	18 100%	9 100%	30 0%	30 100%
(TP)	FAIL	86%	8 75%	5 100%	4 100%	4 75%	4 50%	2 100%	1 100%	7 100%	0 63%
Moto #4	PASS	89%	6 83%	6 83%	6 50%	6 83%	6 100%	6 83%		6 17%	6 100%
(TP)	FAIL	-	0 -	0 -	0 -	0 -	0 -	0 -		0 -	0 -
DPF #1	PASS	100%	9 100%								14 100%
(TP)	FAIL	100%	0 -								3 100%
DPF #2	PASS	100%		2 100%		2 100%	2 100%				2 100%
(TP)	FAIL	100%		1 100%		1 100%	1 100%				1 0%

^ allowing 10% error these percentages become 100%

- For GDIs that have high emission levels (e.g. GDI #1, GDI #3, and GDI #5, >6x10^11 p/km) the PN-PEMS can easily identify a FAIL. Exception PN-PEMS #7' that was underestimating the emissions.
- For GDIs that have emission levels close to the limit or higher (e.g. GDI #2, GDI #4) the PN-PEMS have around 80% success rate (to catch a PASS or FAIL). Some of the PN-PEMS, the most accurate, reach more than 90%. Interestingly, the PMP-TP fails to catch also the PASS, as it is measuring higher (success rate 60-80%). Most PN-PEMS are closer to the PMP-TP.

- For GDIs that have emission levels close to the limit or lower (e.g. GDI #6, GDI #7) the PN-PEMS have high success rate to catch a FAIL. For a PASS the success rate is lower but similar to the PMP-TP.
- For PFIs, the tests were conducted at the CVS and only a limited number of PN-PEMS were tested. The results were satisfactory with similar success rates (typically >80%).
- For motorcycles the success rate was 100% or similar to the PMP-TP when lower.

In general, the results show that the PN-PEMS, with a few exceptions had a high success rate and were able to catch a PASS or FAIL. When this was not the case, they had similar success rates with the PMP-TP.

An interesting note is that changing the emission limit (e.g. to 1x10^12) wouldn't change the results significantly. The reason is that the main reason of a correct result depends on the accuracy of the PN-PEMS (which depends on the calibration) and the precision (scatter) (which is relatively constant for the range examined).

14.4.2 Accuracy (bias and precision)

A second way of evaluating the PN-PEMS was to estimate the differences compared to the PMP-CVS or PMP-TP (bias). This shows whether the calibration was correct and whether the calibration factor is sensitive to the vehicle that is being measured.

Initially the PN-PEMS were compared with the PMP-TP, when both were sampling from the tailpipe (Table 14-4a). This comparison gives the bias and precision of the PN-PEMS. Reasonable differences were considered between -25% and +30% (with standard deviation lower than 20%). These values were based on typical differences between PMP systems at the tailpipe. The best performing systems were #1, #2' (CPC) and #3. PN-PEMS #6' based on limited number of tests also showed good performance until condensation issues. Quite good behaviour was shown by #7' (some issues with absolute levels) and #4 and #5 (but higher scatter of results).

At a next step the PN-PEMS were compared with the PMP-CVS (Table 14-4b). This comparison includes the uncertainty introduced by the different sampling locations. Due to the processes that can take place between tailpipe and dilution tunnel, reasonable differences (bias) were considered between -35% and +50% (with precision less than 25%). These values were arbitrarily selected to include typical differences of the PMP-TP to the PMP-CVS plus some uncertainty for the PN-PEMS (Giechaskiel et al. 2010). The PMP-TP had the best performance (bias better than 20%, precision better than 15%), followed by the PN-PEMS #1', #2' (CPC) and #3. Quite good behaviour was shown by #7' (some issues with absolute levels) and #4 and #5 (but high scatter of results). PN-PEMS #6' had good performance at the tailpipe, but not at CVS without thermal pre-treatment.

It should be noted that the EEPS downstream of a catalytic stripper always connected at the dilution tunnel, which could be considered an advanced DC based PN-PEMS, gave differences to the PMP-CVS between 20% and 40% (-30% to -10% with correction factor following the calibration procedures) (precision 15%).

14.4.3 Cut-off size

The sensitivity of PN-PEMS to smaller than 23 nm (solid) particles was assessed by measuring motorcycles exhaust gas (Moto #3 and Moto #4). The results showed that most CPC based PN-PEMS were only slightly affected (e.g. #2' (CPC) and #7' (CPC)), although differences in the cut-off size resulted in higher scatter of the differences. Some concerns were raised for the CPC of #5' because of its lower than 23 nm cut-off. The DC based PN-PEMS actually were slightly underestimating the emissions (e.g. #1' and #3). PN-PEMS #4 and #5' behaved very well as well.

14.4.4 Volatile removal efficiency

The volatile particle removal efficiency was assessed by measuring exhaust aerosol of a 2-stroke moped (Moto #1) (see Table 14-4). For the systems tested there was no indication of overestimation of emissions. The typical volatile removal approaches from the PN-PEMS were:

1. PMP approach (hot dilution and evaporation tube) with CPC (PN-PEMS #7') or DC (PN-PEMS #3).
2. PMP-like approach and addition of catalytic stripper with DC (PN-PEMS #1', PN-PEMS #5') or CPC (PN-PEMS #5')
3. Hot sampling (>190°C) and dilution at 47°C or direct measurement (e.g. PN-PEMS #6' and #4). PN-PEMS #2' (DC) used an evaporation tube at 350°C and then cold sampling.
4. Cold dilution and a catalytic stripper (PM-PEMS #2 (CPC))

The first approach was sufficient when using high dilution (>100 primary dilution) both when using a CPC and a DC. There are some concerns for DC based systems if a low dilution is used (artefact form re-nucleation), as investigated in the lab (see below).

The second approach was successful at all cases examined.

The third approach in general was sufficient. However PN-PEMS #6' probably had some condensation issues at some point of the campaign. PN-PEMS #4 had high scatter with Moto #2 indicating that even a temperature of 200°C might not be sufficient for the extreme case of motorcycles (high amount of volatiles). PN-PEMS #2 (DC) with evaporation tube and cold dilution was not available for these tests. Probably the diffusion screens would also minimize the effect; however, it needs to be tested.

PN-PEMS #2' (CPC) followed a different approach: the primary dilution was cold, but there was a water trap and a desiccant dryer, then a catalytic stripper and a CPC with 23 nm cut-off size: The draft requirements specified non condensing aerosol (thus no cold dilution of the undiluted hot exhaust). PN-PEMS #2' (CPC) fulfilled this requirement for ambient temperatures of 20°C, and had very good results. Heating of the primary dilution would be necessary for low ambient temperatures. In general the results of PN-PEMS #2' (CPC) were equivalent with the reference instrument. However testing at low and high ambient temperatures and the long term stability of this approach was not investigated.

PN-PEMS #6' was used with 47°C when connected at the dilution tunnel and it was shown that it couldn't efficiently remove the volatiles from the motorcycles. Thus a minimum thermal pre-treatment is absolutely necessary. The results of this study showed that the technical requirements regarding the thermal pre-treatment were

sufficient. However, based on the findings of Phase II for motorcycles, a minimum temperature of 300°C is recommended.

The above findings were in agreement with the lab tests (Annex C) with tetracontane and atomized emery oil tests. Systems with catalytic stripper could handle very high mass of volatiles compared to those only with evaporation tube. Systems with a 23 nm cut-point were also much less sensitive to re-nucleation artifacts or growth of solids below 23 nm. An extra check with atomized oil is recommended in order to distinguish systems that have high volatile removal efficiency.

14.5 Robustness

The Phase II evaluation was done with second generation PN-PEMS. One was even the same unit that was used in Phase I and didn't have any issues, indicating that PN-PEMS can be very robust. On the other hand, there were others that had issues from the beginning. The issues that happened were malfunction of CPC, failure of heated line, condensation at the electrometers, leakage between sampling lines, drift of the diluter. These topics should be addressed by the manufacturers in the future in order to be able to easily identify issues. It should be mentioned though that the PMP system at the tailpipe also showed indications of drift/wear. Nevertheless, this study showed that both DC and CPC based systems can be robust enough for long periods. Specific comments for each system will be given below.

14.6 Specific comments for PN-PEMS

Below some comments for the PN-PEMS examined in this study will be given. Some of them have already been taken into account by the instrument manufacturers.

14.6.1 PN-PEMS #1'

Advantages

It showed excellent comparability in terms of absolute levels (bias) and variability (precision).

Robust during the whole campaign in the lab.

PMP like thermal pre-treatment with catalytic stripper. No volatile artefact was noticed.

Minor effect of solid sub-23 nm particles.

Concerns

Small size dependency (but among the smallest of the DC based systems).

No on-board evaluation (software issues before the tests)

Needs a laptop (not important if integrated in a complete PEMS).

14.6.2 PN-PEMS #2 (CPC)

Advantages

Mini PMP system. It can be calibrated as a PMP system (but only as a whole unit).

It showed excellent comparability in terms of absolute levels (bias) and variability (precision).

Excellent real time correlation with the PMP system at the tailpipe.

Robust for the (short) period that was evaluated.

No effect of solid sub-23 nm particles.

No interference of volatile particles was noticed.

Concerns

The system arrived at the end of the measurement campaign, so it was not thoroughly investigated. Tests after the end of the campaign with 10 more vehicles (tests from the dilution tunnel) didn't indicate any issues.

The VPR is compliant with the draft technical requirements only for ambient temperatures of 20°C (temperature should be higher than the dew point of the exhaust gas).

No on-board evaluation (issues with the software) during the main campaign. At the end of the campaign a limited number of on-board tests showed very good behaviour (Annex D).

No tests were conducted at low ambient temperature, but the CPC is optimized for -10°C to +40°C, so no issues are expected. Heating of the dilution air and the primary diluter would be needed.

Needs a laptop (not important if integrated in a complete PEMS).

Can run up to 4 h in sequence (then wick exchange is needed). Not a problem for PEMS testing but it might be an issue for long testing e.g. in test beds.

CPC control functions are important in order to see the status of the CPC.

Needs exchange of the desiccant dryer approximately weekly (every 5 tests/days)

14.6.3 PN-PEMS #2' (DC)

The system arrived at the end of the measurement campaign, so it was not thoroughly investigated.

The VPR is not fully compliant with the draft technical requirements foe low ambient temperatures (temperature should be higher than the dew point of the exhaust gas). No tests were conducted at low ambient temperature.

No error indication when the dilution air was disconnected.

Needs a laptop (not important if integrated in a complete PEMS).

No on-board evaluation (not available during that period).

14.6.4 PN-PEMS #3

Advantages

It was successfully investigated in Phase I.

PMP thermal pre-treatment

Measured very accurate and precisely at all tests examined.

Minor effect of solid sub-23 nm particles.

No volatile artefact was noticed at high dilutions.

Small and compact without the need of external devices (e.g. laptop)

Robust during the whole campaign
Successfully tested on-board
Estimated PN (and size)

Concerns:
Low dilution can result in re-nucleation and measurement artefact.
High dilution can result in low current and wrong final results (usually overestimation).
Long term robustness hasn't been proven (units of Phase I and II were different). There was a leak after extended use of the system after the end of the campaign.
In case the total current is used (or the LDSA) there is a sensitivity on the measured size distributions.

14.6.5 PN-PEMS #4

Advantages
It was successfully investigated in Phase I.
The same unit was used in Phase II.
The results were similar as in Phase I. Generally the bias is small.
It was robust in both Phases.
Minor effect of solid sub-23 nm particles.
Concerns
It has rather high scatter probably due to the size dependency (low precision).
The temperature of 200°C might not be sufficient for extreme cases (e.g. 2-stroke motorcycles).
It's relatively big and heavy for on-board application of small vehicles.

14.6.6 PN-PEMS #5'

The sampling system includes hot dilution and catalytic stripper. No volatile artefact was noticed.
It has rather high scatter probably due to the size dependency of the DC.
The CPC couldn't be evaluated because there were many issues.
Needs a laptop (not important if integrated in a complete PEMS).

14.6.7 PN-PEMS #6'

When used at the tailpipe the comparability with the reference system was good.
It seems sensitive to condensation.
No need for laptop.
Minor effect of solid sub-23 nm particles.
No on-board evaluation (issues before the tests)

14.6.8 PN-PEMS #7'

Advantages

Mini PMP system (calibrated according to PMP procedures)

Excellent real time correlation with the PMP system at the tailpipe

No effect of solid sub-23 nm particles.

No volatile artefact was noticed.

Concerns

The emissions were generally underestimated

Needs a laptop (not important if integrated in a complete PEMS).

Some connectors were broken easily.

CPC control functions are important in order to see the status of the CPC.

Can run up to 4 h in sequence (then wick exchange is needed). Not a problem for PEMS testing but it might be an issue for long testing e.g. in test beds.

No on-board evaluation (issues with the temperature).

14.7 Calibration in the lab

In Phase I (Giechaskiel et al. 2014) normalized to 100 nm efficiency requirements at sizes between 23 nm and 200 nm were defined (Table 14-2). Efficiency is the ratio of the instrument to a CPC when both are measuring monodisperse aerosol. These efficiency requirements were defined to set upper limits for the size dependency of PEMS. The reason of the normalization at 100 nm was to minimize the extra calibration work that would be needed for PMP systems that could be used for on-board use. In addition this factor was found to minimize the difference of DCs from PMP systems in a wide range of 40-110 nm. Nevertheless, an extra factor was allowed to enable the manufacturers to calibrate their devices for typical exhaust distributions (i.e. adjust the absolute levels measured).

For a few PN-PEMS the calibration procedures described in Giechaskiel et al. (2014) were followed and the measured efficiencies were compared with the draft requirements. Targets of the tests in Phase II were to confirm the requirements for the new generation of PN-PEMS and to define the correct calibration factor.

Regarding the efficiency requirements, Table 14-2 summarizes the results of Phase II and compares them with the requirements of Phase I. The 50 nm requirement cannot be achieved easily. The 200 nm requirement could be more strict (e.g. <2.25), thus further reducing the size dependency of DCs. Also the 23 nm requirement could be a little bit looser to accommodate future PMP systems. But this would mean more strict volatile removal efficiency requirements to ensure no volatile nucleation particles enter the sensor.

Although the calibration procedure is clear, the final extra calibration factor depends on the size (or size distribution) that will be selected to optimize the behaviour of PN-PEMS. It was confirmed also in Phase II, that using the calibration factor of the 100 nm normalization (i.e. extra factor 1) results in underestimation of the emissions compared to the PMP reference system. Thus extra factors were used to calibrate the instruments for typical exhaust size distributions. A factor closer to 1.7 was found the best match for the cases examined. Here, using the exhaust gas particle size distributions of 7 GDIs (see

Figure 14-1), it was also shown that a monodisperse size close to 70 nm (which corresponds to a GMD of 55 nm) gives the best results. Actually for some vehicles (mainly motorcycles) even this size will underestimate the emissions (Figure 14-2).

The CPC based PN-PEMS didn't have this issue. The normal calibration procedures of PMP systems gave the correct calibration factors.

Table 14-2: Efficiency ratios (spark-discharge graphite particles). The extra factor was based on optimization of the DCs' response to GDIs particles (details in relevant chapters).

Efficiency ratios (draft requirements)	**23 nm**	**50 nm**	**100 nm**	**200 nm**	**Extra factor**
	<0.5	**0.4 - 1**	**1**	**<2.5**	
CPC based					
PMP-CVS (Vela 1) (estimation)	0.40	0.95	1.05	1.05	-
PMP-CVS (Vela 2)	0.35	0.84	0.99	1.00	-
PMP-TP	0.36	0.80	0.91	0.91	-
PN-PEMS #2' (CPC)	0.57	0.92	0.99	0.99	-
PN-PEMS #7'	0.38	0.89	1.00	1.00	1.60
DC based					
PN-PEMS #1'	0.06	0.38	1.00	2.17	1.45
PN-PEMS #2 (DC)	0.12	0.26	1.00	2.69	2.20
PN-PEMS #3 (LDSA)	0.10	0.35	1.00	2.23	1.75
PN-PEMS #3 (PN)	0.53	0.77	1.12	1.07	-
PN-PEMS #4 (Phase I)	0.12	0.45	1.00	2.25	2.20

Table 14-3 shows the original (Phase I) requirements for PN-PEMS, the adjusted based on Phase II, and the equivalent requirements by normalizing at 70 nm are shown (in this case no extra calibration factor is allowed). The results refer to soot (propane diffusion flame or spark discharge graphite). Note that the EEPS gave different results between graphite and diffusion flame soot, indicating that the material should be even defined better.

Table 14-3: Comparison of different efficiency proposals.

d_p **[nm]**	**23**	**50**	**70**	**100**	**200**	**Extra**
PMP (estim.)	0.4	0.95	1.0	1.0	1.0	No
PEMS Phase I	<0.5	>0.4	-	1.0	<2.5	Yes
PEMS Phase II	<0.6	>0.6	1.0	<1.6	<3.7	No
PEMS (to confirm)	<0.6	>0.6	0.7 – 1.3	0.7 – 1.3	<2.0	No

These efficiencies refer to the whole system. The system can be measured as one unit or its parts independently. In the second case the VPR has to be calibrated at least at 30, 50, 70 and 100 nm. The sensor has to be calibrated at least at 23, 70 and 200 nm.

In Phase II it was shown that 'advanced' DCs with extra (size) info can have efficiencies very close to CPCs. In addition no extra calibration factor is needed. Thus it could be possible to further restrict the efficiencies as in the new proposal shown in the Table 14-3, which is based partly on the Swiss regulation for construction machinery (Schlatter 2012). However the improved real time operation of these systems was not proved and needs further investigation. The improvement of the correlation to the reference system can be estimated by the experimental data. Assuming that EEPS could be the most advanced DC based PN-PEMS, the differences of advanced DCs would reduce the differences from the range of -35% to 50% to the range of ±30% approximately and the precision from 25% to 15%. Ideally, CPC based systems would further reduce this range to ±20% (precision 15%), based on the comparisons of the reference PMP systems at the dilution tunnel and the tailpipe. As mentioned above, the CPC based systems can easily fulfil even the stricter requirements.

For one system (PN-PEMS #3) the calibration was repeated at the end of the measurement campaign to see drifts or uncertainties in the calibration procedures. The differences were on the order of 15%. Nevertheless, the ratios of the efficiencies for the different sizes were almost identical. The challenge of calibrating DCs is that the current measured is low compared to what measured in real life applications. Higher concentrations cannot be used because of the upper measurement range of the reference instruments during the calibration procedure. This issue was already addressed in Phase I (Giechaskiel et al. 2014) where an experimental uncertainty of 15% was found. It also points out the importance of well-defined procedures, with well calibrated instruments and signals for the DCs that are much higher than their background level. The newly suggested values should cover well preforming instruments and the experimental uncertainties.

14.8 Calibration with exhaust particles

Some of the PN-PEMS were calibrated with GDI exhaust particles by the manufacturers before the measurement campaign (PN-PEMS #1', PN-PEMS #2 (DC), PN-PEMS #4). The absolute levels that were measured in Phase II were in general close to the PMP instruments.

During the measurements it was investigated whether a comparison with a PMP system in a chassis dynamometer during a test cycle could be used to optimize the calibration factor. It was shown that the difference to the PMP system was different between cold and hot cycles, due to the different sizes of the produced particles. Thus a check or calibration in a chassis dynamometer needs attention for DC based systems. It should be mentioned though, that the correction factor adjustment for well calibrated instruments was within the experimental uncertainty and scatter of the chassis results, making the procedure unnecessary (for well calibrated instruments). The second point is that the results at the tailpipe and the dilution tunnel with the PMP systems had also differences thus further questioning the accuracy of the calibration factor adjustment with exhaust gas particles. Finally based on the new efficiency requirements of Phase II no calibration

factor is allowed. The lab measurements can serve only as a check of the proper operation of the systems.

14.9 Key messages

The key findings of Phase II are summarized below:

The sampling location can have an effect on the particle number concentration. The comparison of the two PMP systems (one at the tailpipe and one in the dilution tunnel) showed that this difference is on the order of 10-20% with a scatter of 15% (expressed as one standard deviation). Part of this difference can be attributed to exhaust flow accuracy and time misalignment (that affect also gaseous pollutants) and part to thermopheretic and coagulation losses (that influence only particles).

The feasibility of the on-road measurements with DC-based systems was confirmed. In Phase II two systems (one was the same as in Phase I) showed excellent behaviour (bias less than 30% and precision around 20%, expressed as one standard deviation). One system, as in Phase I, had good agreement with the PMP system but high scatter (up to 60% for some vehicles).

The expected measurement uncertainty of the PN-PEMS includes the 'sampling location' uncertainty (10-20%) and the PN-PEMS uncertainty mainly due to size dependency (30%). The total uncertainty was found to be lower than 50% with scatter better than 25%. These values refer to differences from reference PMP systems at the CVS over a cycle (>10 min duration). These values include the tests with motorcycles and mopeds where the GMD was on the order of 25 nm. For GDIs the results were in general within 30% (20%). The second by second data have higher differences.

The newly developed CPC-based PN-PEMS had promising results, especially for the real time behaviour. However, their robustness has still to be proven. One system that arrived at the end of the campaign had behaviour equivalent with the reference systems (as tests after the measurement campaign with 10 vehicles showed).

The PASS or FAIL results at the 6x10^11 p/km level are almost 100% for some of the PN-PEMS. Nevertheless, the uncertainty mentioned above should be taken onto account.

Many of the PN-PEMS were compact, small and light with low energy consumption. Some of them are ready for on-board use. One of them (DC based) has been already tested with on-board tests successfully. One CPC based also didn't show any issues during on-board tests after the end of the campaign. Nevertheless, there were systems with issues and thus the on-board robustness is a topic that needs to be addressed by the instrument manufacturers. It should be noted that there were indications that the PMP system at the tailpipe also showed wear signs.

The thermal pre-treatment is necessary and the PMP-like approach works (hot dilution and evaporation tube at 300°C). Addition of catalytic stripper in some systems proved that this approach is more robust and can be used at low dilutions too.

Dedicated lab tests showed that the tetracontane tests even at very high concentrations could be passed by the systems tested. Tests with atomized oil showed the limitations at specific high concentrations, which however could be representative of 2-stroke engines. Thus for PN-PEMS (and generally raw exhaust applications) specific volatile removal efficiency tests should be defined.

In Phase I it was required that the PN-PEMS should fulfil some efficiency requirements (to control the size dependency). A correction factor was allowed to adjust the absolute

levels to typical exhaust size distributions. In Phase II the size dependency (efficiencies) and the absolute levels were combined in the new efficiency requirements that are normalized to monodisperse size 70 nm. This size corresponds to a polydisperse distribution of approximately 55 nm which was the mean GMD of the GDIs tested. The GMDs ranged from 35 nm to 75 nm which resulted to differences of ±30% (standard deviation 20%) to the PMP systems.

Some instruments showed even lower size dependency indicating that the requirements could become stricter. However the real time behaviour of these instruments has to be further investigated.

Table 14-4: a) Differences of PN-PEMS to the PMP-TP. b) Differences of PN-PEMS to the PMP-CVS. The mean of the differences and the standard deviation is given, with the number of tests that were available or considered (#). When comparing with PMP-TP (a) in red differences outside the range of -25% to +30%, or standard deviations higher than 20%. When comparing with the PMP-CVS (b) in red differences outside the range of -35% to +50%, or standard deviations higher than 25%. Note: PN-PEMS #6' was connected at the CVS for GDI #6, Moto #3 and Moto #4. At CVS no thermal pre-treatment was used. All results are based on the manufacturers' calibrations. Exception #3 (LDSA) which followed the recommended calibration procedures. PN-PEMS #1' would be shifted +10% and PN-PEMS #2 (DC) -40% if the calibration procedures would be followed.

		PMP-TP			#1'			#2' (CPC)			#2' (DC)			#3			#3 (LDSA)			#4			#5'			#6'			#7'		
		Mean	Dev	#	Mean	Dev	#	Mean	Dev	#	Mean	Dev	#	Mean	Dev	#	Mean	Dev	#	Mean	Dev	#	Mean	Dev	#	Mean	Dev	#	Mean	Dev	#
GDI #1	**CVS**																			18%	27%	9							-56%	21%	10
GDI #2	**TP**	20%	12%	47	-6%	18%	44							6%	22%	47	4%	15%	47	15%	28%	48	26%	51%	47	37%	28%	15	-23%	17%	6
GDI #3	**TP**	12%	13%	40	-16%	27%	34													19%	77%	30	42%	92%	34	12%	28%	29	-4%	17%	17
GDI #4	**TP**	7%	7%	50	-24%	16%	48							18%	11%	50	8%	11%	50	-11%	21%	50	1%	31%	37	-17%	15%	46	9%	15%	31
GDI #5	**CVS**				26%	8%	12																								
GDI #6	**TP**	19%	10%	37	-11%	20%	37	19%	16%	22	63%	41%	37	-15%	8%	26	-10%	12%	26	4%	21%	5	53%	53%	17	113%	135%	37	-10%	18%	16
GDI #7	**TP**	-10%	9%	9	-18%	17%	6	-1%	16%	9				-27%	12%	6	-11%	8%	6				45%	58%	3				-21%	39%	9
GDI #7	**CVS**	-2%	2%	9	3%	9%	9	11%	2%	9																128%	115%	27	-63%	1%	9
PFI #1	**CVS**													1%	11%	6	42%	25%	6												
PFI #2	**CVS**													8%	19%	19	28%	29%	19												
PFI #3	**CVS**				3%	18%	29																								
Moto #1	**CVS**	25%	21%	7	-52%	2%	4	32%	6%	4				64%	41%	3	-4%	13%	3	36%	-	1				46%	154%	3	-51%	14%	4
Moto #2	**TP**	9%	11%	8																102%	102%	7				140%	36%	4	-32%	8%	5
Moto #3	**TP**	-2%	23%	38	-17%	22%	38	25%	37%	29	48%	50%	19	19%	25%	19	-34%	16%	19	-24%	23%	20	-15%	28%	10	555%	331%	38	-23%	33%	38
Moto #4	**TP**	-13%	48%	9	-25%	44%	6	-15%	48%	6	227%	159%	6	9%	33%	6	-40%	37%	6	-21%	55%	6				2388%	1898%	6	-41%	23%	6
DPF #1	**TP**	-19%	9%	17	-28%	6%	9																						-47%	5%	17
DPF #2	**TP**	-16%	3%	3				-9%	1%	3																			-57%	1%	3

			#1'			#2' (CPC)			#2' (DC)			#3			#3 (LDSA)			#4			#5'			#6'			#7'		
			Mean	Dev	#	Mean	Dev	#	Mean	Dev	#	Mean	Dev	#	Mean	Dev	#	Mean	Dev	#	Mean	Dev	#	Mean	Dev	#	Mean	Dev	#
GDI #2	**TP**		-21%	11%	44							-13%	10%	47	-14%	9%	47	-4%	20%	45	4%	36%	47	7%	20%	15	-53%	8%	3
GDI #3	**TP**		-24%	16%	34													4%	56%	30	25%	65%	34	2%	16%	29	-14%	18%	17
GDI #4	**TP**		-30%	14%	48							10%	13%	50	1%	11%	50	-17%	19%	50	-6%	26%	37	-23%	13%	46	7%	22%	35
GDI #6	**TP**		-26%	12%	37	0%	6%	22	38%	34%	37	-15%	8%	26	-19%	16%	26	-10%	8%	5	34%	46%	17				-30%	8%	13
GDI #7	**TP**		-10%	9%	6	9%	7%	9				-21%	8%	6	-3%	3%	6				63%	51%	3				-8%	55%	9
Moto #2	**TP**																	70%	75%	7							-39%	13%	5
Moto #3	**TP**		-14%	18%	38	22%	36%	29	50%	57%	19	26%	15%	19	-30%	14%	19	-28%	24%	20	-19%	28%	10				-21%	34%	38
Moto #4	**TP**		8%	26%	6	15%	18%	6	508%	529%	6	74%	88%	6	-21%	6%	6	3%	23%	6							-10%	43%	6
DPF #1	**TP**		-3%	5%	9																						-34%	6%	17
DPF #2	**TP**					1%	1%	3				-40%		1	44%		1										-50%	2%	3

15 References

Amanatidis, S., Ntziachristos, L. Maricq, M., Rostedt, A., Kauko, J., Tikkanen, J., Samaras, Z. (2014). Estimation of the mean particle size by sampling in parallel with two Pegasor Particle Sensors. ETH conference Switzerland, 2014

Cavina, N., Poggio, L., Bedogni, F., Rossi, V., Stronati, L. (2013). Benchmark comparison of commercially available systems for particle number measurement. SAE 2013-24-0182

EC (2007). Regulation (EC) No 715/2007 of the European Parliament and of the Council of 20 June 2007 "on type approval of motor vehicles with respect to emissions from light passenger and commercial vehicles (Euro 5 and Euro 6) and on access to vehicle repair and maintenance information", Official Journal of the European Union L 171, 1-16, 2007.

EC (2011). European Commission Regulation (EU) No. 582/2011 of May 2011, implementing and amending Regulation (EC) No. 595/2009 of the European Parliament and of the Council with respect to emissions from heavy-duty vehicles (Euro VI) and amending Annexes I to III to Directive 2007/46/EC of the European Parliament and Council

EC (2012). Regulation No. 64/2012 of 23 January 2012, amending Regulation (EU) No. 582/2011 implementing and amending Regulation (EC) No. 595/2009 of the European Parliament and of the Council with respect to emissions from heavy-duty vehicle (Euro VI).

Fierz, M., Burtscher, H., Steigmeier, P., & Kasper, M. (2008). Field measurement of particle size and number concentration with the diffusion size classifier (DiSC). SAE 2008-01-1179.

Fierz, M., Houle, C., Steigmeier, P., & Burtscher, H. (2011). Design, calibration and field performance of a miniature diffusion size classifier. Aerosol Sci. Technol., 45, 1-10.

Fierz, M., Meier, D., Steigmeier, P., Burtscher, H. (2014). Aerosol measurement by induced currents. Aerosol Sci. Technol., 48, 350-357.

Franco V., Kousoulidou M., Muntean M., Ntziachristos L., Huasberger S., Dialra P. (2013). Road vehicle emission factors development: A review. Atmospheric Environment, 70, 84-97

Giechaskiel B., Carriero M., Martini G., Bergmann A., Pongratz H., & Joergl H. (2010). Comparison of particle number measurements from the full dilution tunnel, the tailpipe and two partial flow systems. SAE 2010-01-1299

Giechaskiel B., Riccobono F., & Bonnel P. (2014). Feasibility study on the extension of the Real Driving Emissions (RDE) procedure to Particle Number (PN): Experimental evaluation of portable emission measurement systems (PEMS) with diffusion chargers (DCs) to measure particle number (PN) concentration. EU JRC report EUR 26997 EN

Hall, D., and Dickens, C. (1999). Measurement of the Number and Size Distribution of Particles Emitted from a Gasoline Direct Injection Vehicle," SAE 1999-01-3530

Hedge, M., Weber, P., Gingrich, J., Alger, T., et al. (2011). Effect of EGR on Particle Emissions from a GDI Engine," SAE 2011-01-0636

Johansson, A., Hemdal, S., and Dahlander, P. (2013). Experimental Investigation of Soot in a Spray-Guided Single Cylinder GDI Engine Operating in a Stratified Mode," SAE 2013-24-0052

Khalek, I., Bougher, T., and Jetter, J. (2010). Particle Emissions from a 2009 Gasoline Direct Injection Engine Using Different Commercially Available Fuels," SAE 2010-01-2117,

Mamakos A., Carriero M., Bonnel P., Demircioglu H., Douglas K., Alessandrini S. (2011). EU-PEMS PM evaluation program: Further study on post-DPF PM/PN emissions. Third report. EU 24883

Maricq, M., Podsiadlik, D., and Chase, R. (1999). Examination of the Size-Resolved and Transient Nature of Motor Vehicle Particle Emissions," Environ. Sci. Technol. 33:1618-1626

Maricq, M., Szente, J., Loos, M., and Vogt, R. (2011). Motor Vehicle PM Emissions Measurement at LEV III Levels," SAE 2011-01-0623

Mohr, M., Forss, A., and Steffen, D. (2000). Particulate Emissions of Gasoline Vehicles and Influence of the Sampling Procedure," SAE 2000-01-1137

Mohr, M., Lehmann, U., and Margaria, G. (2003). ACEA Programme on the Emissions of Fine Particulates from Passenger Cars (2): Part 1: Particle Characterisation of a Wide Range of Engine Technologies," SAE 2003-01-1889

Ntziachristos, L., Amanatidis, S., Samaras, Z., Janka, K., & Tikkanen, J. (2013). Application of the Pegasor particle sensor for the measurement of mass and particle number emissions. SAE, 2013-01-1561.

Ntziachristos, L., Mamakos, A., Samaras, Z., Mathis, U., et al. (2004). Characterization of Exhaust Particulate Emissions from Road Vehicles: Results for Light-Duty Vehicles," SAE 2004-01-1985

Okuda H., & Yamada H. (2013). Development of a novel electro mobility analyzer based on a new classifying principle and applications for nanoparticles from different types of vehicles under various conditions. 18th ETH conference, Zurich, Switzerland, 2014

Riccobono, F., Giechaskiel, B., Weiss, M., Bonnel, P. (2014). How to extend the real drive emission test procedure to particle number. Presentation at the 18th ETH Conference on Combustion Generated Nanoparticles, 25th June 2014, Zurich, Switzerland

Rostedt A., Arffman A., Janka K., Yli-Ojanperä J., & Keskinen J. (2014). Characterization and response model of the PPS-M aerosol sensor. Aerosol Sci. Techn. 48:10, 1022-1030

Schlatter, J. (2012). New Swiss legislation on portable particle counters for construction machinery. 16th ETH conference on combustion generated nanoparticles, June 24-27, 2012.

Szybist, J., Youngquist, A., Barone, T., Storey, J., et al. (2011). Ethanol Blends and Engine Operating Strategy Effects on Light-Duty Spark-Ignition Engine Particle Emissions," Energy & Fuels 25(11):4977–4985

U.S. EPA (2005). U.S. Environmental Protection Agency. Engine Testing Procedures, Title 40 Code of Federal Regulations 1065, Subpart J

Weiss M., Bonnel P., Hummel R., & Steininger N. (2013). A complementary emissions test for light duty vehicles: Assessing the technical feasibility of candidate procedures. EU 25572

16 Annex A: Detailed measurement protocol

Test ID	Test cycle	Vehicle Type	Cell	Cell T (°C)	PMP-TP	AVL DC	Horiba DC	Horiba CPC	Matter DC	Pegasor DC	Sensors DC	Sensors CPC	Shimdzu NAM	Maha CPC
20141017_03	Power	Moto #1	VELA 1	25	CVS					CVS				
20140806-02	NEDC hot	PFI #1	VELA 2	23					CVS					
20140806-03	Artemis	PFI #1	VELA 2	23					CVS					
20140806-04	WLTC hot	PFI #1	VELA 2	23					CVS					
20140807-01	WLTC cold	PFI #1	VELA 2	23					CVS					
20140807-02	WLTC hot	PFI #1	VELA 2	23					CVS					
20140807-03	Artemis	PFI #1	VELA 2	23					CVS					
20140811-01	NEDC hot	PFI #2	VELA 2	23					CVS					
20140813-01	NEDC cold	PFI #2	VELA 2	23					CVS					
20140813-02	NEDC hot	PFI #2	VELA 2	23					CVS					
20140813-03	Steady	PFI #2	VELA 2	23					CVS					
20140813-04	WLTC hot	PFI #2	VELA 2	23					CVS					
20140818-01	WLTC cold	PFI #2	VELA 2	23					CVS					
20140818-02	WLTC hot	PFI #2	VELA 2	23					CVS					
20140818-03	WLTC hot	PFI #2	VELA 2	23					CVS					
20140818-04	Steady	PFI #2	VELA 2	23					CVS					
20140819-02	NEDC cold	PFI #2	VELA 2	23					CVS					
20140819-03	NEDC hot	PFI #2	VELA 2	23					CVS					
20140819-04	Steady	PFI #2	VELA 2	23					CVS					
20140820-02	WLTC cold	PFI #2	VELA 2	23					CVS					
20140820-03	WLTC hot	PFI #2	VELA 2	23					CVS					
20140820-04	Steady	PFI #2	VELA 2	23					CVS					
20140821-01	NEDC cold	PFI #2	VELA 2	23					CVS					
20140822-01	NEDC hot	PFI #2	VELA 2	23					CVS					
20140822-03	Steady	PFI #2	VELA 2	23					CVS					
20140825-04	WLTC cold	PFI #2	VELA 2	23					CVS					
20140825-05	WLTC hot	PFI #2	VELA 2	23					CVS					
20141028-02	FTP A	GDI #1	VELA 2	23						CVS				CVS
20141028-02	FTP B	GDI #1	VELA 2	23						CVS				CVS
20141028-02	FTP C	GDI #1	VELA 2	23						CVS				CVS
20141029-01	ECE	GDI #1	VELA 2	23						CVS				CVS
20141029-01	EUDC	GDI #1	VELA 2	23						CVS				CVS
20141029-01	NEDC cold	GDI #1	VELA 2	23						CVS				CVS
20141029-02	FTP A	GDI #1	VELA 2	23						CVS				CVS
20141029-02	FTP B	GDI #1	VELA 2	23						CVS				CVS
20141029-02	FTP C	GDI #1	VELA 2	23						CVS				CVS
20141030_01	ECE40	Moto #2	VELA 1	23	CVS					TP	Issues	Issues	TP	TP
20141030_02	ECE40	Moto #2	VELA 1	23	CVS					TP	Issues	Issues	TP	Low Battery
20141030_03	WHTC	Moto #2	VELA 1	23	CVS					TP	Issues	Issues	TP	Low Battery
20141031_01	WHTC	Moto #2	VELA 1	23	CVS						Issues	Issues		250°C
20141103_01	ECE40	Moto #2	VELA 1	23	CVS					TP	Issues	Issues		TP
20141103_02	WHTC	Moto #2	VELA 1	23	CVS					TP	Issues	Issues		TP
20141103_03	Power	Moto #2	VELA 1	23	CVS					TP	Issues	Issues		TP
20141104_02	WLTC	GDI #2	VELA 2	23						TP				TP
20141105_01	NEDC	GDI #2	VELA 2	8						TP	TP	TP	TP	TP
20141105_02	WLTC	GDI #2	VELA 2	8						TP	TP	TP	TP	TP
20141105_03	Random	GDI #2	VELA 2	8						TP	TP	TP	TP	Issues
20141106_01	NEDC cold	GDI #3	VELA 2	23	TP	TP				TP	TP	TP	TP	TP
20141106_02	WLTC	GDI #3	VELA 2	23	TP	TP				TP	TP	TP	TP	TP
20141106_03	Random	GDI #3	VELA 2	23	TP	TP					TP	TP	TP	TP
20141106_04	WLTC	GDI #3	VELA 2	23	TP	TP				TP	TP	TP	TP	TP
20141107_01	NEDC cold	GDI #3	VELA 2	8	TP	TP				TP	TP	TP	TP	Issues
20141107_02	WLTC	GDI #3	VELA 2	8	TP	TP				TP	TP	TP	TP	Issues
20141107_03	Random	GDI #3	VELA 2	8	TP	TP				TP	TP	TP	TP	Low Battery
20141107_04	WLTC	GDI #3	VELA 2	8	TP	TP				TP	TP	TP	TP	Low Battery
20141111_01	NEDC cold	GDI #4	VELA 2	23	TP	TP			TP	TP	TP	Issues	TP	TP
20141111_02	WLTC	GDI #4	VELA 2	23	TP	TP			TP	TP	Issues	Issues	TP	TP
20141111_03	RDE	GDI #4	VELA 2	23	TP	lost rec			TP	TP	TP	Issues	TP	TP
20141111_04	Steady	GDI #4	VELA 2	23	TP	TP			TP	TP	TP	Issues	TP	TP
20141112_01	NEDC cold	GDI #4	VELA 2	8	TP	TP			TP	TP	TP	Issues	TP	Issues
20141112_02	WLTC	GDI #4	VELA 2	8	TP	TP			TP	TP	TP	Issues	TP	Issues
20141112_03	Random	GDI #4	VELA 2	8	TP	TP			TP	TP	TP	Issues	TP	TP
20141112_04	Steady	GDI #4	VELA 2	8	TP	TP			TP	TP	TP	Issues	TP	Issues
20141113_01	NEDC cold	GDI #4	VELA 2	23	TP	TP			TP	TP	TP	Issues	TP	TP
20141113_02	WLTC	GDI #4	VELA 2	23	TP	TP			TP	TP	TP	Issues	TP	TP

Test ID	Test cycle	Vehicle Type	Cell	Cell T (°C)	PMP-TP	AVL DC	Horiba DC	Horiba CPC	Matter DC	Pegasor DC	Sensors DC	Sensors CPC	Shimdzu NAM	Maha CPC
20141113_03	Random	GDI #4	VELA 2	23	TP	TP			TP	TP	TP	Issues	TP	TP
20141113_04	WLTC	GDI #4	VELA 2	23	TP	TP			TP	TP	TP	Issues	TP	TP
20141114_01	NEDC cold	GDI #4	VELA 2	8	TP	TP			TP	TP	cold	TP	TP	Issues
20141114_02	Random	GDI #4	VELA 2	8	TP	TP			TP	TP	TP	TP	TP	Issues
20141118-2	US06	GDI #5	VELA 2	23		CVS								
20141119-3	NEDC cold	GDI #5	VELA 2	23		CVS								
20141119-4	US06	GDI #5	VELA 2	23		CVS								
20141124-1	NEDC cold	GDI #5	VELA 2	23		CVS								
20141124-2	US06	GDI #5	VELA 2	23		CVS								
20141118-3	NEDC cold	PFI #3	VELA 2	23		CVS								
20141118-4	US06	PFI #3	VELA 2	23		CVS								
20141119-1	NEDC cold	PFI #3	VELA 2	23		CVS								
20141119-2	US06	PFI #3	VELA 2	23		CVS								
20141119-3	US06	PFI #3	VELA 2	23		CVS								
20141119-pre	US06	PFI #3	VELA 2	23		CVS								
20141120-3	NEDC cold	PFI #3	VELA 2	23		CVS								
20141120-4	US06	PFI #3	VELA 2	23		CVS								
20141121-3	NEDC cold	PFI #3	VELA 2	23		CVS								
20141121-4	US06	PFI #3	VELA 2	23		CVS								
20141124-1	NEDC cold	PFI #3	VELA 2	23		CVS								
20141124-2	US06	PFI #3	VELA 2	23		CVS								
20141125_01	NEDC cold	GDI #2	VELA 2	23	TP	TP			TP	TP	TP	Issues	TP	TP
20141125_02	Random	GDI #2	VELA 2	23	TP	TP			TP	TP	TP	Issues	TP	Issues
20141125_03	WLTC cold	GDI #2	VELA 2	8	TP	TP			TP	TP	TP	Issues	TP	Issues
20141125_04	NEDC	GDI #2	VELA 2	8	TP	TP			TP	TP	TP	Issues	Issues	Issues
20141126_01	NEDC cold	GDI #2	VELA 2	23	TP	TP			TP	TP	TP	Issues	Issues	Issues
20141126_02	Random col	GDI #2	VELA 2	23	TP	TP			TP	TP	TP	Issues	Issues	Issues
20141126_03	Random	GDI #2	VELA 2	23	TP	TP			TP	TP	TP	Issues	Issues	Issues
20141127_01	NEDC cold	GDI #2	VELA 2	23	TP	TP			TP	TP	TP	Issues	Issues	Issues
20141127_02	Random col	GDI #2	VELA 2	23	TP	TP			TP	TP	TP	Issues	Issues	Issues
20141127_03	Random	GDI #2	VELA 2	23	TP	TP			TP	TP	TP	Issues	Issues	Issues
20141128_01	WLTC cold	GDI #2	VELA 2	23	TP	TP			TP	TP	TP	Issues	Issues	Issues
20141128_02	WLTC cold	GDI #2	VELA 2	23	TP	TP			TP	TP	TP	Issues	Issues	Issues
20141203_01	WLTC cold	GDI #6	VELA 2	23	TP	TP	TP	Softw	TP				CVS	
20141203_02	WLTC	GDI #6	VELA 2	23	TP	TP	TP	Softw	TP	TP	TP	Issues	CVS	TP
20141203_03	WLTC	GDI #6	VELA 2	23	TP	TP	TP	TP	TP		TP	Issues	CVS	
20141203_04	Artemis	GDI #6	VELA 2	23	TP	TP	TP	TP	TP		TP	Issues	CVS	
20141203_05	NEDC	GDI #6	VELA 2	23	TP	TP	TP	TP	TP		TP	Issues	CVS	TP
20141204_02	NEDC	GDI #6	VELA 2	23	TP	TP	TP	TP	TP			Issues	CVS	
20141204_03	NEDC	GDI #6	VELA 2	23	TP	TP	TP	TP	TP			Issues	CVS	
20141204_04	Artemis	GDI #6	VELA 2	23	TP	TP	TP	TP	TP			Issues	CVS	
20141204_05	WLTC	GDI #6	VELA 2	23	TP	TP	TP	Softw	TP			Issues	CVS	TP
20141205_02	WLTC	GDI #6	VELA 2	23	CVS	TP	TP	TP	TP			Issues	CVS	
20141209-01	R47 not ok	Moto #1	VELA 1	23		CVS		CVS	CVS				CVS	CVS
20141209-02	R47	Moto #1	VELA 1	23		CVS		CVS	CVS				CVS	CVS
20141209-03	Power	Moto #1	VELA 1	23		CVS		CVS	CVS				CVS	CVS
20141210-01	R47	Moto #1	VELA 1	23		CVS		CVS					CVS	CVS
20141211-01	NEDC cold	GDI #7	VELA 1	23	CVS	CVS	CVS	CVS*					CVS	CVS
20141211-02	NEDC cold	GDI #7	VELA 1	23	CVS	CVS	CVS	CVS*					CVS	CVS
20141212-01	NEDC cold	GDI #7	VELA 1	23	CVS	CVS	CVS	CVS*					CVS	CVS
20141212-02	NEDC cold	GDI #7	VELA 1	23	TP		TP	TP*	TP				CVS	TP
20141215-03	NEDC cold	GDI #7	VELA 1	23	TP	TP	TP	TP*	TP				CVS	TP
20141216-02	NEDC cold	GDI #7	VELA 1	23	TP	TP	TP	TP*			TP	TP	CVS	TP
20141217-02	ECE47	Moto #3	VELA 1	23	TP	TP	TP	TP			TP	TP	CVS	TP
20141217-03	ECE47	Moto #3	VELA 1	23	TP	TP	TP	TP		TP	TP	TP	CVS	TP
20141217-04	Power	Moto #3	VELA 1	23	TP	TP	TP	TP		TP	TP	TP	CVS	TP
20141218-01	ECE47	Moto #3	VELA 1	23	TP	TP	TP		TP				CVS	TP
20141218-02	ECE47	Moto #3	VELA 1	23	TP	TP	TP		TP	TP			CVS	TP
20141218-03	Power	Moto #3	VELA 1	23	TP	TP	TP		TP	TP			CVS	TP
20141219-01	WMTC	Moto #4	VELA 1	23	TP	TP	TP	TP	TP	TP			CVS	TP
20141219-02	WMTC	Moto #4	VELA 1	23	TP	TP	TP	TP	TP	TP			CVS	TP
20150118-02	Regener.	DPF #1	VELA 2	23	TP	TP								TP
20150118-03	NEDC	DPF #1	VELA 2	23	TP	TP								TP
20150118-04	WLTC	DPF #1	VELA 2	23	TP	TP								TP
20150130-03	Regener.	DPF #1	VELA 2	23	TP	TP								TP
20150130-04	Artemis	DPF #1	VELA 2	23	TP	TP								TP
20150130-05	WLTC	DPF #1	VELA 2	23	TP	TP								TP

17 Annex B: Comparison of measurements at the tailpipe and the dilution tunnel

When comparing two instruments at different locations (one at the tailpipe and the other at the dilution tunnel) many processes taking place need to be considered. For example, the system sampling from the tailpipe is extracting a flow which will be replaced with dilution air in the dilution tunnel, thus will affect the absolute levels of the emissions (or the exhaust flow rate that is estimated). From the tailpipe until the mixing point of the dilution tunnel losses can occur due to thermophoresis, diffusion or even coagulation when the concentration is high. Finally, the system at the tailpipe needs the exhaust flow rate as an input in order to provide the final emissions in p/km. Any error in the exhaust flow rate measurement and/or in the time alignment between particle concentration signal and exhaust flow rate signal will have an effect on the result. These topics are discussed in the following paragraphs.

17.1 Effect of extracted flow on absolute levels

When instruments sample from the tailpipe, less exhaust flow ends up in the dilution tunnel. This results in lower emissions measured at the dilution tunnel (CVS). At the same time the exhaust flow rate that is estimated by the difference of the total flow in the CVS and the flow of the dilution air is less. Thus the instrument at the tailpipe is using an exhaust flow rate that is lower than in the reality. The final result is that both CVS and tailpipe instruments will give lower absolute emission levels. However, the difference between TP and CVS is not affected; only the absolute levels are affected. In this report no correction was done for the extracted flow rate. The estimated error on the absolute levels is around 2-4%.

17.2 Thermophoretic losses

Thermophoresis makes particles from the hot exhaust go to the cold tube walls. Assuming that the sampling from the tailpipe is only minimally affected, the concentration from the tailpipe will decrease as the exhaust gases are lost at the cold tube walls until the mixing at the dilution tunnel.

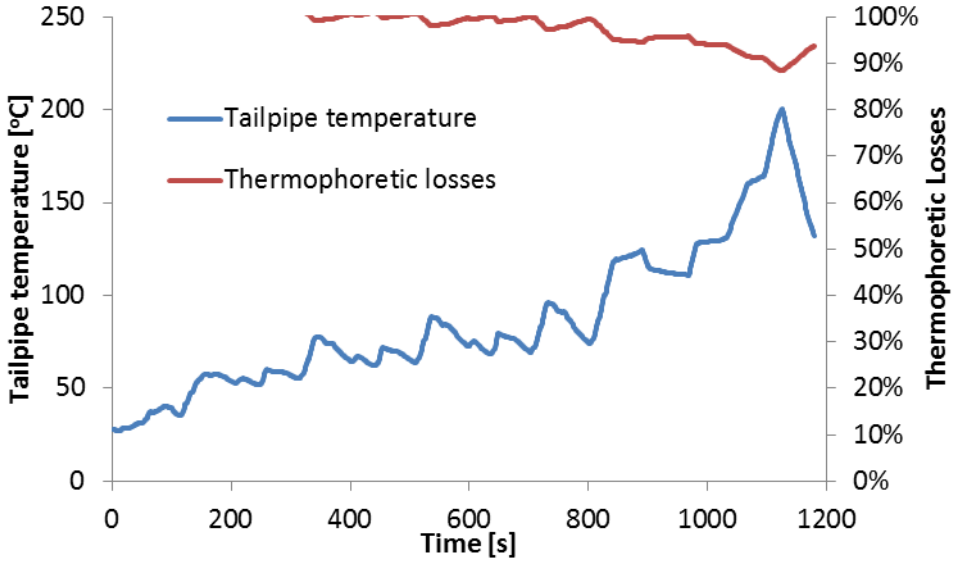

Figure 17-1: Estimated thermophoretic losses over a NEDC cold (20141111-01-NEDC cold).

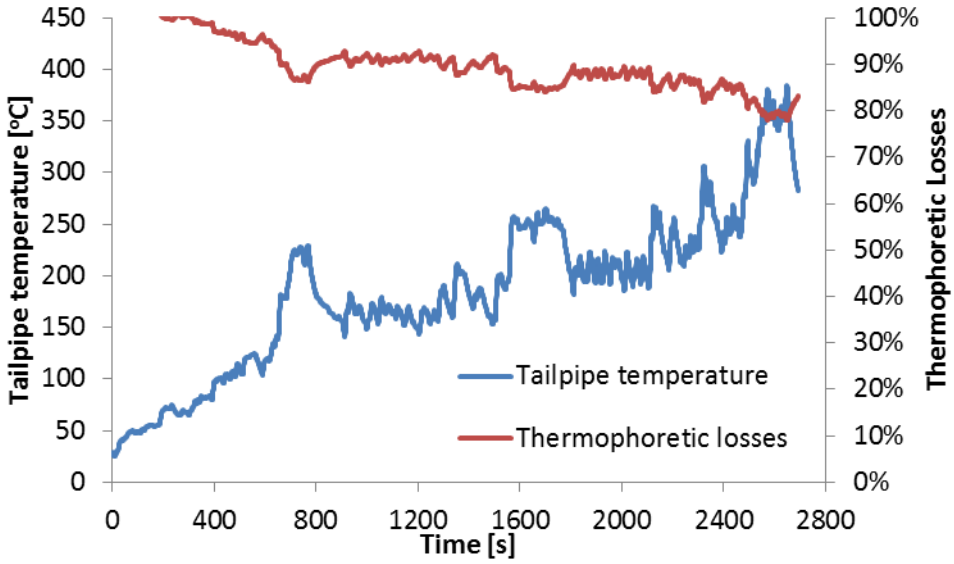

Figure 17-2: Estimated thermophoretic losses over a Random Driving Cycle (20141126-02-Random Driving Cycle).

Assuming that the tube is kept at 100°C, thermophoresis is negligible during cold cycles where the exhaust gas temperature is kept relatively low (Figure 17-1). However, it can reach 10% during more aggressive cycles (Figure 17-2).

17.3 Condensation

During cold start cycles we observed condensation. This lost mass could affect the CVS results (because less exhaust is sampled). We weighted the condensation and we found it around 30 g per test (NEDC). This amount is around 1% of the total exhaust volume. Thus the lost mass is negligible. High amounts of condensation however could lead to particle losses in the condensed liquid that cannot be easily estimated.

17.4 Coagulation

For the highest emitting vehicle (Figure 17-3) the coagulation (agglomeration) effect can be significant. Especially at the beginning of the cycles, where the emissions are highest, 30% reduction of the particle concentration can be observed. However, not the whole percentage is due to coagulation. The dead volume until the CVS also results in particles counted later. Assuming that the PMP-TP measures the correct concentration and the PMP-CVS the decreased from coagulation concentration, for emission levels of 4x10^12 p/km (Figure 17-3) the mean reduction over the cycle is 20%. The comparison between PMPs in function of the measured concentration did not show a clear trend. Thus coagulation probably did not have the most important contribution to the observed deviations.

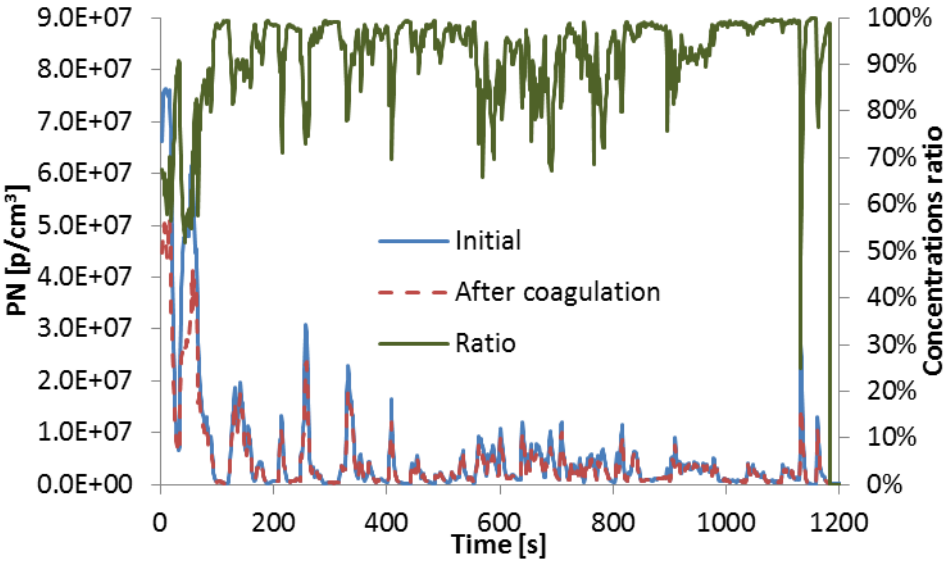

Figure 17-3: Estimated coagulation losses (20141106-01-NEDC cold, GDI #3).

17.5 Exhaust flow

Any error in the exhaust flow rate will have an impact on the final result of the instruments connected to the tailpipe, because they use the exhaust flow rate to estimate the final emissions. The flow rate in this report was estimated as the difference between the total flow rate in the dilution tunnel (CVS) and the dilution air entering the dilution tunnel, measured by pressure difference sensors.

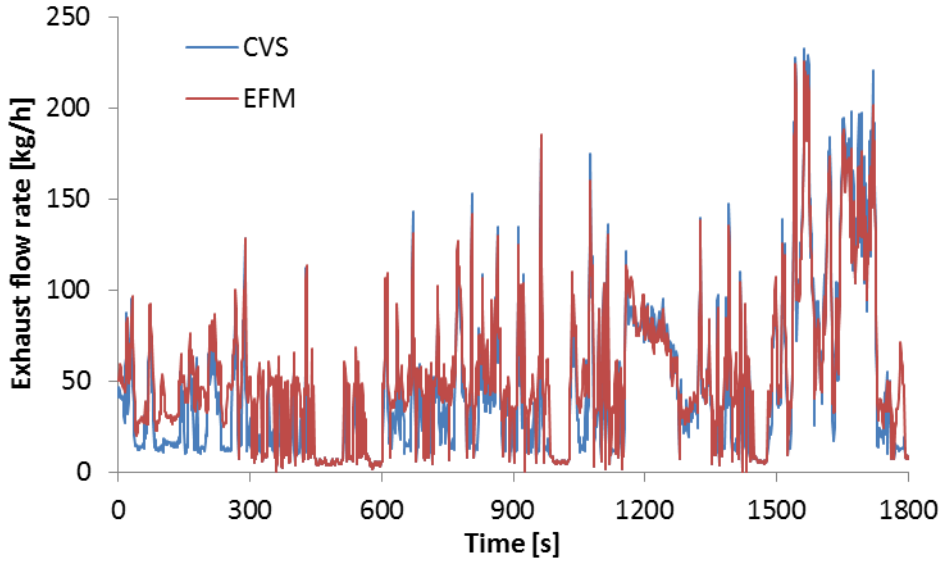

Figure 17-4: Comparison of exhaust flow estimated from the dilution tunnel (CVS) and an exhaust flow meter (EFM).

For some tests an exhaust flow meter (EFM) was connected to the tailpipe of a vehicle (GDI #3) and the flow rates measured by the EFM and the estimated by the CVS were compared (Figure 17-4). The flow rate of the EFM was also used to estimate the emissions of the PMP-TP. The cycle average results had approximately 10% difference.

More discussion on the differences between EFMs and CVS estimated flow can be found elsewhere, but typically are smaller than 10%.

17.6 Time alignment

The time alignment between the exhaust flow rate and the particle concentration can have a significant effect on the final result because these two signals are multiplied with each other. The following figures (Figure 17-5, Figure 17-6, Figure 17-7) show small misalignment of a few seconds and the effect on the final result (of the PMP-TP) (Figure 17-8). One second misalignment can have a 5-10% effect, while 2 seconds can affect 10-15%.

The time alignment in this report was based on the maximum correlation (i.e. assuming that the maximum emissions occur when the exhaust flow rate is maximum). This is not necessarily true and it this approach might have resulted in 5-15% overestimation of the emissions at the tailpipe.

Similar results were found with other vehicles (cycles) (Figure 17-9).

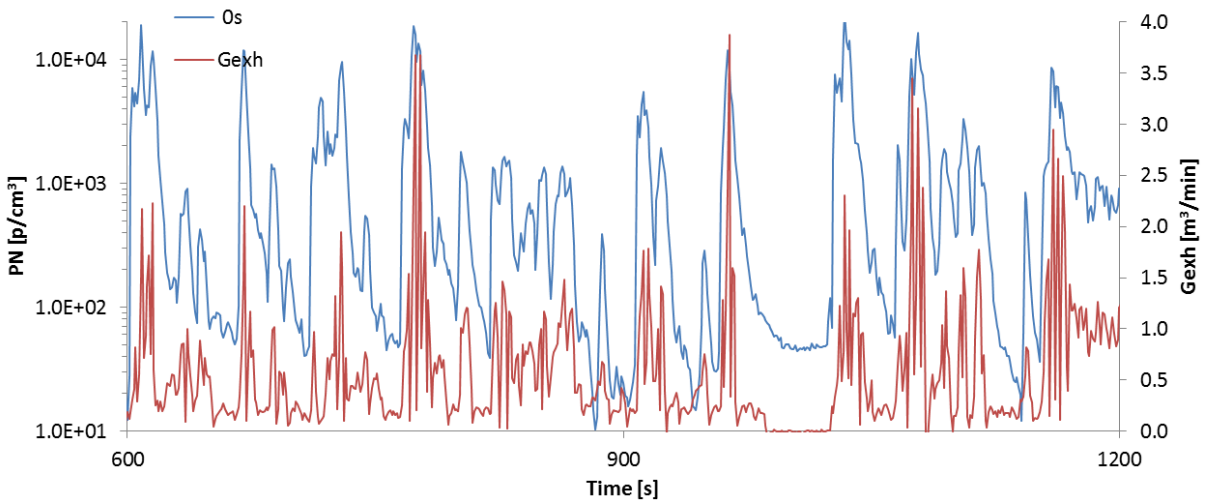

Figure 17-5: Time alignment matching peaks of signals.

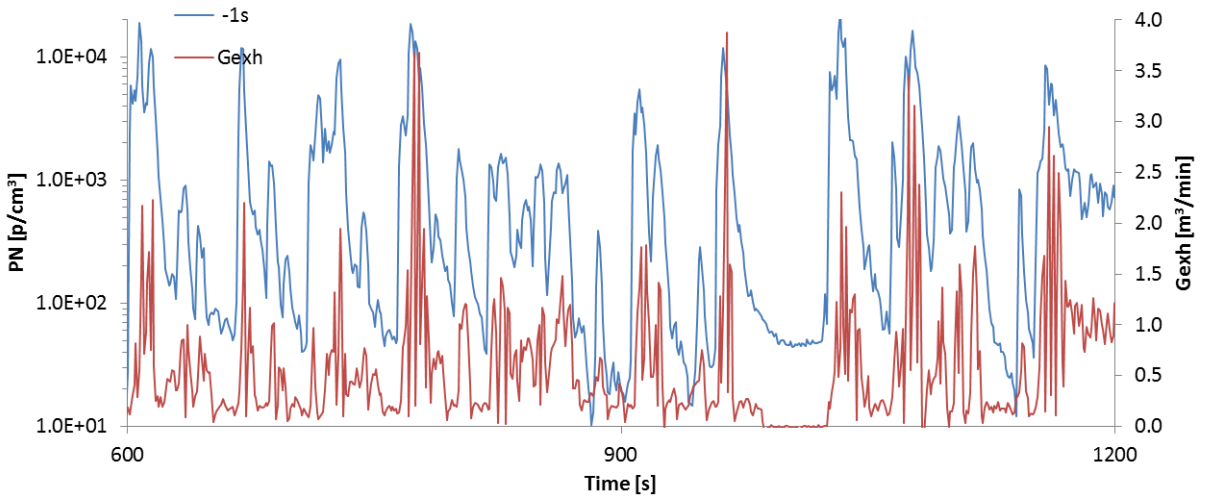

Figure 17-6: Time alignment. PN concentration is 1 s behind.

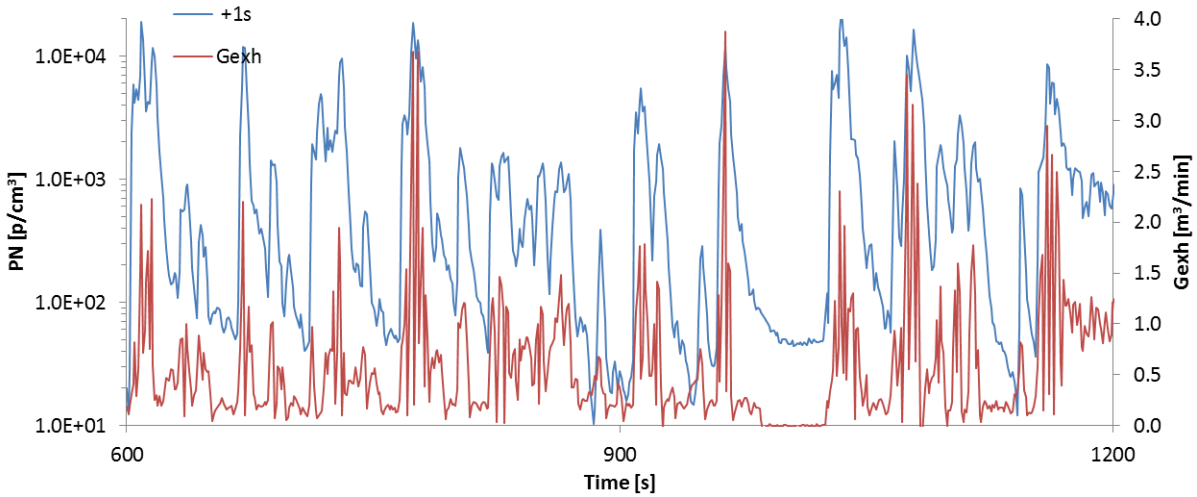

Figure 17-7: Time alignment: PN concentration is 1 s ahead.

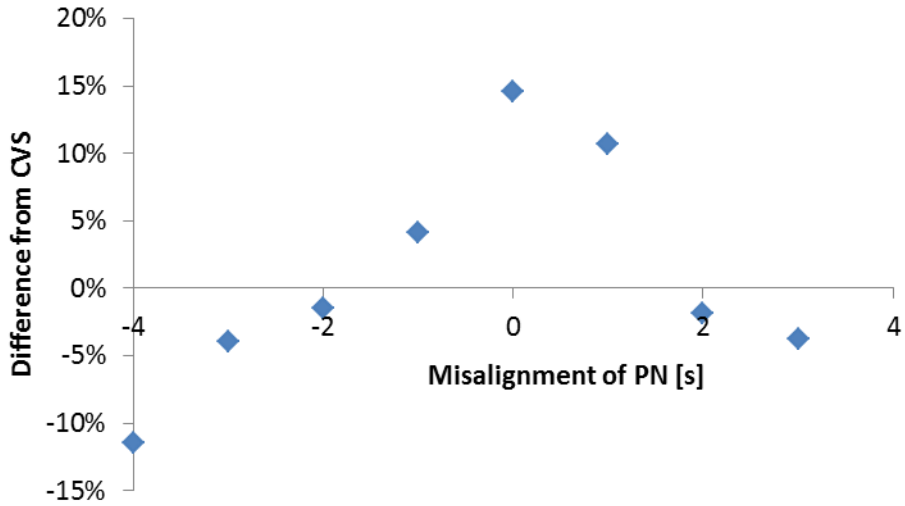

Figure 17-8: Summary of misalignment effect (example of 20141111-02-WLTC, GDI #4).

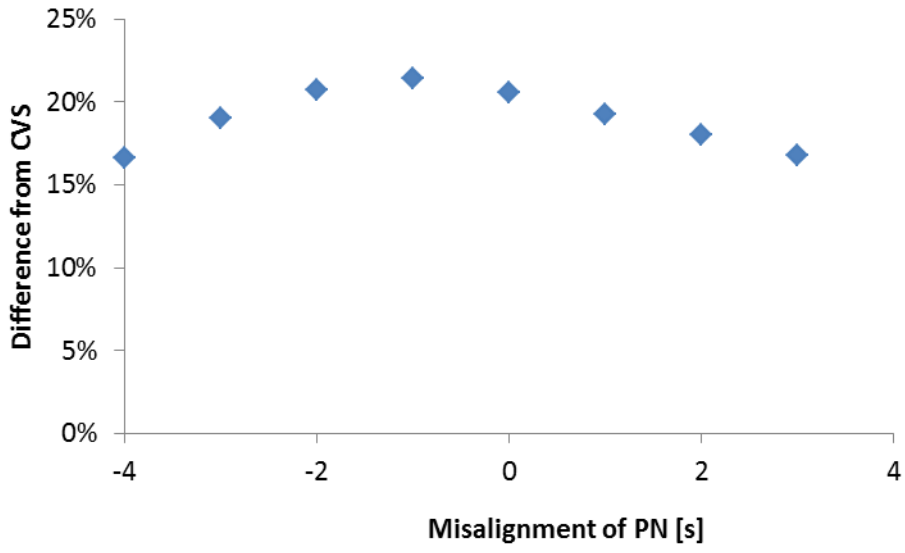

Figure 17-9: Summary of misalignment effect (example of 20141107-01-NEDC, GDI #3).

Similar results were found also with DCs, which in general have faster response than the PMP systems (Figure 17-10).

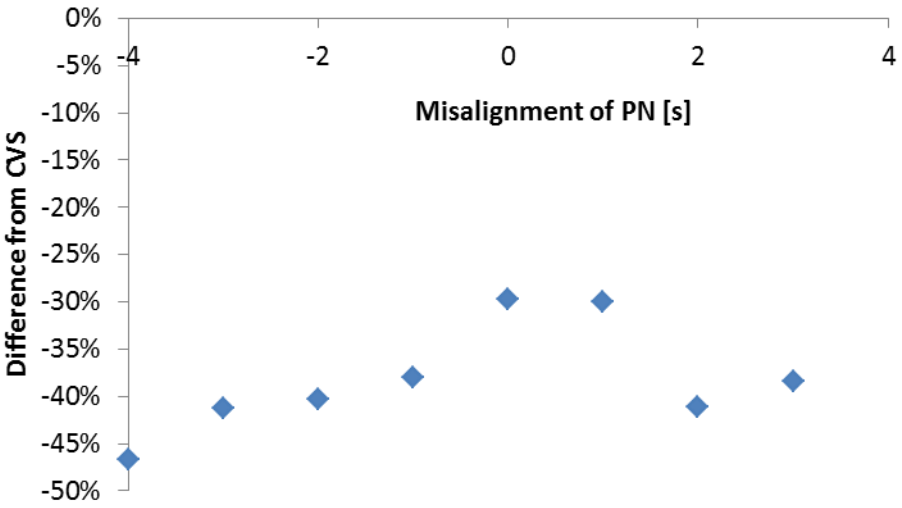

Figure 17-10: Summary of misalignment effect (example of 20141111-02-WLTC for a DC, GDI #4).

18 Annex C: Volatile Removal Efficiency (VRE)

The Volatile Removal Efficiency (VRE) of the systems was evaluated in the main campaign by measuring exhaust of a 2-stroke moped. In the lab two materials were used: Tetracontane and Emery oil. Tetracontane was used because it is required in the legislation (30 nm particles with concentration >10^4 p/cm^3). Atomized emery oil was used to simulate extreme conditions of unburnt lubricant.

The following systems were investigated: PMP-CVS, PN-PEMS #2' (CPC), PN-PEMS #3, PN-PEMS #4. In addition a PMP+CS system was evaluated.

The legislative tetracontane tests were easily passed by all systems (concentration >10^4 p/cm3, monodisperse 30 nm, mass 0.15 µg/m^3). Then polydisperse aerosol with GMD of 120 nm was fed to the instruments (mass 1.5 mg/m^3). Again all systems passed the test with extremely high efficiencies (Table 18-1).

Table 18-1: Volatile Removal Efficiency (VRE) of tetracontane polydisperse aerosol GMD=120 nm, concentration 8x10^5 p/cm^3.

System	PMP	PMP+CS1	#2' (CPC)	#3	#4	CS3 + #4
VRE [%]	100	100	100	97	99	100

The systems were then tested with atomized Emery oil (PALAS AGK 2000 atomizer). The generated size was approximately 200 nm and the concentration was varied by a dilution bridge. An EEPS was always measuring the concentration in parallel with the system under evaluation to quantify the inlet concentration. To put the following results in perspective, a 2-stroke moped can emit >15 mg/m^3 at cold start (measured at the CVS).

Initially the PMP system was evaluated with 23 nm and 10 nm CPCs. The efficiency, as calculated with a CPC of 23 nm, remains high up to approximately 500 µg/m^3 of hydrocarbons at the inlet of the ET. When a 10 nm CPC is considered the efficiency remains high up to 150 µg/m^3. With a 3 nm CPC the upper limit is around 50 µg/m^3 (figure not shown).

The different efficiencies have to do with the growth of the nucleated particles. These values are much lower compared to the estimated mass based on homogeneous nucleation (1500 µg/m^3). Probably the atomized oil had solid residuals that helped heterogeneous nucleation.

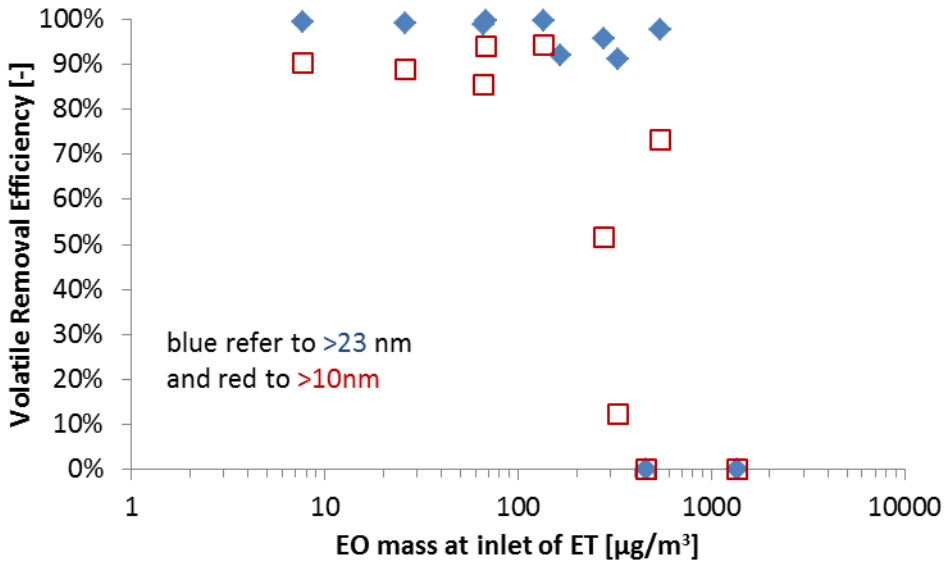

Figure 18-1: VRE of a PMP system

At a second step three CS from different manufacturers in four configurations were examined. The results of the systems with CS can be seen in Figure 18-2. The efficiency of two models was extremely high up to 15 mg/m³ of oil entering the CS. One relatively new CS didn't perform so well, probably because there was no heating section upstream to evaporate the oil.

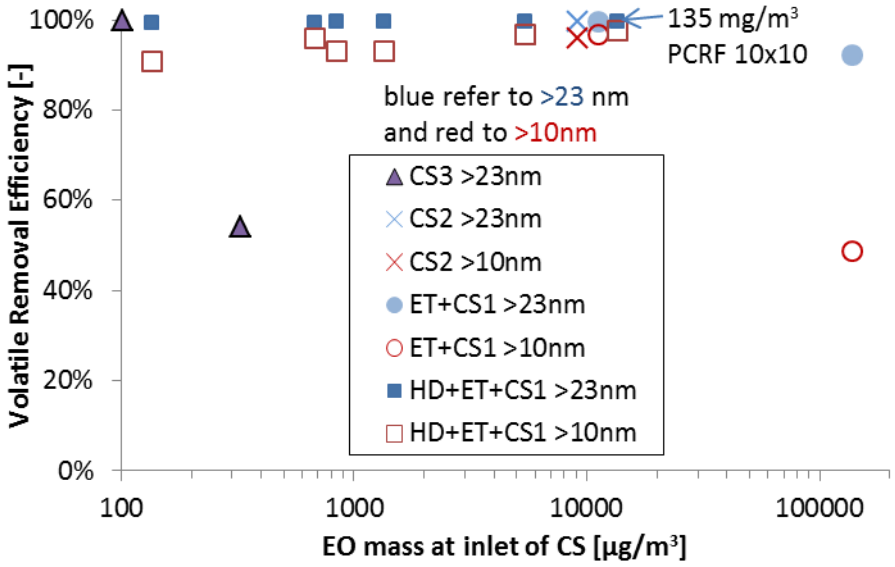

Figure 18-2: VRE of CS based systems. ET=Evaporation Tube, HD=Hot Dilution, CS=Catalytic Stripper.

The results of PN-PEMS #2' (CPC) which includes a CS can be seen in Figure 18-3. The removal efficiency remains high for >1 mg/m³ at the inlet of the CS (>13 mg at the inlet of the device).

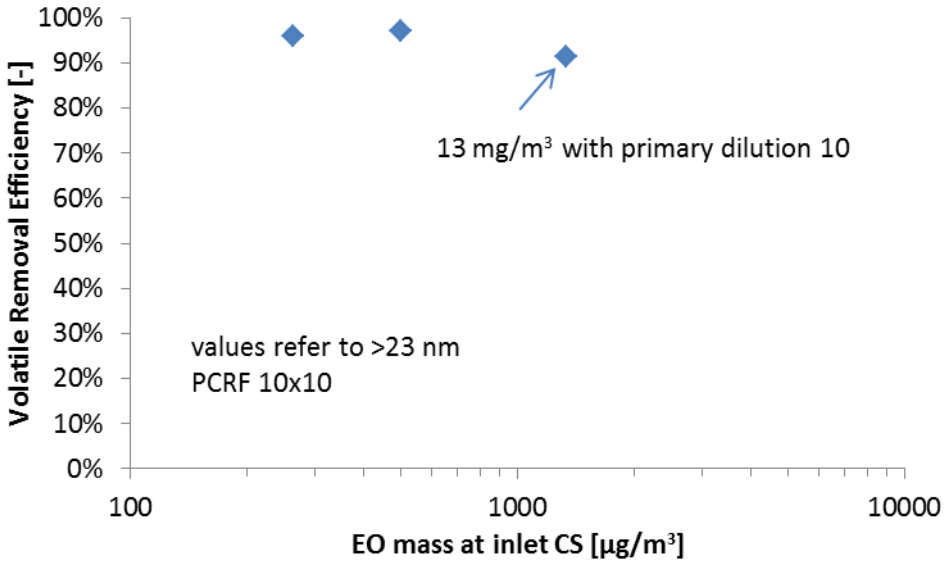

Figure 18-3: VRE of PN-PEMS #2 (CPC).

The results of PN-PEMS #3 which includes primary dilution and an ET can be seen in Figure 18-4. The volatile removal efficiency starts to drop at 50 µg/m³ at the inlet of the ET and a separate nucleation mode is formed at 100 µg/m³ at the inlet of the ET. With the highest dilution of the device approximately up to 13 mg/m³ could be handled.

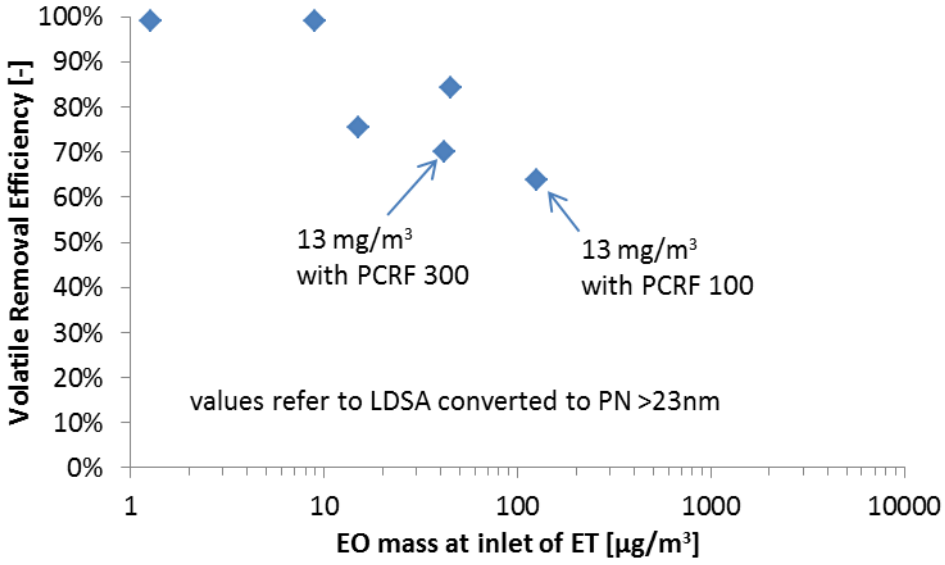

Figure 18-4: VRE of PN-PEMS #3.

The summary of the results can be seen in Figure 18-5 where the mass concentrations of oil at the inlet of the systems is shown (using the available dilutions of the devices). Systems with CS can handle more than 10 mg/m³ while with ET only when using higher dilution ratios.

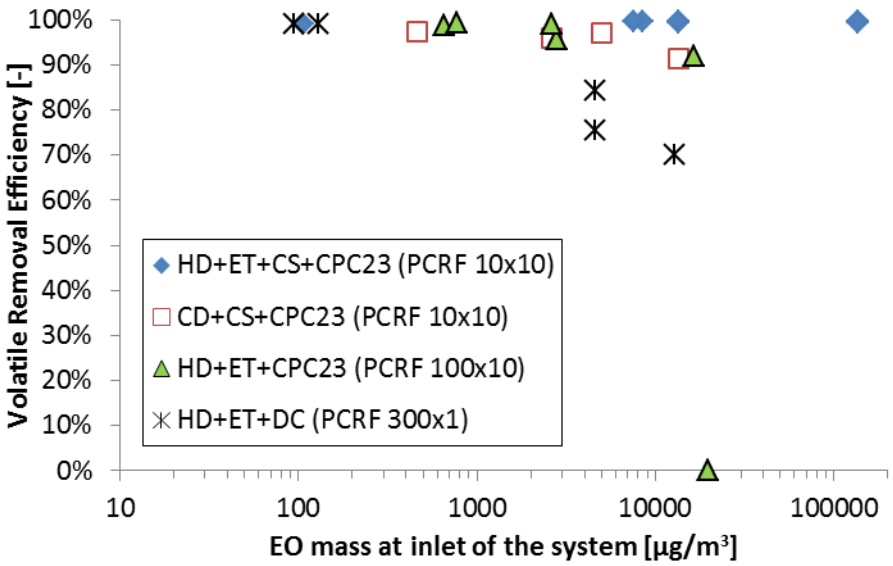

Figure 18-5: Summary of VRE investigations.

For typical applications a high dilution with evaporation tube will be sufficient. For extreme cases (e.g. 2-stroke mopeds) a CS is necessary. However the oxidation efficiency of the CS or its configuration (e.g. heating before the inlet of the CS) need to be well studied and characterized as there can be big differences between different models.

19 Annex D: Further evaluation of PN-PEMS

Two of the PN-PEMS that showed very good results during the main campaign were further evaluated until the beginning of the inter-laboratory exercise with 10 more vehicles: three GDIs, one PFI, one diesel, two diesel with DPF, two motorcycles and one moped (4-stroke). All measurements were conducted from the CVS in the period March – May 2015. In addition a few on-board tests conducted with both systems at 4 vehicles.

The differences compared to the PMP system connected to the CVS (tests both in VELA 1 and VELA 2) can be seen in Figure 19-1. The mean differences of the CPC based system (PN-PEMS #2' (CPC)) to the PMP-CVS are ±15%with a standard deviation of 10%. The DC based system (PN-PEMS #3) had differences of -35% to +15% (PN) or -40% to +40% (LDSA). The standard deviation was approximately 20% (higher for the DPF vehicles). It should be noted that there is a concern that the DC based system drifted during the measurements of the D #1 vehicle and the emissions where underestimated 40% after that point. However it is not clear whether this drop of the efficiency happened during the tests with the diesel vehicle or the on-road tests with a GDI the same period.

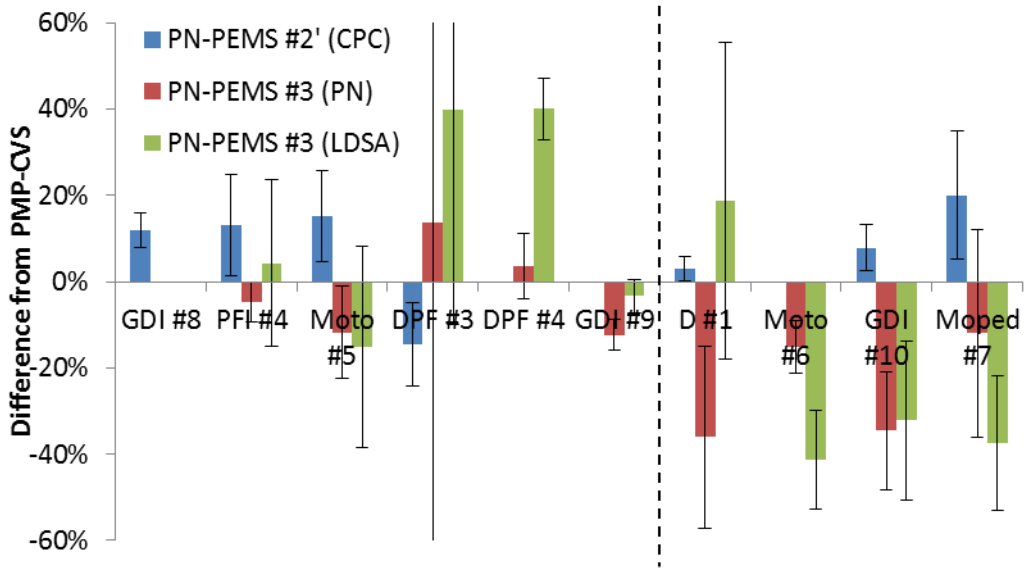

Figure 19-1: Comparison of PN-PEMS with PMP-CVS, all connected to the CVS. The dotted line indicates a possible drift of the DC based system.

A closer look of the behaviour of PN-PEMS #3 can be seen in Figure 19-2. During the period of the measurements of D #1 a 40% drop of the differences compared to the PMP-CVS was observed. This undercounting remained for the rest vehicles tested; this is shown with the tests of GDI #9 over a period of some months. After the May tests the difference to the PMP-CVS was 40%.

The lab evaluation of the system also confirmed the lower efficiency (Figure 19-3). The monodisperse calibration with spark-discharge graphite showed a lower Efficiency compared to the original values (see details in Figure 9-1). This difference is much higher than the 15% experimental uncertainty.

When the system was sent to the manufacturer, it was found out that there was a leakage between the heated line and the diluter

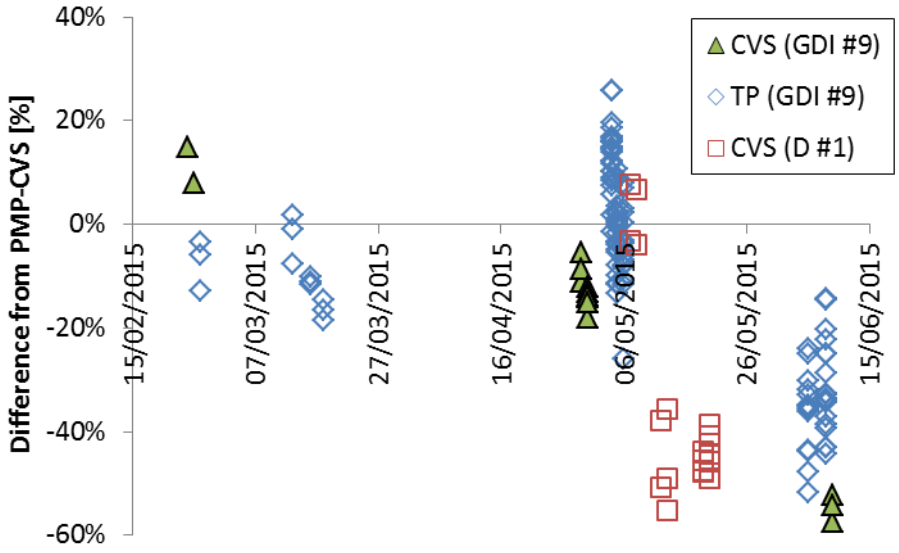

Figure 19-2: Indication of drift of PN-PEMS #3.

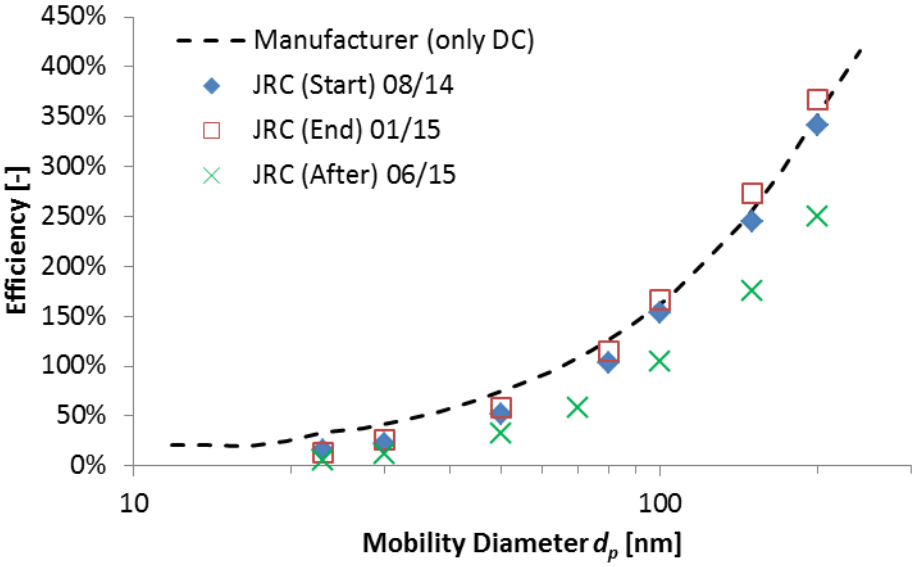

Figure 19-3: Monodisperse calibration of PN-PEMS #3 at different times.

The further evaluation of the two PN-PEMS after the end of the measurement campaign showed:

- The long term robustness of PN-PEMS has to be further investigated by instrument manufacturers: Not only the sensors, but also the dilution and thermal pre-treatment systems might be reason of drifts.
- The CPC based system is promising, especially for the sec to sec data. The tests conducted here didn't indicate any issues. It should be mentioned though that most tests were conducted at the diluted exhaust and only a few at the tailpipe and on-road.

European Commission
EUR 27451 EN – Joint Research Centre – Institute for Energy and Transport

Title: **Feasibility study on the extension of the Real Driving Emissions (RDE) procedure to Particle Number (PN):** Chassis dynamometer evaluation of portable emission measurement systems (PEMS) to measure particle number (PN) concentration: Phase II

Author(s): Barouch Giechaskiel, Francesco Riccobono, Pierre Bonnel

Luxembourg: Publications Office of the European Union

2015 – 149 pp. – 21.0 x 29.7 cm

EUR – Scientific and Technical Research series – ISSN 1831-9424 (online)

ISBN 978-92-79-51003-8 (PDF)

doi:10.2790/74218

LD-NA-27451-EN-N

JRC Mission

As the Commission's in-house science service, the Joint Research Centre's mission is to provide EU policies with independent, evidence-based scientific and technical support throughout the whole policy cycle.

Working in close cooperation with policy Directorates-General, the JRC addresses key societal challenges while stimulating innovation through developing new methods, tools and standards, and sharing its know-how with the Member States, the scientific community and international partners.

Serving society
Stimulating innovation
Supporting legislation

doi: 10.2790/74218

ISBN 978-92-79-51003-8

Publications Office